The Geology, Paleontology and Paleoecology of the Cerro Fortaleza Formation, Patagonia (Argentina)

A Thesis

Submitted to the Faculty

of

Drexel University

by

Victoria Margaret Egerton

in partial fulfillment of the

requirements for the degree

of

Doctor of Philosophy

November 2011

Dedications

To my mother and father

Acknowledgments

The knowledge, guidance and commitment of a great number of people have led to my success while at Drexel University. I would first like to thank Drexel University and the College of Arts and Sciences for providing world-class facilities while I pursued my PhD. I would also like to thank the Department of Biology for its support and dedication.

I would like to thank my advisor, Dr. Kenneth Lacovara, for his guidance and patience. Additionally, I would like to thank him for including me in his pursuit of knowledge of Argentine dinosaurs and their environments. I am also indebted to my committee members, Dr. Gail Hearn, Dr. Jake Russell, Dr. Mike O'Connor, Dr. Matthew Lamanna, Dr. Christopher Williams and Professor Hermann Pfefferkorn for their valuable comments and time.

The support of Argentine scientists has been essential for allowing me to pursue my research. I am thankful that I had the opportunity to work with such kind and knowledgeable people. I would like to thank Dr. Fernando Novas (Museo Argentino de Ciencias Naturales) for helping me obtain specimens that allowed this research to happen. I would also like to thank Dr. Viviana Barreda (Museo Argentino de Ciencias Naturales) for her allowing me use of her lab space while I was visiting Museo Argentino de Ciencias Naturales. I would also like to thank Dr. Roberto Pujana (Museo Argentino de Ciencias Naturales), Ricardo Ponti (Museo Argentino de Ciencias Naturales), Dr. Nora Franco (Universidad de Buenos Aires) and Mary Palacios (Museo Padre Monina) for all of their help and guidance while visiting Argentina.

I would also like to thank the staff and curators of the British Antarctic Survey and the British Natural History Museum for allowing me to search through their collections. I am indebted to the Jurassic Foundation for providing the funding necessary to complete my research.

I am grateful for all the friendships that I have gained during my PhD. I would like the thank Dr. Elizabeth Spudich for being such a good mentor and friend. Her knowledge of anatomy and her teaching style has been inspirational to me. I would also like to thank Jason Poole for his friendship and encouragement. He taught me the importance of communicating science to the public and how to communicate it effectively. I am also indebted to my past lab mates, Jessica Battisto, Elena Schroeter, Christopher Coughenour, Lucio Ibiricu, Jason Schein, Paul Ulman and Zach Boles, for their support and friendship.

I would also like to thank my parents and Phillip Manning whose support has been essential for my success. Without their encouragement and love, I don't know how I could have accomplished all that I have thus far.

TABLE OF CONTENTS

LIST OF TABLES vii
LIST OF FIGURES viii
Abstract xviii
CHAPTER 1: LATE CRETACEOUS GEOLOGY OF THE NORTHERN AUSTRAL BASIN WITH EMPHASIS ON THE CERRO FORTALEZA FORMATION 1
INTRODUCTION 1
Separation of Gondwana 3
Austral Basin Evolution 5
Historical Review of Patagonian Geology 7
LATE CRETACEOUS REGIONAL GEOLOGY OF THE RÍO SHEHUEN VALLEY AND LAGOS VIEDMA AND ARGENTINO 11
Mata Amarilla Formation 11
La Anita Formation 18
Cerro Fortaleza/Pari Aike Formation 23
La Irene Formation 38
Chorrillo Formation 41
Late Cretaceous Depositional Cycles in the area of Lago Viedma/Lago Argentino 45
DISCUSSION 48
CONCLUSIONS 54
CHAPTER 2: GYMNOSPERM WOOD FROM THE CERRO FORTALEZA FORMATION 70
INTRODUCTION 70
GEOLOGICAL SUMMARY 72
METHODS AND MATERIALS 73
SYSTEMATIC PALEOBOTANY 76
DISCUSSION 99
CONCLUSIONS 106
CHAPTER 3: ANGIOSPERM WOOD FROM THE CERRO FORTALEZA FORMATION 125
INTRODUCTION 125
METHODS AND MATERIALS 126
SYSTEMATIC PALEOBOTANY 128
DISCUSSION 135

CONCLUSIONS 140
CHAPTER 4: NEONATAL TEETH IN DIRECT ASSOCIATION WITH A MATURE *TALENKAUEN SANTACRUCENSIS* 155
INTRODUCTION 155
MATERIAL 157
DESCRIPTION 158
DISCUSSION 158
CONCLUSIONS 161
CHAPTER 5: ASSOCIATED SHARK VERTEBRAE FROM THE CRETACEOUS-PALEOGENE BOUNDARY OF NEW JERSEY 165
INTRODUCTION 165
GEOLOGICAL BACKGROUND 166
METHODS 168
DESCRIPTION 170
RESULTS 171
DISCUSSION 172
CONCLUSIONS 173
REFERENCES 182
APPENDIX A: FOSSIL GYMNOSPERM WOOD SAMPLE DESCRIPTIONS AND PLATES 203
APPENDIX B: FOSSIL ANGIOSPERM WOOD SAMPLE DESCRIPTIONS AND PLATES 238
APPENDIX C: ELASMOBRANCH VERTEBRAL MEASUREMENTS. 249
VITAE 253

LIST OF TABLES

Table 1.1. Summary of the nomenclature and age of dinosaur-bearing Upper Cretaceous sediments that crop out on Cerro Fortaleza……...……66

Table 2.1. Anatomical features in the fossil wood from the Cerro Fortaleza Formation ……..112

Table 3.1. Anatomical Features of angiosperm wood from the Cerro Fortaleza Formation……..145

Table 3.2. Comparison of *Hedycaryoxylon* species modified from Poole and Gottwald (2001)…….…….. 149

LIST OF FIGURES

Figure 1.1. Southern Patagonian region of South America. Large inset Figure 1.3. Goggle Maps 2011. 55

Figure 1.2. Austral Basin. Redrawn from Nullo (1999). 56

Figure 1.3. The study region. Triangles indicate hills (cerros) and circles indicate named locations. The location for Lote 119 was based on general area descriptions from Fergulio (1938a, 1944). Inset is Figure 1.4. Google Maps 2011. 57

Figure 1.4. Río La Leona Valley. Major rivers (rios), streams (arroyos), hills (cerros, indicated by triangles) and other notable locations are identified. Note that the Estancia Irene location is based on the description from Macellari et al. (1989). Google Maps 2011..... 58

Figure 1.5. Paleogeography reconstructions showing southern South America for the: a. Middle Jurassic, b. Late Jurassic, c. Early Cretaceous, and d. and Late Cretaceous (Blakey, 2008)..... 59

Figure 1.6. Paleogeographic maps of the Patagonian basins during the mid-late Cretaceous. a. Late Jurassic (Kimmeridgian-Tithonian). b. Early Cretaceous (Valanginian-Hauterivian). c. Early Cretaceous (Aptian). d. Early Cretaceous (Albian). e. Late Cretaceous (Cenomanian-Turonian). f. Late Cretaceous (Campanian-Maastrichtian) (after Spalletti and Franzese, 2007). 60

Figure 1.7. Geological map of Patagonia produced by Charles Darwin, circa 1840, unpublished (Cambridge University Library)..... 61

Figure 1.8. Stratigraphy of the Río Shehuen Valley. The schematic is based on both the text and figure information provided by the cited authors. If the text and figure information differ (e.g. Arbe, 1987) priority is given to the text. If multiple localities are given (e.g., Arbe 1987), a general column was created. Wavy horizontal lines indicates unconformities and dashed lines indicate paraconformities. 62

Figure 1.9. Stratigraphy column of the Río La Leona Valley and partly Lago Argentino. The schematic is based on both the text and figure information provided by the cited authors. If the text and figure information differ (e.g. Arbe, 1987) priority is given to the text. If multiple localities are given (e.g., Arbe 1987), a general column was created. Wavy horizontal lines indicates unconformities and dashed lines indicate paraconformities. 63

Figure 1.10. Paleoenvironments of the Austral Basin during the Late Cretaceous (after, Arbe, 2002). 64

Figure 1.11. Paleogeographic reconstructions of the Austral Basin during the Campanian and Maastrichtian (from, Macellari et al., 1989). 65

Figure 2.1. Map of the southern Patagonia showing the region surrounding Cerro Fortalela. Inset in upper map is Figure 2.2. 107

Figure 2.2. Map of the study region showing the three collection areas. 108

Figure 2.3. Map of the northern collection locality. The numbers correspond to the MPM numbers. The red circles are gymnosperm wood while the white triangles are angiosperm wood. The blue square represents the titanosaur dinosaur quarry. 109

Figure 2.4. Map of the two southern localities (western and eastern) where samples were collected. The numbers correspond to the MPM numbers. The red cicles indicate gymnosperm wood while the white triangles indicate angiosperm wood. 110

Figure 2.5. Pictures showing the variation in the size of fossilized wood in the field. a. MPM-11; scale bar=10 cm. b. MPM-16. c. MPM-19; rock hammer length = 33cm. 111

Figure 2.6. *Agathoxylon* sp. a. TS showing growth rings and a frost ring (arrow). MPM-32, scale bar = 2.5 mm. b. TS showing growth rings (arrow). MPM-23, scale bar = 250 µm. c. RLS showing araucarian uniseriate and alternate biseriate (arrow) pitting. MPM-23, scale bar = 250 µm. d, e, f. RLS showing araucarioid cross-field pits (arrows). MPM-23(d), MPM-32(e), MPM-32(f), scale bars = 50 µm. g. TLS showing uniseriate and biseriate (arrow) rays. MPM-21, scale bar = 50 µm. h. TLS showing long uniseriate rays. MPM-23, scale bar = 250 µm. 117

Figure 2.7. *Planoxylon* sp. MPM-9. a. TS showing growth rings, scale bar = 2.5 mm. b. TS showing growth rings and false rings (arrow), scale bar = 250 µm. c. RLS showing rays and uniseriate bordered pitting (arrow), scale bar = 100 µm. d. RLS showing rare, alternate biseriate tracheid pitting, scale bar = 50 µm. e. RLS showing rounded (piceoid) cross-field pitting (arrow), scale bar = 25 µm. f. RLS showing obliquely angled, slit-like (cupressoid) cross-field pitting (arrow), scale bar = 50 µm. g, h. RLS and TLS showing abietineentüpfelungen (arrows) in the ray cells, scale bars = 25 µm (g) and 50 µm (h). i. TLS showing bordered pits (upper arrow) and uniseriate and biseriate (lower arrow) rays, scale bar = 100 µm. 118

Figure 2.8. *Cupressinoxylon* sp. MPM-26b. a. TS showing growth rings, scale bar = 2.5 mm. b. TS showing growth rings, scale bar = 500 µm. c. RLS showing abietinean

pitting and rays, scale bar = 250 µm. d, e. RLS showing cupressoid cross-field pits (arrow), scale bar = 100 µm. f. TLS showing uniseriate rays (arrow), scale bar = 250 µm. g. TLS showing uniseriate rays, scale bar = 100 µm. 119

Figure 2.9. *Taxodioxylon* sp. 1. a. TS showing growth rings and false ring (arrow). MPM-15, scale bar = 250 µm. b. TS showing pith and growth rings. MPM-18, scale bar = 2.5 mm. c. RLS showing abietinean pitting (arrow) and rays. MPM-15, scale bar = 250 µm. d. RLS showing small, obliquely angled taxodioid cross-field pits (arrow). MPM-15, scale bar = 100 µm. e. RLS showing alternate and opposite biseriate bordered pitting. MPM-15, scale bar = 50 µm. f. TLS showing pitting on an axial parenchyma (arrow). MPM-15, scale bar = 50 µm. g. TLS showing beading on the end walls of the axial parenchyma (arrow). MPM-18, scale bar = 50 µm. h. TLS showing uniseriate tangential rays. MPM-15, scale bar = 250 µm. 120

Figure 2.10. *Taxodioxylon* sp. 2. MPM-11b. a. TS showing growth rings, scale bar = 2.5 mm. b. TS showing growth rings (arrow), scale bar = 250 µm. c. RLS showing abietinean pitting (arrow) and rays, scale bar = 250 µm. d. RLS showing possible xenoxylon bordered pitting on the tracheid walls (arrow), scale bar = 50 µm. e. TLS showing beading on the end walls of the axial parenchyma (arrow), scale bar = 25 µm. f. RLS showing small, obliquely angled taxodioid cross-field pits (arrows), scale bar = 50 µm. g. TLS showing tangential uniseriate rays, scale bar = 250 µm. h. TLS showing uniseriate and biseriate (arrow) tangential rays, scale bar = 100 µm. 121

Figure 2.11. *Podocarpoxylon* sp. a. TS showing growth rings. MPM-30, scale bar = 2.5 mm. b. TS showing axial parenchyma (lower arrow) and a false ring (upper arrow) just after a true growth ring. MPM-30, scale bar = 250 µm. c. RLS showing abietinean pitting (arrow) on the radial wall of the tracheids. MPM-25, scale bar = 200 µm. d. RLS showing cross-field pits (arrow) and spiral checking in the tracheid walls. MPM-30, scale bar = 50 µm. e, f. RLS showing podocarpoid cross-field pitting (arrow). MPM-31(e), MPM-25 (f), scale bar = 50 µm. g. TLS showing uniseriate rays. MPM-25, scale bar = 250 µm. h. TLS showing a rare biseriate ray (arrow). MPM-25, scale bar = 100 µm. .. 122

Figure 2.12. Gymnosperm indet. a. TS showing growth rings. MPM-22, scale bar = 2.5 mm. b. TS showing growth rings including false rings (lower arrow) and diffuse axial parenchyma (upper arrow). MPM-22, scale bar = 250 µm. c. RLS showing poorly preserved ray parenchyma. MPM-1, scale bar = 100 µm. d, e. RLS showing taxodioid cross-field pits (arrows). MPM-1, scale bars = 50 µm (d) and 25 µm (e). f. TLS showing rays and resin-filled parenchyma. MPM-1, scale bar = 50 µm. g. TLS showing very short rays. MPM-7, scale bar = 100 µm. h. TLS showing possible organic crystal deposit (arrow). MPM-7, scale bar = 50 µm. 123

Figure 2.13. Percentages of gymnosperm wood from the Cerro Fortaleza Formation. a. Percentage of gymnosperm wood to angiosperm wood. b. Percentage of each gymnosperm morphogenera to the overall percentage of wood collected from the Cerro Fortaleza Formation. c. Percentage of each gymnosperm morphogenera. 124

Figure 3.1. Map of the Patagonia region of South America and the study region (large inset). The inset in the upper map is Figure 3.2. 141

Figure 3.2. A map showing the region under study and the three fossil wood sites: northern, southwestern and southeastern. Only the northern (Figure 3.3) and southwestern sites (Figure 3.4) yielded permineralizaed angiosperm wood. 142

Figure 3.3. A map showing the northern site. The red circles indicate where fossil wood samples of angiosperms were collected,while the white triangles indicate where fossil wood samples of gymnosperms were collected. The blue square shows the relationship of the fossil wood collected to a titanosaur quarry. 143

Figure 3.4. A map showing the soutwestern sites. The red circles indicate where fossil wood samples of angiosperms were collected, while the white triangles indicate where fossil wood samples of gymnosperms were collected. 144

Figure 3.5. Field photographs of the angiosperm fossil wood from the Cerro Fortaleza Formation. a. MPM-13 *Hedycaryoxylon sp. A* (holotype). b. MPM-12 *Hedycaryoxylon sp. A.* c. MPM-20 *Hedycaryoxylon sp. A.* d. MPM-24 *Hedycaryoxylon sp. A.* e. MPM-26 *Nothofagoxylon corrugatus*. 148

Figure 3.6. *Hedycaryoxylon* sp. A. a. TS with growth rings (arrow). MPM-12; scale bar = 2.5 mm. b. TS showing diffuse porous wood; scale bar = 250 µm. c. RLS showing scalariform perforation plates; scale bar = 100 µm. d, e. RLS showing oval to scalariform vessel-ray pits; scale bars = 50 µm. f. TLS showing scalariform intervessel pitting (arrow); scale bar = 100 µm. g. TLS showing ground fiber with minute bordered pitting; scale bar = 50 µm. h. TLS showing septate fibers (upper arrow) and sheath cell (lower arrow); scale bar = 100 µm. i. TLS showing multiseriate rays and sheath cells (arrow) scale bar = 250 µm. j. RLS showing procumbent, square and upright cells; scale bar = 250 µm. b-j, MPM-13 (holotype). 152

Figure 3.7. *Nothofagoxylon corrugatus*. MPM-26. a. TS showing one faint growth ring (arrow); scale bar = 2.5 mm. b. TS showing diffuse porous wood, solitary vessels, tyloses (arrow) and undulating region; scale bar = 250 µm. c. RLS showing scalariform perforation plate; scale bar = 100 µm. d. RLS showing simple perforation plate; scale bar = 100 µm. e. TLS showing scalariform intervessel pitting; scale bar = 100 µm. f. RLS showing simple vessel-ray pitting (arrow); scale bar = 100 µm. g. RLS showing ground

fiber with minute bordered pitting; scale bar = 100 µm. h. TLS showing rays (lower arrow) and tyloses (upper arrow); scale bar = 250 µm. i. RLS showing cellular composition of ray; scale bar = 250 µm. 153

Figure 3.8. The percentages of angiosperm wood from the Cerro Fortaleza Formation. a. Percentage of angiosperm wood to gymnosperm wood. b. Percentage of each angiosperm morphogenera to the overall percentage of wood collected from the Cerro Fortaleza Formation. c. Percentage of each angiosperm morphogenera. 154

Figure 4.1. MPM-10001. a. Partially articulated body block of *Talenkauen santacrucensis.* b. Reconstruction of *T. santacrucensis* (Novas et al., 2004)..... 162

Figure 4.2. MPM-10001 neonatal teeth. a. Labial view of tooth 1; scale bar = 500 µm. b. Lingual view of tooth 1; scale bar = 500 µm. c. Medial view of lingual surface of tooth 2; scale bar = 200 µm. d. Occlusional view of tooth 2; scale bar = 200 µm. e. Microwear on labial surface of crown of tooth 2; scale bar = 100 µm. 163

Figure 4.3. MPM-10001 left dentary in lateral view (above) and medial view (below). Scale bar equals 5 cm..... 164

Figure 5.1. Shark vertebrae (NJSM 21876) from the Hornerstown Formation..... 175

Figure 5.2. Map of field jacket containing NJSM 21876 and the location of individual vertebrae. Note that some sediment shifting occurred during transport. 176

Figure 5.3. A typical centrum of NJSM 21876 indicating where measurements were taken. DVD, dorsoventral diameter; TD, lateral diameter; CCL, craniocaudal length; and LL lateral length. Scale bar = 10 mm. 177

Figure 5.4. X-ray (left) and the inverse image (right) of a centrum of NJSM 21876. Arrows are pointing to growth lines. Scale bar = 10 mm. 178

Figure 5.5. Linear regression lines of vertebral measurements from NJSM 21876. 179

Figure 5.6. Linear regression lines from NJSM 21786 of vertebral measurements greater than 17.54 mm. 180

Figure 5.7. Map of jacket containing NJSM 21786. Shaded area represents the only significant grouping (p-value <0.001). 181

Figure A.1. Agathoxylon sp. MPM-8. a. TS showing growth rings, scale bar = 250 µm. b. RLS showing araucarian bordered pitting on the tracheids, scale bar = 250 µm. c. RLS showing araucarioid tracheid uniseriate bordered pits, scale bar = 100 µm. d. RLS

showing araucarioid cross-field pits (left arrow) and araucarian bordered pitting (right arrow), scale bar = 50 µm. e, f. TLS showing short, uniseriate rays (arrow), scale bars = 100 µm (e) and 50 µm (f). 218

Figure A.2. *Agathoxylon* sp. MPM-21. a. TS showing growth rings, scales bar = 2.5 mm. b. TS showing growth rings and tracheids, scale bar = 250 µm (b). c. RLS showing uniseriate bordered pits on the radial walls of the tracheids (arrow), scale bar = 100 µm. d. RLS showing araucarioid cross-field pits (arrow), scale bar = 50 µm. e. TLS showing uniseriate and biseriate rays, scale bar = 250 µm. f. TLS showing uniseriate and biseriate rays (arrow), scale bar = 100 µm. 219

Figure A.3. *Agathoxylon* sp. MPM-23. a. TS showing growth rings, scale bar = 2.5 mm. b. TS showing false rings (arrow), scale bar = 250 µm. c. RLS showing araucarian uniseriate and alternate biseriate pitting (arrow), scale bar = 250 µm. d. RLS showing araucarioid cross-field pits (arrow), scale bar = 100 µm. e, f. TLS showing tangential rays, scale bars = 250 µm (e) and 100 µm (f). 220

Figure A.4. *Agathoxylon* sp. MPM-32. a. TS showing growth rings and frost rings (arrow), scale bar = 2.5 mm. b. TS showing growth rings and frost ring, scale bar = 250 µm. c. RLS with uniseriate (arrow) and biseriate alternate pitting on the tracheid walls, scale bar = 100 µm. d. RLS with the arrow pointing to araucarioid cross-field pitting, scale bar = 100 µm. e. TLS showing predominantly uniseriate rays, scale bar = 250 µm. f. TLS showing uniseriate rays and pitting on tangential wall of some tracheids, scale bar = 100 µm. 221

Figure A.5. *Planoxylon* sp. MPM-9. a. TS showing growth rings, scale bar = 2.5 mm. b. TS showing growth rings and false rings (arrow), scale bar = 250 µm. c. RLS showing rays and uniseriate bordered pitting (arrow), scale bar = 100 µm. d. RLS showing rare, alternate biseriate tracheid pitting, scale bar = 50 µm. e. RLS showing rounded (piceoid) cross-field pitting (arrow), scale bar = 25 µm. f. RLS showing obliquely angled, slit-like (cupressoid) cross-field pitting (arrow), scale bar = 50 µm. g, h. RLS and TLS showing abietineentüpfelungen (arrows) in the ray cells, scale bars = 25 µm (g) and 50 µm (h). i. TLS showing bordered pits (upper arrow) and uniseriate and biseriate (lower arrow) rays, scale bar = 100 µm. 222

Figure A.6. *Cupressinoxylon* sp. MPM-26b. a. TS showing growth rings, scale bar = 2.5 mm. b. TS showing growth rings, scale bar = 500 µm. c. RLS showing abietinean pitting and rays, scale bar = 250 µm. d, e. RLS showing cupressoid cross-field pits (arrow), scale bar = 100 µm. f. TLS showing uniseriate rays (arrow), scale bar = 250 µm. g. TLS showing uniseriate rays, scale bar = 100 µm. 223

Figure A.7. Taxodioxylon sp. 1. MPM-10. a. TS showing growth rings, scale bar = 2.5 mm. b. TS showing growth rings and possible false ring, scale bar = 250 µm. c. TS showing diffuse axial parenchyma (arrow) in earlywood, scale bar = 250 µm. d. RLS showing bordered pitting of the tracheid wall (arrow) and rays, scale bar = 100 µm. e, f. RLS showing taxodioid-cupressoid cross-field pitting (arrow), scale bars = 50 µm. g. TLS showing uniseriate rays, scale bar = 250 µm. 224

Figure A.8. *Taxodioxylon* sp. 1. MPM-15. a. TS showing growth rings, scale bar = 2.5 mm. b. TS showing growth rings (lower arrow) and false ring (upper arrow), scale bar = 250 µm. c. RLS showing abietinean pitting (arrow) and rays, scale bar = 250 µm. d. RLS showing small, obliquely angled taxodioid cross-field pits (arrow), scale bar = 100 µm. e. RLS showing alternate and opposite biseriate bordered pitting, scale bar = 50 µm. f. TLS showing pitting on an axial parenchyma (arrow), scale bar = 50 µm. g. TLS showing uniseriate tangential rays, scale bar = 250 µm. 225

Figure A.9. *Taxodioxylon* sp. 1. MPM-16. a. TS showing growth rings, scale bar = 2.5 mm. b. TS showing growth rings (arrow), scale bar = 250 µm. c. TS showing wound wood (?), scale bar = 250 µm. d. RLS showing abietinean bordered pitting (arrow) on the tracheid walls, scale bar = 250 µm. e, f. RLS showing cross-field pitting (arrow), scale bars = 50 µm (e) and 100 µm (f). g. TLS showing uniseriate tangential rays, scale bar = 250 µm. 226

Figure A.10. *Taxodioxylon* sp. 1. MPM-18. a. TS showing pith and growth rings, scale bar = 2.5 mm. b. TS showing growth rings, false ring, and diffuse axial parenchyma (arrow), scale bar = 250 µm. c. RLS showing rays (arrow), scale bar = 250 µm. d. RLS showing cross-fields with taxodioid cross-field pits (arrow), scale bar = 100 µm. e. TLS showing short rays, scale bar = 250 µm. f. TLS showing beading on the end walls of the axial parenchyma (arrow), scale bar = 50 µm. 227

Figure A.11. *Taxodioxylon* sp. 2. MPM-11b. a. TS showing growth rings, scale bar = 2.5 mm. b. TS showing growth rings (arrow), scale bar = 250 µm. c. RLS showing abietinean pitting (arrow) and rays, scale bar = 250 µm. d. RLS showing possible xenoxylon bordered pitting on the tracheid walls (arrow), scale bar = 50 µm. e. TLS showing beading on the end walls of the axial parenchyma (arrow), scale bar = 25 µm. f. RLS showing small, obliquely angled taxodioid cross-field pits (arrows), scale bar = 50 µm. g. TLS showing tangential uniseriate rays, scale bar = 250 µm. h. TLS showing uniseriate and biseriate (arrow) tangential rays, scale bar = 100 µm. 228

Figure A.12. *Podocarpoxylon* sp. MPM-6. a. TS showing growth rings, scale bar = 2.5 mm. b. TS showing growth ring, scale bar = 250 µm. c. TS showing axial parenchyma, scale bar = 250 µm. d. RLS showing rays and tracheid bordered pitting, scale bar = 250

µm. e. RLS showing uniseriate abietinean pitting on the tracheid walls (arrow), scale bar = 100 µm. f. RLS showing podocarpoid cross-field pits (arrow), scale bar = 50 µm. g. TLS showing uniseriate rays, scale bar = 250 µm. 229

Figure A.13. *Podocarpoxylon* sp. MPM-11a. a. TS showing growth rings, scale bar = 2.5mm. b. TS showing growth rings and axial parenchyma, scale bar = 250 µm. c. RLS showing abietinean bordered pitting (arrow) and rays, scale bar = 250 µm. d. RLS showing podocarpoid-cupressoid cross-field pits (arrow), scale bar = 100 µm. e. TLS showing uniseriate rays, scale bar = 250 µm. f. TLS showing a biseriate ray (arrow), scale bar = 100 µm. 230

Figure A.14. *Podocarpoxylon* sp. MPM-25. a. TS showing growth rings, scale bar = 2.5 mm. b. TS showing a growth ring and axial parenchyma (arrow), scale bar = 250 µm. c. RLS showing abietinean pitting (arrow) on the radial wall of the tracheids, scale bar = 200 µm. d. RLS showing narrow slit-like podocarpoid cross-field pitting (arrow), scale bar = 100 µm. e. TLS showing uniseriate rays, scale bar = 250 µm. f. TLS showing uniseriate rays, scale bar = 100 µm..... 231

Figure A.15. *Podocarpoxylon* sp. MPM-30. a. TS showing growth rings, scale bar = 2.5 mm. b. TS showing a false ring just after a true growth ring (arrow), scale bar = 250 µm. c. RLS showing spiral checking (arrow) in the tracheid walls, scale bar = 100 µm. d. RLS showing abietinean pitting and silt-like podocarpoid cross-field pitting (arrow), scale bar = 100 µm. e, f. TLS showing tangential rays, scale bar = 250 µm (e) and 100 µm (f). . 232

Figure A.16. *Podocarpoxylon* sp. MPM-31. a. TS showing growth ring, scale bar = 2.5 mm. b. TS showing growth ring (arrow), scale bar = 250 µm. c. RLS showing abietinean uniseriate pitting on the tracheids (arrow), scale bar = 100 µm. d, e. RLS showing podocarpoid cross-field pitting (arrows), scale bars = 100 µm. f, g. TLS showing uniseriate rays, scale bars = 250 µm (f) and 100 µm (g). 233

Figure A.17. Gymnosperm indet. MPM-1. a. TS showing growth rings, scale bar = 2.5mm. b. TS showing diffuse axial parenchyma, scale bar = 250 µm. c. RLS showing rays, scale bar = 100 µm. d, e. RLS showing taxodioid cross-field pits, scale bars = 50 µm. f., g. TLS showing short, uniseriate rays, scale bars = 100 µm (f) and 50 µm (g).. 234

Figure A.18. Gymnosperm indet. MPM-7. a. TS showing growth rings, scale bar = 2.5 mm. b. TS showing growth ring and diffuse axial parenchyma, scale bar = 250 µm. c. RLS showing rays, scale bar = 250 µm. d. RLS showing rays and taxodioid cross-field pits (arrow), scale bar = 50 µm. e. TLS showing short tangential rays, scale bar = 100 µm. f. TLS showing possible organic crystal deposit, scale bar = 25 µm. 235

Figure A.19. Gymnosperm indet. MPM-19. a. TS showing growth rings, scale bar = 2.5 mm. b. TS showing growth rings and diffuse axial parenchyma (arrow), scale bar = 250 µm. c. RLS showing rays and possible cross-field pits, scale bar = 250 µm. d. RLS showing rays and possible cross-field pits (arrow), scale bar = 50 µm. e. TLS showing tangential rays, scale bar = 250 µm. f. TLS showing axial parenchyma and rays, scale bar = 100 µm. 236

Figure A.20. Gymnosperm indet. MPM-22. a. TS showing growth rings, scale bar = 2.5mm. b. TS showing growth rings including false rings (upper arrow) and diffuse axial parenchyma (lower arrow), scale bar = 250 µm. c. TLS showing axial parenchyma with smooth end walls, scale bar = 100 µm. d. RLS showing rays, scale bar = 100 µm. e, f. RLS showing possible taxodioid cross-field pits, scale bars = 50 µm. g. TLS showing short, uniseriate rays, scale bar = 100 µm. 237

Figure B.1. *Hedycaryoxylon* sp. A. MPM-13. a. TS showing diffuse porous wood; scale bar = 2.5 mm. b. TS showing diffuse porous wood; scale bar = 250 µm. c. RLS showing scalariform perforation plates; scale bar = 100 µm. d, e. RLS showing oval to scalariform vessel-ray pits; scale bars = 50 µm. f. TLS showing scalariform intervessel pitting (arrow); scale bar = 100 µm. g. TLS showing ground fiber with minute bordered pitting; scale bar = 50 µm. h. TLS showing septate fibers (upper arrow) and sheath cell (lower arrow); scale bar = 100 µm. i. TLS showing multiseriate rays and sheath cells (arrow) scale bar = 250 µm. j. RLS showing procumbent, square and upright cells; scale bar = 250 µm. 244

Figure B.2. *Hedycaryoxylon* sp. A. MPM-12. a. TS showing growth rings (arrow) and diffuse porous wood; scale bar = 2.5 mm. b. TS showing diffuse porous wood and crushed vessels; scale bar = 250 µm. c. RLS showing scalariform perforation plate; scale bar = 100 µm. d. RLS showing oval to scalariform vessel-ray pits (arrow); scale bar = 50 µm. e. TLS showing scalariform intervessel pitting (arrow); scale bar = 50 µm. f. TLS showing ground fiber with minute bordered pitting (arrow); scale bar = 50 µm. g. TLS showing septate fibers (arrow); scale bar = 50 µm. h. TLS showing multiseriate rays; scale bar = 250 µm. i. RLS showing rays with procumbent, square and upright cells; scale bar = 100 µm. 245

Figure B.3. *Hedycaryoxylon* sp. A. MPM-20. a. TS with growth rings (arrow); scale bar = 2.5 mm. b. TS showing diffuse porous wood, thickened fibers at growth rings, solitary and rarely paired vessels; scale bar = 250 µm. c. RLS showing scalariform perforation plate and fibers with bordered pitting (arrow), scale bar = 50 µm. d. TLS showing scalariform intervessel pitting (arrow); scale bar = 50 µm. e. RLS showing simple vessel-ray pitting; scale bar = 50 µm. f. TLS showing septate fibers (arrow); scale bar =

100 µm. g. TLS showing multiseriate rays; scale bar = 250 µm. h. RLS showing cellular composition of rays; scale bar = 250 µm. 246

Figure B. 4. *Hedycaryoxylon* sp. A. MPM-24. a. TS with growth rings; scale bar = 2.5 mm. b. TS showing a growth ring, diffuse porous wood and tyloses (arrow); scale bar = 250 µm. TS showing diffuse porous wood and vessel cluster (arrow), scale bar = 250 µm. d. RLS showing scalariform perforation plates, scale bar = 50 µm. e. RLS showing simple vessel-ray pitting, scale bar = 100 µm. f. TLS showing scalariform intervessel pitting, scale bar = 50 µm. g. TLS showing fiber with bordered pitting, scale bar = 25 µm. h. TLS showing septate fibers (arrow), scale bar = 100 µm. i. TLS showing multiserate rays and fiber dissecting ray (arrow), scale bar = 250 µm. j. RLS showing procumbent (lower arrow) and upright (upper arrow) ray cells, scale bar = 100 µm. 247

Abstract

The Geology, Paleontology and Paleoecology of the Cerro Fortaleza Formation, Patagonia (Argentina)

Victoria M. Egerton

The Cerro Fortaleza Formation, in southern-most Patagonia (Argentina), contains a unique flora and fauna from the Late Cretaceous (Campanian). This study is the first to assess, analyze and interpret the paleobotany of the Cerro Fortaleza Formation. Twenty-five fossil wood samples have been collected, thin-sectioned and studied. Gymnosperm morphogenera identified in this study include: *Agathoxylon*, *Planoxylon*, *Taxodioxylon*, *Cupressinoxylon* and *Podocarpoxylon*. This is the first record of *Planoxylon*, *Taxodioxylon* and possibly *Cupressinoxylon* from Argentina. The gymnosperm wood samples all possess distinct growth rings, providing strong evidence for seasonal growth regimes in the region. Additionally, two morphogenera of angiosperm wood, *Hedycaryoxylon* and *Nothofagoxylon*, have also been identified for the first time in Argentina. Of these, a new morphospecies of angiosperm wood is described. All wood morphogenera from the Cerro Fortaleza Formation, except *Planoxylon*, have also been described from Late Cretaceous sediments of the Antarctic Peninsula. Thus, the presence of these taxa in both regions supports Late Cretaceous plant dispersal between them. Despite sharing the same taxa, the floras from the Cerro Fortaleza Formation and the Antarctic Peninsula exhibit strikingly different relative abundances. The relative abundance of gymnosperm to angiosperm wood in the Cerro Fortaleza Formation is 75:25; whereas, coeval floras from the Antarctic Peninsula are ~25:75. This floristic

difference could be a function of regional floristic differences or a result of different depositional and/or preservational environments.

In addition to the flora, minute dinosaur teeth and bone fragments from the Cerro Fortaleza Formation are also described. This material was discovered during the preparation of the holotype of a medium-sized ornithopod, *Talenkauen santacrucensis* (MPM-10001). The tooth crowns are 1 mm in apicobasal height and 1.7 mm in mesiodistal width. The morphology, size and wear of the teeth and the small bone fragments suggest that the fossils were from a neonatal *T. santacrucensis.* This is the first record of neonatal ornithopod remains from South America. In conclusion, the work undertaken here will provide important floral and faunal data for future studies on the evolution of the Austral Basin.

CHAPTER 1: LATE CRETACEOUS GEOLOGY OF THE NORTHERN AUSTRAL BASIN WITH EMPHASIS ON THE CERRO FORTALEZA FORMATION

INTRODUCTION

The Patagonian region of South America has long fascinated explorers and scientists (Figure 1.1). Its rugged terrain and poorly charted geography have sustained a constant stream of research in this region. The geology of Patagonia has been studied since 1834 when Charles Darwin followed the Río Santa Cruz to try to discover its source (Darwin, 1833-1834, 1846). Despite this long history, the geology of the region is still relatively unclear.

The separation of Gondwana and the uplift of the Andes led to the contortion of the rocks of the region such that the geology of many areas is still ambiguous. One of these regions is the north-central portion of the Austral Basin. The Austral Basin was one of the major basins of Patagonia during the Cretaceous and has been posited to be the largest depocenter in Patagonia (Spalletti and Franzese, 2007). The basin spans most of the Santa Cruz and Tierra del Fuego provinces of Argentina (Figure 1.2). Within the Austral Basin is the Río La Leona Valley in the Santa Cruz Province. The Río La Leona flows southward from the southeastern shore of Lago Viedma to Lago Argentino (Figures 1.3, 1.4). The geology of this area has been studied since 1892; however, the interpretation and age of the sediments exposed here is still debated.

The stratigraphy of the rocks of this region is essential to understanding the paleobiogeographic relationship between South America and Antarctica during the Late Cretaceous. Throughout the Cretaceous, South America and the Antarctic Peninsula shared a continental-continental plate boundary. It is not clear whether this connection was subaerial, covered by an epeiric sea, or whether it alternated between these states. Limited terrestrial vertebrate data is available from Antarctica to examine the paleobiogeographic relationship between South America and Antarctica during the Late Cretaceous (Cambiaso et al., 2002; Case et al., 2000; Case et al., 2007; Crame et al., 2004; Crame et al., 1991; Gasparini et al., 1987; Hooker et al., 1991; Molnar et al., 1996). However, fossil wood spans both of these locations and provides a potentially useful tool for understanding vertebrate paleoenvironments and paleobiogeography.

The Cerro Fortaleza Formation, located in the Río La Leona Valley, contains both well-preserved silicified wood and dinosaur fossils. Additionally, many other fossil faunal elements are preserved in this formation, making the Cerro Fortaleza Formation an essential unit for deciphering the Cretaceous paleoenvironments of southern Patagonia. However, the literature for the Cerro Fortaleza Formation contains contradicting names, ages and interpretations. Before the paleontology of the formation is discussed (Chapters 2, 3 and 4), the name, age and geology of the Cerro Fortaleza Formation must be defined. In this chapter I discuss the break-up of Gondwana, the formation and evolution of the Austral Basin and the major geological formations surrounding Lagos Viedma and Argentino, with particular emphasis on the Cerro Fortaleza Formation.

Separation of Gondwana

Antarctica can be described as the keystone of the Gondwanan super-continent during the Mesozoic. Connections among the southern continents, Arabia and India allowed for biotic pathways for both flora and fauna. This, consequently, led to closely related Gondwanan biota (e.g., Chatterjee and Scotese, 1999; Cracraft, 2001; Gheerbrant and Rage, 2006; Hay et al., 1999; Kleinschmidt, 2007; Parrish, 1990; Sanmartín and Ronquist, 2004; Scher and Martin, 2006; Spalletti and Franzese, 2007; Upchurch, 2008). This southern landmass was separated by its northern counterpart, Laurasia, by an equatorial seaway, the Tethys.

The separation of the Gondwanan landmasses began during the Middle Jurassic (ca. 183-177 Ma) (Eagles and König, 2008) (Figure 1.5a). Southwest rotation of East Gondwana (Australia, Antarctica, India, and southern Africa) from West Gondwana (northern Africa, Arabia, and South America) resulted in rifting between Australia and India and between Australia and Antarctica (Eagles and König, 2008; Li and Powell, 2001). Continental extension along the Kenya-Somali coastline resulted in Madagascar and India moving southeast away from Africa (Hay et al., 1999; Li and Powell, 2001; Veevers, 2004). To the west, extensional tectonics led to the opening of the Weddell Sea, initiating the separation of South America, Antarctica, and Africa. The southeastern-most Patagonian basin, the Austral (Magellanes) Basin, formed ~150 Ma from an influx of Pacific waters along the western and southwestern margins of the newly formed Andean volcanic arc and from the growing Weddell Sea. Further expansion of this region initiated the opening of the southern Atlantic Ocean (Figure 1.5b) (Spalletti and Franzese, 2007).

By the beginning of the Early Cretaceous (145.5-99.6 Ma), rifting had resulted in the arrangement of four continental blocks: India-Madagascar, Australia-Antarctica, Africa-Arabia, and South America (Figure 1.5c) (Li and Powell, 2001; Veevers, 2004). Loose terrestrial connections still occurred among these landmasses; however, they would have been heavily influenced by sea level. Rifting between Australia and India (132 Ma) resulted in the opening of the Indian Ocean. Rotation of the India-Madagascar block continued until ~114 Ma, at which point movement between Africa and Madagascar stopped and seafloor spreading continued to widen the Indian Ocean (Li and Powell, 2001; Veevers, 2004). Australia slowly rifted from Antarctica throughout the Cretaceous, thereby creating a shallow seaway between the two continents (Blakey, 2008; Li and Powell, 2001). Uplift of the Andes closed the Pacific Ocean portal and isolated the southern Atlantic Ocean (Spalletti and Franzese, 2007). The Atlantic Ocean spread northward, rifting and parting South America from Africa-Arabia so that, by the mid-Cretaceous, South America and Africa-Arabia were separated, but not necessarily isolated (Blakey, 2008; Li and Powell, 2001).

The Late Cretaceous (99.6-65.5 Ma) was dominated by the opening and closing of major ocean basins (Figure 1.5d). Rotation and northward movement of Africa and Arabia closed the western Tethys Ocean that separated Laurasia and Gondwana (Blakey, 2008; Li and Powell, 2001). The Indian Ocean underwent rapid seafloor spreading, separating Madagascar from India and forcing India northward (Ali and Aitchison, 2008; Li and Powell, 2001). Separation of New Zealand from Australia resulted in the opening of the Tasman Sea. Furthermore, the Atlantic mid-ocean ridge continued to part South America from Africa (Blakey, 2008; Li and Powell, 2001).

The final break-up of Gondwana occurred between Australia-Antarctica and South America-Antarctica during the Cenozoic (65.5-15 Ma). The spreading rate between Australia and Antarctica increased ~45 Ma resulting in separation of the two landmasses by 35 Ma (Blakey, 2008; Li and Powell, 2001). Separation between South America and Antarctica occurred in three phases: 1) opening, 2) narrowing and 3) subsequent re-widening of the Drake Passage (Lagabrielle et al., 2009). The initial opening of the Drake Passage occurred ~37-34 Ma, resulting in the formation of the Antarctic Circumpolar Current (ACC) (Barbeau et al., 2009; Lagabrielle et al., 2009; Scher and Martin, 2006). Subsequent narrowing of the Drake Passage occurred between 29-22 Ma due to competing faults (North and West Scotia faults) and further uplift of Tierra del Fuego. The ACC was able to flow through the Drake Passage during this time; however, there was a substantially decreased flow. The most recent widening of the Drake Passage began ~15 Ma and continues today (Lagabrielle et al., 2009).

Austral Basin Evolution

The Patagonia region of South America extends from Lago Nahuel Huapi (41°S) south to the Straits of Magellan (~53°S) (Riccardi and Rolleri, 1980). This region underwent extensive geographic and geologic transformations during the Mesozoic. The Austral (Magellanes) Basin is the southernmost basin in South America and trends NNW (Biddle et al., 1986) (Figure 1.2). The Austral Basin is bounded by the Deseado Massif to the north, the Scotia Plate to the south, the Río Chico Dorsal of the Dungeness Arch to the east and the Western Andes to the west. From the Jurassic-Neogene, it is postulated

that between 7000-9000 m of sediment was deposited in the Austral Basin (Biddle et al., 1986; Marenssi et al., 2003).

The Austal Basin has undergone three major tectonic events due to the separation of Gondwana: extensional tectonics and uplift; thermal subsidence and the formation of a marginal sea; and the development of a foreland basin to the east of a magmatic arc (Arbe, 1987, 2002; Biddle et al., 1986; Marenssi et al., 2003). Starting in the Triassic and occurring though the Jurassic, extension between the South American and African plates led to a faulted terrain of grabens and half grabens and magmatic intrusion in southern South America. The extensional tectonics and localized cooling of the magmatic bodies led to subsidence of the region (Biddle et al., 1986). Subsequently, the subsidence led to the initial formation of the Austral Basin (~150 Ma). Waters from the Pacific Ocean and Weddell Sea filled the basin. Rifting between South America and Africa led to further expansion of this region and initiated the opening of the southern Atlantic Ocean (Figure 1.6a) (Spalletti and Franzese, 2007).

Uplift of the Andes closed off the conduit between the Pacific Ocean and the Austral Basin by the beginning of the Early Cretaceous (Spalletti and Franzese, 2007). The Atlantic Ocean continued to spread northward, rifting South America from Africa so that, by the mid-Cretaceous, South America and Africa were separated, but not necessarily isolated (Blakey, 2008; Li and Powell, 2001). During the Early Cretaceous, shales and mudstones were predominantly deposited in the Austral Basin. Continental deposits were first laid down during the Aptian in the northwestern-most portion of the basin. Early foreland development occurred during the Albian due to the uplift of the

western volcanic arc and compressional tectonics (Figure 1.6b, c, d) (Spalletti and Franzese, 2007).

During the Late Cretaceous, the Atlantic mid-ocean ridge continued to part South America from Africa (Blakey, 2008; Li and Powell, 2001). Uplift in the southern and western portions of the Austral Basin occurred (Biddle et al., 1986). This led to eastward migration of the foredeep during the Cenomanian-Turonian (Figure 1.6e) (Biddle et al., 1986; Spalletti and Franzese, 2007). To the northwest, further development and progradation of continental and nearshore deposits occurred. Additionally, extensive faulting (strike-slip) along the Shackleton fault system, in what is now Tierra del Fuego, led to an east-west oriented ridge. This ridge divided the Austral Basin and the Weddell Sea (Biddle et al., 1986; Spalletti and Franzese, 2007). During the Campanian-Maastrichtian, the Austral Basin underwent a general regression which allowed for progradation of continental deposits southward (Figure 1.6f) (Spalletti and Franzese, 2007).

Historical Review of Patagonian Geology

Charles Darwin was the first scientist to conduct geological surveys of the Patagonian region of South America (Darwin, 1846). Early exploration of this region had been limited to basic geographical surveys. On April 18, 1834, Robert FitzRoy (1805-1865) disembarked on an expedition up the Río Santa Cruz to reach its source (FitzRoy, 1839). Darwin recorded topographical, geological, and biological observations in his Banda Oriental Notebook (p. 38-103) and created the first geological map of the region (Figure 1.7). On May 1, Darwin collected silicified wood in a Tertiary sandstone

unit containing numerous *Ostrea* sp. He suggested that both sets of fossils were redeposited from an upstream location. The discovery of fossil wood marks the first recorded terrestrial fossil in the region (Darwin, 1833-1834). Four days later, the expedition ceased their westerly direction, just several miles short of Lago Argentino and returned to the *H.M.S. Beagle* (Darwin, 1846; FitzRoy, 1839).

The first systematic geological survey of Patagonia was conducted from 1875-1880 with a second survey conducted from 1890-1895. Francisco Moreno, founder of the Museo de La Plata, initiated these expeditions to explore, describe and collect biological, archeological and paleontological remains for his new museum (Riccardi, 2008). In the later expeditions (1891-1892), Hermann Konrad Burmeister (or Carlos Germán Conrado Burmeister), director of the Museo de Buenos Aires (now Museo Nacional de Buenos Aires), led the team into the Santa Cruz Territory. He produced one of the first generalized descriptions of the Cretaceous geology of the region: the oldest beds belong to the calcareous Guaranítica unit that contains the bivalve *Inoceramus* sp; the overlying unit is described as red and pink sandstones with yellow clays containing "gigantic" dinosaurs; and the youngest unit is characterized by red sandstones, conglomerates, and yellow clays that contain lignite and "enormous" petrified tree trunks (Burmeister, 1892, 1901). One of the primary regions his team explored was around Lagos Argentino and Viedma. While exploring the eastern side of the Río La Leona, Burmeister discovered dinosaur bones and silicified wood at the base of a hill he named Cerro Fortaleza (Figure 1.4) (Burmeister, 1892; Riccardi, 2008). The fossil bones were preliminarily identified as "Iguanodontid" based on the shape and size of the bones. The diameter of some bones was recorded to be approximately 10-12 cm; while the femur

measured 33 cm in mid-shaft width (not diameter) and 1.15 m long. The femur was not collected because it was considered to be too weathered (Burmeister, 1892). Rather, Burmeister collected several vertebrae from Cerro Fortaleza and deposited these fossils in the Museo de La Plata. The bones were identified as posterior caudal vertebrae belonging to a sauropod; however, they were too fragmentary to be identified to any known genus (Lydekker, 1893). These vertebrae were later donated to the Museo Nacional de Buenos Aires on January 10, 1918 by a collector, Mr. Teodoro Caillet-Bois (Huene, 1929). Carlos Ameghino identified these bones as those collected by Burmeister from the eastern side of the Río La Leona. The vertebrae were subsequently redescribed and identified by Huene (1929) as belonging to the titanosaur *Argyrosaurus superbus*.

In the late 19th century, vast numbers of fossils were collected by Carlos Ameghino and described by Florentino Ameghino (e.g. Ameghino, 1893, 1898, 1899a, b, 1900, 1906; Podgorny, 2005; Riccardi, 2008). Carlos Ameghino discovered dinosaur bones in the Par Aïk (Pari-Aik) area while exploring this and the Río Shehuen realm (Figure 1.3). The material was discovered in a weathered out portion of a red sandstone unit situated above sediments containing abundant *Ostrea guaranitica* (Ameghino, 1899a, 1906). This suite of rocks was considered to be part of the "Séhuénéen éstage," one of several continental stages of the Upper Cretaceous Guaranítica Formation. The sandstone unit contained both marine and terrestrial fossils including: shark teeth (*Oxyrhina mantelli*, *Scapanorhynchus subulatus*, etc.), bony fishes (*Protosphyraena* sp., *Lepidotes* sp., *Ceratodus* sp., etc.), a vertebra belonging to a mammal the size of *Notostylops* sp., sauropod ("Clasmodosaurus spatula*"*) and theropod dinosaurs ("carnosaur" teeth and "Loncosaurus argentinus*"* the latter is now considered an

ornithopod) (Ameghino, 1898, 1899a, 1906; Coria and Salgado, 1996b; Huene, 1929). Here it is important to note that Florentino Ameghino had long hypothesized that advanced mammals lived during the Cretaceous (Salgado, 2007).

In the late 1930s and well into the 1940s, there was a renewed interest in Patagonian geology. Egidio Feruglio was one of the most influential geologists working in the region. In February and April 1935, Egidio Feruglio, Joaquín Frenguelli and Alejandro Piátnitzky studied both sides of the Río Shehuen, around Piedra Clavada and Mata Amarilla (Figure 1.3). They came to the conclusion that the age of this region ranged from the Turonian to the Danian (Feruglio, 1935; Frenguelli, 1936; Piatnitzky, 1936). Additionally, Feruglio (1935) identified Upper Cretaceous marine deposits and sandstone units that contained abundant fossils in the Lago Argentino region. In 1938 Feruglio published two papers on the geology of the Río Shehuen Valley (including Los/Tres Lagos, Estancia Mata Amarilla and Estancia Pari Aike), the Río La Leona Valley (including the Arroyo Guanaco and Barrancas Blancas) and the region south of Lago Argentino (including Cerro Calafate and Estancia Anita). The first paper (Feruglio, 1938a) described the geology in terms of horizons (e.g. Horizons A, B, C, etc.) while the subsequent paper (Feruglio, 1938b) established distinct names for each of the horizons (e.g., Strata Mata Amarilla, Anita, Pari Aike, etc.). He differentiated the horizons/stratum of the Río Shehuen and Río La Leona valleys from those exposed south of Lago Argentino (Figures 1.3, 1.4). Interestingly, he called explicit sedimentary units "Estrato," or Statum, rather than Formation despite the recommendation of the Argentine Department of Exploration to do the latter (Fossa-Mancini, 1938). The region was described in greater detail with more stratigraphic sections in 1944 (Feruglio, 1944).

Additionally, Feruglio applied the term “Estratos con Dinosaurios” in conjunction with named strata that contain dinosaur bones (i.e., “Estratos del Chorrillo o Estratos con Dinosaurios” and “Estratos del Pari Aike o Estratos con Dinosaurios”). This follows how previous authors have identified particular strata in Argentina (e.g., Keidel, 1917; Piatnizky, 1936; Roll, 1936). Thus “Estratos con Dinosaurios” can refer to several formations, depending on the source. The geographical range of the strata can be as far north as the Río Chico, east to Lago San Martín and south to Lago Argentina (Arbe, 2002).

More recent work in the regions around the Río Shehuen, Lago Viedma, Río La Leona and Lago Argentino has led to further understanding of the evolution of the Austral Basin . A review of this literature is organized based on each formation. Controversies regarding the name and age of the Cerro Fortaleza Formation are discussed in that section.

LATE CRETACEOUS REGIONAL GEOLOGY OF THE RÍO SHEHUEN VALLEY AND LAGOS VIEDMA AND ARGENTINO

Mata Amarilla Formation

The Mata Amarilla Formation was first described by Feruglio (1938a). He tentatively named the formation Horizon B (Feruglio, 1938a) but later changed the designation to “Estratos de Mata Amarilla” (Figure 1.8) (Feruglio, 1938b). This stratum was initially described as consisting of 340-350 m of sediment in the Río Shehuen Valley and 155 m of the uppermost section in the Río La Leona Valley (Figures 1.3, 1.4). The

stratum differs between the two aforementioned regions. The localities described in the Río Shehuen Valley include: the "right-side" (no cardinal direction given) of the Río Shehuen near Tres Lagos, the valley between the estancias Mata Amarilla and Pari Aike, Meseta (Cerro) Pari Aike and the "narrows" between the Estancia Pari Aike and Estancia Claudia (probably located south of the Río Shehuen and just west of Mata Amarilla). The Río Shehuen Valley consists mostly of grey to dark grey claystone, containing *Exogyra guaranitica*, and is interlayered with banks of sandstone which contain dinosaur bones (uppermost layers). The Río La Leona Valley, however, is described as being composed of grey and grey-green resistant sandstone layers that alternate with grey, grey-green, and black clays that contain rare selachian teeth (Feruglio, 1938a, 1944). Additional fossils identified from the Mata Amarilla Stratum include: *Trigonia wilkensi*, *Eriphyla shehuena* and *Nerinea* sp. (Feruglio, 1938b, 1944). Feruglio (1938a) interpreted the lowermost stratum to be from a marine environment based on the presence of marine invertebrate fossils and the uppermost stratum to be from a continental environment based on its presence of dinosaur fossils.

The final Mata Amarilla Formation nomenclature was coined by Bianchi (1967) and Leanza (1972). Leanza (1972) designated the type locality to be 15 km east of Piedra Clavada on the "right" side of the Río Shehuen. He proposed that the Mata Amarilla Formation continues to crop out south to Cerro Indice and west to Lago Viedma (Figure 1.3). This formation overlies the Piedra Clavada Formation and is overlain by the Man Aike Formation (Figure 1.8). Leanza (1972) stated that the Mata Amarilla Formation consists of 300 m of hard yellow-dark grey clayey sandstone that alternates with friable clayey and compact sandstones. Marine fossils such as *Corula shehuena*, *Exogyra*

guaranitica, and *Potamides patagoniensis*, are extremely common throughout the succession and may consist of millions of individuals. Furthermore, Leanza (1972) estimated the age of this formation to be Coniacian based on the ammonite *Peroniceras santacrucense.*

Riccardi and Rolleri (1980) further defined the geographical range of the Mata Amarilla Formation as the Tres Lagos region, south to Lago Viedma and in the region to the east (Figure 1.3 and 1.4). Furthermore, they estimated the maximum thickness of the formation to be approximately 350 m southeast of Tres Lagos and south of the Río Shehuen. They defined the Mata Amarilla Formation as consisting primarily of grey-green claystone and siltstone layers with some conglomeratic lenses. The lower part of the formation contains banks of marine invertebrate fossils (*Corbula shehuena, Exogyra guaranitica*, *Natica sehuena*, *Potamides patagoniensis*); while the upper part contains vertebrate bones and petrified wood. Riccardi and Rolleri (1980) listed six vertebrates identified from the Mata Amarilla Formation; however, half of the identified species are now considered to be either *nomina vana* or *nomina dubia*: "Loncosaurus argentines*,"* *"*Clasmodosaurus spatula*"* and "Tryonix argentina" (Coria and Salgado, 1996b; Powell, 2003; Wood and Patterson, 1973). A lungfish described from the formation, "Ceratodus*"* *iheringi*, was recently renamed *Atlantoceratodus iheringi* (synonym: *Ameghinoceratodus*) (Agnolin, 2010; Apesteguia et al., 2007; Cione et al., 2007). Lastly, *Simptosuchus contortidens* (Ameghino, 1899b) and *Platemys sehuenensis* (Ameghino, 1900, 1906) have only been described in the original literature, with no mention of the taxa or material in over one hundred years. Riccardi and Rolleri (1980) suggestd that, based on the lithology and paleontology, the lower unit was deposited in a marine

environment while the upper unit was deposited in a coastal environment. They also agreed with Leanza (1972) that the age of the Mata Amarilla Formation is Coniacian (Figure 1.8).

The geographical range of the Mata Amarilla Formation was further refined by Nullo et al (1981a) to include the Río Shehuen Valley, Piedra Clavada, Cerro Indice, Cerro Bagual (Cerro Mata Amarilla) and on the estancias Mata Amarilla and Pari Aike. However, they later confined the formation to be only within the Río Shehuen Valley (including the Estancia Mata Amarilla) (Nullo et al., 1999). They described the Mata Amarilla Formation as consisting of friable clayey sandstones with intercalations of compact sandstone. It grades from fine (pelitic) to coarse (psammitic) sandstones from west to east, respectively. Nullo et al. (1999; 1981a) interpreted these sediments as having been deposited in a shallow marine environment based on the sediments and marine fossils such as ammonites (*Peroniceras santacrucense*, *Placenticeras patagonicum* and *P. washbournei*). The Mata Amarilla Formation concordantly overlies the Piedra Clavada Formation and is coeval to the continental Cardiel Formation to the north and laterally grades with the deeper marine rocks of the Río Guanaco Formation to the west (Nullo et al., 1981a).

Arbe (2002) delineated the geographical range of the Mata Amarilla Formation as the southern shores of Lago Cardiel, Lago San Martin, the Estancia Mata Amarilla and the region to the east of the Estancia Pari Aike. This formation was measured at approximately 350 m thick and consists of sandstones and mudstones with tidal deposits. The sedimentary environment is proposed to be a fluvial/littoral environment. Fossils identified in this formation include: bivalves (*Eriphyla sehuena*, *Corbula sehuena* and

Exogyra guaranitica), gastropods (*Potamides patagonensis*), algae (*Botryococcus* sp., *Palambages* sp. and *Schizoaporis reticulata*) and terrestrial plant fossils (*Laucophyllum* sp. and *Araliaephyllum* sp.) (Arbe, 2002; Arrondo, 1983). Arbe (2002) asserted that the Mata Amarilla Formation is bounded by Upper Cenomanian-Lower Turonian and Lower Santonian unconformities, respectively.

The vertebrate paleontology of the Mata Amarilla Formation was examined by Goin et al. (2002). They described the formation as consisting of light and dark grey massively bedded mudstones composed mostly of quartz and with lesser amounts of feldspars, smectite, illite and kaolinite. Unidirectional ripples, carbonaceous layers and unimodal, trough cross-bedded sandstone banks (up to 4 m thick) occur intermittently. Goin et al. (2002) collected over 2000 vertebrate fossils from the Estancia Mata Amarilla, which include dipnoan tooth plates (*Atlantoceratodus iheringi*), bony fish teeth (*Lepidotes* sp.), ganoid scales (Semionotiformes or Lepisosteiformes), turtle scutes (Chelidae indet., *Pharynops* sp. and *Chelus* sp.), crocodyliform scutes and sauropod dinosaur teeth and bone fragments. Based on the lithology and paleontology of the Mata Amarilla Formation, Goin et al. (2002) interpreted its paleoenvironment to be a series of floodplains, either fluvial or distal alluvial, and swamps that occurred in a humid, warm temperate climate (Goin et al., 2002).

Iglesias et al. (2007) collected and described 500 fossil leaf impressions from two localities in the Mata Amarilla Formation. They cited Berry (1928; 1937) and Frenguelli (1953) as conducting the first studies of the fossil flora in this formation. Iglesias et al. (2007) distinguished two discrete sections in the Mata Amarilla Formation. The lower section was interpreted as consisting of interdistributary ribbon channel facies containing

vertebrate fossils and silicified logs and also delta plain facies bearing marine invertebrates, fossil leaves and an *in situ* fossil forest comprised only of coniferous trees (trunk diameters up to 1.2 m). Iglesias et al. (2007) described 12 leaf morphotypes consisting of angiosperms (82%), ferns (10%) and conifers (8%). They proposed that the leaves accumulated in a delta plain (coastal) environment that consisted of a canopy of coniferous trees with an understory of herbaceous angiosperms and ferns. The upper section is interpreted to have been deposited in a meandering fluvial environment with associated floodplains and adjacent lacustrine environments. This section bears vertebrate fossils, fossil leaves, silicified wood and charcoalified plant remains. The leaf fossils are poorly preserved compared to those in the lower section. Iglesias et al. (2007) suggested these leaves were preserved in a high-energy fluvial environment, hence the poor preservation. They concluded that the Mata Amarilla Formation contains greater morphological variation of fossil leaves than other coeval Gondwanan formations (Iglesias et al., 2007).

Additional paleontological research conducted in the Mata Amarilla Formation includes O'Gorman and Varela's (2010) work on plesiosaurs. Teeth, one propodium, two cervical, one "pectoral" and two dorsal vertebrae were collected from two localities and assigned to Elasmosauridae indet. Both localities produced plesiosaur material in the lower section of the Mata Amarilla Formation. O'Gorman and Varela (2010) interpreted the lower section to have been deposited in an estuarine environment that was strongly influenced by tides. They also added that these sediments were deposited during the foreland stage of the Austral Basin. The Mata Amarilla Formation transitionally overlies

the Piedra Clavada Formation is overlain by the La Anita Formation (Figure 1.8) (O'Gorman and Varela, 2010).

The most recent research regarding the geology of the Mata Amarilla Formation has been conducted by Varela (Varela, 2009, 2010a, b; Varela et al., 2010). He studied 15 sections to assess the stratigraphic relationships of the Piedra Clavada, Mata Amarilla and La Anita Formations (Figure 1.8). The Pari Aike, Cerro Fortaleza, Arroyo Guanaco and, possibly, the Puesto El Álamo formations were compounded into the Mata Amarilla Formation.

Varela and colleagues (Varela, 2009, 2010a, b; Varela et al., 2010) proposed that the Mata Amarilla Formation increases in thickness to the south because the underlying thin oceanic crust allows for greater flexure than the continental crust to the north. Additionally, the sediments of the Mata Amarilla Formation are significantly different than those from the underlying and overlying formations in that they contain: abundant quartz, moderate to low amounts of plagioclase and feldspars, and lesser amounts of calcite, palygorskite, pyrite, dolomite, hematite and magnetite. The clays primarily consist of smectite with lesser amounts of kaolinite (Varela, 2010a). Extensive paleosols (histosols, vertisols, alfisols and inceptisols) produce vertical and lateral variations in the formation which are, in turn, influenced by extrinsic (e.g., tectonic, eustatic or climatic) and intrinsic factors (e.g., distance from main channel), respectively (Varela, 2010a, b). Tsunami deposits are described in the lower part of the formation. These deposits consist of alternating sandstones and mudstones with interbedded bioclastic deposits that are "periodically interrupted" by bioclastic sand, coquina, and shell deposits containing autochthonous and allochthonous marine and freshwater mollusks (Varela, 2010a; Varela

et al., 2010). Varela (2010a) suggests that the following paleoenvironments are present within the Mata Amarilla Formation: lagoon, estuary and bayhead delta, coastal plain, distal fluvial system, meandering fluvial system with low sinuosity, meandering river with high sinuosity and braided fluvial system. Additionally, he describes hydromorphic soils preserved in the formation and postulates that these soils indicate that the Mata Amarilla paleoclimate was humid and seasonally tropical (consistent with the Cenomanian "greenhouse") (Varela, 2010a, b). This interpretation is further suggested by thick paleosols and carbonaceous layers containing *in situ* trees of the "Maria Elena" Petrified Forest. The forest is preserved in anastomosing fluvial deposits (Varela, 2010a, b). Varela (2010a) concludes the Mata Amarilla Formation was initially deposited during a marine transgression that was followed by a forced regression and finally another marine transgression. The sea level changes that occurred are proposed to be due to tectonic changes to the Andean fold-thrust belt rather than eustatic changes. The Mata Amarilla Formation marks the beginning of foreland basin for the Austral Basin. The middle section of this formation is dated to 96.23 ± 0.71 Ma (Cenomanian) (Varela, 2010a).

La Anita Formation

The La Anita Formation was first named the "Estratos o Areniscas de la Anita" by Feruglio (1938b). His description of the stratum corresponds to his previous description of Horizon 1 that crops out south of Lago Argentino (Figure 1.3) (Feruglio, 1938a). This unit consists of 300 m of well-cemented sandstones containing conglomeratic lenses and intercalations of mudstones. The fossil fauna includes: *Exogyra guaranitica*, *Lahilla*

luisa, Notodonax sp., *Holodiscus hauthali* and fossil leaves and wood (Feruglio, 1938a, b).

South of Lago Argentino, Feruglio (1944) established three Upper Cretaceous "strata". The lowermost stratum was the "Estratos La Anita." The type section for this stratum is on the plateau south of the Estancia La Anita. The Estratos La Anita are also exposed in the upper valley of the Río Shehuen, the southern shore of Lago Viedma, Arroyo Guanaco, Cerro Fortaleza, the northern (Estancia Maria Antonia) and the southern shores of Lago Argentino. Feruglio (1944) described the type section as consisting of grey, grey-green or teal, fine, cross-bedded sandstone that is very compact and resistant to weathering. The sandstone is interbedded with grey-dark grey, friable sandy claystones and conglomerate lenses. This unit is 300-350 m thick with beds generally dipping to the southeast. Marine mollusks can be found at several levels at the type locality and include: *Astarte* cf. *venatorum*, *Venus* cf.*venatorum*, *Mytilus* aff. *decipiems*, *Cinulia pauper* and *Holodiscus hautali*. Marine fossils at other localities include: *Exogyra guaranitica, Cucullaea argentina, Pugnellus* aff. *uncatus*, *Trigonia* sp. and a selachian tooth. Additionally, fossil wood and angiosperm leaves are preserved. The Estratos La Anita also crops out at the base of the Cerro Fortaleza and consists of light grey-green coarse sandstone with small lenses of soft clay. Additional sedimentary profiles for these strata are described from the southern shore of Lago Viedma on either side of Arroyo Guanaco (Feruglio, 1944).

The La Anita Formation was established by Bianchi (1967) after Feruglio's (1944) "Estratos La Anita." Furque and Camacho (1972), following Bianchi (1967), observed that this formation occurs both north and south of Lago Argentino with the best

exposure being on the Estancia La Anita (250 m thickness). These sediments consist of clayey to conglomeratic sandstones that are stratified and frequently cross-bedded. A diverse fauna of mollusks were found throughout the formation. Furque and Camacho (1972) interpreted the La Anita Formation as Upper Campanian (?) to Lower Maastrichtian marine facies deposited during a transgression.

Leanza (1972) further added that the Upper Cretaceous outcrops in the Lagos Argentino and Viedma region are distinct from the Upper Cretaceous strata in the Río Shehuen Valley; therefore, these regions contain their own unique formations. Additionally, the La Anita Formation is composed of compact sandstones with intercalations of white-grey or blue-grey lenticular conglomerates and unlithified clayey sandstone. The section is nearly 400 m thick at the type section (on the Estancia La Anita) and contains ammonites (*Pseukossmaticeras hauthali*) that indicate an age of lower Maastrichtian (Leanza, 1972) (Figure 1.9).

Arbe and Hechem (1984) divided the La Anita Formation into four members: the La Barco, Chachorro, La Asunción and La Irene. The first two were originally named by Furque (1973). The oldest member, the La Barco Member, was deposited during two stages of sedimentation. The first stage resulted in a "low-stand delta," formed south of what is now Lago Argentino, due to a sudden regression. This developed a type I unconformity (type I sequence boundary). The second stage resulted in the abandonment of the original delta and the formation of a series of destructive deltas caused by subsidence and the westward migration of the depocenter. The Chachorro Member is interpreted as a constructive delta system including delta front and plains. The La Asunción Member consists of subtidal to intertidal deposits that contributed to the

westward movement of marginal delta deposits associated with each deltaic cycle. Arbe and Hechem (1984) suggested that the movement was linked to tectonic reactivation of subsidence areas to the east. The La Irene Member was formed by southward to westward expansion of a river system, followed by river avulsion and, lastly, coastal deposits. This final member occurred during a "transgressive" cycle in the upper Campanian and was separated from the overlying Calafate Formation by a type II discordance. According to Arbe and Hechem (1984) the marine fauna in the formation include: *Cucullaea* cf. *argentina*, "Cytherea" cf. *australis*, *Gryphaea* sp., *Natica cerreria* and *Lahilla* cf. *tetrica.* The La Anita Formation is overlain by (Cachorro Member), laterally interdigitates with (La Barco and La Asunción Members) and overlies (La Irene Member) the Cerro Fortaleza Formation (Figure 1.9) (Arbe and Hechem, 1984).

Macellari et al. (1989) also included the La Asunción, Cachorro and La Barco Members as distinct units within the La Anita Formation. They excluded the La Irene Member and designated it as a separate formation. The La Asunción Member consists of 20-30 m of marine, subtidal and intertidal deposits of a transgressive system tract. The Cachorro Member is only exposed south of Lago Argentino. It is 320-370 m thick and is interpreted to be a prograding shallow marine prodelta followed by distributary channel fill with some marine influences. This member contains oysters and plant fossils. The overlying La Barco Member is 840 m thick and contains shallow marine bivalves and ammonites (*Baculites* sp.). Macellari et al. (1989) interpreted this member to be a lower delta plain to submerged delta plain facies that is further divided into lower and upper strata. The lower stratum is interpreted as consisting of barrier island deposits, followed by bay deposits and then fluvial distributary channel fill. The upper stratum consists of a

subaqueous delta plain, followed by bay and shallow marine deposits. The La Barco Member interdigitates and is overlain by the Cerro Fortaleza Formation (Figure 1.9). Macellari et al. (1989) agreed with previous assertions that the La Anita Formation was deposited during the upper Campanian.

The La Anita Formation was additionally analyzed be Kraemer and Riccardi (1997). The formation is thickest to the west and tapers eastward. It overlies the Alta Vista Formation and is overlain by the Pari Aike (Cerro Fortaleza) Formation (Figure 1.9). Only the La Asunción and La Barco Members are exposed in the study region; the Cachorro Member only occurs south of Lago Argentino and is therefore not discussed. The La Asunción Member lies along the margin of the Río La Leona and the Arroyo Turbio. This member consists of sub-tidal to intertidal siltstone and fine sandstone beds (fining upward) deposited in a high energy environment. Bivalves are commonly found in the upper layers. The La Barco Member is exposed further to the west and is 500 m thick. It is interpreted to be a delta deposit that consists of four transgressive/regressive cycles. Many ammonite, gastropod and bivalve species have been identified from the La Anita Formation. Based on this information, Kraemer and Riccardi (1997) biostratigraphically dated the formation to the Campanian-Maastrichtian.

Marenssi et al. (2003) conducted a thorough investigation of the Upper Cretaceous outcrops south of Lago Viedma. In their Barrancas Blancas section, only the uppermost 28 m of the La Asunción Member is exposed. It is divided into two facies (A and B). Facies A is comprised of 8 m of yellowish-brown, fine-coarse grained, massive, friable, muddy sandstone. It is heavily bioturbated (*Thalassinoides* sp. burrows), but some current ripples and cross-bedding (herringbone and trough) are preserved. Pebbles

are scattered throughout this facies. Facies A is interpreted to be a low-energy subtidal deposit. Facies B is 21 m thick and consists of lenticular sandstone banks that contain some gravel. The sandstone banks (0.5-0.8 m thick) are laterally continuous for hundreds of meters and contain ripples, planar, herringbone, tabular and trough cross-bedding. This facies is interpreted as a high energy subtidal (shoreface) environment, dominated by waves and storms (Marenssi et al., 2003).

The first plesiosaur discovered in the Santa Cruz Province was "Polyptychodon patagonicus*"* and was named based on two teeth (Ameghino, 1893). The material was collected around Lago Argentino in the "Fomación Santacrueña" ("Sehuenense") (Ameghino, 1906; O'Gorman and Varela, 2010). O'Gorman and Varela (2010) putatively designate this species as a *nomen vanum* because the type material has been lost. They considered the "Sehuenense" unit to be a junior synonym of the Mata Amarilla Formation; however, the Mata Amarilla Formation has never been identified in the Lago Argentino region where these teeth were found. Additionally, Ameghino (1898, 1906) defined the Sehuenense stage as containing Upper Cretaceous sediments with little geographical reference. Thus, based on the evidence provided, the "P. patagonicus" indet. teeth were possibly collected from the marine rocks of the La Anita Formation.

Cerro Fortaleza/Pari Aike Formation

The name Pari Aike has been used, in some form, since at least 1906 for the same location. The different possible spellings that have been used include: "Par Aïk" and "Pari-Aik" (Ameghino, 1906); "Par Aik" and "Parri Aike" (Huene, 1929); and "Pari

Aiken" (Feruglio, 1938b). The most recent spelling of "Pari Aike" was established by Feruglio (1944).

The "Estratos de Pari Aiken" designation is attributed to Feruglio (1938b) based on previously described rocks tentatively named Horizon C (Table 1.1) (Feruglio, 1938a). The Estratos de Pari Aiken are estimated to be 250 m thick in both the Río Shehuen Valley and Río La Leona Valley; however, the sedimentology of this unit differs between the two rivers (Figures 1.3 and 1.4). In the Río Shehuen Valley, Horizon C is described from an exposure located on the northeastern portion of Lote 119, about 15-20 km from Cerro Pari Aike and in the "narrows" between estancias Claudia and Pari Aike (Figure 1.4). The sediments consist of light to dark grey claystones with intercalations of sandstones and conglomerates. In the Río La Leona Valley, the strata consist of two thick, yellow banks of friable sandstone that contain layers of grey, grey-green, black and purple clays. Dinosaur bones have been discovered in both areas; however, the Río La Leona Valley also contains silicified wood and is noted to be completely devoid of marine fossils (Feruglio, 1938a). Feruglio (1938) suggests that these rocks were deposited in an estuarine environment during a regression in the Late Cretaceous.

Feruglio (1944) further describes the "Estratos de Pari Aike" or the "Estratos con Dinosaurios" in a profile of Cerro Fortaleza (Figure 1.4). The "Estratos con Dinosaurios" is discussed in the text; however, the "Estratos de Pari Aike" is only mentioned in the text. The "Estratos de Pari Aike" overlies the Estratos La Anita and is approximately 250 m thick (Table 1.1). The base of this stratum is composed of light, friable sandstones interbedded with bands of purple, grey to dark grey clays with a conchoidal fracture. About halfway through the stratum, a distinct, 8 m thick layer of grey to black

carbonaceous clays containing gypsum veins covered with a rusty colored film occurs. Above this layer is a layer of grey clays overlain with banks of grey to light green friable sandstone. The next layer is comprised of grey clay that contains concretions that are enveloped by a film of black manganese oxide or hyrdroxide. The final layer is composed of grey to dark grey clays with purple mottling and interspersed pockets of sand. The uppermost layer contains numerous fragments of dinosaur bones (Feruglio, 1944). Additional sedimentary profiles for these strata are described from the southern shore of Lago Viedma on either side of Arroyo Guanaco (Feruglio, 1944).

Leanza (1972) described the Pari Aike Formation as being composed of light to dark grey claystone with thick, friable, sandstone layers and conglomeratic lenses. The only fossils contained within the formation are dinosaur bones. He stated that the type locality is on the Estancia Pari Aike, approximately 20 km due south of Piedra Clavada (Figure 1.4). This would place the type section on or near Cerro Pari Aike. However, in the Río Shehuen Valley, Feruglio (1938a) described an exposure that he identified as Horizon C (Estratos de Pari Aiken) located about 15-20 km from Cerro Pari Aike and in the "narrows" between the estancias Claudia and Pari Aike. Leanza (1972) may have referred to the latter area as the type section, but neither Feruglio (1938a, b, 1944) nor Leanza (1972) provided maps identifying this area. Leanza (1972) considered the Pari Aike Formation to be a junior synonym of the Mata Amarilla Formation because he asserted that there is no distinct transition between the two formations (Table 1.1).

The Pari Aike Formation was conserved by Riccardi and Rolleri (1980) despite Leanza's (1972) suggestion that it was equivalent to Mata Amarilla (Table 1.1). They stated that the Pari Aike Formation spans north to Lago Pueyrredón (northwestern Santa

Cruz Province), south to Lago Argentino, east to Lago Cardiel and west to Lago San Martín (Figure 1.3). The geology consists of red, purple and black clays and tuffs interbedded with friable sandstones and conglomerates. Riccardi and Rolleri (1980) reported mollusks, dinosaur bones, silicified wood and leaf fragments in this formation. According to these workers, there are some regional differences in the Pari Aike Formation. In the northern region, the thickness and consolidation of sediments increases and the colors of the sediments become more uniform (mainly reds and greens). Additionally, the topography is not the same as in the south. To the south, around Lago Argentino, the sediment consists of a fining-upward sequence with banks of conglomerates. The sediment packages are thickest in the northern-most region, ~500 m thick, compared to the south, ~250 m. Additionally, the age of the unit decreases southward. Around Lago San Martin, the Pari Aike Formation overlies the Cenomanian-Turonian? Piedra Clavada Formation and is separated from this unit via a disconformity. In the Río Shehuen and Río La Leona Valleys, Riccardi and Rolleri (1980) stated that the Pari Aike Formation interdigitates with the Mata Amarilla Formation (Coniacian), Alamo Formation (Santonian?-Campanian) and Anita Formation (Maastrichtian). The Pari Aike is overlain (separated via a disconformity), in the north, by Posadas Basalt, Río La Leona Formation and Centinela Formation (Eocene-Oligocene). In the south, it is conformably overlain by the Man Aike Formation (Maastrichtian-Paleocene) (Figure 1.9). Therefore, based on the ages of the underlying and overlying formations, the Pari Aike Formation ranges from Turonian to Maastrichtian (over 25 My), which Riccardi and Rolleri (1980) indicated in one of their tables. However, these authors stated in the text of the paper that the age range is from the Aptian/Albian-Maastrichtian (~47 My) (Figure 1.9). Based on

the fossils and lithology of this formation, they suggest that the Pari Aike Formation represents a continental environment (Riccardi and Rolleri, 1980). Riccardi and Rolleri (1980) considered the Chorrillo Formation (south of Lago Argentino) to be a junior synonym of the Pari Aike Formation. They argued that it was misinterpreted by Feruglio (1938a, b) because the upper portion of the type section of the Pari Aike Formation was covered in vegetation so as to preclude an unambiguous correlation (Riccardi and Rolleri, 1980).

Alternatively, Nullo et al. (1981a) asserted that the Pari Aike Formation is a junior synonym of the Chorrillo Formation (Table 1.1). They suggested that the Chorrillo Formation is exposed on the southern margin of Lago Argentino and north to Cerro Fortaleza. The type section for the Chorrillo Formation is approximately 100 m thick and is located at the headwaters of the Arroyo Chorrillo Malo just west of the Estancia Anita. Nullo et al. (1981a) suggested that the Chorrillo Formation represents a period of continentalization from north to south during the Upper Cretaceous. They further infered that its age is upper Campanian or Maastrichtian based on the ages of the underlying (La Anita Formation) and overlying (Calafate Formation) formations (Nullo et al., 1981a).

Arbe and Hechem (1984) proposed a new formation, the Cerro Fortaleza Formation, to encompass the upper Cretaceous continental sediments that crop out along the Río La Leona and Barrancas Blancas (Table 1.1). These sediments had previously been included within the Pari Aike Formation. Arbe and Hechem (1984) argue that these rocks should not be included in the Pari Aike Formation because of lithological differences: the former consisting primarily of continental fluvial deposits and the latter

consisting primarily of mudstones. Furthermore, the authors distinguished the Pari Aike Formation from the Chorrillo Formation based on sedimentological differences (Arbe and Hechem, 1984).

The type section of the Cerro Fortaleza Formation is located on the eastern bank of the Río La Leona on Cerro Fortaleza. The Cerro Fortaleza Formation is 350 m thick at its type section (Cerro Fortaleza) and 500 m thick at Barrancas Blancas and the southwestern side of Cerro Ratón (Figure 1.4) (Arbe and Hechem, 1984). Arbe and Hechem (1984) divided the Cerro Fortaleza Formation into five distinct facies (P, Q, R, S, and T) that range in age from the middle to upper Campanian. The oldest facies, Facies P, is a grey-yellow, medium to fine grained quartz sandstone with tabular banks and herringbone crossbedding that occur in sets up to 0.40 m thick. Flaser bedding occurs between these sets. These beds grade into laminated siltstones and claystones containing intercalations of fine to very fine sands. This facies contain some bivalves, mollusks (e.g., *Ostrea* sp.), gastropods, ostracods (i.e., *Ovocytheridea*? sp.) and tricolpate (angiosperm) pollen. Arbe and Hechem (1984) interpreted this facies as having been deposited in intertidal and lagoonal environments. Facies P primarily occurs in the southern-most exposure of the formation (Arbe and Hechem, 1984).

The next facies, Facies Q, consists of layers and banks of trough cross-bedded, grey-yellow sandstones and conglomeratic sandstones that contain a "tuffaceous" matrix. The sandstones grade from medium to fine-grained and have tabular and planar crossbeds. Intercalations of olive to olive brown, laminar or massively bedded, bioturbated (by rootlets) claystones and siltstones occur. This facies is laterally associated with Facies R and overlain by Facies S. Facies Q is interpreted to have been deposited in

a moderate energy "sinuous" river environment that drained into a vegetated alluvial plain (Arbe and Hechem, 1984).

Facies R consists of grey-yellow sandstone with a clayey/tuffaceous matrix. The base of the unit contains load casts and abundant mudstone clasts. The sandstone bedding consists of large (3 m thick) tabular beds that contain distinct planes and low angle, wavy micro-bedding and medium to coarse-grained planar bedding or trough cross-bedding. Overall, Facies R is a coarsening and thickening upward sequence. Arbe and Hechem (1984) reported dinosaur bones, silicified wood and indeterminate plant fossils from this facies. They interpreted Facies R to consist of "sheet-flood" deposits (probably crevasse splays) from basins that occurred lateral to the main river (Facies Q) (Arbe and Hechem, 1984).

Facies S consists of grey-olive and dark grey, mottled, non-expandable, tuffaceous siltstones and claystones. Thin, wavy-bedded intercalations of fine to very fine calcareous sands occur. This unit consists of massive bedding, linsen, undulating laminations and varve deposits. Weathering of Facies S produces light and dark banding that is distinctive for the Cerro Fortaleza Formation. Arbe and Hechem (1984) suggested this unit to represent a fluvio-palustrine environment. Facies S overlies Facies Q and R in the northern regions of the outcrop belt and over Facies P in the southern. It also interdigitates with the La Barco Member of the La Anita Formation and is overlain by Facies T in the north and the La Irene Member of the La Anita Formation to the south (Arbe and Hechem, 1984).

Facies T is the uppermost unit of the Cerro Fortaleza Formation. It consists of massively bedded, expandable, red and purple siltstones and mudstones containing

indeterminate plant fragments. This facies is separated from the overlying Calafate Formation (to the north) by a disconformity and, in the south, interdigitates with and is overlain by the La Irene Member (Arbe and Hechem, 1984).

Arbe and Hechem (1984) interpreted the Cerro Fortaleza Formation as having been deposited during a time of increased western "continentalization" (Facies P, Q and R) and eastern tectonic subsidence (Facies R, S and T). Overlying the type section of the Cerro Fortaleza Formation is the Calafate Formation, with an erosional unconformity separating the two formations. However, on the Estancia Irene and southwards, the Cerro Fortaleza Formation is overlain by the La Irene Member of the La Anita Formation (Figure 1.9) (Arbe and Hechem, 1984).

Arbe (1987) treated the Pari Aike Formation as a discrete formation from the Cerro Fortaleza Formation. He identified outcrops belonging to the Pari Aike Formation at the base of Cerro Indice. Here, the Pari Aike Formation is 150 m thick and consists of sandstones and tuffaceous siltstones deposited in a fluvio-palustrine environment. It overlies the Mata Amarilla Formation and is, in turn, overlain by the Man Aike Formation (separated by an unconformity). He further suggested that the Pari Aike Formation is coeval with the Cardiel and Puesto El Moro Formations (Figure 1.8). Arbe (1987) speculated that the Pari Aike Formation was deposited during a regression in the upper Coniacian-lower Santonian.

The Cerro Fortaleza Formation was further described by Macellari et al. (1989) (Table 1.1). They agreed with Arbe and Hechem (1984) that the Cerro Fortaleza Formation is a distinct formation apart from the older Pari Aike Formation. Additionally, Macellari et al. (1989) further agreed with Arbe and Hechem (1984) that

the two formations are divided by an unconformity. However, Arbe and Hechem (1984) never mentioned an unconformity separating the two units. Macellari et al. (1989) described the Cerro Fortaleza Formation as consisting of 460 m of light-dark grey friable claystones with intercalations of poorly cemented sandstone. It decreases in thickness towards the south and west. They divided the Cerro Fortaleza Formation into two members, a lower and an upper, that are up to 220 m and 240 m thick, respectively. The lower member consists of fining-upward cycles of yellowish silty sandstones to grey mudstones. This member is interpreted as a low-sinuous meandering fluvial environment that had a high fine sediment load and a constant discharge. Macellari et al. (1989) suggested that the lack of lateral accretion indicates that the fluvial system was influenced by rapid subsidence of the basin. The upper member consists of unconsolidated grey, olive green and purple mudstones with friable sandstone intercalations (1-3 m thick) occurring approximately 100 m apart. Layers of coal in the upper beds contain poorly preserved plant material and fossil wood. Westward, the sediments continue in fining-upward cycles (5-10 m thick), but pass from conglomerates to cross-bedded sandstones and lastly to mudstones. This upper stratum is interpreted as a meandering river system that included proximal and distal meandering river facies, in addition to occasional fluvio-lacustrine periods with thick overbank deposits. Additionally, Macellari et al. (1989) proposed that the climate was humid (based on the presence of grey clays) with intervals of high rainfall and a high water table (based on the presence of coal beds). The Cerro Fortaleza Formation was interpreted to be late Campanian in age due to the underlying and coeval La Anita Formation and the overlying La Irene Formation (Figure 1.9) (Macellari et al., 1989).

Kraemer and Riccardi (1997) conserved the name Pari Aike Formation, over Cerro Fortaleza Formation, for the sediments cropping out along the Río La Leona Valley between Lago Viedma and Lago Argentino (Table 1.1). They maintained the name in order to prevent the application of too many names to similar lithostratigraphic units. Thus, Kraemer and Riccardi (1997) stated that the Pari Aike Formation crops out along the Río La Leona Valley, Arroyo Turbio, Cañadón Hondo and the southern margin of Arroyo Guanaco. It ranges in thickness from 175-300 m south of the Arroyo Turbio, 350 m on Cerro Fortaleza and 500 m along Barrancas Blancas. They stated that the Pari Aike Formation is easily distinguishable from the other formations in the region because it appears like "standard badlands" sediments with dark banding throughout the formation. The Pari Aike Formation consists of poorly cemented banded claystones with sandy intercalations. Several carbonaceous layers containing indeterminate plant fossils and silicified wood occur. Dinosaur vertebrae and silicified branches were identified in Kraemer and Riccardi's (1997) horizon n17. Horizons n16 and n18 yields additional fossils identified by Oviedo (1982): *Ostrea ultima*, *Melanopsis* sp., internal molds of Pholadomydae and Ostreidae, fossil pollen and marine microplankton. Kraemer and Riccardi (1997) interpreted the Pari Aike Formation as representing a meandering fluvial environment with possible fluvio-lacustrine intervals. They proposed its age to range from the late Coniacian-Maastrichtian based on stratigraphic relationships. However, in their generalized stratigraphic column, the Pari Aike Formation is situated between the La Anita and the La Irene formations; thereby implying its age late Campanian-early Maastrichtian (Figure 1.9). To the west, the Pari Aike Formation is replaced by the La Anita Formation (Kraemer and Riccardi, 1997).

Arbe (2002) reassessed the Cerro Fortaleza Formation by adding to and altering some of the information that was discussed in his previous works (Table 1.1) (Arbe, 1987; Arbe and Hechem, 1984). The Cerro Fortaleza Formation ranges in thickness from 350 m on Cerro Fortaleza to 500 m in Barrancas Blancas and Cerro Ratones. It crops out as far north as Lago San Martín, east to Lago Viedma, and throughout the Río La Leona Valley. Arbe (2002) describes the Cerro Fortaleza Formation as consisting of olive and red siltstones and claystones with paleosols. These sediments are interpreted as having been deposited in fluvial, fluvial-palustrine and coastal plain environments. Furthermore, he speculates that the red siltstones and claystones have been oxidized in palustrine environments. The Cerro Fortaleza Formation is coeval with the deltatic facies of the La Anita Formation and is overlain by the La Irene Formation (separated via a disconformity) (Figure 1.9). Arbe (2002) placed the Cerro Fortaleza Formation between the 85 and 77.5 Ma (Santonian-Campanian) unconformities.

Arbe (2002) differentiated the "Estratos de Pari Aike" (Feruglio, 1938a, b) from the Cerro Fortaleza Formation. The former consists of transgressive tidal deposits (littoral facies with tidal deposits) that exclusively crop out on Lote 119 near Cerro Castillo. He states that the "Estratos de Pari Aike" overlie the continental La Irene Formation (Maastrichtian) (Arbe, 2002).

Goin et al.(2002) proposed that the Pari Aike Formation (including the Cerro Fortaleza Formation) is a junior synonym of the Mata Amarilla Formation (Table 1.1). They justified this based upon the presence of periodic marine deposits in both formations. They correlated these intercalations of marine deposits and fossils of the Pari

Aike and Mata Amarilla formations and determined that the units are too similar to be considered distinct formations (Goin et al., 2002).

The name Pari Aike was also conserved by Novas et al. (2002) for the Upper Cretaceous continental formation exposed on the southern margin of Lago Viedma, Barrancas Blancas and on the western side of the Río La Leona (Cerro los Hornos) (Table 1.1). Novas et al. (2002) stated that the Pari Aike Formation is 300 m thick in this region and consists of fining-upward cycles of unconsolidated sandstone. They divided the Pari Aike Formation into two sections: a lower section exposed at Barrancas Blancas (120 m thick) and an upper on Cerro Los Hornos (180 m thick). The lower section consists of grey to light olive-grey, sandy siltstones with very fine sandstones organized in fine laminations, medium-fine grained sandstone banks and cross-bedded channels containing medium-small conglomerates. Lateral accretion surfaces occur. Sandstone channels increase in frequency and size in the upper portion of this facies. Silicified wood is frequently found in the lower facies. Novas et al. (2002) interpreted this section to have been deposited in a low to moderately sinuous fluvial environment where there was an increase in energy and avulsion through time. The upper stratum consists predominantly of grey to grey-green siltstones and tuffaceous claystones. However, channels do occur and are composed of coarse-grained sandstones and conglomerates that fine upward to fine grained sandstones. Volcanic ash layers have been identified in this upper section. The top of the upper section contains load deformation structures (Novas et al., 2002). Additionally, intercalations of marine facies containing microphytoplankton and mollusks have been identified towards the top of the formation on Cerro Fortaleza (Novas et al., 2002; Oviedo, 1982). Invertebrate burrows, leaves,

large silicified trunks (diameter 1.2 m) and dinosaur bones can be found in mudstone and carbonaceous layers. Novas et al. (2002) interpreted this upper section as a coastal plain and fluvial environment that was dominated by floodplains. The fluvial facies are composed primarily of fine grained sediments. The river system flowed from the southwest and is proposed to have been more sinuous and to contain less avulsions than the lower section. Dinosaur bones occur predominantly in channel deposits (80%) in the upper two-thirds of the Pari Aike Formation. Novas et al. (2002) suggested that the age of the formation is Coniacian-Santonian based on the presence (titanosaurian sauropods) and absence (hadrosaurian ornithopods) of dinosaur clades discovered in the formation and its stratigraphic relationship to the Mata Amarilla Formation. According to Novas et al. (2002) the Pari Aike Formation interdigitates with and overlies the Mata Amarilla Formation)

The Upper Cretaceous continental sediments exposed in the Río La Leona Valley were again identified as belonging to the Cerro Fortaleza Formation by Marenssi et al. (2003) (Table 1.1). Their primary study localities were also Barrancas Blancas and Cerro Los Hornos. The Barrancas Blancas section of the Cerro Fortaleza Formation is 390 m thick and conformably overlies the La Asunción Member of the La Anita Formation. Marenssi et al. (2003) divided the formation into three facies (Facies C, D and E). Facies C occurs at the base of the formation. It consists of 30 m thick fining-upward cycles of whitish-brown sandstone to dark-banded massive mudstones. Sandbars contain ripples, trough cross-bedding and planar laminations of fine to very fine sands. Marenssi et al. (2003) interpreted this facies as a progradational coastal facies that included a transitional or lagoon/coastal plain environment with fluvial influences. The overlying facies, Facies

D, is comprised of 105 m of alternating highly consolidated mudstones and large sandstone channels that are laterally continuous for hundreds of meters (up to 300 m). The base of the facies consists of fining-upward cycles of cross-bedded (trough and tabular) conglomerates. These are followed by fining-upward cycles of cross-bedded (containing some ripple marks) or massively bedded sandstones that fine upward to mudstone. Floodplain deposits consisting of tabular banks, massive mudstones and fine laminations (including small ripples) are also common in Facies D. There are no lateral accretion surfaces evident in this facies. Dinosaur bones and silicified wood found in this facies are typically associated with channel and floodplain deposits, respectively. Marenssi et al. (2003) interpretd this facies as a low energy, low sinuousity fluvial environment with south to southwst flow direction. Overlying Facies D is the thickest of the three facies, Facies E (225 m). Facies E is comprised of well-cemented, cross-bedded (including ripples) sandstones and massively bedded, laminated mudstones that occur in stacking cycles between 10-15 m thick. Lateral accretion surfaces are present in this facies. The mudstones contain both ripple and plant root marks. The uppermost portion of this facies consists of laminated sands that contain iron botryoidal concretions and are interbedded with massively bedded sandstone lenses that contain ripple marks. Dinosaur bones and wood are common in this uppermost package. Facies E is interpreted as representing a lower energy, moderately sinuous meandering fluvial system that would have been subject to tides. Channel depth was 4-6 m with the width estimated to be 60-100 m. Lateral accretion surfaces are between 70 m and 100 m wide. Marenssi et al. (2003) stated that the features present in Facies E are typical of a deltaic distributary floodplain. The overall fluvial system is interpreted to have run south-soutwest and to

have added to the progradational sequence of the La Anita Formation (Marenssi et al., 2003).

Most recently, authors (O'Gorman and Varela, 2010; Varela, 2010a) have again suggested that the Pari Aike Formation (including the Cerro Fortaleza Formation) is a junior synonym of the Mata Amarilla Formation (Table 1.1). O'Gorman and Varela (2010) suggested that the middle and upper sections of the Mata Amarilla Formation contain the dinosaur fossils previously ascribed to the Pari Aike Formation. Furthermore, Varela (pers. comm.) claims that the middle section of the Mata Amarilla Formation, radiometrically dated to 96.23 ± 0.71 Ma (middle Cenomanian), is correlative to the fossil-bearing layers at Cerro Los Hornos, Barrancas Blancas and Cerro Fortaleza.

Limited information has been published on the fossil fauna and flora of the Pari Aike/Cerro Fortaleza Formation. Despite being known as "Estratos con Dinosaurios," only four dinosaurs have been described from this formation: *Talenkauen santacrucensis* (Novas et al., 2004), *Puertasaurus reuili* (Novas et al., 2005b), *Orkoraptor burkei* (Novas et al., 2008) and *Austrocheirus isasii* (Ezcurra et al., 2010). *T. santacrucensis, P. reuili, O. burkei* were discovered on and around Cerro Los Hornos while *A. isasii* was discovered along Hoyada Arroyo Sec (near Estancia La Irene) (Ezcurra et al., 2010; Novas et al., 2004; Novas et al., 2005a; Novas et al., 2008). A new titanosaurian genus is currently under study by the research group at Drexel University and their collaborators. This dinosaur was discovered on the northwestern base of Cerro Fortaleza. The only other vertebrate material that has been described from this formation are teeth of an elasmobranch (*Archaeolamna kopingensis*) found on the south-eastern slope of Cerro Fortaleza (Schroeter et al., in prep). Additional titanosaur bones,

semionotiform/lepisoteid scales, testudine fragments, elasmobranch, dipnoan, ornithopod and theropod teeth have been discovered but not yet described. Furthermore, there has only been a section from an unpublished (and, so far, unobtainable) dissertation and a short abstract on the palynology of the Cerro Fortaleza Formation (Oviedo, 1982; Povilauskas et al., 2003).

La Irene Formation

The La Irene Formation was established as a distinct formation, rather than a member of the La Anita Formation (see above), by Macellari et al. (1989). The type section is located on the Estancia La Irene on the southwestern banks of the Río La Leona (Figure 1.4). Outcrops are also exposed along the Río La Leona Valley and on the southern shore of Lago Argentino. The La Irene Formation ranges in thickness from 20 to 200 m, tapering to the south and east. It unconformably overlies the La Anita Formation at the type section. This formation consists of fining-upward cycles of cross-bedded conglomerates, laminated sandstones and mudstones. Macellari et al. (1989) interpreted the La Irene Formation as representing deposition in a high energy braided fluvial environment that was the distal-most portion of a meandering river system. Throughout the region, the La Irene Formation overlies the La Anita and Cerro Fortaleza formations and interdigitates with and is overlain by the Chorrillo Formation (Figure 1.9) (Macellari et al., 1989).

Kraemer and Riccardi (1997) defined the La Irene Formation as all of the conglomeratic layers that is above the Pari Aike Formation north of Lago Argentino. These include the conglomerate layers of the Man Aike Formation (Furque, 1973; Leanza, 1972; Riccardi and Rolleri, 1980), Calafate Formation (Nullo et al., 1981b) and

the La Irene Member of the La Anita Formation (Arbe and Hechem, 1984). Kraemer and Riccardi (1997) agreed with Macellari et al. (1989) that the La Irene Formation should not be included in the La Anita Formation because the Pari Aike Formation sintervenes between these two units. Additionally, the La Irene Formation exhibits a clear discordance and marked facies differences from the La Anita Formation. Kraemer and Riccardi (1997) limited the La Irene Formation to the area north of Lago Argentino and pointed out that this formation does not necessarily correlate with the units south of this lake. Its thickness ranges from 20 m in the Río La Leona Valley and increases in thickness southward. The La Irene Formation is composed of fining-upward cycles (6-10 m thick) of cross-bedded, well-rounded conglomerates interpreted as being laid down in a high energy anastomosing (braided) river. Silicified tree trunks were identified at Cerro Los Hornos. Kraemer and Riccardi (1997) suggested the age of the La Irene Formation to be Maastrichtian based on the fact that the overlying formation (Man Aike Formation) contains Tertiary bivalves and the underlying formation (Pari Aike Formation) contains dinosaur bones (Figure 1.9) (Kraemer and Riccardi, 1997).

Arbe (2002) stated that the La Irene Formation crops out along the western margin of the Río La Leona Valley and on the northern and southern banks of Lago Argentino, contrary to Kraemer and Riccardi (1997). He also suggested that these sediments were previously included in the Calafate Formation (e.g. Bianchi, 1967; Furque, 1973; Nullo et al., 1981b; Riccardi and Rolleri, 1980). Arbe (2002) interpreted the sedimentary packages of the La Irene Formation as consisting of fluvial and transgressive tidal deposits laid down during the upper Campanian (77.5 Ma) and Maastrichtian, respectively (Figure 1.9). The fluvial system would have been oriented

north-northwest and south-southeast. The La Irene Formation was deposited during a time of rapid continentalization of the basin due to a eustatic fall in sea level (Arbe, 2002).

The palynology of the La Irene Formation was studied by Povilauskas et al. (2008). They agreed with Arbe (2002) regarding the areas where the La Irene Formation is exposed. In the Río La Leona Valley, the La Irene Formation is separated from the underlying Cerro Fortaleza Formation by an unconformity; however, south of Lago Argentino (near the town of El Calafate) there is no apparent unconformity separating the La Irene Formation and the underlying La Anita Formation. Povilauskas et al. (2008) collected sediments on and around Cerro Calafate for palynological analysis. They divided the La Irene Formation into lower and upper facies. The lower facies is 110 m thick and consists of light-colored sandstones and dark mudstones. These sediments form fining-upward sequences that thicken and increase in overall grain size through the succession. Banks of fine- to coarse-grained sandstone range between 2-9 m thick and intercalations of mudstones (sometimes carbonaceous) range in thickness from 15 m at the base to 1 m at the top. Povilauskas et al. (2008) interpreted the lower facies as being deposited in a transitional/delta plain environment with both fluvial and (some) marine influences. The upper facies is 120 m thick and is comprised primarily of fining-upward conglomeratic sandstone banks containing rare mudstones. This facies is interpreted as more continental fluvial channel deposits. In both facies spores and pollen are relatively well-preserved. A few marine palynomorphs (dinoflagellate cysts) were discovered; however, the assemblage is predominantly composed of terrestrial plants. Angiosperm pollen is dominated by Chloranthaceae (*Clavatipollenites* sp.) and Arecaceae (*Arecipites*

spp., *Longapertites* sp., *Spinizonocolpites hialinus*) with lesser amounts of Liliaceae (*Liliacidites* spp.), Proteaceae (*Proteacidites* sp., *Peninsulapollis gillii*, *Retidiporites camachoii)*, Ericaceae (*Ericipites scabratus*), Nyssaceae (*Nyssapollenites* cf. *squamosus*) and Symplocaceae (*Senipites* sp.) palynomorphs. The gymnosperm palynomorphs include: Podocarpaceae (*Podocarpidites* spp.), Ephedraceae (*Equisetosporites* sp.) and Cycadales/Bennettitales (*Cycadopites nitidus*). Additionally, lesser amounts of bryophyte spores and fungal remains were identified. Povilauskas et al. (2008) conclude that the continental assemblage of the La Irene Formation is dominated by ferns (e.g., Cyatheaceae, *Laevigatosporites*) and angiosperms with lesser quantities of gymnosperms. They suggest that the Podocarpaceae pollen was transported in from other environments because of its low frequency (podocarps release large amounts of pollen). The paleoclimate would have been warm-temperate to warm-wet at least locally based on the species present and their abundance. Additionally, the palynological evidence (species, species ranges and similarity of flora) has convinced Povilauskas et al. (2008) to agree with earlier interpretations that the La Irene Formation is Maastrichtian in age.

Chorrillo Formation

In 1935, Feruglio identified Upper Cretaceous marine deposits that contain abundant fossils south of Lago Argentino. This unit consists of grey-green sandstones with variegated clays and conglomeratic lenses. Feruglio (1935) discovered abundant fossils in these sediments, including dinosaurs, plants (gymnosperms and angiosperms), brachiopods (i.e., *Terebratula* sp. and *Bouchardia* sp.), bivalves (e.g., *Malletia* sp.,

Trigonia sp., *Lahillia* sp., *Ostrea* sp. and *Exogyra* sp.), gastropods (e.g., *Pleurotomaria* sp. and *Turritella* sp.), cephalopods (*Nautilus* sp.) and sharks (*Scapanorhynchus* sp.).

The same deposits were identified as Horizon 2 by Feruglio (1938a) and later named "Estratos del Chorrillo" (Feruglio, 1938b). Feruglio (1938a) initially postulated that Horizon 2 might correlate with his Horizon B, which is exposed north of Lago Argentino. However, he later distinguished the two horizons as distinct strata (Feruglio, 1938b). In both 1938 publications he described this unit as 140-240 m of mottled mudstone and sandstone that contains dinosaur bones, dicot leaves and marine mollusks (Feruglio, 1938a, b).

Later, Feruglio (1944) also called these strata the "Estratos del Chorrillo o Estratos con Dinosaurios." These beds overlie the "Estratos de La Anita" and are overlain by the "Estratos de Calafate". Along with the Estratos de La Anita, the type section of the Estratos del Chorrillo is also located on the plateau south of the Estancia Anita and also crops out in other areas south of Lago Argentino. Feruglio (1944) described the Estratos del Chorrillo as consisting of yellow, grey and grey-blue sandy clay and clayey sandstone layers that separate yellow, violet, grey-blue and grey-green sandstone banks that are up to 50 m thick. Lenses of white puddingstone also occur. Furthermore, he identified terrestrial plants (leaves and wood), fragments of dinosaur bones and occasional marine mollusks interspersed at different levels in the strata. In particular, he noted that the upper-most portion of the Estratos del Chorrillo yields well-preserved dicot leaves. This strata is estimated to be at least 140 m to perhaps 230 m thick. Feruglio (1944) proposed that this strata is continental based on the presence of dinosaur bones.

Furque and Camacho (1972) described the Chorrillo Formation as being exposed in the Arroyo Moyano and on the western slope of Cerro Redondo. Here, the unit is 200 m thick and its lithology consists predominantly of fine sandstones and claystones with a few horizons containing conglomerates, concretions and coal lenses. Dinosaur bone fragments, fossil leaves and wood were identified; however, no invertebrate fossils were discovered despite Feruglio's earlier report of such fossils in these strata (Feruglio, 1938a, b). Furque and Camacho (1972) suggested that the age of the Chorrillo Formation is Maastrichtian based on sequence stratigraphy (lying above the La Anita Formation and below the Calafate Formation). They concluded that the Chorrillo Formation represents continental facies deposited during a regression (Furque and Camacho, 1972).

Leanza (1972) described the Chorrillo Formation as a 300 m thick, occasionally clayey, sandstone unit that was laid down in a continental environment. The only fossils that he was able to find were dinosaur bones. Furthermore, he also suggested that the Chorrillo Formation is Maastrichtian based on the underlying and overlying units (Leanza, 1972).

The Chorrillo Formation was later described as cropping out from the southern margin of Lago Argentino north to Cerro Fortaleza by Nullo et al. (1981a). They described the type section as being located at the headwaters of the Arroyo Chorrillo Malo located just to the west of the Estancia Anita. Furthermore, Nullo et al. (1981a) considered the "Estratos de Pari Aike" and Horizon C of Feruglio (1938a) as a junior synonym to the Chorrillo Formation. They proposed that the Chorrillo Formation represents a period of southward continentalization of the basin. In agreement with previous authors, they also postulated that the age of the Chorrillo Formation is Upper

Campanian or Maastrichtian based on the underlying (La Anita) and overlying (Calafate) formations (Nullo et al., 1981a).

Arbe and Hechem (1984) distinguished the Chorrillo Formation as distinct from the Cerro Fortaleza (Pari Aike) Formation because of the sediments and cycles of deposition. They identified outcrops belonging to the Chorrillo Formation in the northern and southwestern sections of Lago Argentino. This formation overlies and is separated from the La Irene Member of the La Anita Formation by a paraconformity (Figure 1.9). The Chorrillo Formation consists of conglomerates deposited in a high energy environment followed by deposition of siltstones and claystones in a palustrine environment and, lastly, by medium grained cross-bedded sandstones from a meandering river environment. The base of the Chorrillo Formation contains dinosaur skeletons and other vertebrate remains, while the uppermost section contains plant fossils (i.e., *Podocarpus* sp., *Myrica mira*, *Cladophlebis* sp., *Laurelia* sp., *Nothofagus* sp. and *Blechnum* sp.) (Arrondo, 1983). Arbe and Hechem (1984) suggested that a drop in sea level, further subsidence to the east, and reactivation of a sediment supply to the north created westward continental (fluvio-palustrine) expansion that led to the deposition of the Chorrillo Formation.

Macellari et al. (1989) proposed that the Chorrillo Formation is much thicker than previously estimated. They posited that the thickness of the formation ranges from 50 m (near El Calafate) to 820 m (~30 km southwest of El Calafate). This unit is primarily comprised of fining-upward cycles of sandstones and shales with tuff horizons occurring in the uppermost portion. Additionally, shallow marine bivalves, oysters and plant fossils occur in two specific horizons. Macellari et al. (1989) interpreted this formation as

representing a meandering fluvial environment with thick overbank deposits. Southward, these deposits include possible estuarine and shallow water facies. This formation interdigitates with and overlies the La Irene Formation (Figure 1.9) (Macellari et al., 1989).

Late Cretaceous Depositional Cycles in the area of Lago Viedma/Lago Argentino

Arbe and Hechem (1984) were the first to propose depositional cycles for the Upper Cretaceous strata in the area of the Río La Leona and Lago Viedma and Lago Argentino. The formations (Alta Vista, La Anita, Cerro Fortaleza, Chorrillo and Calafate) in this region represent two depositional cycles in the Austral Basin. The first comprising the Alta Vista, La Anita and Cerro Fortaleza formations, was a result of regression and continental expansion (via deltas, rivers and wetlands) that occurred throughout the Campanian. The delta and river systems deposited by these Upper Cretaceous formations appear to trend north to south, overall, while developing subaerial environments on the western margin of the basin. To the east, tectonic subsidence prevented well-established continental habitats from occurring; rather it only permitted marshy-type environments to persist. The second cycle that Arbe and Hechem (1984) proposed occurred during the upper Campanian-Maastrichtian (Chorrillo and Calafate Formations). This cycle also consists of a regression and subsequent transgression that resulted in the sedimentation of extensive fluvial and estuarine deposits, respectively (Arbe and Hechem, 1984).

Macellari et al. (1989) also analyzed the Upper Cretaceous-Paleocene depositional systems of the Austral Basin. They divided these sediments into three

sequences, all bounded by unconformities. Sequence I consists of the Tres Pasos, Alta Visa, La Anita and Cerro Fortaleza formations (Figure 1.11). This sequence began with the deposition of the marine Tres Pasos and Alta Vista formations during a lowstand system tract. The subsequent transgressive system tract deposited the shallow marine Asunción Member of the La Anita Formation northward as sea level inundated the continental shelf. The highstand system tract that followed led to continental expansion consisting of a southwestward progradating delta system (El Barco Member) and meandering river valley (Cerro Fortaleza Formation) (Figure 1.11). Sandstone petrography indicates a continental margin provenance (predominantly metamorphosed quartz, quartzite and recycled siliceous volcanic rocks) for the La Anita, Cerro Fortaleza and La Irene formations. The source of the sediments are postulated to have been from the northeast and northwest (Macellari et al., 1989). An erosional unconformity separates sequence 1 and 2. The unconformity may be due to either eustatic changes or tectonic reactivation of the sedimentary source. Sequence 2 thickens southward from 25 m (Cerro Fortaleza) to 760 m (~30 km south of Lago Argentino) and ranges in age from the Maastrichtian-earliest Paleocene (Macellari et al., 1989). There is no delta system in this sequence. Rather, the northern part of the basin consists of braided fluvial systems (La Irene Formation) that grade into meandering fluvial and fluvio-lacustrine (Chorrillo Formation) and finally into marine (Cerro Cazador Formation) facies. Reactivation of volcanoes to the west during the early part of the sequence led to the deposition of andesite dominated sediments. Abundant volcanism continued in the region into the early Tertiary (Figure 1.11) (Macellari et al., 1989).

In his most recent publication, Arbe (2002) reexamined the tectono-sedimentary cycles for the Cretaceous of Santa Cruz Province that he had originally described (Arbe, 1986, 1987; Arbe and Hechem, 1984). The sedimentary cycles are grouped into distinct units bounded by unconformities (disconformity or paraconformity), and are interpreted to have been as the result of the tectono-sedimentary evolution of the basin. Both second and third order depositional cycles are recognized and described by Arbe (2002). The third-order depositional cycles are proposed to have been a function of eustatic control while the second-order cycles were tectonically derived. The sequences are as follows: Río Mayer (Berriasian-early Aptian), Lago San Martín (early Aptian-Early Turonian), and Lago Viedma (early Turonian-Maastrichtian). The sediments exposed around Lago Viedma and Lago Argentino are placed within the Lago Viedma Cycle. This cycle is separated from the San Martín Lago Cycle by a discontinuity at 93 Ma. The Lago Viedma Cycle is subdivided into the Mata Amarilla and Anita Sub-Cycles (Arbe, 1986, 1987). The Mata Amarilla Sub-Cycle is a transgressive aggradational-progradational parasequences that contains the Puesto El Moro Formation (continental), Mata Amarilla Formation (littoral), Puesto El Álamo Formation (platform) and Cerro Toro Formation (bathyal and abyssal) (Figure 1.10). This sub-cycle ranges from the late Cenomanian/Early Turonian (93-91.5) to the early Santonian (85 Ma) (Arbe, 1986, 1987; Arbe and Hechem, 1984; Nullo et al., 1999). The subsequent Anita Sub-Cycle is a regressional parasequence consisting of the Cardiel (continental), La Anita (littoral), Cerro Fortaleza (continental), La Irene (continental), Chorrillo (continental) and Cerro Cazador (continental/littoral) Formations (Figure 1.10). This sub-cycle ranges from the late Santonian-Maastrichtian (85-68 Ma).

DISCUSSION

The geology of the region surrounding Lago Viedma and Lago Argentino is adequately established with the exception of the Cerro Fortaleza/Pari Aike Formation. The basic geological framework of the region was established by Feruglio (1938a, b; 1944). He coined the names Mata Amarilla, Pari Aike, Anita and Chorrillo for the Upper Cretaceous strata in the region.

The Mata Amarilla Formation is primarily found in the Río Shehuen Valley (including Tres Lagos, Piedra Clavada and Estancia Mata Amarilla). Outcrops have been reported further to the north, south and west; however, there is little consensus as to the full geographical extent of the formation (Arbe, 2002; Feruglio, 1938a, b, 1944; Goin et al., 2002; Iglesias et al., 2007; Leanza, 1972; Nullo et al., 1999; Nullo et al., 1981a; O'Gorman and Varela, 2010; Riccardi and Rolleri, 1980; Varela, 2009, 2010a, b; Varela et al., 2010). The Mata Amarilla Formation consists predominantly of mudstones in its lower half and interbedded mudstones and sandstones in its upper half (Arbe, 2002; Feruglio, 1938a, 1944; Goin et al., 2002; Iglesias et al., 2007; O'Gorman and Varela, 2010; Varela, 2009, 2010a, b; Varela et al., 2010). Tidal and tsunami deposits have been reported in the lower strata (Arbe, 2002; Varela, 2010a; Varela et al., 2010). Additionally, paleosols are present throughout the formation, but are particularly frequent in the upper horizons (Varela, 2010a, b). Fossils occur throughout the Mata Amarilla Formation but marine fossils are predominantly situated in the lower half of the unit. Fossils that have been discovered include: algae, angiosperms, gymnosperms, ferns bivalves, gastropods, ammonites, lungfish, semionotiforms/lepisosteiforms, plesiosaurs, dinosaurs, turtles and crocodilians (Agnolin, 2010; Arbe, 2002; Arrondo, 1983; Feruglio,

1938a, b, 1944; Goin et al., 2002; Iglesias et al., 2007; Leanza, 1972; Nullo et al., 1999; Nullo et al., 1981a; O'Gorman and Varela, 2010; Riccardi and Rolleri, 1980; Varela, 2009, 2010a, b; Varela et al., 2010). Overall, the Mata Amarilla Formation is interpreted to be composed of marine and fluvial paleoenvironments. Most authors agree that the lower half of the formation was deposited in coastal environments with periodic marine incursions. The upper half of the formation is interpreted to have been laid down in a fluvial environment that experienced frequent flooding events (Arbe, 2002; Feruglio, 1938a, b, 1944; Goin et al., 2002; Iglesias et al., 2007; Leanza, 1972; Nullo et al., 1999; Nullo et al., 1981a; O'Gorman and Varela, 2010; Riccardi and Rolleri, 1980; Varela, 2009, 2010a, b; Varela et al., 2010). A complete list of proposed Mata Amarilla paleoenvironments include: lagoon, estuary/bayhead delta, coastal plain, distal fluvial system, meandering fluvial system with low sinuosity, meandering river with high sinuosity, and braided fluvial system (Varela, 2010a). Based on the geology and fossils of the Mata Amarilla Formation, it is interpreted to have experienced a humid, warm temperate (seasonally tropical) paleoclimate (Goin et al., 2002; Varela, 2010a, b). The age of the formation is currently considered to range from the Cenomanian-Coniacian (Figure 1.8) (Leanza, 1972; O'Gorman and Varela, 2010; Varela, 2009, 2010a, b; Varela et al., 2010). Lastly, the Mata Amarilla Formation is an aggradational-progradational parasequence that was deposited during a transgressive cycle (Arbe, 1986, 1987, 2002).

The La Anita Formation crops out north and south of Lago Argentino and along the Río La Leona. It is composed of well-cemented cross-bedded sandstones, interbedded with mudstones and conglomerate lenses (Arbe, 1986, 1987, 2002; Arbe and Hechem, 1984; Feruglio, 1938a, c, 1944; Kraemer and Riccardi, 1997; Leanza, 1972;

Macellari et al., 1989; Marenssi et al., 2003). The La Anita Formation is divided into three members: El Barco, Chachorro and La Asunción. These members were laid down in a prograding delta system that includes delta front, plain and margin facies (Arbe, 1986, 1987, 2002; Arbe and Hechem, 1984; Kraemer and Riccardi, 1997; Macellari et al., 1989). Thus, the formation consists of subtidal, intertidal and coastal deposits (Arbe, 1986, 1987, 2002; Arbe and Hechem, 1984; Macellari et al., 1989; Marenssi et al., 2003). Fossil leaves, wood, bivalves, gastropods, ammonites, selachian teeth, and at least one plesiosaur are reported from the La Anita Formation (Arbe, 1986, 1987, 2002; Arbe and Hechem, 1984; Feruglio, 1938a, c, 1944; Kraemer and Riccardi, 1997; Leanza, 1972; Macellari et al., 1989; Marenssi et al., 2003). Most authors agree that the age of this formation is late Campanian based on the biostratigraphy (Arbe, 1986, 2002; Arbe and Hechem, 1984; Furque and Camacho, 1972; Kraemer and Riccardi, 1997; Macellari et al., 1989). The La Anita Formation is proposed to have been deposited during a regression which resulted in continental expansion to the south and west (Arbe, 1986, 1987, 2002; Arbe and Hechem, 1984; Macellari et al., 1989)

The La Irene Formation was initially defined as a member of the La Anita Formation; however, it is now considered to be a discrete formation (Arbe, 1987, 2002; Arbe and Hechem, 1984; Kraemer and Riccardi, 1997; Macellari et al., 1989; Povilauskas et al., 2008). It crops out both north and south of Lago Argentino and along the Río La Leona (Arbe, 2002; Arbe and Hechem, 1984; Macellari et al., 1989). The La Irene Formation is composed of fining upward cycles of cross-bedded conglomerates, sandstones and mudstones. It is interpreted to have been laid down in a high energy, possibly braided, fluvial environment with putative tidal influences (Arbe, 2002; Arbe

and Hechem, 1984; Kraemer and Riccardi, 1997; Macellari et al., 1989; Povilauskas et al., 2008). Angiosperms, gymnosperms, ferns, bryophytes, fungi and dinoflagellates have all been identified from the La Irene Formation (Kraemer and Riccardi, 1997; Povilauskas et al., 2008). Furthermore, the paleoclimate is interpreted to have been warm-temperate to warm-wet based on the palynological evidence (Povilauskas et al., 2008). Most authors agree that the La Irene Formation is Maastrichtian in age (Arbe, 2002; Kraemer and Riccardi, 1997; Macellari et al., 1989; Povilauskas et al., 2008).

Overlying the La Irene Formation is the Chorrillo Formation. Outcrops belonging to the Chorrillo Formation are exposed south of Lago Argentino (Feruglio, 1935, 1938a, b, 1944; Leanza, 1972; Macellari et al., 1989; Nullo et al., 1981a). The unit is composed of sandstones, mudstones units that contain conglomerate lenses (Arbe, 1986; Arbe and Hechem, 1984; Feruglio, 1935, 1938a, b, 1944; Furque and Camacho, 1972; Macellari et al., 1989). These are considered to have been deposited in a high energy meandering fluvial environment and low energy lacustrine/palustrine environments (Arbe and Hechem, 1984; Macellari et al., 1989). Angiosperms, gymnosperms, brachiopods, bivalves, gastropods, sharks and dinosaurs have all been reported from the Chorrillo Formation (Arbe and Hechem, 1984; Feruglio, 1935, 1938b; Leanza, 1972; Macellari et al., 1989). It is interpreted to be Maastrichtian in age based on the overlying (Calafate) and underlying (La Irene) formations (Arbe, 1987, 2002; Arbe and Hechem, 1984; Furque and Camacho, 1972; Leanza, 1972; Macellari et al., 1989; Nullo et al., 1981a).

Compared to the aforementioned formations, the Cerro Fortaleza/Pari Aike Formation is not as clearly agreed upon regarding paleoenvironments, stratigraphic relationships and ages. The “Estratos de Pari Aike” were initially named by Feruglio

(1938a, b) for outcrops in both the Río Shehuen (type section area) and the Río La Leona Valleys. He stated that the geology of the two localities is significantly different.

Confusion regarding the location of the type section and stratigraphic relationships of the Pari Aike Formation has led to a series of name changes for this and forthe Cerro Fortaleza Formation. Arbe and Hechem (1984) named the Upper Cretaceous fluvial outcrops in the Río La Leona Valley the Cerro Fortaleza Formation. They distinguished the Cerro Fortaleza Formation as a distinct from the Pari Aike Formation. Despite this, some authors have maintained the name Pari Aike Formation for the Upper Cretaceous outcrops in the Río La Leona Valley (e.g., Kraemer and Riccardi, 1997; Novas et al., 2002). Other authors consider the Pari Aike and Cerro Fortaleza formations to be junior synonyms of the Mata Amarilla Formation (Goin et al., 2002; Leanza, 1972; O'Gorman and Varela, 2010; Varela, 2010a) or the Chorrillo formations (Nullo et al., 1981a).

Based on the general location of the type locality of the Pari Aike Formation (around Lote 119) relative to the Mata Amarilla type section, it would not be surprising if, indeed, the Pari Aike Formation is one and the same as the Mata Amarilla Formation (Figure 1.3). The type section of the Pari Aike Formation is described as consisting of grey claystones with intercalations of sandstone and conglomerates (Arbe, 2002; Feruglio, 1938a, 1944; Goin et al., 2002; Iglesias et al., 2007; O'Gorman and Varela, 2010; Varela, 2009, 2010a, b; Varela et al., 2010). This is the same type of lithology described for the Mata Amarilla Formation. There has been virtually no consensus on the age or stratigraphic relationships of the Pari Aike Formation (outcrops far to the east of the Río La Leona Valley) (Arbe, 2002; Arbe and Hechem, 1984; Riccardi and Rolleri,

1980). Riccardi and Rolleri (1980) stated that, around Lago San Martín, the Pari Aike Formation overlies the Piedra Clavada Formation (Cenomanian) and in the Río Shehuen Valley, it is coeval with the Mata Amarilla Formation (Coniacian). Additionally, Arbe (1987) suggested that the Pari Aike Formation overlies the Mata Amarilla Formation and is overlain by the Man Aike Formation. Conversely, Arbe (2002) stated that the Pari Aike Formation overlies the La Irene Formation (Maastrichtian). Thus, further work is needed to establish if the Pari Aike Formation is a distinct formation from the Mata Amarilla Formation.

The Cerro Fortaleza Formation crops out along the Río La Leona and south of Lago Viedma. The type section is located on Cerro Fortaleza and, from hereon, any description of Upper Cretaceous, dinosaur-bearing sediments on or around Cerro Fortaleza, despite the name (e.g., Pari Aike, Mata Amarilla or Chorrillo) is included (Arbe, 1986, 1987; Arbe and Hechem, 1984). The Cerro Fortaleza Formation consists predominantly of cross-bedded friable sandstones interbedded with layers of mudstones and occasional coal horizons (Arbe, 1986, 1987; Arbe and Hechem, 1984; Feruglio, 1938a, 1944; Kraemer and Riccardi, 1997; Macellari et al., 1989; Marenssi et al., 2003; Novas et al., 2002; Riccardi and Rolleri, 1980). Paleosols and volcanic ash layers have also been reported (Arbe, 2002; Novas et al., 2002). Most authors consider the bulk of the Cerro Fortaleza Formation to have been deposited in a southwestern oriented meandering fluvial environment with the base also consisting of coastal plain environments (Arbe, 1986, 1987; Arbe and Hechem, 1984; Kraemer and Riccardi, 1997; Macellari et al., 1989; Marenssi et al., 2003; Novas et al., 2002; Riccardi and Rolleri, 1980). Based on the presence of paleosols and coal horizons, it is interpreted that the

climate was humid with intervals of high rainfall and a high water table (Macellari et al., 1989). Dinosaur bones, silicified wood, fossil pollen, bivalves, gastropods, ostracods and marine microplankton have been discovered in the Cerro Fortaleza Formation (Arbe and Hechem, 1984; Burmeister, 1892; Egerton et al., 2010; Ezcurra et al., 2010; Feruglio, 1935, 1938a, b, c, 1944; Kraemer and Riccardi, 1997; Lacovara et al., 2004; Marenssi et al., 2003; Novas et al., 2002; Novas et al., 2004; Novas et al., 2008; Novas et al., 2005b; Oviedo, 1982; Povilauskas et al., 2003). The Cerro Fortaleza Formation interdigitates with and overlies the deltatic facies of the La Anita Formation (Arbe, 1986, 1987, 2002; Arbe and Hechem, 1984; Kraemer and Riccardi, 1997; Macellari et al., 1989). In turn, the La Irene Formation overlies the Cerro Fortaleza Formation (Arbe, 2002; Arbe and Hechem, 1984; Kraemer and Riccardi, 1997; Macellari et al., 1989).

CONCLUSIONS

In conclusion, the name Cerro Fortaleza Formation should be retained for the Upper Cretaceous fluvial outcrops that overlie the La Anita Formation and are overlain by the La Irene Formation. Additionally, based on the well-established ages of the underlying La Anita (Campanian) and overlying La Irene (Maastrichtian) formations, the age of the Cerro Fortaleza Formation should be considered to be middle/late Campanian-early Maastrichtian.

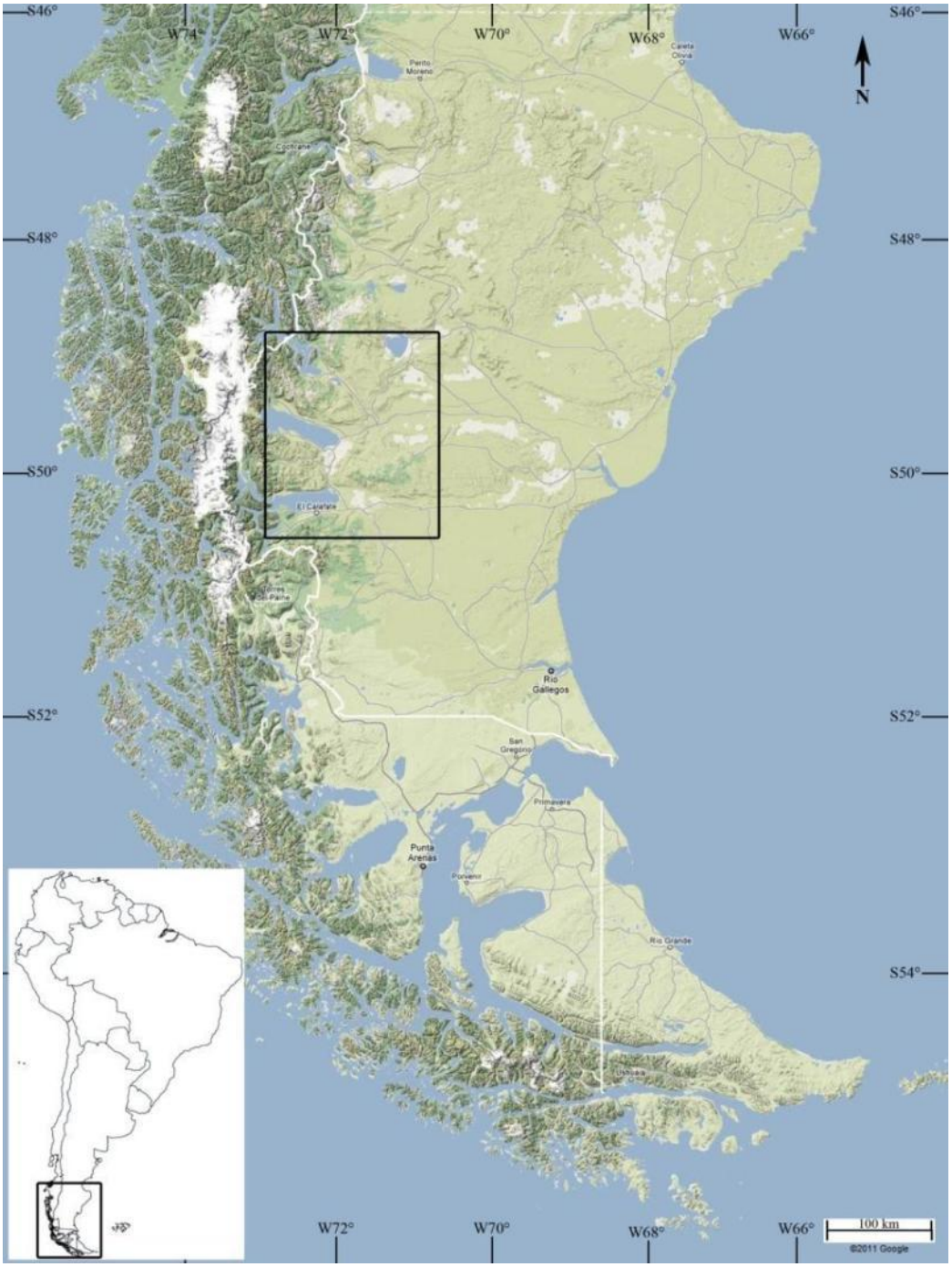

Figure 1.1. Southern Patagonian region of South America. Large inset Figure 1.3. Goggle Maps 2011.

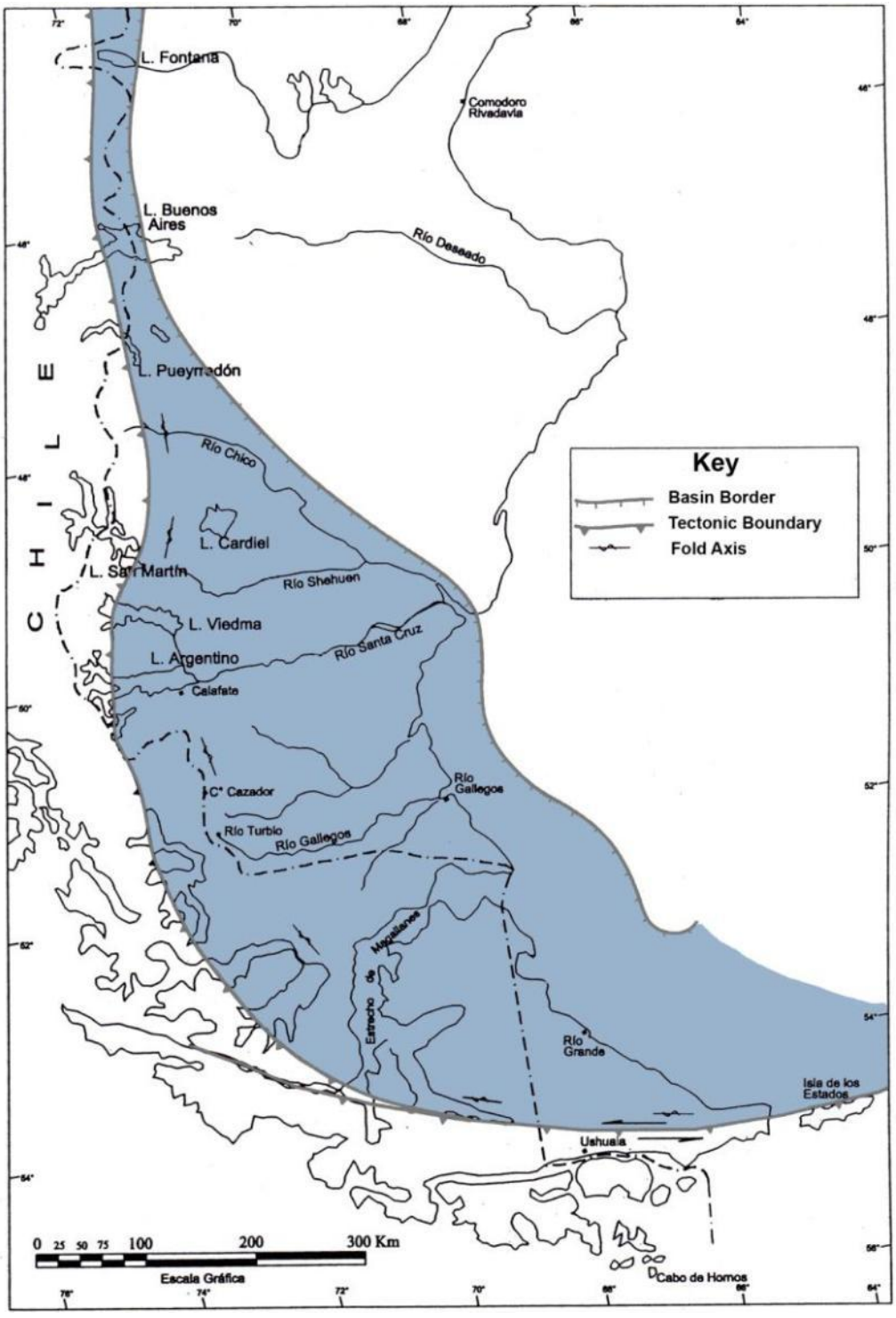

Figure 1.2. Austral Basin. Redrawn from Nullo (1999).

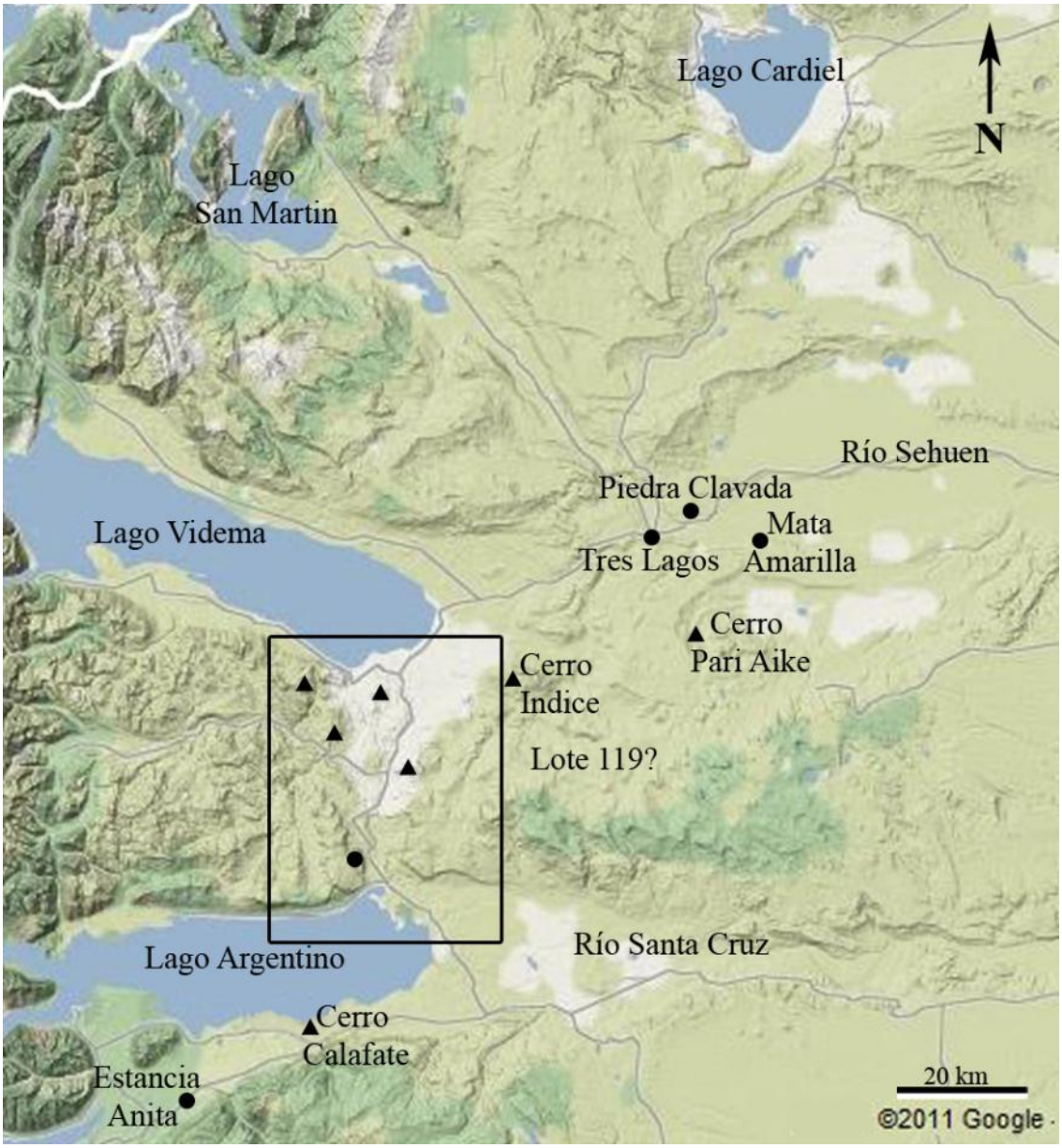

Figure 1.3. The study region. Triangles indicate hills (cerros) and circles indicate named locations. The location for Lote 119 was based on general area descriptions from Fergulio (1938a, 1944). Inset is Figure 1.4. Google Maps 2011.

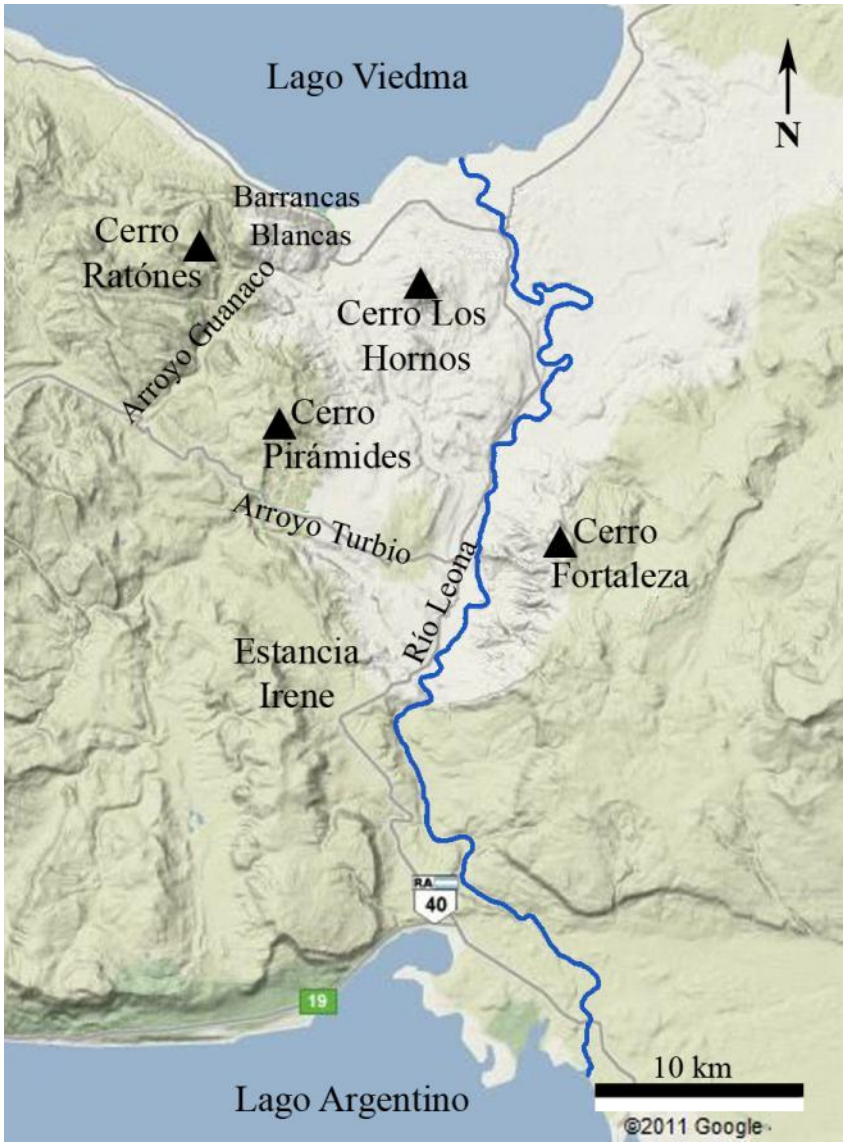

Figure 1.4. Río La Leona Valley. Major rivers (rios), streams (arroyos), hills (cerros, indicated by triangles) and other notable locations are identified. Note that the Estancia Irene location is based on the description from Macellari et al. (1989). Google Maps 2011.

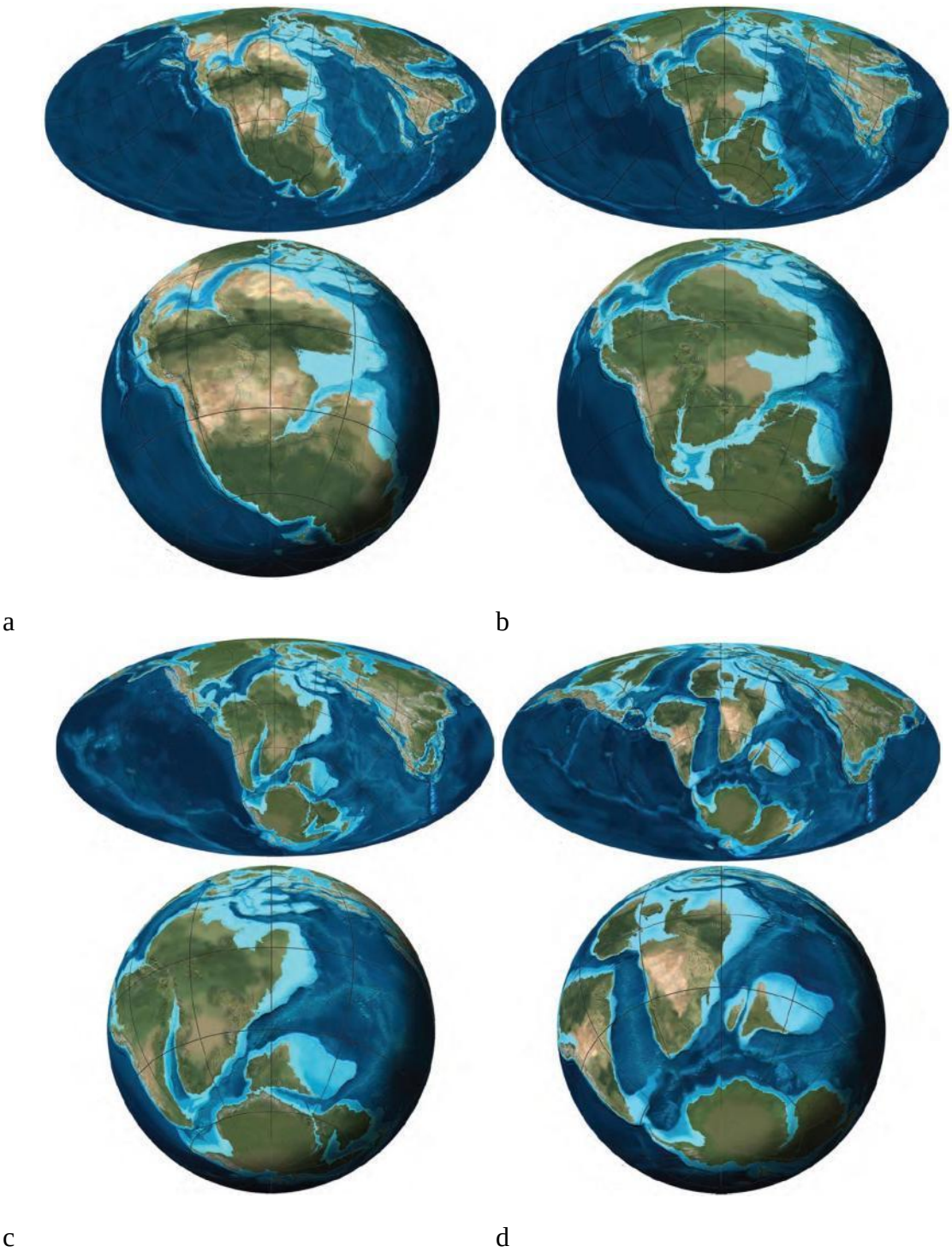

Figure 1.5. Paleogeography reconstructions showing southern South America for the: a. Middle Jurassic, b. Late Jurassic, c. Early Cretaceous, and d. and Late Cretaceous (Blakey, 2008).

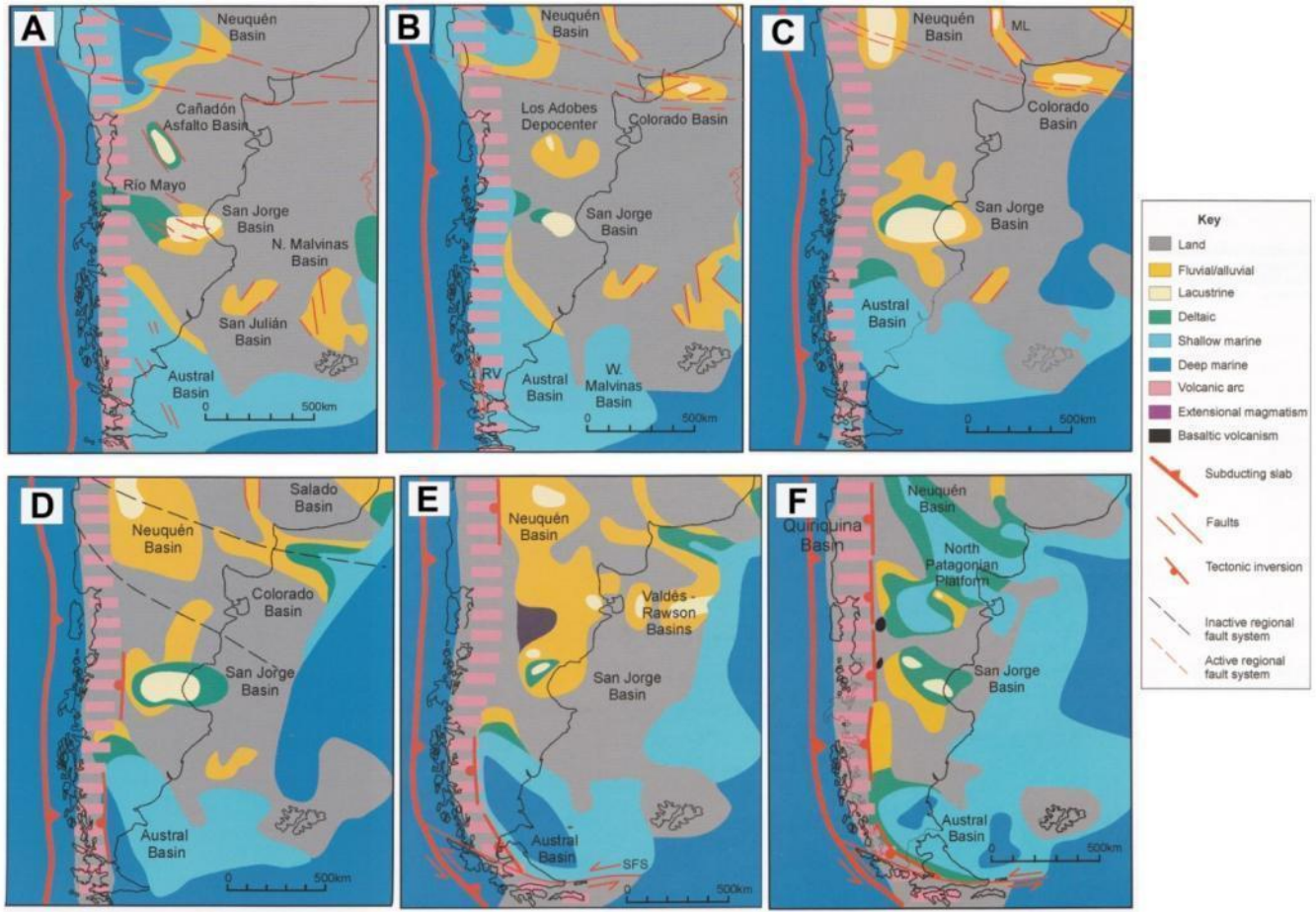

Figure 1.6. Paleogeographic maps of the Patagonian basins during the mid-late Cretaceous. a. Late Jurassic (Kimmeridgian-Tithonian). b. Early Cretaceous (Valanginian-Hauterivian). c. Early Cretaceous (Aptian). d. Early Cretaceous (Albian). e. Late Cretaceous (Cenomanian-Turonian). f. Late Cretaceous (Campanian-Maastrichtian) (after Spalletti and Franzese, 2007).

Figure 1.7. Geological map of Patagonia produced by Charles Darwin, circa 1840, unpublished (Cambridge University Library).

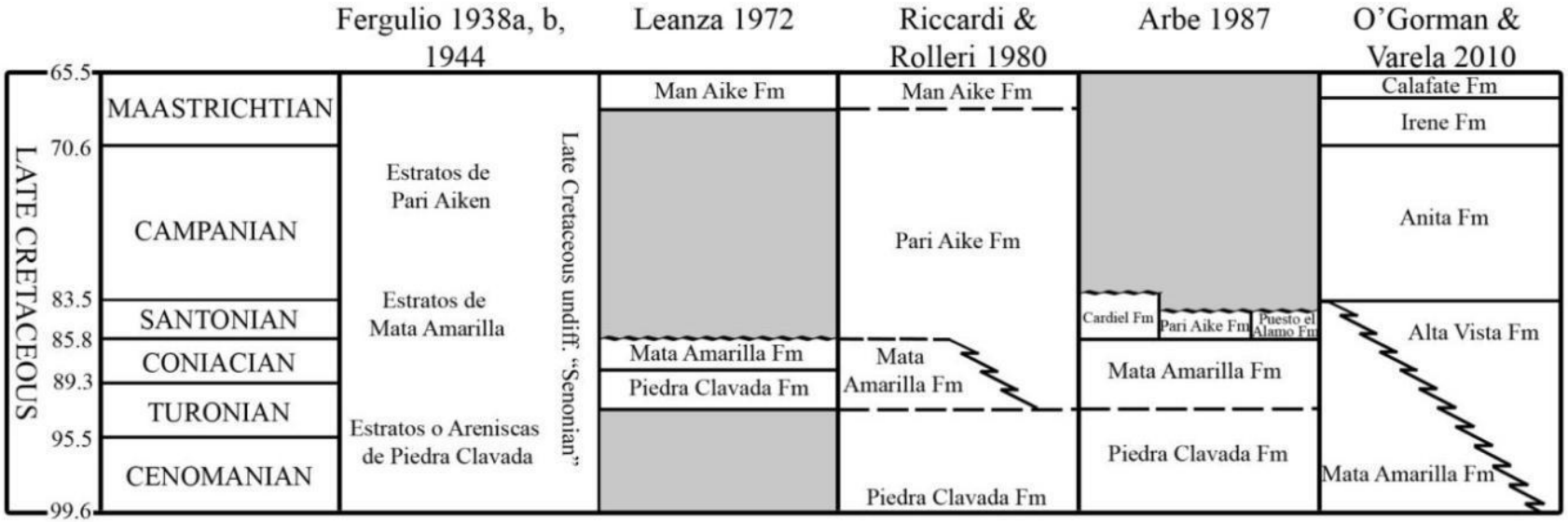

Figure 1.8. Stratigraphy of the Río Shehuen Valley. The schematic is based on both the text and figure information provided by the cited authors. If the text and figure information differ (e.g. Arbe, 1987) priority is given to the text. If multiple localities are given (e.g., Arbe 1987), a general column was created. Wavy horizontal lines indicates unconformities and dashed lines indicate paraconformities.

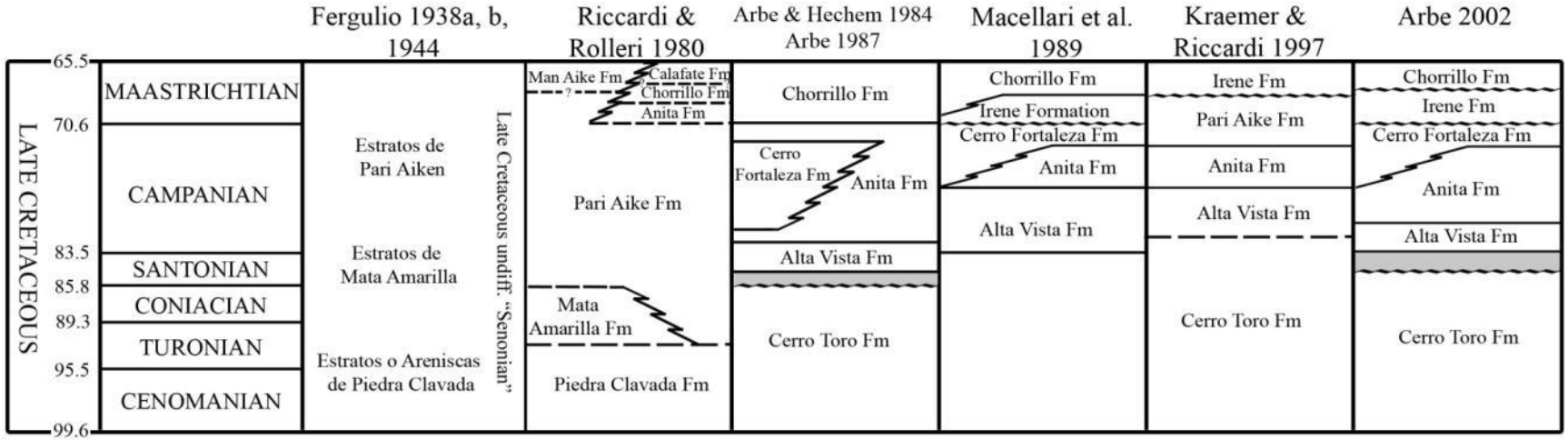

Figure 1.9. Stratigraphy column of the Río La Leona Valley and partly Lago Argentino. The schematic is based on both the text and figure information provided by the cited authors. If the text and figure information differ (e.g. Arbe, 1987) priority is given to the text. If multiple localities are given (e.g., Arbe 1987), a general column was created. Wavy horizontal lines indicates unconformities and dashed lines indicate paraconformities.

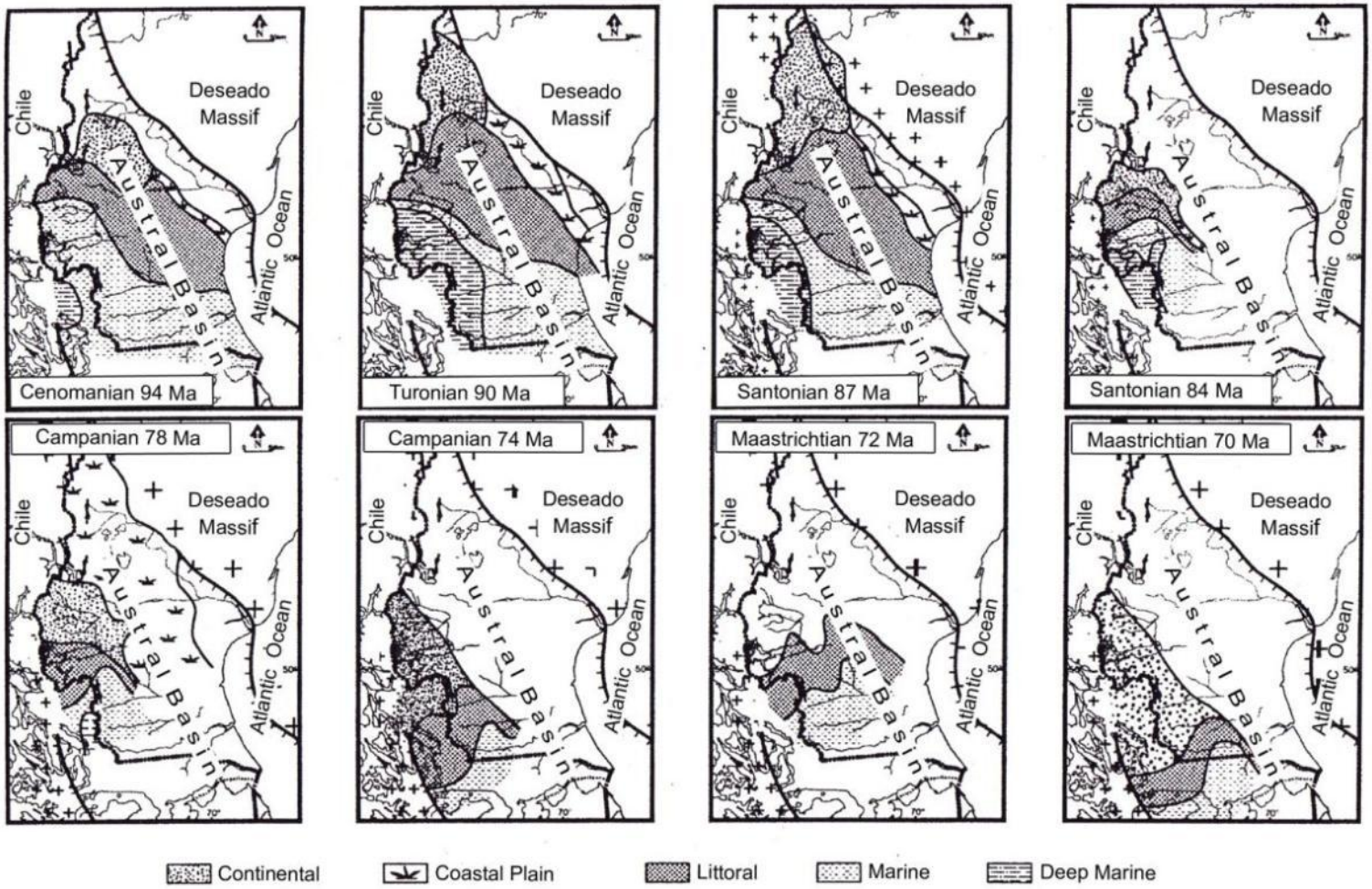

Figure 1.10. Paleoenvironments of the Austral Basin during the Late Cretaceous (after, Arbe, 2002).

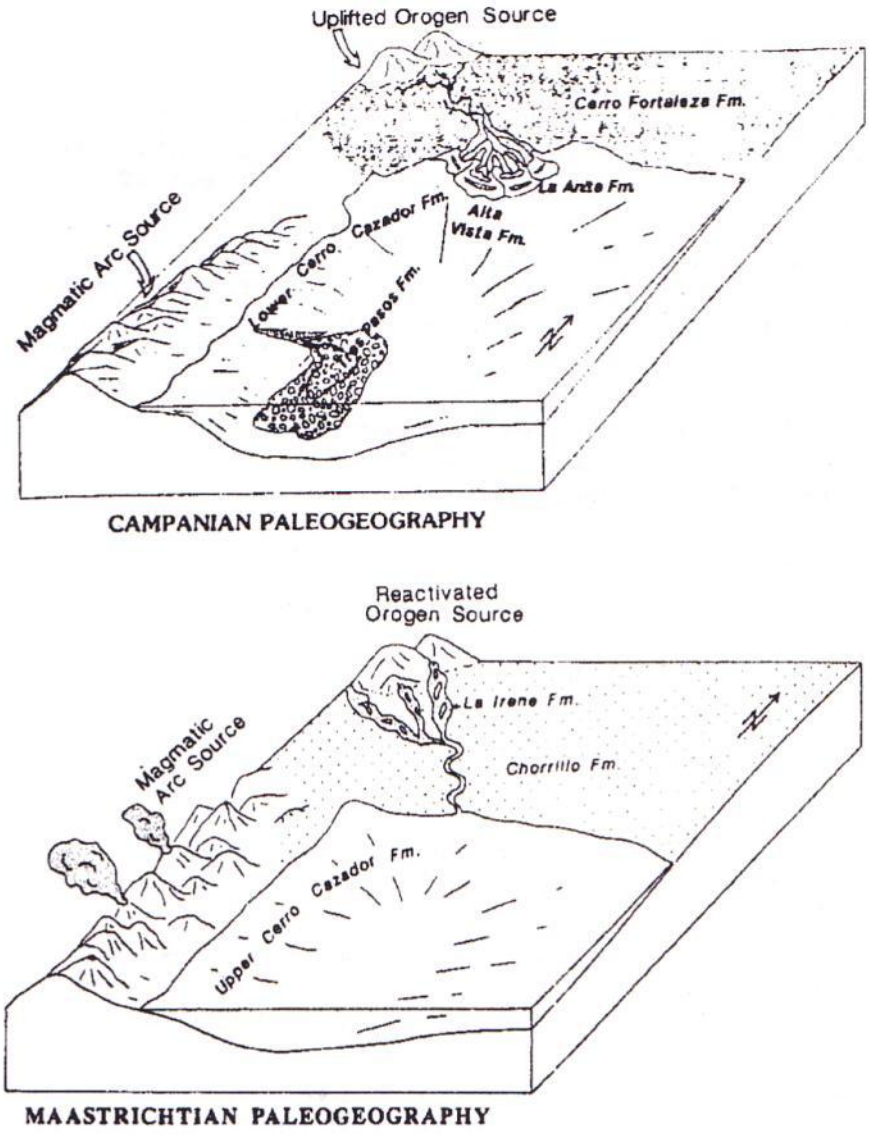

Figure 1.11. Paleogeographic reconstructions of the Austral Basin during the Campanian and Maastrichtian (from, Macellari et al., 1989).

Table 1.1. Summary of the nomenclature and age of dinosaur-bearing Upper Cretaceous sediments that crop out on Cerro Fortaleza.

Author(s)	Strata Name(s)	Age(s)	Location(s)	Paleoenvironment(s)	Fossils
Feruglio, 1938a, b	Horizon C	Late Cretaceous	Río Shehuen Valley (including Mata Amarilla and Pari Aike Estancias) and Leona Rio Valley	Estuarine, continental	Dinosaur bones, silicified wood
Feruglio, 1944	Estratos con Dinosaurios (text); Estratos de Pari Aike (table)	Late Cretaceous	Southeasterm shore of Lago Viedma, the Río Leona Valley, south to Lago Argentino	Continental	Dinosaur bones, silicified wood
Leanza, 1972	Mata Amarilla Fm	Coniacian	20 km south of Río Shehuen, on the same longitude line as Piedra Clavada	Not given	Dinosaur bones
Riccardi and Rolleri, 1980	Pari Aike Fm	Aptian/Albian-Maastrichtian	Lago Pueyrredón (north), to Lago Argentino (south), to the southern shores of the Río Shehuen (east), and Lago Cardiel (west)	Continental	Dinosaur bone, silicified wood, fragments

Table 1.1. continued

Author(s)	Strata Name(s)	Age(s)	Location(s)	Paleoenvironment(s)	Fossils
Nullo et al., 1981	Pari Aike	late Campanian-Maastrichtian	Lago Argentino north to Cerro Fortaleza	Continental	Dinosaur bones
Arbe and Hechem 1984; Arbe, 1986, 1987	Cerro Fortaleza Fm	early-mid Campanian	Along the Río Leona, Barrancas Blanca	Fluvial to palastrine and lagoons	Dinosaur bones, silificied wood, indet. plant fragments, gastropods, ostracods, angiosperm pollen
Macellari, et al. 1989	Cerro Fortelaza Fm	late Campanian	Río Leona Valley south to Lago Argentino	Meandering fluvial	Plants
Kraemer and Riccardi, 1997	Pari Aike Fm	Coniacian-Maastrichtian (text); Maastrichtian (fig.)	Río Leona Valley, Arroyo Turbio, Cañadón Hondo and the southern margin of the Arroyo Guanaco	Meandering fluvial	Dinosaur bones, silicified wood, indeterminate plant material, bivalves (e.g. *Ostrea* sp., *Melanopsis* sp.), gastropods, pollen, microplankton

Table 1.1. continued

Author(s)	Strata Name(s)	Age(s)	Location(s)	Paleoenvironment(s)	Fossils
Arbe, 2002	Cerro Fortaleza Fm	Campanian (fig. 1); Santonian-Campanian (fig. 6)	South of San Martin Lake, east of Lake Viedma,and along the Río Leona Valley	Fluvial to wetlands	Dinosaur bones, bivalve and gastropod traces
Novas, et al. 2002	Pari Aike Fm	Coniacian-Santonian	Southern shore of Lago Viedma, Barrancas Blancas and along the Río Leona	Meadering fluvial	Dinosaur bones, silicified wood, microplankton, mollusks
Goin et al., 2002	Mata Amarilla	Upper Cretaceous	Río Shehuen Valley and Río Leona Valley	Continental	Vertebrate bones, marine fossils
Marenssi, et al. 2003	Cerro Fortelaza Fm	Campanian-Maastrichtian	Río Leona Valley	Transitional, lagoon/coastal plain and fluvial	Dinosaur bones, silicified wood

Table 1.1. continued

Author(s)	Strata Name(s)	Age(s)	Location(s)	Paleoenvironment(s)	Fossils
O'Gorman and Varela, 2010; Varela, 2010a	Mata Amarilla Fm	Cenomanian	Río Shehuen Valley and Río Leona Valley	Mata Amarilla: lagoon, estuary and bayhead delta, coastal plain, distal fluvial system, meandering fluvial system with low sinuosity, meandering river with high sinuosity, and a braided fluvial system	Dinosaur bones, plesiosaurs

CHAPTER 2: GYMNOSPERM WOOD FROM THE CERRO FORTALEZA FORMATION

INTRODUCTION

The record of Cretaceous gymnosperm wood in southern South America is relatively incomplete compared to the rest of Gondwana (Herbst et al., 2007; Philippe et al., 2004). The fossil record of wood is an essential component for understanding major flora turnover events such as the Late Cretaceous gymnosperm to angiosperm turnover. During the Late Cretaceous, world-wide gymnosperm abundance and diversity declined as angiosperm abundance and diversity increased (e.g. Crane, 1987; Stewart and Rothwell, 1993; Willis and McElwain, 2002). The Gondwanan floras were no different. The relative abundance of gymnosperm woods in the Antarctic Peninsula decreased from 75-80% of the overall fossil wood flora during the Early Cretaceous, down to 25% by the Late Cretaceous. Thus, the overall forest canopy and understory changed dramatically in a relatively short time (Cantrill and Poole, 2005). This turnover would have had dramatic effects on the general ecology of the region and the world.

The study of southern Patagonia Cretaceous paleobotany is still in its infancy. The Austral Basin is no different. Only two primary studies have been published on the paleobotany of this region. The first study was conducted by Iglesias et al. (2007) on fossil leaves from the Mata Amarilla Formation (Coniacian). They found that the gymnosperms were relatively rare and comprised a small fraction of the overall flora (8%) (Iglesias et al., 2007). A second study focused on the palynology of the Irene

Formation (Maastrichtian) (Povilauskas et al., 2008). They reaffirmed that fern and angiosperm palynomorphs were far more abundant than those produced by gymnosperm. Other than those two studies, there has been little published on the fossil flora of the Austral Basin despite it being ephemerally mentioned in the literature. The Mata Amarilla Formation (Coniacian) is known for its petrified wood, including the "Maria Elena" Petrified Forest; with published abstracts being the only literature published on this material (Iglesias et al., 2007; Riccardi and Rolleri, 1980; Varela, 2010a, b). The Irene Formation (Maastrichtian) is also reported to yield silicified wood and fossil leaves (Arbe and Hechem, 1984; Arrondo, 1983; Feruglio, 1938a, b, 1944; Furque and Camacho, 1972; Kraemer and Riccardi, 1997; Macellari et al., 1989).

Fossil wood assemblages from the Cerro Fortaleza Formation (Campanian) has been studied since 1892 (Burmeister, 1892). Subsequent researchers have also noted the presence of silicified wood and other plant material (Arbe and Hechem, 1984; Feruglio, 1938a; Kraemer and Riccardi, 1997; Macellari et al., 1989; Marenssi et al., 2003; Novas et al., 2002; Riccardi and Rolleri, 1980) and one unpublished (and unattainable) dissertation has examined the fossil pollen (Oviedo, 1982). However, very little is known about this flora (Egerton et al., 2010; Povilauskas et al., 2003). The aim of this chapter is to identify and describe the gymnosperm fossil wood from the Cerro Fortaleza Formation and to compare this wood flora to others from Gondwana. Additionally, the relative abundance of gymnosperm to angiosperm fossil wood occurrences is examined to ascertain the magnitude of the gymnosperm to angiosperm turnover had on this flora.

GEOLOGICAL SUMMARY

The Cerro Fortaleza Formation is located in the Río La Leona Valley of Santa Cruz Province, Argentina. This formation consists predominantly of cross-bedded friable sandstones interbedded with layers of mudstones and occasional coal horizons (Arbe, 1986, 1987; Arbe and Hechem, 1984; Feruglio, 1938a, 1944; Kraemer and Riccardi, 1997; Macellari et al., 1989; Marenssi et al., 2003; Novas et al., 2002; Riccardi and Rolleri, 1980). Paleosols, volcanic ash and marine intercalations have also been reported within the succession (Arbe, 2002; Novas et al., 2002). Most authors consider the bulk of the Cerro Fortaleza Formation to have been deposited in a southwestern oriented meandering fluvial environment; however, the base of the formation also consists of coastal floodplain environments in the uppermost strata of the formation (Arbe, 1986, 1987; Arbe and Hechem, 1984; Kraemer and Riccardi, 1997; Macellari et al., 1989; Marenssi et al., 2003; Novas et al., 2002; Riccardi and Rolleri, 1980). Based on the presence of paleosols and coal horizons, it is interpreted that the climate was humid with intervals of high rainfall and a high water table (Macellari et al., 1989). Dinosaur bones, turtle bones, silicified wood, fossil pollen, shark teeth, lungfish tooth plates, fish scales, mollusks, bivalves, gastropods, ostracods and marine microplankton have been discovered in the Cerro Fortaleza Formation (Arbe and Hechem, 1984; Egerton et al., 2010; Ezcurra et al., 2010; Feruglio, 1938a, 1944; Kraemer and Riccardi, 1997; Lacovara et al., 2004; Marenssi et al., 2003; Novas et al., 2002; Novas et al., 2004; Novas et al., 2008; Novas et al., 2005b; Oviedo, 1982; Povilauskas et al., 2003; Schroeter et al., in prep).

The Cerro Fortaleza Formation interdigitates and overlies the deltaic facies of the La Anita Formation (Early-Mid Campanian) (Arbe, 1986, 1987, 2002; Arbe and Hechem, 1984; Kraemer and Riccardi, 1997; Macellari et al., 1989). In turn, the braided fluvially lain La Irene Formation (Maastrichtian) overlies the Cerro Fortaleza Formation (Arbe, 2002; Arbe and Hechem, 1984; Kraemer and Riccardi, 1997; Macellari et al., 1989). The age of the Cerro Fortaleza Formation, based on the underlying La Anita (Campanian) and overlying La Irene (Maastrichtian) Formations, is at most Late Campanian and at least Early Maastrichtian (Arbe, 1987, 2002; Arbe and Hechem, 1984; Kraemer and Riccardi, 1997; Macellari et al., 1989).

METHODS AND MATERIALS

Permineralized wood was collected from the Cerro Fortaleza Formation in February 2009. The samples were collected from three primary localities on the western flank of Cerro Fortaleza, near the Río La Leona. The three areas include: northern, southwestern and southeastern sites (Figures 2.1-2.4). The northern locality is close to a titanosaur dinosaur quarry (Figure 2.3); while the southwestern locality occurs near the banks of the Río La Leona; and the southeastern locality is high on a hill where titanosaur material was collected in 2003 (Figure 2.4). These areas were thoroughly explored in ordered to collect as many samples as possible. A total of twenty-five hand samples were collected from the exposures. The fossilized wood included fragments, over half a meter diameter logs and greater than 2.5 m long trunks (Figure 2.5). Latitude and longitude coordinates were recorded for each sample (Garmin eTrex Legend GPS unit) and all the

localities were photographed. Wood samples were initially examined with a 10x hand-lens to look for anatomical features in order to justify collection and subsequent thin-sectioning.

The fossil wood samples were made into polished thin-sectioned in Buenos Aries using standard techniques (Hass and Rowe, 1999). Each sample was sectioned along three different planes, transverse (TS), tangential longitudinal (TLS) and radial longitudinal (RLS), and mounted on glass slides. All three planes were required to identify and analyze salient morphological features. The thin sections were examined in February 2010 using transmitted light spectroscopy (a Leica DM2500 microscope with a Leica DFC290 camera attachment and an Olympus BX51 microscope with a DP25 camera attachment) at the Museo Argentino de Ciencias Naturales, Buenos Aires, Argentina. Digital photomicrographs were taken of all key morphological features. Descriptions and identification were conducted through reference to literature (e.g., Barefoot and Hankins, 1982; Hoadley, 1990; IAWA, 2004; Philippe and Bamford, 2008) and computerized wood databases (e.g., InsideWood, 2004-onwards). The permineralized wood was described in accordance to the International Association of Wood Anatomists (IAWA) standards of wood morphology (IAWA, 2004). The specimens are curated at the Museo de Perito Moreno in Rio Gallegos, Argentina.

Precise measurements were taken of specific morphological features that were diagnostic to each taxon. The percentage of uniseriate to biseriate bordered pits on the radial walls of tracheids (RLS) was determined from 100 independent sections of tracheids (mid-section and one end of the tracheid). Earlywood radial and tangential

diameters were measured in TS and for 50 tracheids. The bordered pit width on the radial walls of the tracheids (RLS) was determined for 50 pits. Lastly, the ray height in number of cells in TLS and the percentage of uniseriate to biseriate rays were recorded for 50 rays. When more than one sample occurred for a particular morphogenus (e.g. *Agathoxylon*), the average of all of the measurements for that taxon was given in the description. The original measurements for each specimen have been listed in Table 2.1.

Gymnosperm wood is morphologically very conservative with only subtle differences separating extant families and genera. The differences between genera can be so subtle that it is often difficult to assign extant wood to a particular genus or, especially, to the species level. Additionally, significant variation in wood morphology can occur throughout an individual tree. Branches, roots and the trunk (pith and cambrium) can all yield slight to significant variations in morphology (e.g. tracheid size and abundance of axial parenchyma). Ontogeny (e.g. sapling vs. mature stems) can also affect the morphology of many anatomical features (Barefoot and Hankins, 1982; Falcon-Lang and Cantrill, 2000; Wheeler and Baas, 1998; Wheeler and Lehman, 2005). Lastly, the taphonomic history can affect the preservation of key features (e.g. cross-field pitting type) (Gerards et al., 2007; Tarmian et al., 2011; Wheeler and Baas, 1998). Therefore, no attempt was made to assign any specimen to a particular morphospecies. If there were differences among specimens assigned to the same morphogenus, they were denoted by the morphogenus name and a number (e.g. *Taxodioxylon* sp. 1 and *Taxodioxylon* sp. 2).

SYSTEMATIC PALEOBOTANY

Order: Coniferales

Family: Araucariaceae

Morphogenus: *Agathoxylon* Hartig 1848

Type species: *Agathoxylon cordaiatum* Hartig 1848

Agathoxylon sp.

Material: MPM-8, MPM-21, MPM-23, MPM-32

Description: Growth rings are distinct with a narrow latewood zone (1-6 cells high). Growth rings from MPM-32 are distinguished due to earlywood crushing at the latewood/earlywood boundary and frost rings (Figure 2.6a, b). False rings are present in all the specimens. Axial parenchyma and resin canals are absent. The mean earlywood tracheid diameters are, radially, 32.5 µm (range 14-76 µm) and, tangentially, 26.5 µm (range 10-67 µm). Bordered pitting on the radial walls of the tracheids is predominantly uniseriate (95-100%) with a minor amount of alternate biseriate pitting and no opposite biseriate pitting. The bordered pits are arranged in a typical araucarian arrangement where the bordered pits touch and slightly compress neighboring pits (Figure 2.6c, e). The average diameter of the bordered pits is 14.5 µm (range 7-24 µm).

Ray parenchyma are horizontal with smooth end walls (Figure 2.6d, e, f). Ray tracheids are absent. Cross-field pits consist of 2-6, unordered, crowded pits with narrow, angled, elliptical apertures consistent with araucarioid cross-field pits (Figure 2.6d, e, f).

Tangential rays are predominantly uniseriate (69-100%) with some rays containing biseriate sections (Figure 2.6g, h). The average tangential ray height is 6.13 cells with the range being 1-28 cells.

Identification: Following both Kräusel's (1949) and Philippe and Bamford's (2008) keys, MPM-8, MPM-21, MPM-32 and MPM-23 belong to the morphogenera "Araucarioxylon" and *Agathoxylon*, respectively. "Araucarioxylon" has long been a commonly used morphogenera for Araucarian woods; however, its validity is debated (for complete discussion see Philippe, 2011). "Araucarioxylon" (Kraus, 1870) is considered to be a junior synonym to *Agathoxylon* (Hartig, 1848) because the latter is the earliest valid name (Philippe, 1993, 2011). Despite being officially designated as an illegitimate named by Philippe (1993), the morphogenus "Araucarioxylon" is still being used. *Agathoxylon* is distinguished by araucarian bordered pits on the radial walls of the tracheids, thin and unpitted ray walls thin, cross-fields containing many araucarioid pits and no resin canals (Hartig, 1848; Kräusel, 1949; Philippe and Bamford, 2008). All of the fossil wood described here (MPM-8, MPM-21, MPM-23 and MPM-32) are similar except that the overall tracheid size, bordered pit size and ray length in MPM-23 are greater than in the other specimens. Size variation may occur within an individual tree or

several trees of the same species; therefore , MPM-23 is lumped together with the other specimens (Falcon-Lang, 2005).

These Argentine specimens are similar to other material from Argentina, Antarctica and Chile. Pujana et al. (2007) describe seven specimens belonging to *Agathoxylon* from the Bajo Barreal Formation (Late Cretaceous) in Argentina. The diameters of the tracheids are larger (mean tangential diameter 35 µm, range 25-50 µm) in the Bajo Barreal material than in the Cerro Fortaleza material. Despite having larger tracheids, the border pit diameter in the Bajo Barreal material is approximately the same (~13 µm). Overall, the ray height of the Bajo Barreal material is much shorter than the Cerro Fortaleza material, typically 1-5 cells and up to 8 cells high; but the height does closely corresponds to one specimen, MPM-8, from Cerro Fortaleza. "Araucarioxylon" *chapmanae* was described from the Late Cretaceous of Livingston Island, Antarctic Peninsula (Poole and Cantrill, 2001a). In the Livingston Island material, there is significantly more biseriate bordered pitting (74% biseriate, 21% uniseriate, 5% triserate) and more pits per cross-field (2-11) than in the Cerro Fortaleza material. Additionally, the shape of the bordered pits is more polygonal-shaped in the Livingston Island material due to crowding in the tracheid. Terada et al. (2006b) identify two "Araucarioxylon" species from Eocene sediments in Chile: A. *pichasquense* and A. cf. *kellerense*. The tracheid diameters in "Araucarioxylon" *pichasquense* are, on average, larger (41.1 µm radially, 31.8 µm tangentially) than in the Cerro Fortaleza material. Additionally, there are more pits per cross-field 5-9 and only uniseriate rays. "Araucarioxylon" cf. *kellerense* is also quite different from the Cerro Fortaleza material in that the growth rings are indistinct; the bordered pitting on the radial walls of the tracheids are more

scattered; there are 4-6 pits per cross-field; and the rays are shorter 1-11 (mean 4.5) (Terada et al., 2006b).

Gondwanan distribution: Extant araucarians are restricted to the southern hemisphere. All extant araucarians are trees, some that exceeding 60 m in height (Kunzmann, 2007; Panti et al., 2011; Taylor et al., 2009). During the Mesozoic, Araucariaceae occurred in both hemispheres, primarily in high latitudes (Kunzmann, 2007). It has been proposed that Araucariaceae evolved during the Early Triassic (Kunzmann, 2007); however, other authors suggest that, based on wood anatomy, they occurred as far back as the Carboniferous and possibly even Devonian (Philippe, 2011). At least 400 morphospecies have been described and many more not ascribed to a particular species (e.g. *Agathoxylon* sp.) (Philippe, 2011). *Agathoxylon* has been recorded from at least 16 countries (including the continent of Antarctica) of the southern hemisphere from the Jurassic-Cretaceous (Philippe et al., 2004). From South America 17 *Agathoxylon* species have been recorded from the Jurassic-Cretaceous. Only 4 *Agathoxylon* species have been identified from the Jurassic of the Santa Cruz Province and none have been recognized from the Cretaceous until now (Panti et al., 2011). The majority of the material from the Cretaceous of this region (between 46°S and 52°S) has been identified from Chile and includes: *Agathoxylon* sp. (Philippe et al., 2000), "Araucarioxylon" sp. (Nishida et al., 1990), "Araucarioxylon" *ohzanum* (Nishida et al., 1992), "Araucarioxylon" *pichasquense* and "Araucarioxylon" *kellerense* (Nishida et al., 1992; Nishida et al., 1990).

Order: Coniferales

Family: Protopinaeae Kräusel (1949)

Morphogenus: *Planoxylon* Stopes (1916)

Type species: *Planoxylon hectori* Stopes (1916)

Planoxylon sp.

Material: MPM-9

Description: Growth ring boundaries are distinct with a narrow latewood zone and some earlywood crushing (Figure 2.7a, b). False rings are present throughout the specimen (Figure 2.7a, b). Axial parenchyma are present but rare. The mean earlywood tracheid diameter, radially, is 47 µm (range 29-79 µm) and, tangentially, is 39 µm (range 23-63 µm). Bordered pitting on the radial wall of the tracheid is a mix of both araucarian (dominant) and abietinean and consists of uniseriate (98%) and rare biseriate (exclusively alternate) pits (Figure 2.7c, d). The biseriate pits are restricted to the end walls of the tracheids (Figure 2.7d). Bordered pits are circular; although, more often, they are semi-circular due to slight compression from neighboring pits (Figure 2.7c, d). The average diameter of the bordered pits is 14 µm with the range being 8-20 µm. Spiral checking is present in some tracheids.

Cross-field pits are araucarioid, cupressoid and piceoid and contain 1-6 pits per cross-field, with the majority containing 2-4 pits and rarely 5-6 pits. These pits are

commonly obliquely angled with the pit aperture elliptical to slit-like (araucarioid and cupressoid); although some apertures are rounded (piceoid) (Figure 2.7e, f). Ray tracheids are absent. Abietineentüpfelungen ('abietinean pitting') can be identified on the transverse walls of some of the ray cells in both RLS and TLS (Figure 2.7g, h).

In TLS, rays are predominantly uniseriate (97%) with some local biseriation (Figure 2.7i). The mean ray height is 8.7 cells with a range of 2-21 cells. Tangential tracheid walls contain some bordered pits (Figure 2.7i).

Identification: Based on both Kräusel's (1949) and Philippe and Bamford's (2008) keys, this fossilized wood belongs to the morphogenus *Planoxylon*. However, *Planoxylon* only differs slightly from another morphogenus, *Araucariopitys.* It has been proposed that the two morphogenera should by unified into one; however, they are currently considered to be two unique morphogenera (see Philippe and Hayes, 2010) Following the Kräusel (1949) key, *Planoxylon* and *Araucariopitys* are both distinguished based on having a mixture of abietinean and araucarian bordered pits and abietineentüpfelungen tangential ray walls. Furthermore, Philippe and Bamford's (2008) key identifies both *Planoxylon* and *Araucariopitys* based on the terminal walls of ray cells either being pitted or thickened, abietineentüpfelungen (pitting) present on the transverse walls of the ray cell, and a mixture of araucarian and abietinean pitting on the radial walls of tracheids. In both keys, the two genera are only distinguished by whether araucarian (*Planoxylon*) or abietinean (*Araucariopitys*) bordered pitting on the radial walls of the tracheids is dominant. Kräusel (1949) further distinguishes the two based on the degree of

mulitseriation (*Planoxylon* 1-3 and *Araucariopitys* 1-2) on the radial walls of the tracheids. Philippe and Bamford's (2008) key also divides the two based on their biogeography, *Planoxylon* being a Gondwanan taxon and *Araucariopitys* being a Laurasian taxon. Both morphogenera have been described from Gondwana (e.g. *Planoxylon austral* and *Araucariopitys antarcticus*). Differentiation of morphogenera based on geography is arguable because the geographical location of a fossil should be irrelevant to its taxonomy. Lastly, Philippe and Hayes (2010) further add that a unique feature for *Planoxylon* is the high number of pits per cross-field, typically 5 pits. In MPM-9, the number of cross-field pits does range from 1-6 pits per cross-field; however, the typical number of pits per cross-field is between 2-4 pits.

MPM-9 is similar to *P. hectori* (Stopes, 1916) from the Cretaceous of New Zealand. They both have the general characteristics for the morphogenera; additionally, resin canals are absent in both MPM-9 and *P. hectori* and wood parenchyma is infrequent in both. They also differ in that abietineentüpfelungen on the ray walls is more prevalent in *P. hectori* than MPM-9; the orientation of the cross-field pits in *P. hectori* are more regular ('vertical pairs' of 1-3 per cross-field) than in MPM-9; and *P. hectori* has uniseriate, biseriate and triseriate bordered pitting on the radial walls of the tracheids in the earlywood while MPM-9 only has uniseriate and biseriate bordered pitting. This specimen also shares some similarities with *P. austral* from the Late Permian of New Caladonia (Vozenin-Serra and Salard-Cheboldaeff, 1992) and the Middle Jurassic (La Marilde Formation) of Argentina (Gnaedinger, 2007a). The cross-field pits are the most similar, as they both have very obvious cupressoid pits. The average diameters of the tracheids are smaller in *P. austral* (radial 33 µm, tangential 32 µm) than in MPM-9

(radial, 47 µm, tangential 39 µm). The bordered tracheid pits are more abietinean than araucarian and are more commonly biseriate (32%) or triseriate (3%) in *P. austral* than in MPM-9 whereas the bordered pits are more araucarian and are rarely biseriate (2%) and never triseriate. Additionally, in *P. austral*, there is a greater range in height of the rays in terms of the number of cells (2-32 cells in *P. austral* and 2-21 in MPM-9); although the average height is the same in both (~9 cells). Lastly, biseriate and triserate rays are more common (32% and 3%, respectively) in *P. austral* than in MPM-3 (3% and 0%, respectively) (Gnaedinger, 2007a).

It is certainly worth comparing MPM-9 to the *Araucariopitys* species recorded from the Antarctic Peninsula. Falcon-Lang and Cantrill (2000) were the first to formally identify *Araucariopitys* sp. from the Antarctic Peninsula (Late Albian of Alexander Island). The eight specimens are described as primarily having a mean maximum earlywood tracheid diameter 22.7 µm; predominantly uniseriate bordered pitting on the tracheids (75.5%); biseriate bordered pits predominantly alternate (~89%) and rarely opposite; adjacent bordered pits "almost always touching" (~99%); circular/hexagonal araucarioid cross-field pits (1-4 per cross-field) with slit-like, inclined apertures; rays uniseriate with the average ray height being 3.6 cells (range 1-15 cells). Poole and Cantrill (2001) identified and proposed a new species, *A. antarcticus* from the Williams Point Beds on Livingston Island, Antarctica (Cenomanian). Overall, the morphology was comparable with the material from Alexander Island. The difference between the two is that *A. antarcticus* includes: triseriate bordered pits in addition to uniseriate and biseriate and cross-fields containing more pits per cross-field (2-9 pits with average 6 pits). The description of these Antarctic specimens is nearly identical to MPM-9 with the exception

of the Antarctic material having narrower tracheids, a greater proportion of multiseriate pitting to uniseriate pitting and shorter rays. The only features that are not mentioned for the Antarctic specimens concerns the presence of axial parenchyma and pitting on the transverse ray walls. It is worth noting that in figure 6 of Poole and Cantrill (2001), there appears to be pitting on the transverse walls of the rays. Lastly, the suite of features in the Antarctic specimens more closely relates to *Planoxylon* rather than *Araucariopitys*.

Gondwanan distribution: *Planoxylon* has been recorded from the Late Permian to Middle Cretaceous of Gondwana (India, New Zealand, New Caledonia, Uruguay and Argentina).

The oldest *Planoxylon* material (Upper Permian) belongs to *P. stopesii* from Indonesia (Pasad, 1981), *P. gnaedingeriae* from Uruguay (Crisafulli, 2004), *P. austral* and *P. lacunosum* from New Caledonia (Salard, 1968; Vozenin-Serra and Salard-Cheboldaeff, 1992). Only one specimen has been identified from the Triassic, *P. indicum* from the Lower Triassic of India (Vagyani and Mahabale, 1974). From the Jurassic, *P. austral* has been described from Argentina (Gnaedinger, 2007a) and it has been proposed that *Araucarioxylon zeelandicum* (Crié, 1889) from the Jurassic–Early Cretaceous of New Zealand should be reassigned to the morphogenus *Planoxylon* (Philippe et al., 2004). Lastly, there have only been two specimens discovered in Cretaceous rocks from Gondwana, *Planoxylon* sp. from the Early Cretaceous of India (Prabhakar, 1987) and *P. hectori* from the Mid-Cretaceous of New Zealand (Stopes, 1916).

Order: Coniferales

Family: Cupressaceae

Morphogenus: *Cupressinoxylon* Göppert (1850)

Type species: *Cupressinoxylon gothanii* Kräusel (1920)

Cupressinoxylon sp.

Material: MPM-26b

Description: Growth rings are distinct and have a narrow latewood zone with a thickness of only two to six cells (Figure 2.8a, b). A few false rings are present. Axial parenchyma are diffuse (Figure 2.8b). The mean earlywood tracheid radial and tangential diameters are 25 µm (range 14-39 µm) and 24 µm (range 11-41 µm), respectively. The radial walls of the tracheids contain only uniseriate bordered pits (mean diameter 12 µm); however, most of the length of the tracheid is smooth (Figure 2.8c). The bordered pits are either isolated or form short chains of 2-8, rarely touching, pits (Figure 2.8c, d). The apertures of the bordered pits are either elliptical or slit-like.

Ray parenchyma have smooth walls and ray tracheids are absent (Figure 2.8c). Rays are commonly resin-filled. Cross-field pits consist of 1-2 bordered pits per cross-field with an aperture narrower than the border and angled ~45° (Figure 2.8d, e). These features are consistent with cupressoid pits. Spiral checking on the tracheid wall occurs in small sections throughout the specimen.

Tangential rays are uniseriate with no biseriation present in the thin-section (Figure 2.8f, g). The average ray height is 4.5 cells with a range from 1-11 cells (standard deviation 2.21). A few bordered pits occur on the tangential wall of the tracheids (Figure 2.8).

Identification: Following Kräusel (1949) and Philippe and Bamford (2008) morphogenera keys, the features in MPM-26b are consistent with *Cupressinoxylon*. The primary features that distinguish this morphogenus include: abietinean bordered pitting, ray cells smooth and the cross-field pits being cupressoid (obliquely angled). The general characteristics of *Cupressinoxylon* are similar to that of extant Cupressaceae (Stewart and Rothwell, 1993).

MPM-26b is very similar to *Cupressinoxylon* sp. material (Poole et al., 2001) from the Eocene of King George Island, Antarctic Peninsula. The specimens both contain few uniseriate pits that often form short rows (one to eight pits) on the radial walls of the tracheids with the pit aperture ranging from circular to slit-like and one or two cupressoid pits per cross-field. They also share a similar ray height (*Cupressionxylon* sp. 1-14 cells high, MPM-26b 1-11 cells high). *Cupressinoxylon* sp. (Harland et al., 2007) from the Aptian-Albian of Ellesmere Island and Spitsbergen are also comparable with this specimen. The most striking similarity is the nearly identical ray height with the Arctic material having a range of 1-12 cells high and a mean value of 4-5 cells. The primary differences between MPM-26b and the Arctic material is the Arctic material contains abundant pitting on the radial wall of the tracheids that are also more closely associated

to each other (more araucarian) and there are more pits per cross-field than in both MPM-26b and Antarctic material (Harland et al., 2007; Poole et al., 2001). *Cupressinoxylon kotaens* (Rajanikanth and Sukh-Dev, 1989) and *C. rajmahalense* (Bhardwaj, 1953) from the Early Cretaceous and Jurassic, respectively, of India also shares similarities with this Argentine specimen. However, *C. korens* and *C. rajmahalense* are quite distinct from MPM-26b by having abundant bordered pitting, occasional biseriate pitting, and rims of Sanio on the radial walls of the tracheids (Bhardwaj, 1953). Additionally *C. korens* contains more pits per cross-field (2-4) and *C. rajmahalense* contains taller rays (1-23 cells, mean 7) (Bhardwaj, 1953; Rajanikanth and Sukh-Dev, 1989).

Gondwanan distribution: *Cupressinoxylon* has been described from both the northern and southern hemispheres and its occurrence spans from the Early Jurassic well into the Miocene (e.g. Falcon-Lang, 2003; Falcon-Lang and Cantrill, 2001; Lutz, 1930; Morgans et al., 1999; Philippe et al., 2004; Ru-feng et al., 1996). Southern hemisphere *Cupressinoxylon* species are rare; and the validity of most have been questioned (Philippe et al., 2004; Torres and Philippe, 2002). Philippe et al., (2004) reexamined Jurassic-Early Cretaceous Gondwanan specimens belonging to this genus and established that only *C. kotaense* (Rajanikanth and Sukh-Dev, 1989) and *C. rajmahalense* (Bhardwaj, 1953) from the Early Jurassic and Early Cretaceous, respectively, of India belong to this genus. The only other Gondwanan specimen is *Cupressinoxylon sp*. (Poole et al., 2001) from the Middle Eocene of the Antarctic Peninsula.

A number of putative *Cupressinoxylon* specimens have been described from Argentina; however, all have had their validity questioned. Conwentz (1885) first described *Cupressinoxylon* sp., *C. latiporosum* and *C. patagonicum* of the Oligocene from Rio Negro Province (Herbst et al., 2007). But, the material is poorly preserved and defies assignment into separate *Cupressinoxylon* species much less positive identification to the genus (Kräusel, 1949; Lutz, 1930). *Cupressinoxylon* sp. Gothan (1915) and *C. krauselii* Eckhold (1923) are both from the Early-Middle Jurassic from Neuquén Provence. The generic assignment has been questioned for this material because of poor preservation, particularly of the cross-field pits for *C. krauselii* (possibly araucarioid and not cupressoid) (Florin, 1940; Kräusel, 1949; Philippe et al., 2004; Torres and Philippe, 2002; Vaudois and Privé, 1971). Jaworski (1915, 1926a, b) described '*Cedroxylon* or *Cupressinoxylon* sp.' from the Lower Jurassic from Mendoza Province. The material was reassessed by Torres and Philippe (2002) as being *Agathoxylon* sp. Lastly, Vaudois and Privé (1971) suggest that *C. hallei* Krausel (1949) from the Cretaceous(?) or Tertiary(?) of Patagonia (location not specified) may belong to the genus *Widdringtonioxylon*.

Order: Coniferales

Family: Cupressaceae

Morphogenus: *Taxodioxylon* Hartig (1848) emend. Gothan (1905)

Type species: *Taxodioxylon goeppertii* Hartig (1848)

Taxodioxylon sp.1

Material: MPM-10, MPM-15, MPM-16, MPM-18

Description: Growth rings are distinct with an abrupt, narrow latewood zone (Figure 2.9a, b). False rings are present (Figure 2.9a). MPM-18 is branch wood that includes the pith (Figure 2.9b). Axial parenchyma are rare and occur in both the earlywood and the latewood. Moderate beading occurs on the transverse end walls of some of the axial parenchyma (Figure 2.9f, g). The tracheids are square to hexagonal in shape with the mean radial and tangential earlywood tracheid diameters being 29µm (range 13-55 µm) and 26 µm (range 13-43 µm), respectively. The radial wall of the tracheids predominantly contain uniseriate (98% - 100%) bordered pits (Figure 2.9c, d), and rarely biseriate alternate pits (Figure 2.9e). Bordered pitting consists of a mix of abietinean and araucarian pitting, depending on the depth of field, with the former being dominant. These bordered pits range in size from 6-19 µm with an average being 13 µm.

Ray parenchyma horizontal and end walls are smooth. Ray tracheids are absent. Rays are often filled with a dark resinous material. Cross-field pits consist of 2 to 4 small, unorganized taxodioid/cupressoid pits per cross field (Figure 2.9d). In tangential longitudinal section, the ray height ranges from 1 to 18 cells with the average being 4.65 cells (Figure 2.9h).

*Taxodioxylon sp.*2

Material: MPM-11b

Description: Growth rings are abrupt with a narrow latewood zone (2-6 cells thick) and a wide earlywood zone (Figure 2.10a, b). The earlywood has been crushed in many of the

growth rings (Figure 2.10b). False rings are present. Axial parenchyma are diffuse and occur in both the earlywood and the latewood. Beading is present on the transverse end walls of some of the axial parenchyma (Figure 2.10e). The tracheids are rectangular to hexagonal in shape. The mean radial earlywood tracheid diameter is 27 µm (range 16-40 µm) and the mean tangential tracheid diameter is 26 µm (range 10-37 µm). The radial walls of the tracheids bear abundant araucarian bordered pits and possible xenoxylon bordered pits (Figure 2.10c, d). Bordered pits are predominately uniseriate (99%) with one set of opposite biseriate pits. The average diameter of the bordered pits is 16 µm (range 12-27 µm).

Ray parenchyma horizontal and end walls are smooth and straight; ray tracheids are absent (Figure 2.10c, f). Rays are often filled with a dark resinous material. Cross-field pitting consists of 1-2 obliquely angled taxodioid/cupressoid pits in both the earlywood and the latewood (Figure 2.10f).

In tangential longitudinal section, ray height ranges from 2-21 cells high with the average being 7.26 cells high (standard deviation 4.22). Rays are predominately uniseriate (98%) with some local biseriation (Figure 2.10g, h).

Identification: The two *Taxodioxylon* species described here are identified on the presence of the following features: distinct growth rings, ray cell walls smooth, predominately uniseriate rays 1-30 cells high, small taxodioid/cupressoid cross-field pits, rare axial parenchyma and pitting on the end walls the of axial parenchyma. Additionally, resin canals and spiral thickenings are absent (Dolezych et al., 2010;

Harland et al., 2007; Kräusel, 1949; Philippe and Bamford, 2008). The distinction of the two species is the number of pits per cross-field (2-4 pits in sp. 1 and 1-2 pits in sp. 2), the arrangement of cross-filed pits (aligned in *Taxodioxylon* sp. 1 and not aligned in *Taxodioxylon* sp. 2), the average ray height (4.66 cells in sp. 1, 7.26 cells in sp. 2) and the border pitting type (abietinean in *Taxodioxylon* sp. 2 and araucarian in *Taxodioxylon* sp.2). The general characteristics of *Taxodioxylon* are similar to that of extant Taxodiaceae and Cupressaceae (Stewart and Rothwell, 1993).

Taxodiaceous wood is morphologically very conservative; resulting in similar morphology among the different genera. Notably *Taxodioxylon*, *Glyptostroboxylon* and *Sequoioxylon* are all nearly identical in their morphology (Dolezych and Van Der Burgh, 2004; Hartig, 1848; Philippe and Bamford, 2008; Torrey, 1923; Williams et al., 2010). The similarity is so striking that Philippe and Bamford's (2008) key places both *Taxodioxylon* and *Sequoioxylon* together. However, *Taxodioxylon* can be distinguished from *Sequoioxylon* by the presence of ray tracheids and smooth axial parenchyma end walls in *Sequoioxylon* (Andrews, 1936; Blokhina et al., 2010). Additionally, the *Glyptostroboxylon* morphogenus description is identical to that of *Taxodioxylon* except for the presence of glyptostroboid pits in the earlywood cross-fields (Dolezych and Van Der Burgh, 2004; Williams et al., 2010). Many authors have used various morphological features such as cross-field pitting number, cross-field pit shape and smooth *versus* nodular end walls on axial parenchyma to distinguish between morphogenera; however, these features can vary within a single individual, let alone a population (Williams et al., 2010, references therein).

Following Kräusel's (1949) morphogenera key, *T*. sp. 1 corresponds with *T. taxodii* and *T*. sp. 2 with *T. burgessi*. The key for the *Taxodioxylon* species is very general and only uses the number of pits per cross-field, presence or absence of pitting on the end walls of axial parenchyma and the presence or absence of wound wood. As previously mentioned, these features can vary within a species, let alone an individual, and thus, cannot be readily used for identification of morphospecies (Williams et al., 2010, references therein).

There are several unique features that distinguish *Taxodioxylon*. sp. 1 and *Taxodioxylon.* sp. 2 from other *Taxodioxylon* species. One feature that occurs in *Taxodioxylon* sp. 1 and is not common in other *Taxodioxylon* species is the presence of alternate biseriate bordered pits (Figure 2.9c) (Dolezych et al., 2010; Dolezych and Van Der Burgh, 2004; Harland et al., 2007; Kräusel, 1949; Philippe and Bamford, 2008; Torrey, 1923). Commonly, biseriate pits occur next to (opposite) the neighboring pit. The alternate nature of these pits could be due to morphology or taphonomy. The tracheids containing the pits are skewed rather than straight. This distortion could result in what looks like alternative pitting, but may actually be opposite, in some of the tracheids. Another feature prominent in many *Taxodioxylon* species is the presence of crassulae (Sanio Rims) between pairs of biseriate pits. Both *Taxodioxylon* sp.1 and sp.2 lack crassulae.

Falcon-Lang and Cantrill (2000) have reported *Taxodioxylon* sp. from the Late Albian of Alexander Island, Antarctica. The Antarctic species are somewhat similar to both of the species reported here; however, there are several striking differences. The

bordered tracheid pitting on the Antarctic material is predominantly abietinean, as is *Taxodioxylon* sp. 1. Moreover, the Antarctic material contains more biseriate pitting (11%) than in the Argentine material, but contains alternate biseriate pitting as in *Taxodioxylon* sp. 2. The mean earlywood tracheid diameter in the Antarctic material is much larger (55 µm) than in either of the Argentine specimens (*Taxodioxylon* sp. 1, 29 µm and 26 µm; *Taxodioxylon* sp. 2, 27 µm and 26 µm). Additionally, the mean number of ray cells (TLS) for the Antarctic material is 8.3 cells (range 1-31 cells) and is relatively similar to that of *Taxodioxylon* sp. 2 (7 cells, range 1-21 cells) but is very different compared to *Taxodioxylon* sp. 1 (5 cells, range 1-18 cells).

Taxodioxylon has also been recently described from the Arctic (late Paleocene-early Eocene) by Williams et al. (2010). Again, the overall description is very similar but there are notable differences. The tracheid diameter (radial) is much wider in the Arctic material (max 75 µm) than in the Argentine material; however, the tangential diameter of the Arctic material is on par with the Argentine (Arctic 20-40 µm; Argentine, overall, 10-43 µm). Again, the ray height (in cell numbers) is more numerous in the Arctic (range 2-36) than in the Argentine material.

Gondwana Distribution: This is the first record of *Taxodioxylon* in Argentina. The *Taxodioxylon* morphogenus is typically associated with high latitudes in the northern hemisphere. Taxodiaceous conifers are common in the northern hemisphere from the Early Cretaceous through the Recent (e.g., Dolezych et al., 2010; Harland et al., 2007; LePage et al., 2005; LePage, 2007; Visscher and Jagels, 2003; Williams et al., 2010).

Only a few specimens have been described in the southern hemisphere. As previously discussed, one well-preserved specimen has been described from Antarctica (late Albian of Alexander Island) (Falcon-Lang and Cantrill, 2000). The only other material that has been described is, *Taxodioxylon* sp. (Bhardwaj, 1952) and *Taxodioxylon rajmahalense* (Bhardwaj, 1953), from the Early Cretaceous of India. Nevertheless, Philippe et al. (2004) suggest these identifications may not be correct.

Order: Coniferales

Family: Podocarpaceae

Morphogenus: *Podocarpoxylon* Gothan 1905

Type species: *P. juniperoides* Gothan 1905

Podocarpoxylon sp.

Material: MPM-6, MPM-11a, MPM-25, MPM-30

Description: Growth rings are distinct; the transition of earlywood to latewood is typically abrupt (only 3-9 latewood cells thick), but a few growth rings have a more gradual transition. False rings are present in all the specimens except MPM-25 and are 2-3 cells thick (Figure 2.11a, b). Earlywood deformation is present in MPM-11a. Axial parenchyma are present, but are not abundant (Figure 2.11b). The average earlywood tracheid diameters are, radially, 35.8 µm (range 14-62 µm) and, tangentially, 29.5 µm

(range 13-49 µm). Bordered pitting on the radial walls of the tracheids is predominantly uniseriate (97-100%) with only a few occurrences of adjacent and opposite biseriate pits. The bordered pits are round with the apertures either round to slit-like and form short chains of closely associated (less than one cell space apart) pits (abietinean pitting) (Figure 2.11c). The mean bordered pit diameter is 13.2 µm with the range being 7-21 µm.

Ray parenchyma are horizontal and have smooth, unpitted walls. Ray tracheids are absent. Cross-field pitting generally occurs as 1-2 pits per cross-field that have sub-parallel, narrow apertures. These features are consistent with podocarpoid pits (Figure 2.11d, e, f). Spiral checking on the tracheid walls occurs periodically throughout MPM-30 at approximately a 45 degree angle (Figure 2.11d).

In tangential section, rays are predominately uniseriate (97-100%) (Figure 2.11g). The average tangential ray height is 6.86 cells with a range being 1-37 cells (Figure 2.11h). Bordered pits occur on the tangential walls of the tracheids.

Identification: Following Kräusel's (1949) and Philippe and Bamford's (2008) keys, this material belongs to the morphogenus *Podocarpoxylon*. *Podocarpoxylon* is distinguished by having: predominantly uniseriate, abietinean bordered pits on the radial walls of the tracheids; biseriate bordered pits opposite; primarily uniseriate rays; ray walls smooth; cross-field pits having less than 4 pits per cross-field; cross-field pits taxodioid/podocarpoid; resin canals and spiral thickenings absent.

Several *Podocarpoxylon* species are reported from Gondwana. Poole and Cantrill (2001a) named three species, *P. chapmanae*, *P. verticalis* and *P. communis*, from Livingston Island (Late Cretaceous), Antarctic Peninsula. *P. chapmanae* is distinguished based on rare to absent parenchyma; 1-4 cross-field pits; cross-field pit apertures round to obliquely inclined; cross-field pits are pairs alternately arranged; and small bordered pits on the tangential walls (either isolated or in rows of up to 4). *P. verticalis* is diagnosed by having 1-5 pits per cross-field, cross-field pit apertures vertical when in pairs and significantly less biseriate pitting than *P. chapmanae* (6-9.4%). Lastly, *P. communis* is distinguished by containing 1-4 (rarely 4) pits per cross-field; circular to obliquely elliptical cross-field pits; and pairs of cross-field pits arranged next to (opposite) each other. All of these specimens differ from the Cerro Fortaleza material by having a greater number of pits per cross-field. Additionally differences among the Cerro Fortaleza material and the Antarctic material includes: greater percentage of biseriate (39-51%) and triserate (0.5%) bordered pits in *P. chapmanae*; arrangement of pairs of cross-field pits in *P. chapmanae* and *P. communis*; and the cross-field pit size and shape in *P. chapmanae* (smaller) and *P. communis* (more circular). The Cerro Fortaleza material is closely comparable to other *Podocarpoxylon* material, *P. garciae*, from Late Cretaceous deposits in Río Negro Province, Argentina. *P. garciae* and the Cerro Fortaleza material share similar growth ring widths, tracheid diameters, bordered pit frequency on the radial walls of the trachieds and the number of pits per cross-field. However, the cross-field pits in *P. garciae* are circular rather than slit-like and the rays are much shorter, commonly 2-3 cells high (range 1-15 cells) (Del Fueyo, 1998).

Gondwanan Distribution: Extant members of the Podocarpaceae family are restricted to the southern hemisphere (Taylor et al., 2009). *Podocarpoxylon* has been reported from the Jurassic-Miocene of Gondwana (e.g. Gnaedinger, 2007b; Philippe et al., 2004; Terada et al., 2006a); however, this morphogenera has been proposed to be as old as the Early Permian (Crisafulli, 2004; Crisafulli and Herbst, 2008; Crisafulli and Herbst, 2009). This taxon has been reported from at least eight Southern Hemisphere countries (e.g. Crisafulli, 2004; Crisafulli and Herbst, 2009; Del Fueyo, 1998; Philippe et al., 2004; Terada et al., 2006a; Terada et al., 2006b).

Only a few Podocarpoxylon taxa have been discovered in Argentina: *P. austroamericanum* and *P. feruglioi* from the Middle Jurassic of Santa Cruz Province (Gnaedinger, 2007b), *P. garciae* from the Late Cretaceous of Rio Negro Province (Del Fueyo, 1998), *P. dusénii* from the "Tertiary" of Santa Cruz Province (Kräusel, 1924) and *P. mazzonii* from the Paleogene of Chubut Province (Brea et al., 2011; Raigemborn et al., 2007). Kräusel (1924) named *P. dusénii* from a fragment of wood recovered from the "Tertiary" on the Río La Leona (50° 10'S, 71°12'W). The coordinates given do not correspond to the Río La Leona, rather, they plot in Lago Argentino. If the latitude line is decreased (~50° 09'30" S) so as to be on land rather than in the lake, then the closest formations would be either the Anita Formation or the Cerro Fortaleza Formation, based on the most recent geological map of the area (Kraemer and Riccardi, 1997). Without more information it is impossible to determine which formation it could be from; however, it is unlikely to have come from Tertiary beds.

Order: Coniferales

Gymnosperm indet.

Material: MPM-01, MPM-07, MPM-19, MPM-22

Description: Growth rings are distinct and contain a thick latewood zone and some earlywood crushing. False rings are present (Figure 2.12a, b). The average earlywood tracheid radial and tangential diameters are 34.75 µm (range 2-58 µm) and 29.75 µm (range 15-51 µm), respectively. Axial parenchyma is abundant and diffuse in both the earlywood and the latewood (Figure 2.12b). The end walls of the parenchyma are smooth. Parenchyma are often filled with dark resinous material (Figure 2.12c).

The radial walls of the tracheids contain bordered pitting, although poor preservation prevents identification of abietinean or araucarian pitting. Bordered pits are only preserved in MPM-19 and average 14 µm in diameter (32 measured pits) with a range of 10-21 µm. Some cross-field pits in MPM-07 and MPM-01 are preserved (Figure 2.12d, e). In both specimens, there is only one, centrally located, cupressoid/taxodioid pit per cross-field preserved.

Tangential rays are exclusively uniseriate with an average ray height of 3.83 cells and range of 1-11 cells (Figure 2.12f, g). There appear to be organic crystal deposits in the axial parenchyma in most of the specimens (MPM-01, MPM-07 and MPM-22) (Figure 2.12 h).

Identification: Due to poor preservation, MPM-01, MPM-07, MPM-19 and MPM-22 can only be confidently identified as Gymnosperm. Putative family assignments may be Podocarpaceae, Cupressaceae or Cephalotaxaceae based on the presence of diffuse axial parenchyma (Richter et al. 2004). The type of cross-field pitting in two of the four specimens suggests that the wood may belong to *Taxodioxylon*.

DISCUSSION

This study reveals a high percentage of coniferous wood (80%) relative to angiosperm wood (20%) (see Chapter 3 for details) for the Cerro Fortaleza Formation (Figure 2.13a). Five morphogenera are recognized: *Agathoxylon*, *Planoxylon*, *Cupressinoxylon*, *Taxodioxylon* and *Podocarpoxylon*. Additionally, there are four specimens that could not readily be identified. Out of the 20 conifer specimens collected, 50% of the material is either *Taxodioxylon* or *Podocarpoxylon*, 20% belongs to *Agathoxylon* and 10% is either *Planoxylon* or *Cupressinoxylon* (Figure 2.13c). This is the first record of *Planoxylon*, *Taxodioxylon* and possibly *Cupressinoxylon* from Argentina. Furthermore, *Agathoxylon* and *Podocarpoxylon* have each been only identified once from the Late Cretaceous of Argentina (Del Fueyo, 1998; Pujana et al., 2007).

The distribution of coniferous wood around the study area is difficult to assess; but its association with dinosaur bones is interesting (Figure 2.2). The northern site yields all of the *Taxodioxylon* material (5 specimens), 3 *Podocarpoxylon*, 2 *Agathoxylon*

specimens, as well as, the only *Planoxylon* specimen and several indeterminate gymnosperm specimens (Figure 2.3). The southwestern site only yielded a specimen of *Podocarpoxylon* and an indeterminate gymnosperm fossil (Figure 2. 4). Lastly, the northeastern site only yielded one specimen each of *Agathoxylon* and *Podocarpoxylon* (Figure 2.4). It is difficult to assess any trends among these localities. Certainly the most productive fossil wood sedimentary horizons occur in the northern locality. The northern site also contains abundant Titanosaur bones. Two *Podocarpoxylon* specimens (MPM-6 and MPM-30) were discovered with or in near proximity to Titanosaur bones. MPM-6 was collected approximately 3 meters from a long bone (possibly a tibia); while MPM-30 was discovered directly next to an extremely large pile of weathered bone fragments. Thus, the fossil wood and dinosaur bones are being recovered from some of the same horizons which indicate that these plants and animals may have lived, died and became buried in the same environments.

Growth rings are present in all of the conifer wood material. Additionally, all of the material, except for one *Agathoxylon* specimen, contain false rings. Growth rings are formed during periods when cell division temporarily slows or stops because the conditions for growth are unfavorable. In temperate regions, growth rings are commonly indicative of seasonal growth. The ring boundaries are emphasized by smaller, thicker-walled cells of the latewood and the large, thinner-walled cells of the earlywood. False rings occur when cell division slows or stops because of sudden unfavorable conditions (e.g. drought) during the growth season. Furthermore, one sample, MPM-32, contains frost rings. These develop because of damage to the cells due to conditions like a late frost (Creber and Francis, 1999).

Both the Austral Basin and the Antarctic Peninsula were located in the Warm Temperate Biome during the Late Cretaceous (Iglesias et al., 2011; Poole et al., 2005). Warm, low latitudinal oceanic currents followed along the coast from South America to at least the northern part of the Antarctic Peninsula. This resulted in a maritime climate for the latter region (Cantrill and Nagalingum, 2005; Dutra and Batten, 2000; Poole et al., 2005). It has been suggested that the climate close to the Atlantic Coast of the Austral Basin, during the Coniacian, was humid with a seasonally tropical climate (Varela, 2010a, b). Macellari et al (1989) posit that the climate of the Cerro Fortaleza Formation (Campanian) was humid with intervals of high rainfall and a high water table (Macellari et al., 1989). Moreover, it has been proposed that the climate for the Austral Basin, during the Maastrichtian, was warm-temperate to warm-wet (Povilauskas et al., 2008).

There has been very little work on Cretaceous fossil flora in southern Argentina. Most of the fossil woods described from the Cretaceous of Argentina are only descriptions based on one or two specimens (e.g. Del Fueyo, 1998; Herbst et al., 2007; Martínez and Lutz, 2007; Pujana et al., 2007). Most of what we know about the floras is from pollen and fossil leaves (e.g. Archangelsky et al., 2009; Barreda and Archangelsky, 2006; Iglesias et al., 2011; Quattrocchio et al., 2011). Based on the latter information, a generalized paleobotanical history can be constructed for the Cretaceous. During the Cretaceous, most of Patagonia, western Antarctica, New Zealand, Australia, Tasmania, India, Madagascar and southern Africa were in a warm temperate biome. The latter regions have very similar floras from the Early Cretaceous through the Paleogene (Iglesias et al., 2011). During the Early Cretaceous, there was a diversification of conifers (Araucariaceae, Podocarpaceae and Taxodiaceae), ferns, cycads, bennettites and

pteridosperms in Patagonia (Iglesias et al., 2011; Passalia, 2007). The first angiosperm floras in Patagonia occur during the Early Cretaceous in the Austral Basin (Spring Hill Formation) and were probably small herbaceous plants (Archangelsky et al., 2009; Iglesias et al., 2011). During the Late Cretaceous, angiosperms diversified and began to dominate most ecosystems. Bennettites and cycads underwent significant decline at the beginning of the Late Cretaceous. The decline in abundance and diversity increased and resulted in the bennettites becoming extinct at the beginning of the Late Cretaceous. In southern-most Argentina, podocarps were the dominant forest components of Patagonia with some araucarian trees (Iglesias et al., 2011; Iglesias et al., 2007).

Due to the extensive paleobotanical work in the Antarctic Peninsula, a detailed paleobotanical history of the region can be reconstructed. At the beginning of the Late Cretaceous (Cenomanian-Turonian), understory floras transitioned from being fern and club moss dominated to angiosperm dominated. The coniferous overstory underwent very little change; however, there was a significant decline in the species diversity of all the understory floras except the angiosperms (Cantrill and Poole, 2002, 2005; Poole and Cantrill, 2001b). Angiosperm diversity rapidly increased with angiosperms conquering disturbed environments and migrating into and out-competing other floras in established environments. Thus, colonizing plants, such as bennettites, were the first to decrease in diversity (Cantrill and Poole, 2002). Angiosperm leaf physiognomy suggests that the climatic regime for the Antarctic Peninsula was subtropical to tropical (Francis et al., 2008). Within 10 million years after the first angiosperms appeared in the Antarctic Peninsula, angiosperm floras represented up to 75% of the floral diversity. The dominant conifer wood families during the Coniacian-Santonian continued to be Podocarpaceae

and Araucariaceae; however, angiosperm wood became more abundant later in the Cretaceous (Cantrill and Poole, 2005). Mosses and liverworts decreased in diversity to become only a minor understory component and bennettites underwent extirpation (local extinction) (Cantrill and Poole, 2002). Ferns and club mosses slightly recovered in diversity but were a lesser ecological component than in previous times (Cantrill and Poole, 2002). This rebound may have been from exploitation of new habitats carved out by the angiosperms (Poole and Cantrill, 2001b). By the end of the Cretaceous (Campanian-Maastrichtian), the first modern angiosperm floras appear in Antarctica. These floras were dominated by Nothofagaceae, Lauraceae, and Cunoniaceae woods and most closely resembled the cool temperate rainforests of Valdivia in Southern Chile (Poole and Cantrill, 2001b; Poole et al., 2003). The understory component remained dominated by ferns and clubmosses; but further reduction in the species diversity of these floras continued (Cantrill and Poole, 2002).

Comparatively, fossil wood from the Antarctic Peninsula is well-studied (see Cantrill and Poole, 2005). Fossil wood is the major botanical element preserved in Antarctica and is recorded in many formations. Fossil wood has been, and continues to be, collected in paleolatitudes between 59-62° (Francis and Poole, 2002; Poole et al., 2005). Cantrill and Poole (2005) created a database of over 500 specimens of fossil wood from the Aptian-Eocene of the Antarctic Peninsula. Within the Cretaceous, they concluded that there were four distinct phases that occurred. The first phase occurred during the Aptian-Albian and consisted of a conifer dominated flora with *Podocarpoxylon* dominating most of the environments (60-85%). The next phase occurred during the Cenomanian-Turonian and is marked by the possibility of

angiosperm wood being discovered. Phase three occurred during the Coniacian-Santonian and is denoted by the appearance and extreme diversification and abundance of angiosperm dominated floras (up to 75%). Lastly, phase four occurred during the Campanian-Maastrichtian and is marked by additional diversification and radiation of more modern groups such as nothofagaceous woods (Cantrill and Poole, 2005).

The relative abundance of the fossil wood from the Cerro Fortaleza is quite unique to the overall paleobotany of both Argentina and Antarctica in the latest Cretaceous (Campanian-Maastrichtian). By the Late Cretaceous, both Antarctica and Argentina were angiosperm dominated floras with subsidiary amounts of gymnosperms. In Argentina, this is evident in both fossil leaf and pollen floras. In Antarctica, leaf, pollen and fossil wood floras exhibit this dominance. However, with the Cerro Fortaleza floras, angiosperms only consist of 20% of the total flora and gymnosperms represent 80%.

In addition to being a gymnosperm dominated environment, rather than angiosperm dominated environment, the Cerro Fortaleza Formation also has a relatively high diversity of gymnosperm taxa. Both *Podocarpoxylon* and *Taxodioxylon* are equally represented (25% each), unlike the fossil wood floras of the Antarctic Peninsula. Only one *Taxodioxylon* sp. has only been recorded from Albian beds in the Antarctic Peninsula (Falcon-Lang and Cantrill, 2000). The abundance of *Podocarpoxylon* in the Cerro Fortaleza Formation is approximately the same as it is for the Antarctic Peninsula during the Campanian-Maastrichtian (Cantrill and Poole, 2005). *Agathoxylon* is more abundant in the Cerro Fortaleza Formation than in coeval Formations from the Antarctic Peninsula. This is the earliest record of *Cupressinoxylon* for both the Argentina and Antarctica. This

morphogenus is not recognized in the Antarctic Peninsula until the Eocene. Additionally, this is the first record of *Planoxylon* for both Argentina and the Antarctic Peninsula.

As previously mentioned, there are diverse opinions regarding the age of the Cerro Fortaleza Formation (see Chapter 1 for full discussion). It has been suggested to have been as old as the Coniacian (e.g. Novas et al., 2002; Riccardi and Rolleri, 1980; Varela, 2010a) and as young as the Maastrichtian (Kraemer and Riccardi, 1997). Based on the overlying (La Irene Formation) and underlying (La Anita Formation) formations, both of which have been dated, the Cerro Fortaleza Formation should be Campanian in age. Understanding the age of this formation is essential to understanding how the fossil flora fits in with the general pattern observed in Patagonia and the Antarctic Peninsula. If the Cerro Fortaleza Formation is considered to be Coniacian, then the relative abundance and morphogenera of the gymnosperms agrees with the trends in other areas of Patagonia and the Antarctic Peninsula. By contrast, with the Cerro Fortaleza Formation being Campanian in age, the relative abundance of gymnosperms to angiosperms is not necessarily consistent with the rest of Patagonia and the Antarctic Peninsula. The inconsistency could be due the result of two major factors. First, there are very few Late Cretaceous fossil wood localities in Patagonia, thus it is difficult to compare floras. Secondly, when compared to similar floras in the Antarctic Peninsula, differences could be due to sample size differences, preservation biases (e.g., soil alkalinity or acidity during burial), depositional environment (i.e., fluvial for the Cerro Fortaleza and coastal for the Antarctic Peninsula), ecology or regional climatic regime differences.

CONCLUSIONS

Extensive exposures of Cretaceous strata in Argentina have yielded many well-preserved fossil leaves and pollen. To date, research has primarily been limited to these types of fossil plant materials. This study one of the first extensive investigations of Late Cretaceous wood morphotaxa to be conducted in Argentina. The fossil coniferous wood from the Cerro Fortaleza Formation is comparable to many conifer woods from the rest of Gondwana. Typical Gondwanan morphotaxa such as *Agathoxylon* and *Podocarpoxylon*, are represented. Much rarer morphogenera, such as *Planoxylon, Taxodioxylon* and *Cupressinoxylon*, are also represented. This is the first record of *Planoxylon, Taxodioxylon* and possibly *Cupressinoxylon* for the Mesozoic of Argentina. All of the material collected exhibits growth rings which are indicative of a seasonal environment. Both the Antarctic Peninsula and Patagonia experienced a major floral turn-over during the Campanian, where angiosperms came to dominate most environments. However, the Cerro Fortaleza floras are still gymnosperm dominated (80%).

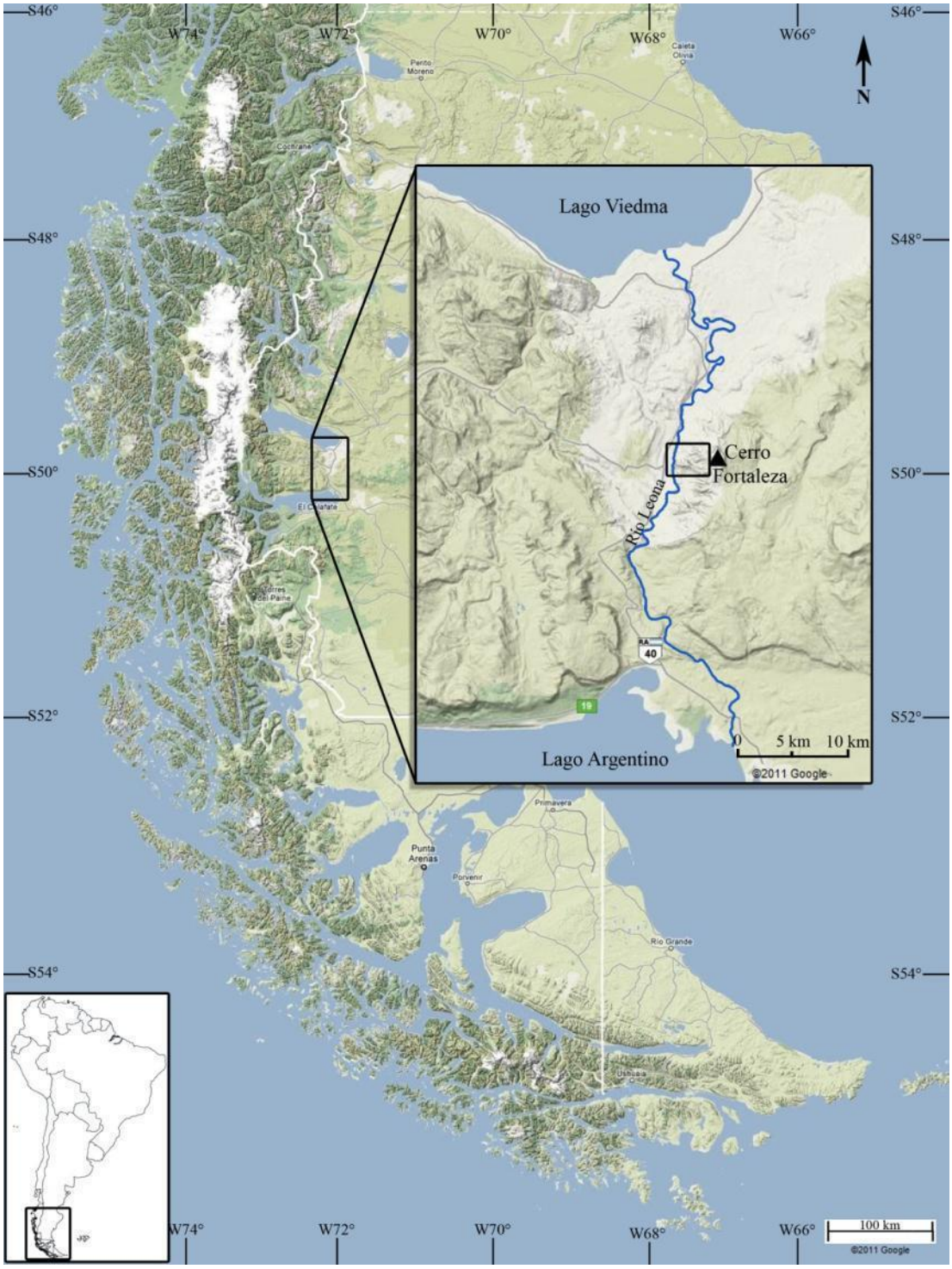

Figure 2.1. Map of the southern Patagonia showing the region surrounding Cerro Fortalela. Inset in upper map is Figure 2.2.

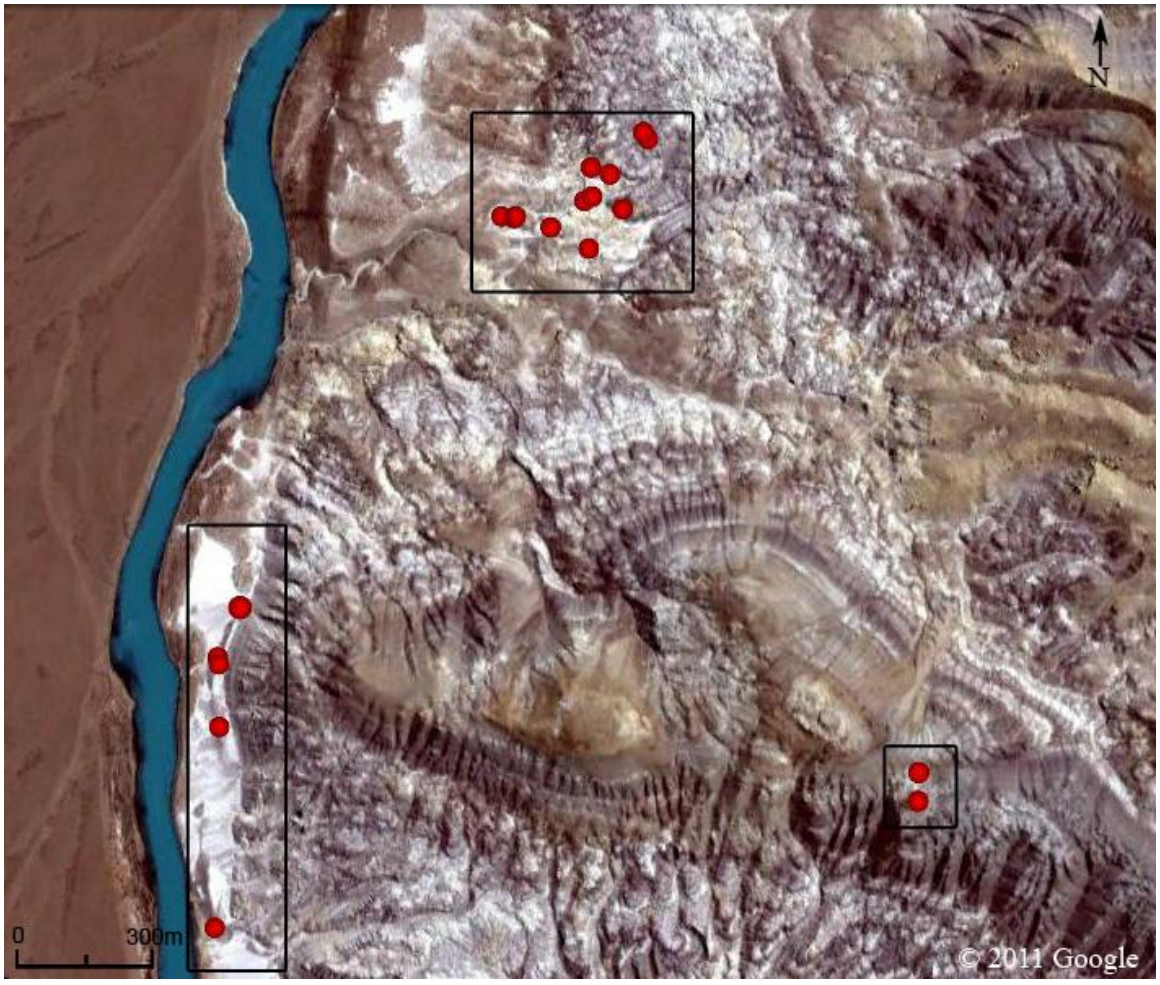

Figure 2.2. Map of the study region showing the three collection areas.

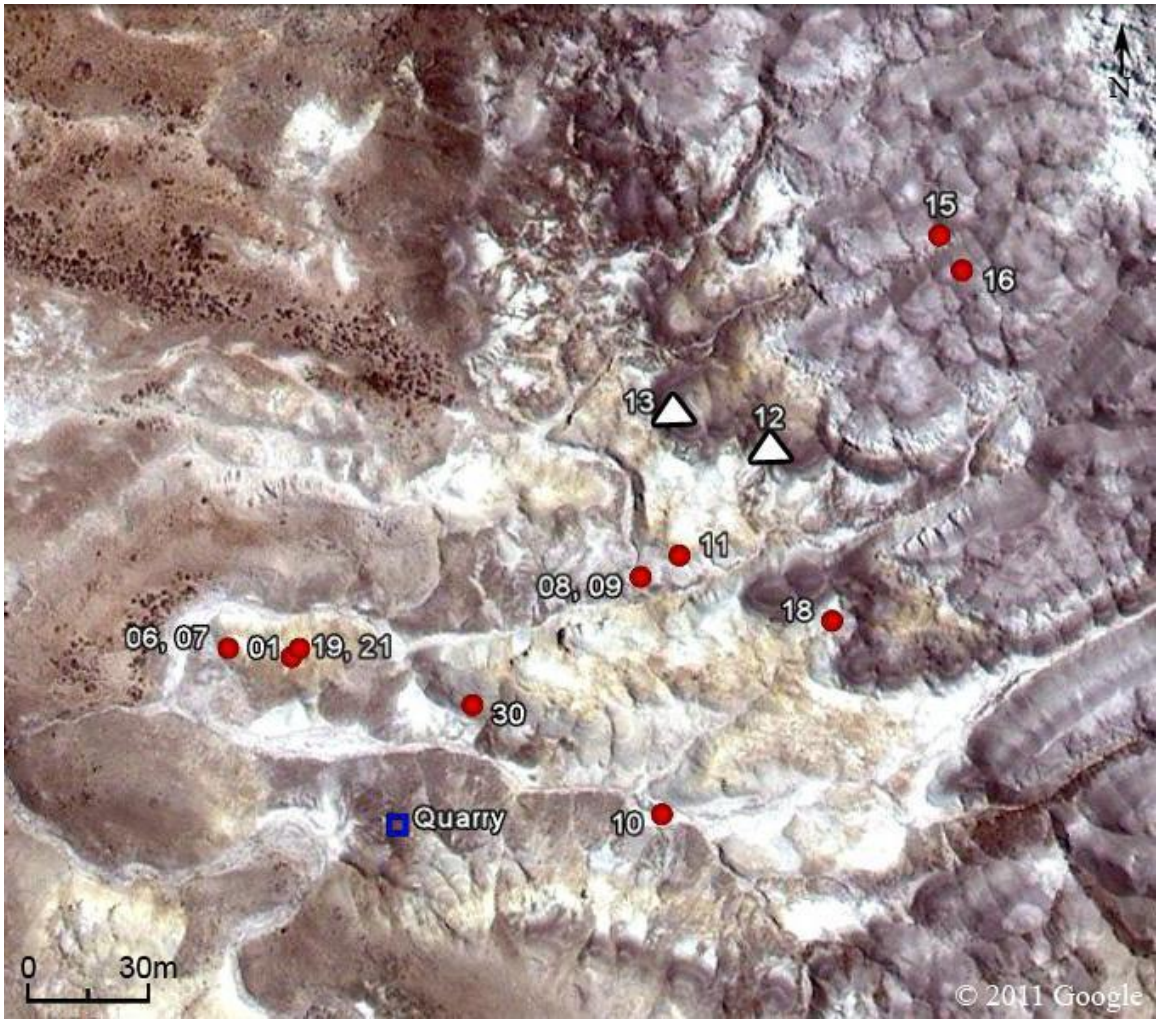

Figure 2.3. Map of the northern collection locality. The numbers correspond to the MPM numbers. The red circles are gymnosperm wood while the white triangles are angiosperm wood. The blue square represents the titanosaur dinosaur quarry.

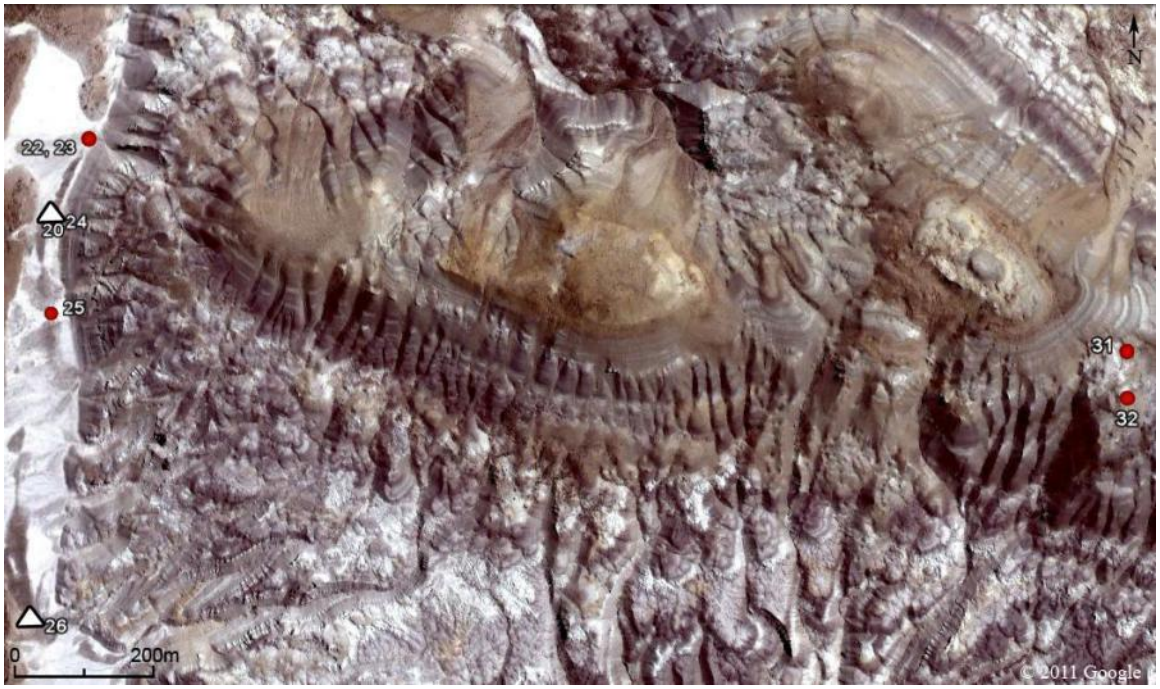

Figure 2.4. Map of the two southern localities (western and eastern) where samples were collected. The numbers correspond to the MPM numbers. The red cicles indicate gymnosperm wood while the white triangles indicate angiosperm wood.

Figure 2.5. Pictures showing the variation in the size of fossilized wood in the field. a. MPM-11; scale bar=10 cm. b. MPM-16. c. MPM-19; rock hammer length = 33cm.

Table 1. Anatomical features in the fossil wood from the Cerro Fortaleza Formation.

Feature	MPM-8 Agathoxylon sp.	MPM-21 Agathoxylon sp.	MPM-23 Agathoxylon sp.	MPM-32 Agathoxylon sp.
Growth rings	distinct	weakly distinct	distinct	distinct
False rings	present	absent	present	present
Earlywood tracheid diameter (radial) (µm)	mean 22; st dev. 3; median 21; range 14-31	mean 30; st dev. 5; median 30; range 15-41	mean 44; st dev. 11; median 42; range 24-76	mean 35; st dev. 7; median 35; range 20-47
Earlywood tracheid diameter (tangential) (µm)	mean 18; st dev. 4; median 17; range 10-27	mean 22; st dev. 3; median 21; range 15-31	mean 36; st dev. 9; median 35; range 22-67	mean 30; st dev. 7; median 29; range 18-49
Tracheid bordered pitting type	predominantly araucarian	predominantly araucarian	predominantly araucarian	predominantly araucarian
Bordered pitting diameter (µm)	mean 10; st dev. 3; median 9; range 7-16	mean 15; st dev. 2; median 15; range 11-18	mean 17; st dev. 3; median 17; range 8-24	mean 16; st dev. 2; median 15; range 11-22
Uniseriate tracheid bordered pitting (percent)	100	100	97	95
Biseriate tracheid bordered pitting alternate/opposite (percent)	0/0	0/0	66.7/33.3	100/0
Axial parenchyma	absent	absent	absent	absent
Axial parenchyma end walls	n/a	n/a	n/a	n/a
Ray tracheid	absent	absent	absent	absent
Ray parenchyma walls	smooth	smooth	smooth	smooth
Cross-field pitting (type and number)	araucarioid 2-6	araucarioid 2-6	araucarioid 2-6	araucarioid 2-6
Ray height (cell number)	mean 3.96; st dev. 1.48; median 4; range 2-9	mean 6.05; st dev. 3.29; median 5; range 1-15	mean 8.31; st dev. 6.27; median 7; range 1-28	mean 6.48; st dev. 3.95; median 6; range 1-19
Percentage of uniseriate/ biseriate rays	100/0	96/4	97/3	69/31

Table 1. Continued.

Feature	MPM-9 Planoxylon sp.	MPM-26b Cupressinoxylon sp.	MPM-10 Taxodioxylon sp. 1	MPM-15 Taxodioxylon sp. 1
Growth rings	distinct	distinct	distinct	distinct
False rings	present	present	present	present
Earlywood tracheid diameter (radial) (µm)	mean 47; st dev. 10; median 46; range 29-79	mean 25; st dev. 7; median 25; range 14-39	mean 30; st dev. 6; median 29; range 17-45	mean 31; st dev. 8; median 32; range 16-55
Earlywood tracheid diameter (tangential) (µm)	mean 39; st dev. 9; median 37; range 23-63	mean 24; st dev.8; median 23; range 11-41	mean 26; st dev. 7; median 23; range 15-42	mean 27; st dev. 6; median 28; range 13-43
Tracheid bordered pitting type	predominantly araucarian	predominantly abietinean	predominantly abietinean	predominantly abietinean
Bordered pitting diameter (µm)	mean 14; st dev. 3; median 14; range 8-20	mean 12; st dev. 2; median 12; range 8-17	mean 14; st dev. 2; median 13; range 8-19	mean 14; st dev. 3; median 14; range 9-19
Uniseriate tracheid bordered pitting (percent)	98	100	100	98
Biseriate tracheid bordered pitting alternate/opposite (percent)	100/0	0/0	0/0	100/0
Axial parenchyma	diffuse (rare)	diffuse	diffuse	diffuse
Axial parenchyma end walls	smooth	smooth	pitted and smooth	pitted and smooth
Ray tracheid	absent	absent	absent	absent
Ray parenchyma walls	pitting	smooth	smooth	smooth
Cross-field pitting (type and number)	araucarioid-cupressoid 2-6 pits	cupressoid	taxodioid pits 2-4	taxodioid pits 2-4
Ray height (cell number)	mean 8.70; st dev. 4.3; median 8; range 2-21	mean 4.50; st dev. 2.21; median 4; range 1-11	mean 5.76; st dev. 3.33; median 4.5; range 2-18	mean 4.49; st dev. 2.06; median 4; range 2-11
Percentage of uniseriate/ biseriate rays	97/3	100/0	100/0	100/0

Table 1. Continued.

Feature	MPM-16 Taxodioxylon sp. 1	MPM-18 Taxodioxylon sp. 1	MPM-11b Taxodioxylon sp. 2	MPM-11a Podocarpoxylon sp.
Growth rings	distinct	distinct	distinct	distinct
False rings	present	present	present	present
Earlywood tracheid diameter (radial) (µm)	mean 29; st dev. 7; median 30; range 16-44	mean 27; st dev. 6; median 27; range 13-39	mean 27; st dev. 5; median 26; range 16-40	mean 34; st dev. 6; median 34; range 22-45
Earlywood tracheid diameter (tangential) (µm)	mean 25; st dev. 7; median 26; range 13-39	mean 25; st dev. 7; median 25; range 13-43	mean 26; st dev. 6; median 23; range 10-37	mean 29; st dev. 6; median 30; range 14-44
Tracheid bordered pitting type	abietinean	predominantly abietinean	predominantly araucarian	predominantly abietinean
Bordered pitting diameter (µm)	mean 12; st dev. 2; median 12; range 6-15	mean 11; st dev. 2; median 11; range 7-14	mean 16; st dev. 3; median 16; range 12-27	mean 13; st dev. 2; median 13; range 9-16
Uniseriate tracheid bordered pitting (percent)	100	100	100	100
Biseriate tracheid bordered pitting alternate/opposite (percent)	0/0	0/0	0/0	0/0
Axial parenchyma	diffuse (rare)	diffuse	diffuse	diffuse
Axial parenchyma end walls	pitted and smooth	pitted and smooth	pitted and smooth	smooth
Ray tracheid	absent	absent	absent	absent
Ray parenchyma walls	smooth	smooth	smooth	smooth
Cross-field pitting (type and number)	taxodioid pits, 2-4	taxodioid pits 2-4	taxodioid pits 1-2	podocarpoid 1-2
Ray height (cell number)	mean 4.74; st dev. 2.04; median 5; range 2-14	mean 3.64; st dev. 1.31; median 3; range 1-8	mean 7.26; st dev. 4.22; median 6; range 1-21	mean 9.09; st dev. 5.92; median 8; range 2-25
Percentage of uniseriate/ biseriate rays	100/0	100/0	98/2	97/3

Table 1. Continued.

Feature	MPM-6 Podocarpoxylon sp.	MPM-25 Podocarpoxylon sp.	MPM-30 Podocarpoxylon sp.	MPM-31 Podocarpoxylon sp.
Growth rings	distinct	distinct	distinct	distinct
False rings	present	absent	present	present
Earlywood tracheid diameter (radial) (μm)	mean 41; st dev. 7; median 42; range 24-53	mean 38; st dev. 9; median 35; range 24-62	mean 22; st dev. 4; median 22; range 14-30	mean 44; st dev. 9; median 44; range 22-61
Earlywood tracheid diameter (tangential) (μm)	mean 35; st dev. 6; median 36; range 23-47	mean 28; st dev. 8; median 27; range 14-49	mean 23; st dev. 6; median 22; range 13-37	mean 32; st dev. 8; median 30; range 18-49
Tracheid bordered pitting type	predominantly abietinean	predominantly abietinean	predominantly abietinean	predominantly abietinean
Bordered pitting diameter (μm)	mean 13; st dev. 2; median 13; range 9-16	mean 14; st dev. 1; median 14; range 10-18	mean 11; st dev. 1; median 11; range 7-14	mean 15; st dev. 2; median 14; range 10-21
Uniseriate tracheid bordered pitting (percent)	99	100	99	97
Biseriate tracheid bordered pitting alternate/opposite (percent)	0/100	0/0	0/100	66.7/33.3
Axial parenchyma	diffuse	diffuse	diffuse	diffuse
Axial parenchyma end walls	smooth	smooth	smooth	smooth
Ray tracheid	absent	absent	absent	absent
Ray parenchyma walls	smooth	smooth	smooth	smooth
Cross-field pitting (type and number)	podocarpoid 1-2	podocarpoid 1-2	slit-like 1-4	podocarpoid 1-2
Ray height (cell number)	mean 4.39; st dev. 2.01; median 4; range 2-12	mean 10.13; st dev. 7.56; median 8.5; range 1-37	mean 4.43; st dev. 2.08; median 4; range 2-11	mean 6.24; st dev. 4.11; median 5; range 2-20
Percentage of uniseriate/ biseriate rays	100/0	98/2	99/1	98/2

Table 1. Continued.

Feature	MPM-1 Gymnosperm indet.	MPM-7 Gymnosperm indet.	MPM-19 Gymnosperm indet.	MPM-22 Gymnosperm indet.
Growth rings	distinct	distinct	distinct	distinct
False rings	present	present	present	present
Earlywood tracheid diameter (radial) (µm)	mean 39; st dev. 7; median 39; range 20-58	mean 36; st dev. 7; median 36; range 20-50	mean 31; st dev. 6; median 31; range 20-44	mean 33; st dev. 7; median 32; range 20-53
Earlywood tracheid diameter (tangential) (µm)	mean 32; st dev. 5; median 33; range 19-43	mean 29; st dev. 6; median 29; range 15-49	mean 25; st dev. 4; median 25; range 15-34	mean 33; st dev. 7; median 32; range 20-51
Tracheid bordered pitting type	?	?	?	?
Bordered pitting diameter (µm)	?	?	mean 14; st dev. 2; median 14; range 10-21	?
Uniseriate tracheid bordered pitting (percent)	?	?	?	?
Biseriate tracheid bordered pitting alternate/opposite (percent)	?	?	?	?
Axial parenchyma	diffuse (abundant)	diffuse (abundant)	diffuse (abundant)	diffuse (abundant)
Axial parenchyma end walls	smooth	smooth	smooth	smooth
Ray tracheid	absent?	absent?	absent?	absent?
Ray parenchyma walls	smooth	smooth	smooth	smooth
Cross-field pitting (type and number)	?	small cupressoid-taxodiod pits 1-?	?	?
Ray height (cell number)	mean 3.76; st dev. 1.96; median 4; range 1-8	mean 3.95; st dev. 3; median 3; range 1-9	mean 3.76; st dev. 1.78; median 3; range 1-11	mean 3.85; st dev. 1.843; median 4; range 1-7
Percentage of uniseriate/ biseriate rays	100/0	100/0	100/0	100/0

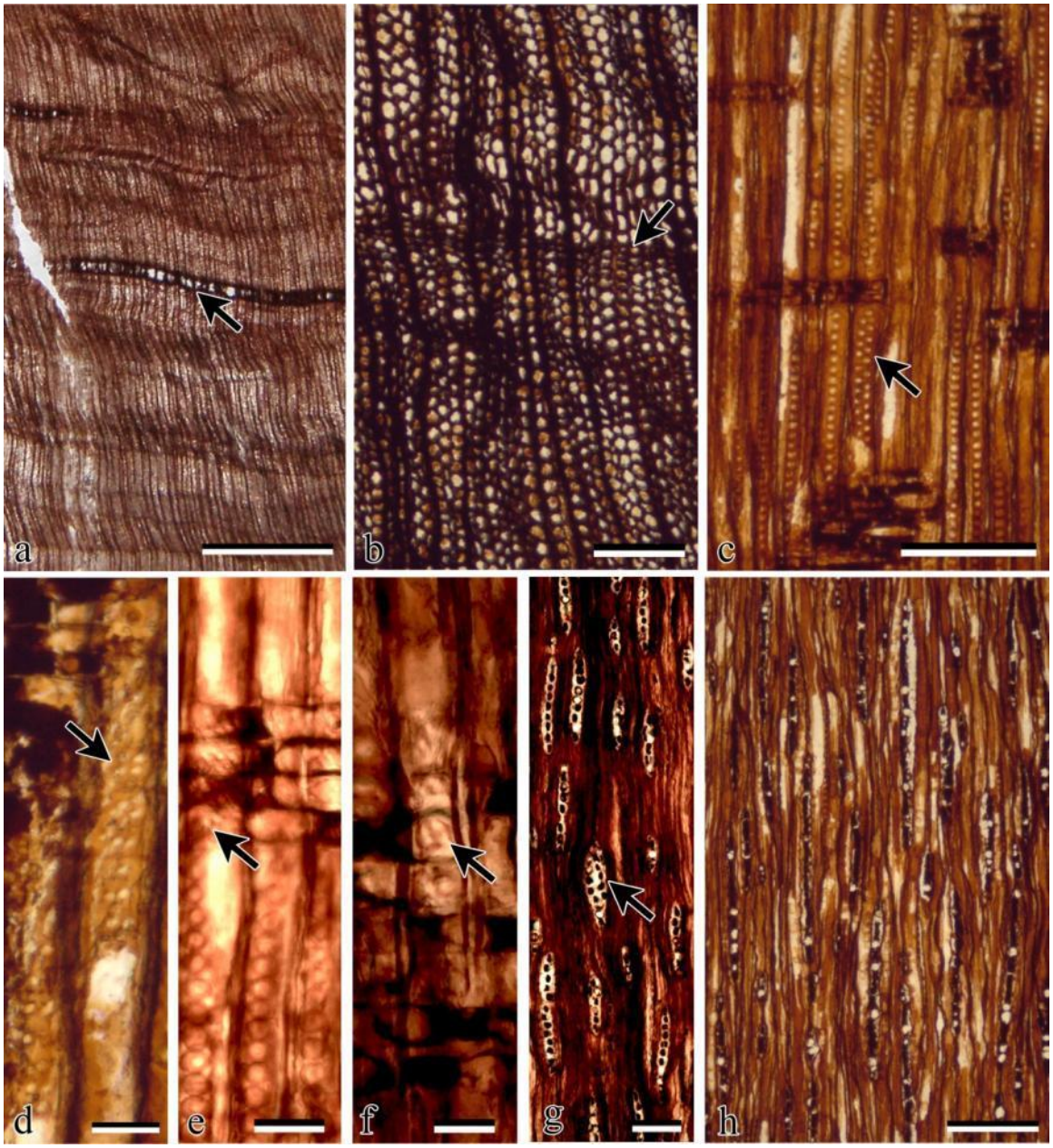

Figure 2.6. *Agathoxylon* sp. a. TS showing growth rings and a frost ring (arrow). MPM-32, scale bar = 2.5 mm. b. TS showing growth rings (arrow). MPM-23, scale bar = 250 µm. c. RLS showing araucarian uniseriate and alternate biseriate (arrow) pitting. MPM-23, scale bar = 250 µm. d, e, f. RLS showing araucarioid cross-field pits (arrows). MPM-23(d), MPM-32(e), MPM-32(f), scale bars = 50 µm. g. TLS showing uniseriate and biseriate (arrow) rays. MPM-21, scale bar = 50 µm. h. TLS showing long uniseriate rays. MPM-23, scale bar = 250 µm.

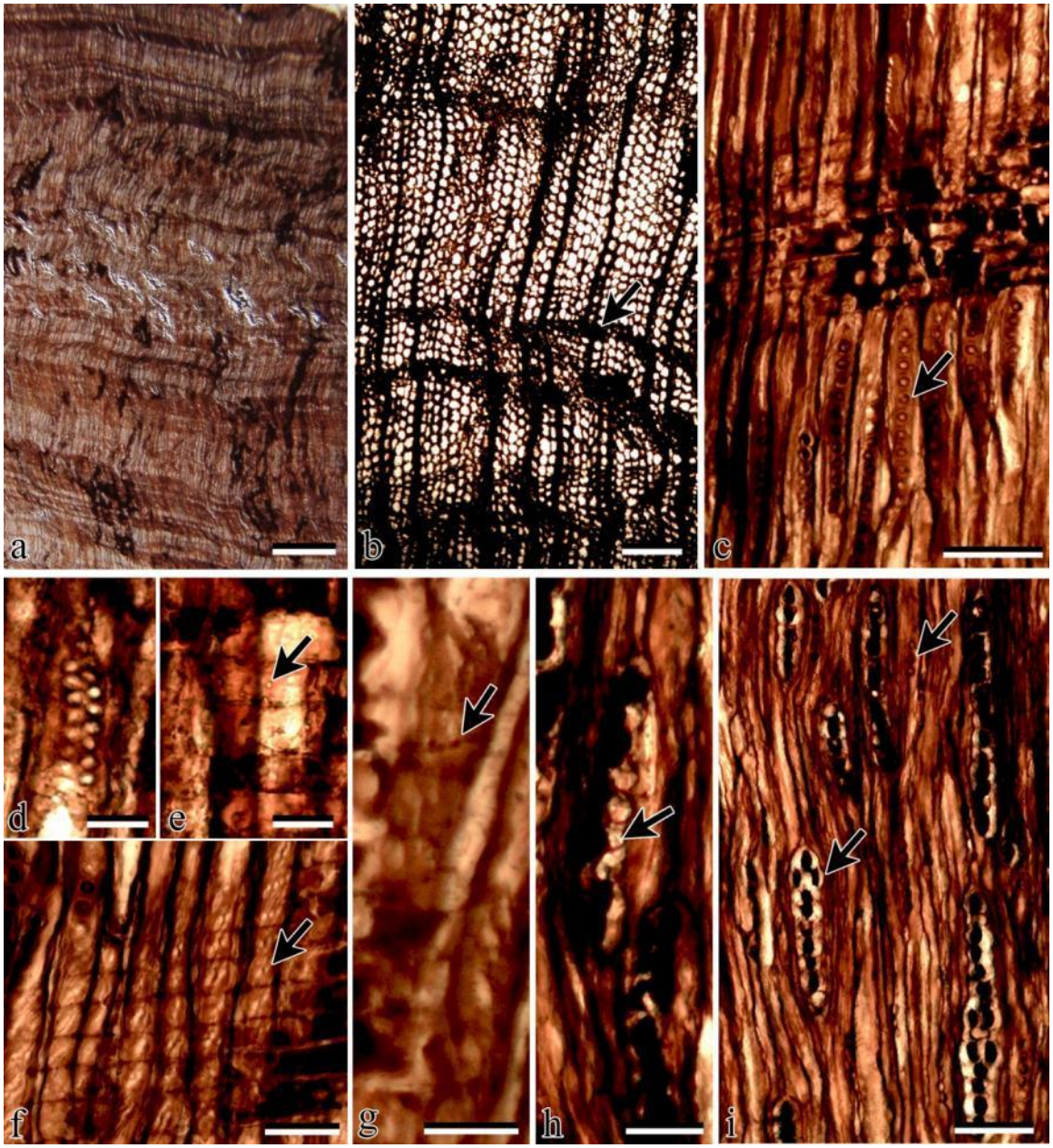

Figure 2.7. *Planoxylon* sp. MPM-9. a. TS showing growth rings, scale bar = 2.5 mm. b. TS showing growth rings and false rings (arrow), scale bar = 250 µm. c. RLS showing rays and uniseriate bordered pitting (arrow), scale bar = 100 µm. d. RLS showing rare, alternate biseriate tracheid pitting, scale bar = 50 µm. e. RLS showing rounded (piceoid) cross-field pitting (arrow), scale bar = 25 µm. f. RLS showing obliquely angled, slit-like (cupressoid) cross-field pitting (arrow), scale bar = 50 µm. g, h. RLS and TLS showing abietineentüpfelungen (arrows) in the ray cells, scale bars = 25 µm (g) and 50 µm (h). i. TLS showing bordered pits (upper arrow) and uniseriate and biseriate (lower arrow) rays, scale bar = 100 µm.

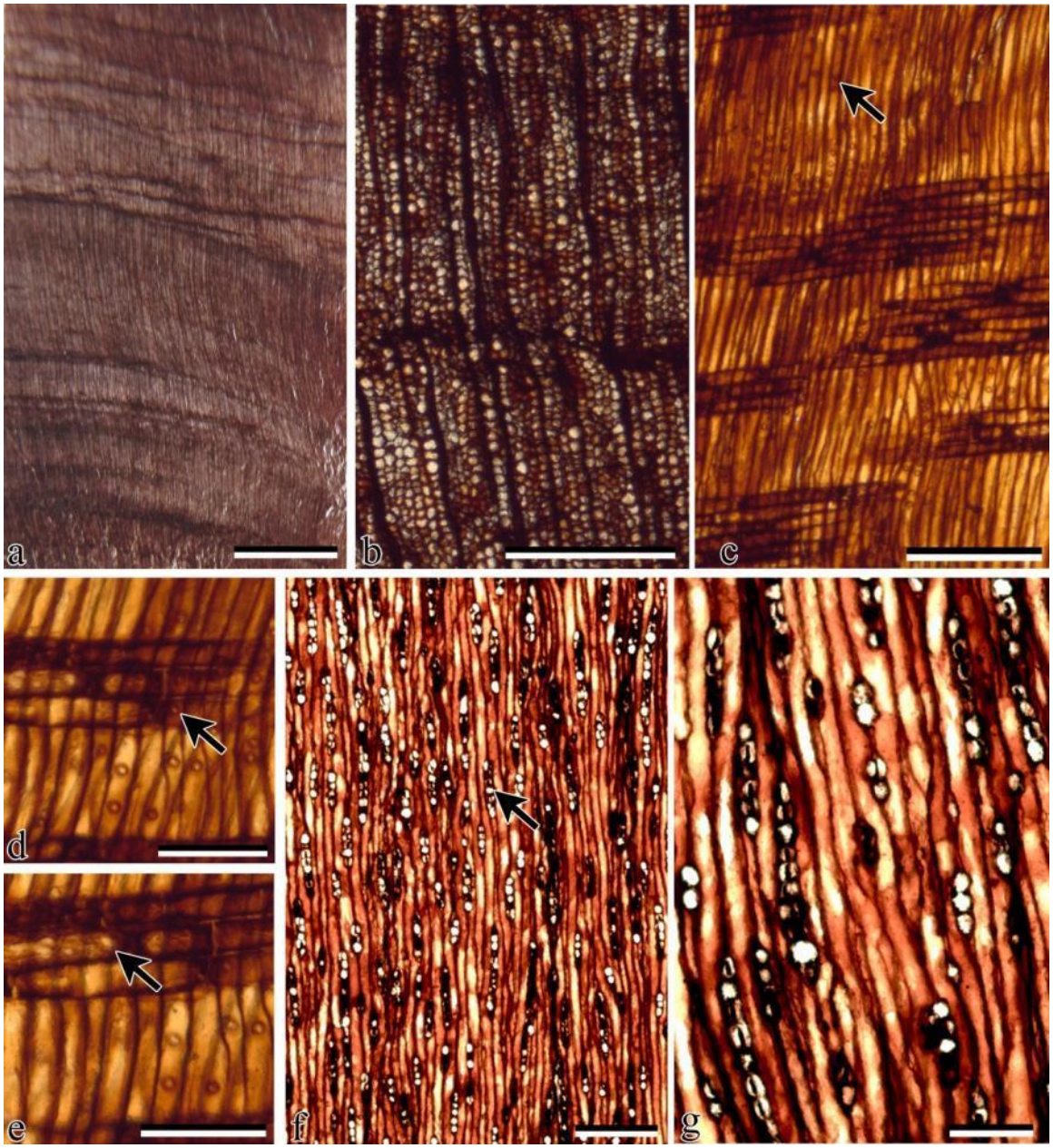

Figure 2.8. *Cupressinoxylon* sp. MPM-26b. a. TS showing growth rings, scale bar = 2.5 mm. b. TS showing growth rings, scale bar = 500 µm. c. RLS showing abietinean pitting and rays, scale bar = 250 µm. d, e. RLS showing cupressoid cross-field pits (arrow), scale bar = 100 µm. f. TLS showing uniseriate rays (arrow), scale bar = 250 µm. g. TLS showing uniseriate rays, scale bar = 100 µm.

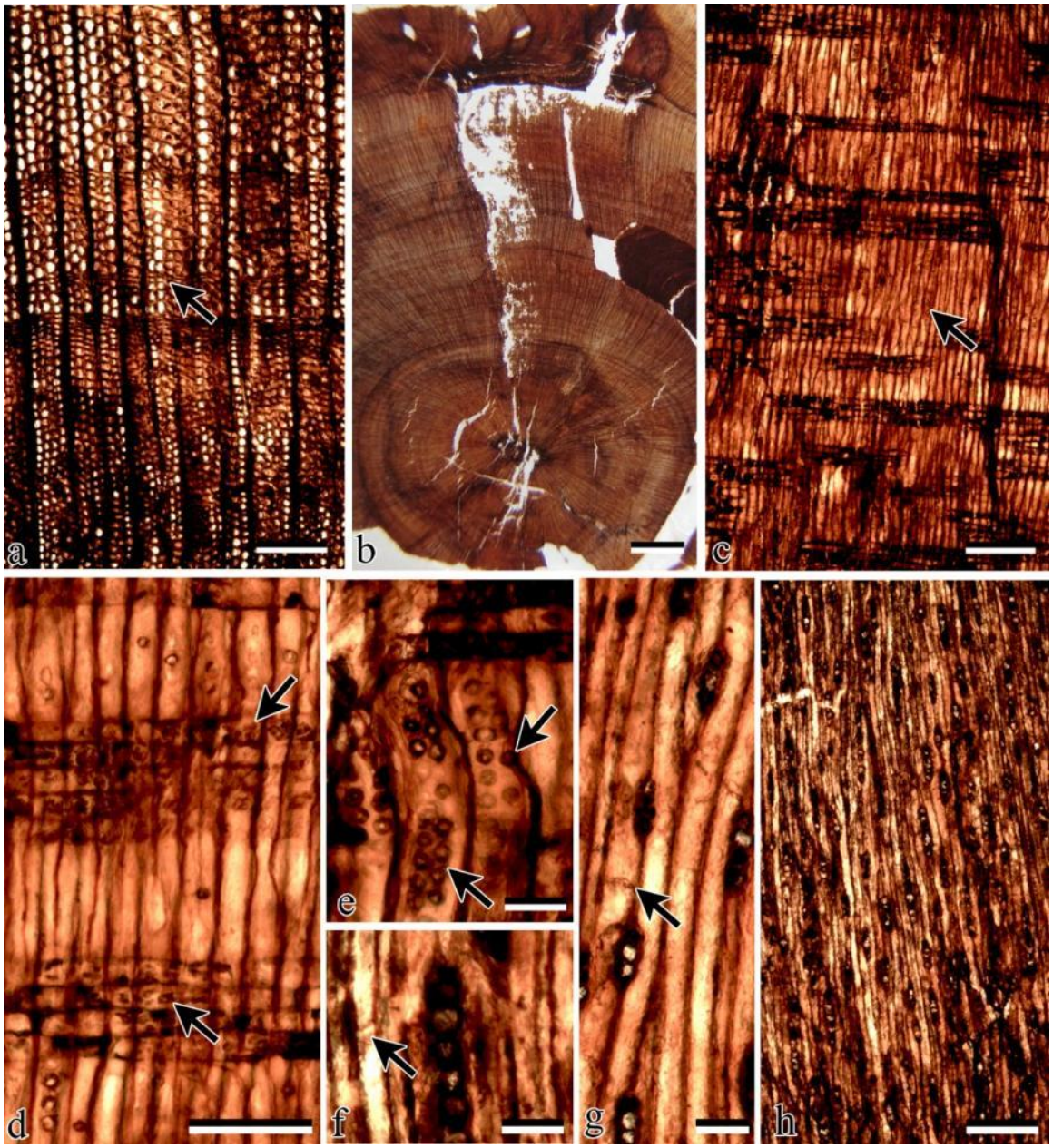

Figure 2.9. *Taxodioxylon* sp. 1. a. TS showing growth rings and false ring (arrow). MPM-15, scale bar = 250 µm. b. TS showing pith and growth rings. MPM-18, scale bar = 2.5 mm. c. RLS showing abietinean pitting (arrow) and rays. MPM-15, scale bar = 250 µm. d. RLS showing small, obliquely angled taxodioid cross-field pits (arrow). MPM-15, scale bar = 100 µm. e. RLS showing alternate and opposite biseriate bordered pitting. MPM-15, scale bar = 50 µm. f. TLS showing pitting on an axial parenchyma (arrow). MPM-15, scale bar = 50 µm. g. TLS showing beading on the end walls of the axial parenchyma (arrow). MPM-18, scale bar = 50 µm. h. TLS showing uniseriate tangential rays. MPM-15, scale bar = 250 µm.

Figure 2.10. *Taxodioxylon* sp. 2. MPM-11b. a. TS showing growth rings, scale bar = 2.5 mm. b. TS showing growth rings (arrow), scale bar = 250 µm. c. RLS showing abietinean pitting (arrow) and rays, scale bar = 250 µm. d. RLS showing possible xenoxylon bordered pitting on the tracheid walls (arrow), scale bar = 50 µm. e. TLS showing beading on the end walls of the axial parenchyma (arrow), scale bar = 25 µm. f. RLS showing small, obliquely angled taxodioid cross-field pits (arrows), scale bar = 50 µm. g. TLS showing tangential uniseriate rays, scale bar = 250 µm. h. TLS showing uniseriate and biseriate (arrow) tangential rays, scale bar = 100 µm.

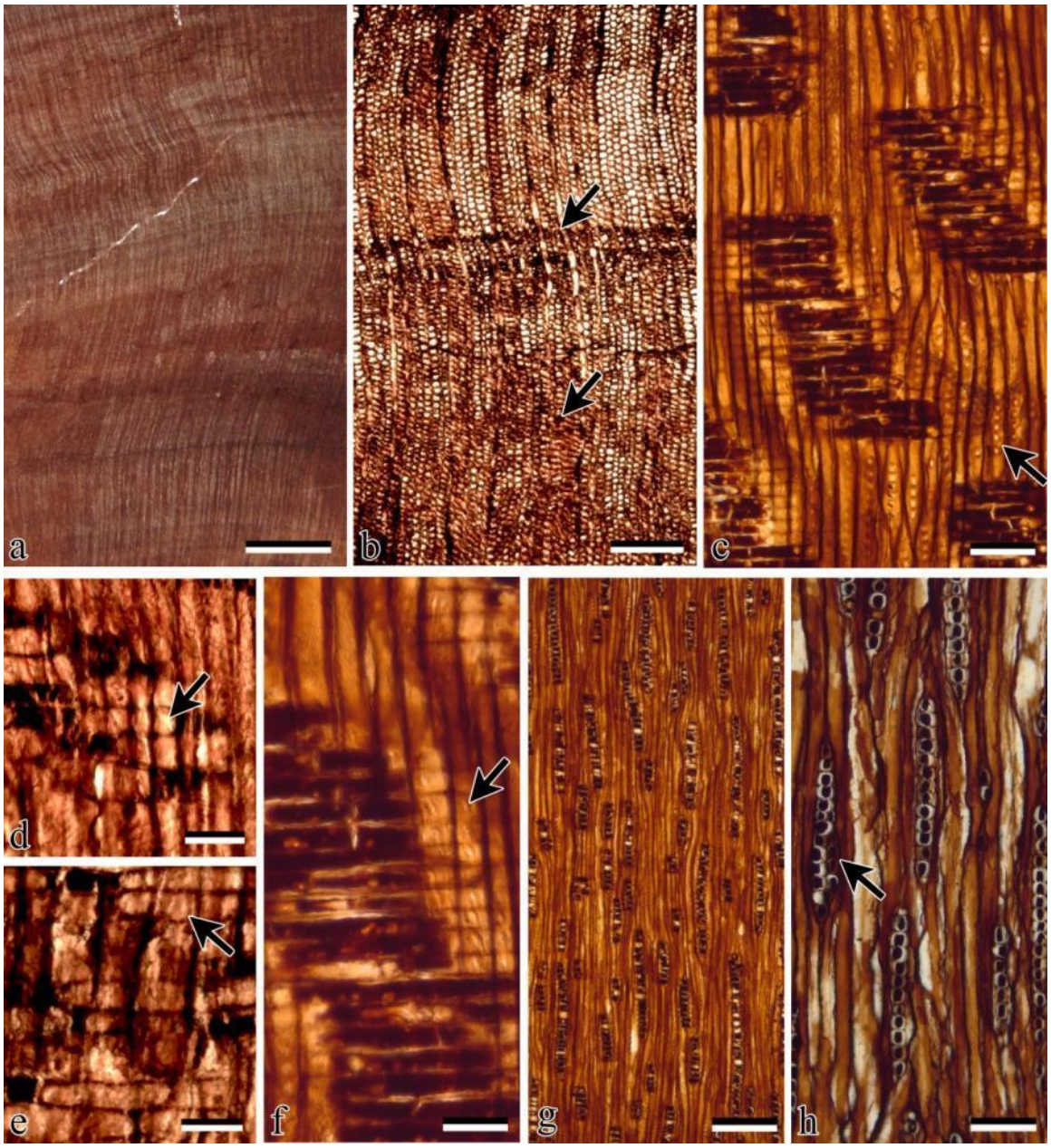

Figure 2.11. *Podocarpoxylon* sp. a. TS showing growth rings. MPM-30, scale bar = 2.5 mm. b. TS showing axial parenchyma (lower arrow) and a false ring (upper arrow) just after a true growth ring. MPM-30, scale bar = 250 µm. c. RLS showing abietinean pitting (arrow) on the radial wall of the tracheids. MPM-25, scale bar = 200 µm. d. RLS showing cross-field pits (arrow) and spiral checking in the tracheid walls. MPM-30, scale bar = 50 µm. e, f. RLS showing podocarpoid cross-field pitting (arrow). MPM-31(e), MPM-25 (f), scale bar = 50 µm. g. TLS showing uniseriate rays. MPM-25, scale bar = 250 µm. h. TLS showing a rare biseriate ray (arrow). MPM-25, scale bar = 100 µm.

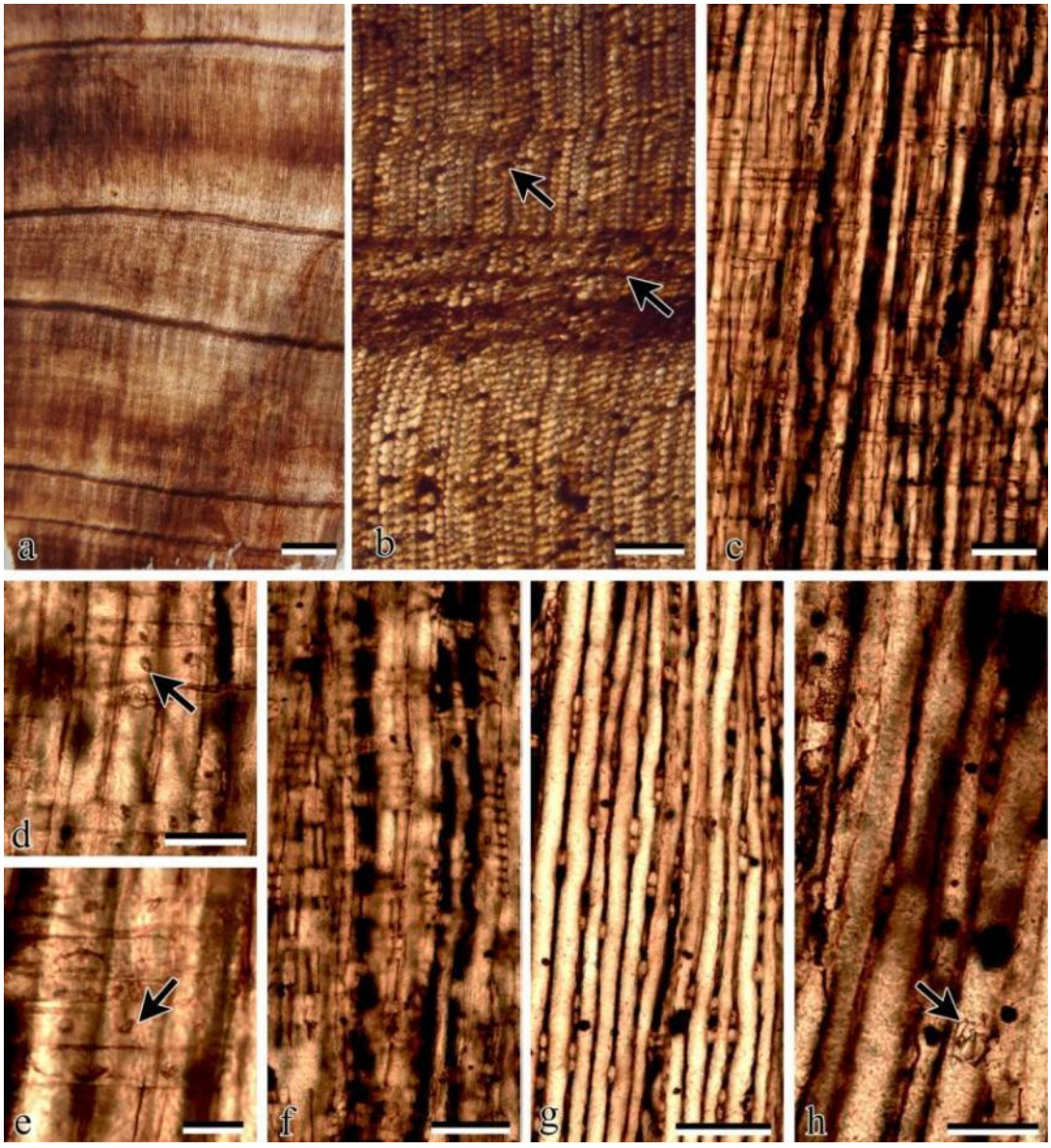

Figure 2.12. Gymnosperm indet. a. TS showing growth rings. MPM-22, scale bar = 2.5 mm. b. TS showing growth rings including false rings (lower arrow) and diffuse axial parenchyma (upper arrow). MPM-22, scale bar = 250 µm. c. RLS showing poorly preserved ray parenchyma. MPM-1, scale bar = 100 µm. d, e. RLS showing taxodioid cross-field pits (arrows). MPM-1, scale bars = 50 µm (d) and 25 µm (e). f. TLS showing rays and resin-filled parenchyma. MPM-1, scale bar = 50 µm. g. TLS showing very short rays. MPM-7, scale bar = 100 µm. h. TLS showing possible organic crystal deposit (arrow). MPM-7, scale bar = 50 µm.

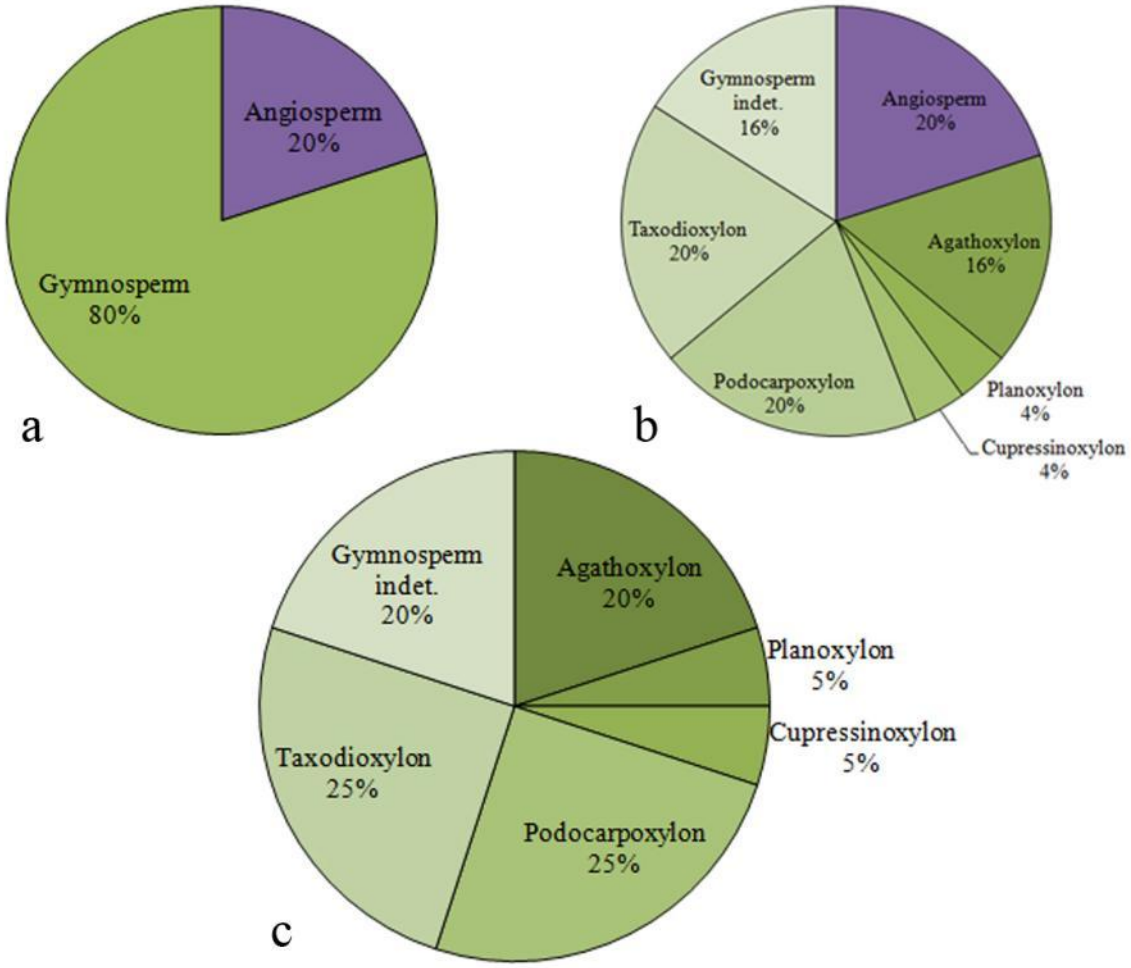

Figure 2.13. Percentages of gymnosperm wood from the Cerro Fortaleza Formation. a. Percentage of gymnosperm wood to angiosperm wood. b. Percentage of each gymnosperm morphogenera to the overall percentage of wood collected from the Cerro Fortaleza Formation. c. Percentage of each gymnosperm morphogenera.

CHAPTER 3: ANGIOSPERM WOOD FROM THE CERRO FORTALEZA FORMATION

INTRODUCTION

Extant angiosperms consist of approximately 400 families with over 400,000 species (Taylor et al., 2009). Approximately 95% of all vascular plants today are angiosperms. These plants live in more diverse environments and ecological niches than any other plant group, from oceans to rivers and deserts to rainforests. Their morphology is incredibly diverse as a function of their environments. Angiosperms are evolutionarily a relatively young group, with most of the modern families only originating between 130-90 million years ago (Davies et al., 2004; Stewart and Rothwell, 1993; Taylor et al., 2009; Willis and McElwain, 2002).

The sudden apparent emergence and diversification of angiosperms have been pondered by scientists since at least the 1870's. Charles Darwin notability called this "an abominable mystery" when discussing the subject in a letter written to Joseph Hooker (Davies et al., 2004). While many still consider this a difficult period from which there is little data, a far greater number of angiosperm fossils have been discovered since Darwin's time.

As discussed in previous chapters, the Cerro Fortaleza Formation contains abundant Late Cretaceous plant material. Silicified wood (Arbe and Hechem, 1984; Burmeister, 1892; Egerton et al., 2010; Ezcurra et al., 2010; Feruglio, 1935, 1938a, b, c,

1944; Kraemer and Riccardi, 1997; Lacovara et al., 2004; Marenssi et al., 2003; Novas et al., 2002; Novas et al., 2004; Novas et al., 2008; Novas et al., 2005b; Oviedo, 1982; Povilauskas et al., 2003), leaf (Arbe and Hechem, 1984; Novas et al., 2002; Riccardi and Rolleri, 1980) and palynomorphs (Arbe and Hechem, 1984; Kraemer and Riccardi, 1997; Oviedo, 1982; Povilauskas et al., 2003) have been identified from this formation. The palynomorphs are the only plant material to be studied up to this point. However, only two reports have discussed these microflora: an unpublished, unattainable dissertation (Oviedo, 1982) and an abstract (Povilauskas et al., 2003). The abstract only reports the occurrence of algae (*Pediastrum*), bryophyte and pteridophyte (*Azollopsis*) spores, and angiosperm and gymnosperm pollen. This chapter reports new angiosperm fossils from the Cerro Fortaleza Formation and their significance to understanding the paleobotany of the region.

METHODS AND MATERIALS

Permineralized wood was collected from the Cerro Fortaleza Formation in February 2009. This formation has been interpreted to have been deposited by a meandering fluvial system near the Atlantic shore of the Austral Basin during the Middle Campanian-Early Maastrichtian (Arbe, 1986, 1987; Arbe and Hechem, 1984; Kraemer and Riccardi, 1997; Macellari et al., 1989; Marenssi et al., 2003; Novas et al., 2002; Riccardi and Rolleri, 1980). Twenty-five samples were collected from three primary localities on the western flank of Cerro Fortaleza: northern, southwestern and southeastern sites (Figures 3.1-3.4). Latitude and longitude coordinates were recorded

for each sample using a Garmin eTrex GPS unit. All the samples were photographed in the field (Figure 3.5). Wood samples were initially examined with a 10x hand-lens to look for anatomical features in order to justify collection and subsequent thin-sectioning.

The fossil wood samples were thin-sectioned in Buenos Aries using standard techniques (Hass and Rowe, 1999). Thin-sections were made from three different planes for each sample: transverse (TS), tangential longitudinal (TLS) and radial longitudinal (RLS). All three planes were required to identify standard morphological features that permit analysis of morphological features. These thin sections were examined in February 2010 using transmitted light microscopy (a Leica DM2500 microscope with a Leica DFC290 camera attachment and an Olympus BX51 microscope with a DP25 camera attachment) at the Museo Argentino de Ciencias Naturales, Buenos Aires, Argentina. Digital photomicrographs were taken of all key morphological features (e.g. vessels, fibers, rays, ect.). Descriptions and identification were conducted using reference literature (e.g., Barefoot and Hankins, 1982; Carlquist, 2010; Hoadley, 1990; IAWA, 1989; Metcalfe, 1987; Metcalfe and Chalk, 1950, 1983; Philippe and Bamford, 2008) and computerized wood anatomy databases (e.g., InsideWood, 2004-onwards). The permineralized wood was described in accordance to the International Association of Wood Anatomists (IAWA) standards of wood morphology (IAWA, 1989). The specimens are curated at the Museo de Perito Moreno in Rio Gallegos, Argentina.

Precise measurements were made in accordance to recommendations from the IAWA. Vessel measurements were made in transverse section. The average tangential diameter of vessels was based upon fifty randomly chosen vessels. The number of vessels

per square millimeter was based upon ten randomly selected fields of view. The number of bars per scalariform perforation plate was based upon a minimum of ten plates. Ray measurements were made on tangential sections and are based upon measurements made on 25 rays. The ray width was based upon the number of cells in the thickest portion of the ray. The ray height was measured in microns and based on measurements made of 25 randomly assigned rays. The number of rays per linear millimeter was based upon ten randomly chosen fields of view of the thin section. A summary of the characteristics for each angiosperm wood sample has been recorded in Table 3.1.

The angiosperms were named using the International Code for Botanical Nomenclature (ICBN). Unlike gymnosperms, angiosperms show significant diversity in their morphological features. These features can distinguish taxa down to the genus and species levels in extant species (Carlquist, 2010; Metcalfe, 1987). Using this approach to identify and name taxa is typical for fossil angiosperms (Gottwald, 1992; Poole and Cantrill, 2001a; Poole et al., 2000a; Poole and Francis, 1999, 2000; Poole and Gottwald, 2001; Poole et al., 2000b; Wheeler and Lehman, 2009).

SYSTEMATIC PALEOBOTANY

Order: Laurales

Family: Monimiaceae

Subfamily: Monimioideae

Morphogenus: *Hedycaryoxylon* Süss 1960 emend.

Type species: *Hedycaryoxylon subaffine* Vater 1884

Hedycaryoxylon sp. A

Material: MPM-13, MPM-12, MPM-20, MPM-24

Type locality: Eastern side of the Río La Leona, northwest of Cerro Fortaleza. 49°56' S; 072°03' W

Formation: Cerro Fortaleza

Age: Campanian

Repository: Museo de Perito Moreno in Rio Gallegos, Argentina

Generic diagnosis: The emended generic diagnosis (translated by Poole and Gottwald 2001) for *Hedycaryoxylon* includes: diffuse porosity; solitary, short radial rows or small groups of vessels; scalariform perforation plates; bordered, opposite to scalariform intervessel pits; large, oval to scalariform ray-vessel pits; septate fibers with simple to bordered pits; scarce, diffuse, occasionally paratracheal axial parenchyma; tall (up to 5 mm), multiseriate (> 7 cells wide), heterocellular rays; uniseriate, upright rays; and oil idioblasts absent (Süss, 1960).

Species diagnosis: The species diagnosis for *Hedycaryoxylon* sp. A includes: weakly distinctive to distinctive growth rings; diffuse porosity; predominately solitary vessels; rare radial groups or clusters of up to 5 vessels; tangential diameters range from 21-90 µm; <47 vessels per square mm; rare axial parenchyma; oval to scalariform intervessel pits; rare uniseriate rays; multiseriate rays 2 to 9 cells wide; ray height of 0.46-2.17 µm; minute to distinctly bordered pits on the fibers; square, procumbent, upright and sheath cells.

Description: The holotype (MPM-13) and MPM-12 have been broken from permineralized logs that are at least a half meter in diameter. MPM-20 and MPM-24 have been recovered from spoil piles at the base of a hill and could have been from either trunk wood or branch wood (Figure 3.5). The only geological formation that crops out near where these specimens were found is the Cerro Fortaleza Formation. Growth rings are weakly distinct (MPM-13) to very distinct (MPM-12 and MPM-20) and can be distinguished based upon fiber diameter. The growth rings in MPM-13 can only be distinguished in the hand sample; whereas in MPM-12 and MPM-20, growth rings can be identified in both the hand samples and the thin sections. The vessels are distributed in a diffuse porous pattern and are randomly arranged to loosely radially arranged (Figure 3.6a, b). They have a circular to oval outline and occur predominantly as solitary vessels, but occasionally occur as paired and rarely in radial multiples or in clusters (3-5 vessels per grouping). Vessel walls are thin compared to fibers and parenchyma. The mean tangential diameter of the vessel lumina is 73 µm with a range of 21-90 µm. The average

number of vessels per square millimeter is 35 vessels with a range of 19-65 vessels. Perforation plates are scalariform with between 9-32 bars per plate (Figure 3.6c). Vessel-ray pitting consists of simple, horizontal (scalariform) pits (Figure 3.6d, e). Intervessel pitting is scalariform (Figure 3.6f). Helical thickenings in vessel elements are absent. Tyloses are common. Ground tissue fibers contain distinct bordered pits that can be seen in both radial and tangential longitudinal section (Figure 3.6g). Both septate and nonseptate fibers occur in the specimen (Figure 3.6f). Fiber walls are thin to thick. Axial parenchyma is diffuse and is occasionally paratracheal, occurring either above and/or below a vessel. Rays are predominantly multiseriate with a mean width of 5 cells (range, 1-17 cells) with the majority of the rays being 3, 4 or 5 cells wide (Figure 3.6h). Uniseriate rays are rare. The mean ray height is 1.03 mm with a range of 0.46-2.17 mm. The mean number of rays per millimeter is 13 rays with a range of 6-16 rays. Ray cells are procumbent (centrally located in the ray), square and upright (toward the margins of the ray). Larger sheath cells predominantly occur at the ends of the rays and often extend the rays an additional 0.25-0.5 mm (Figure 3.6h,i).

Identification: There have been four previously assigned *Hedycaryoxylon* species: *H. hortonioides* from South Africa (Mädel, 1960), *H. tambourissoides* from Antarctica (Poole and Cantrill, 2001a; Poole and Gottwald, 2001), *H. subaffine* (Süss, 1960) and *H. vasicentrosum* from Germany (Gottwald, 1992). All the species except *H. vasicentrosum* are from Upper Cretaceous strata (Gottwald, 1992).

The species described here, *H.* sp. A, is distinct from those previously described. Two of the primary differences between *H.* sp. A and the other described species includes: the presence of growth rings and distinctive bordered pits on the fiber walls in *H.* sp. A. None of the described species contain distinctive growth rings. Moreover, putatively, they do not have distinctive bordered pitting on the fiber walls. The InsideWood online wood database lists both *H. hortonioides* and *H. vasicentrosum* as containing bordered pits on their fibers; however, neither their descriptions nor their figures suggest the presence of this feature (Gottwald, 1992; InsideWood, 2004-onwards; Mädel, 1960). Thus, until further descriptions are published to the contrary, it is assumed that these species do not have bordered pitting on the fiber walls. Specific differences with other species include: *H. hortonioides* containing smaller, more abundant vessels, a greater abundance of axial parenchyma and rhombic crystals; *H. tambourissoides* having larger, less abundant vessels, less bars on the scalariform perforation plates and higher rays; *H. subaffine* containing smaller vessels, less bars on the scalariform perforation plates, absent tyloses and higher rays; and *H. vasicentrosum* having larger vessels, more bars per perforation plate, higher rays and rhombic crystals present (Table 3.2).

Hedycaryoxylon sp. A is very similar to wood of the extant members of the family Monimiaceae, in particular, *Hedycarya* and, to a lesser extent, *Tambourissa*. The general family characteristics include: predominantly diffuse porous wood; vessel tangential diameter between 50-100 µm; predominantly solitary with occasional short radial multiples/clusters of vessels; scalariform perforation plates; scarce to diffuse axial parenchyma; and predominantly wide multiseriate rays. Additional *Hedycaryoxylon* sp. A features which may also be found in extant *Hedycarya* and *Tambourissa* are wide

multiseriate rays (8-16 cells wide), fibers that may be septate and small bordered pits on the fiber walls (InsideWood, 2004-onwards; Metcalfe, 1987; Metcalfe and Chalk, 1950; Poole and Gottwald, 2001).

Order: Fagales

Family: Nothofagaceae

Morphogenus: *Nothofagoxylon* Gothan 1908

Type species: *Nothofagoxylon scalariforme* Gothan 1908

Nothofagoxylon corrugatus Poole Hunt et Cantrill 2001

Material: MPM-26

Description: This sample was collected from a spoil pile at the base of an outcrop of interbedded channel sands and muds (Figure 3.4). There are no other geological formations, other than the Cerro Fortaleza Formation, on the hill above where the specimen was found. It notably has ancient insect borings on it and through it (Figure 3.5e). There are only a few distinct growth rings present (Figure 3.7a, b). In most cases, the growth ring boundaries are relatively indistinct with minimal structural changes (i.e. vessel density and fiber thickness) except for an undulating band (Figure 3.7b). The wood is semi-ring porous to diffuse porous. The vessels are almost exclusively solitary (Figure 3.7b). The number of vessels per square millimeter averages 30 (standard

deviation 5.09, median 29) with a range of 23-39. The vessels are oval-shaped with the long axis being radially aligned (Figure 3.7b). The mean tangential diameter of the vessel is 64µm (standard deviation 19.07 µm, median 61 µm) with a range of range 56-92 µm. Both simple and scalariform perforation plates are present, the latter being dominant (Figure 3.7c, d). Scalariform perforation plates consist of 20-40 bars. Vessel-ray pits have simple borders with mostly rounded pits and fewer scalariform pits (Figure 3.7f). Intervessel pits are predominantly scalariform; however, opposite pits do occur (Figure 3.7e). Tyloses are very common (Figure 3.7b, h). Fibers are thin-walled and contain distinct bordered pits that can be seen in radial longitudinal section (Figure 3.7g). Septate fibers are present. Axial parenchyma are absent. Rays are primarily biseriate (average number of cells, 2.2); uniseriate and triserate rays are less common (Figure 3.7h). The average height of the rays is 715 µm (standard deviation, 1.23 µm, median 739 µm) with a range of 337-1074 µm. The average number of rays per square millimeter is 12 (standard deviation, 1.23; median 12) with the range begin 11-14 rays. The cellular composition of the rays is procumbent, square and upright cells (Figure 3.7i).

Identification: MPM-26 is identified as *Nothofagoxylon corrugatus* based on the following characteristics: growth rings present and undulating; vessels solitary; vessels elliptical; perforation plates simple to scalariform; vessel-ray pitting oval to scalariform; intervessel; uni-, bi-, or triseriate rays; crystals absent; thin-walled fibers with distinct bordered pits on the fiber wall (Poole, 2002; Poole et al., 2001). *N. corrugatus* has been established as a species by Poole et al. (2001) from six specimens of the Eocene from

King George Island, Antarctic Peninsula. Four additional specimens have been recovered from latest Maastrichtian-earliest Paleocene sediments from Seymour Island, Antarctica (Poole, 2002). There are only slight differences between MPM-26 and the Antarctic material. The Antarctic material has more abundant vessels per square millimeter; while MPM-26 has septate fibers and more frequent biseriate rays. Poole et al. 2001 state that one specimen, P 3023.13, contains exclusively biseriate rays. The only possible difference that could warrant a new species would be the presence of septate fibers; however, Poole (2002) admits that the fibers are poorly preserved. Other than that, there is not enough difference to identify MPM-26 as a new species. Poole et al. (2002) state that *Nothofagoxylon corrugatus* is most similar to the extant *Nothofagus* subgenus *Fuscospora*, in particular *Nothofagus solandri* and *Nothofagus fusca.*

DISCUSSION

This is the first extensive study of angiosperm wood from the Cretaceous of southern Argentina. The fossilized angiosperm wood from the Cerro Fortaleza Formation has a low abundance and diversity, especially when compared to the gymnosperm wood (Figure 3.8). However, both the apparent low abundance and diversity might well be a function of taphonomy, with the paleoassemblage only partly reflecting the original paleocommunity. Only two morphospecies have been identified: *Hedycaryoxylon sp. A* and *Nothofagoxylon corrugatus*. *H. sp. A* is a newly described taxon based on four specimens: two of the specimens (MPM-12 and MPM-13) are from

the northern site, while the other two (MPM-20 and MPM-24) are from the southwestern site (Figures 3.3 and 3.4). This material consists of a mixture of wood types including trunk wood (Figure 3.5 a, b) and, possibly, branch wood (Figure 3.5 c, d) *N. corrugatus* is from the southern-most portion of the southwestern site (Figure 3.4). The sample is possibly from branch wood, although it is difficult to determine whether it was branch or trunk wood. Notably, there are insect borings on and through the specimen (Figure 3.5e).

Cretaceous angiosperm fossils have been discovered on all the Southern Hemisphere continents; however, the abundance of such fossils is not as plentiful as in the Northern Hemisphere (Archangelsky et al., 2009; Iglesias et al., 2007). Extensive studies on Argentine angiosperm fossils have been conducted in recent years and have helped scientists to better understand the evolution of angiosperms (e.g. Archangelsky et al., 2009; Iglesias et al., 2007; Passalia, 2007; Povilauskas et al., 2008; Quattrocchio et al., 2006). Archangelsky et al. (2009) have analyzed angiosperm palynomorphs and leaf impressions from the late Barremian-Coniacian of 19 formations from 5 of the Argentinian Basins. They recognize three distinct stages of angiosperm evolution. The first stage occurs during the Late Barremian-Aptian and is demarcated by the first appearance of angiosperm pollen and leaves in Patagonia. The second stage includes diversification of angiosperm floras during the latest Aptian-earliest Albian. The third stage clearly reflects a sudden increase in both diversity and abundance of angiosperms throughout Argentina (2009). Similar world-wide patterns have been reported during the Cretaceous (Archangelsky et al., 2009; Stewart and Rothwell, 1993; Taylor et al., 2009).

Within the Late Cretaceous of the Austral Basin, the angiosperm record has only been studied in a few formations. The Cenomanian fossil flora of the Mata Amarilla Formation is well-known. Berry (1928; 1937) and Frenguelli (1953) are recognized for conducting the first studies of the fossil flora in this Formation. Recently, the fossil leaves from Mata Amarilla Formation have been studied by Iglesias et al. (2007). The fossil flora includes 500 preserved leaves from two localities that represent two different paleocommunities (lowland and highland). The lowland community consists predominantly of accumulated angiosperm (82%), fern (10%) and conifer (8%) leaves from a delta plain environment (coastal). Based on the leaf data and the presence of coniferous wood, Iglesias et al. (2007) posit that the Mata Amarilla flora represents an environment consisting of a canopy of coniferous trees with smaller, herbaceous angiosperms and ferns. The upland paleocommunity deposit has been interpreted to have been deposited in a meandering fluvial environment with associated floodplains and adjacent lacustrine environments. This section bears vertebrate fossils, fossil leaves, silicified wood and charcoalified plant remains. The leaf fossils are poorly preserved compared to those in the lower section. Iglesias et al. (2007) suggests these leaves had been deposited in a high-energy fluvial environment, hence the poor preservation. They conclude that the Mata Amarilla Formation contains a greater morphological variation of fossil leaves than coeval Gondwanan formations (Iglesias et al., 2007).

More recently, the Maastrichtian La Irene Formation microflora have been studied by Povilauskas et al. (2008). Samples taken from two horizons, a lower and an upper, have yielded 42 morphotypes of non-fungal spores and pollen and 2 species of dinoflagellate cysts. The paleoassemblage is predominantly composed of terrestrial

plants with ferns being the most abundant, followed by angiosperms and, to a lesser amount, gymnosperms. Angiosperm pollen is dominated by Chloranthaceae (*Clavatipollenites* sp.) and Arecaceae (*Arecipites* spp., *Longapertites* sp., *Spinizonocolpites hialinus*) with lesser amounts of Liliaceae (*Liliacidites* spp.), Proteaceae (*Proteacidites* sp., *Peninsulapollis gillii, Retidiporites camachoii),* Ericaceae (*Ericipites scabratus*), Nyssaceae (*Nyssapollenites* cf. *squamosus*) and Symplocaceae (*Senipites* sp.) palynomorphs. Based on the data from the microflora, Povilauskas et al. (2008) conclude that the continental assemblages of the La Irene Formation is dominated by ferns and angiosperms with lesser quantities of gymnosperms. They suggest that the Podocarpaceae pollen had been transported in from other environments because of the low frequency of pollen (Podocarps release high amounts of pollen). The paleoclimate would have been warm-temperate to warm-wet at least locally based on the species present and their abundance (Povilauskas et al., 2008). They do note the lack of Nothofagaceae pollen. Coeval angiosperm floras in the Antarctic Peninsula are dominated by Nothofagaceae. Povilauskas et al. (2008) have proposed that Nothofagaceae had not reached this region of South America by the Maastrichtian. However, based on the newly identified *Nothofagoxylon* species from the Cerro Fortaleza Formation, we know that Nothofagaceae species were present from the Campanian of South America.

Records of Cretaceous angiosperm wood from the Antarctic Peninsula far outweighs coeval angiosperm wood from Argentina (see Cantrill and Poole, 2005; Herbst et al., 2007). Eight angiosperm families have been recorded from Cretaceous beds of Anatrctica: Lauraceae, Cunoniaceae, Illiciaceae, Winteraceae, Nothofagaceae,

Monimiaceae, Atherospermataceae, Myrtaceae (Cantrill and Poole, 2005; Poole, 2002; Poole and Cantrill, 2001a; Poole et al., 2000a; Poole and Francis, 1999, 2000; Poole and Gottwald, 2001; Poole et al., 2000b; Poole et al., 2003; Poole et al., 2000c). Angiosperm wood (*Antarctoxylon* and *Weinmannioxylon*) is first reported as early as the Coniacian from the Antarctic Peninsula (Poole and Cantrill, 2001a; Poole et al., 2000a). Significant increases in the abundance and diversity of angiosperm wood are such that, by the Santonian, 70% of the fossil wood recovered from the Antarctic Peninsula is angiosperm. Thus, the overall forest canopy changes from the predominantly coniferous canopy of the Early Cretaceous to a diverse angiosperm dominated canopy during the Late Cretaceous. A slight decline (down to 63%) in the relative abundance of angiosperms occurs during the Campanian (Cantrill and Poole, 2005). During this phase, *Hedycaryoxylon* makes its first and last appearance in the Antarctic Peninsula. *H. tambourissoides* has only been identified from five specimens from Campanian beds on James Ross and Livingston Islands (Poole and Cantrill, 2001a; Poole and Gottwald, 2001). Woods belonging to Nothofagaceae appear during the Early Campanian and rapidly increase in abundance to the point where nearly half of all angiosperm woods from the Campanian of the Antarctic Peninsula belong to *Nothofagoxylon* (Cantrill and Poole, 2005). Five different species of *Nothofagoxylon* have been identified from the Antarctic Peninsula during the Cretaceous: *N. scalariforme*, *N. ruei*, *N, kraeuseli*, *N. aconcaguaense* and *N. corrugatus*.

CONCLUSIONS

Despite the abundance of fossil angiosperm discoveries in the Austral Basin, this is the first description of Cretaceous angiosperm wood in this region. *Hedycaryoxylon* and *Nothofagoxylon* have both been identified in coeval sediments from the Antarctic Peninsula. The Cerro Fortaleza angiosperm flora is not as diverse as those in Antarctica; however, only a limited number of fossil wood fragments have been found in the Cerro Fortaleza Formation. The new species of *Hedycaryoxylon* described in this study adds valuable information to the diversity and distribution of this group that will no doubt have implications for the biogeography of this morphogenus and for the Monimiaceae family. Additionally, the *Nothofagoxylon* species recovered from the Cerro Fortaleza Formation proves to be the oldest Nothofagaceae fossil in Argentina. The presence of these two morphospecies in coeval rocks in southern South America and Antarctica indicates the possibility of the dispersal of plants between these two locations.

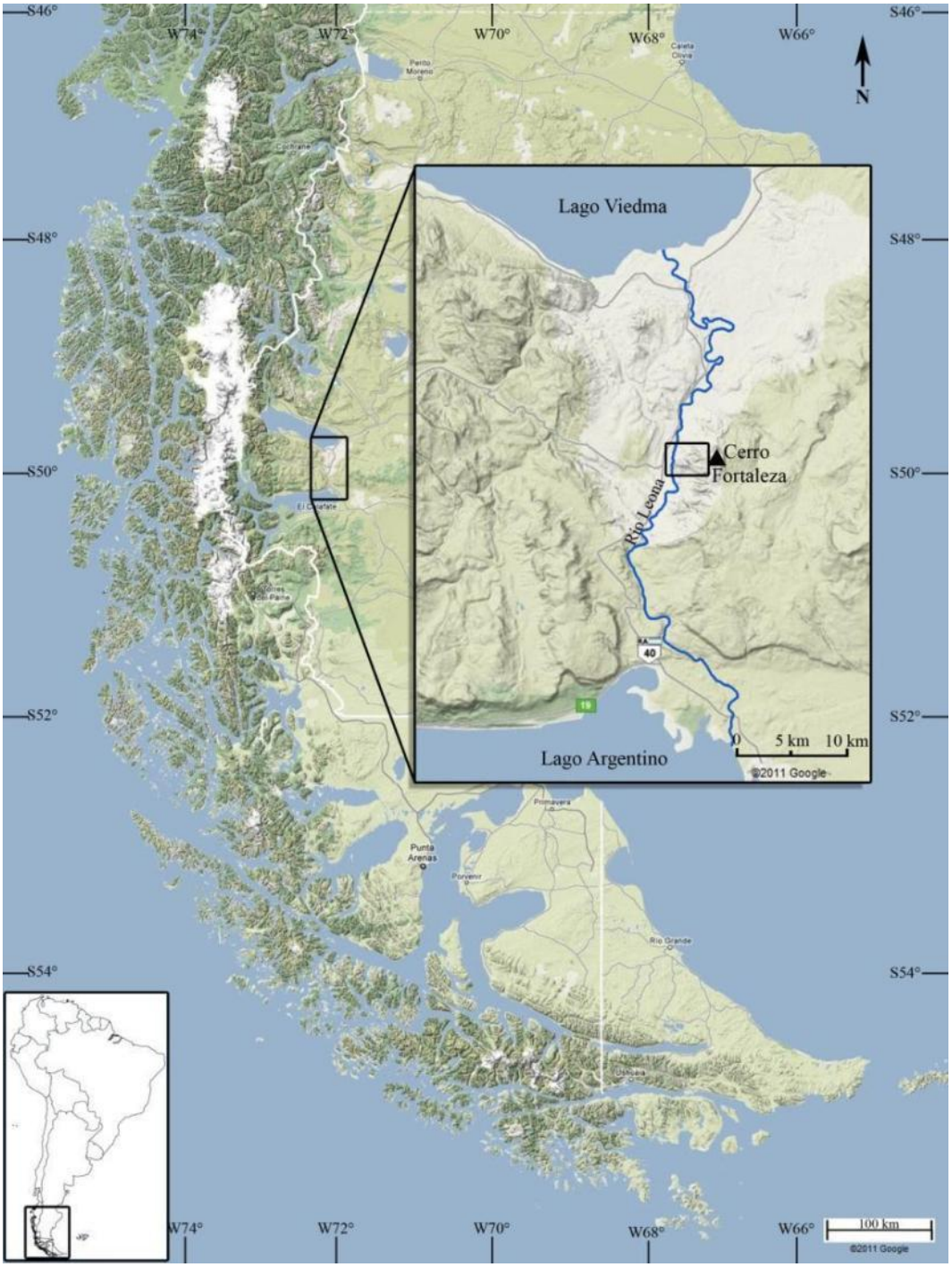

Figure 3.1. Map of the Patagonia region of South America and the study region (large inset). The inset in the upper map is Figure 3.2.

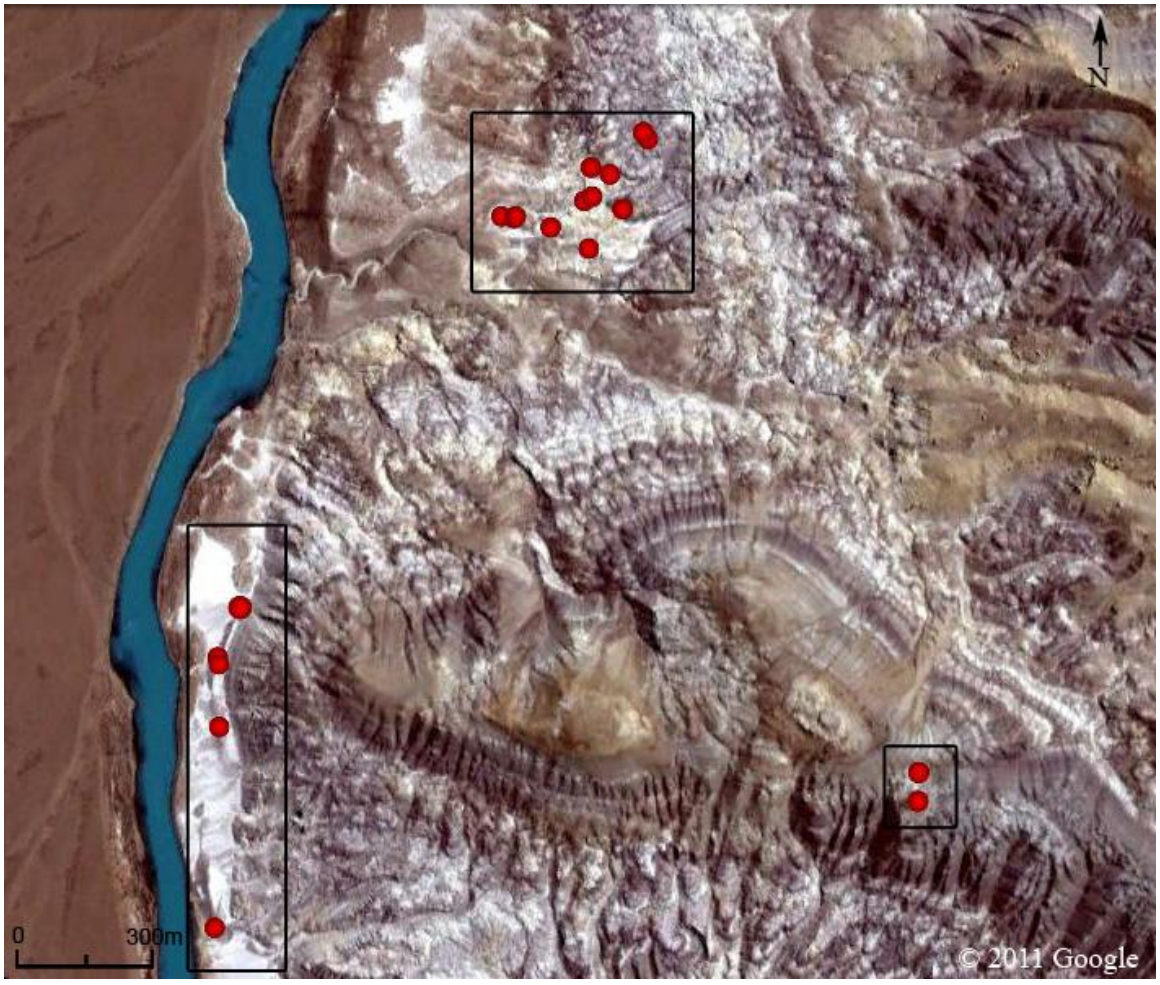

Figure 3.2. A map showing the region under study and the three fossil wood sites: northern, southwestern and southeastern. Only the northern (Figure 3.3) and southwestern sites (Figure 3.4) yielded permineralizaed angiosperm wood.

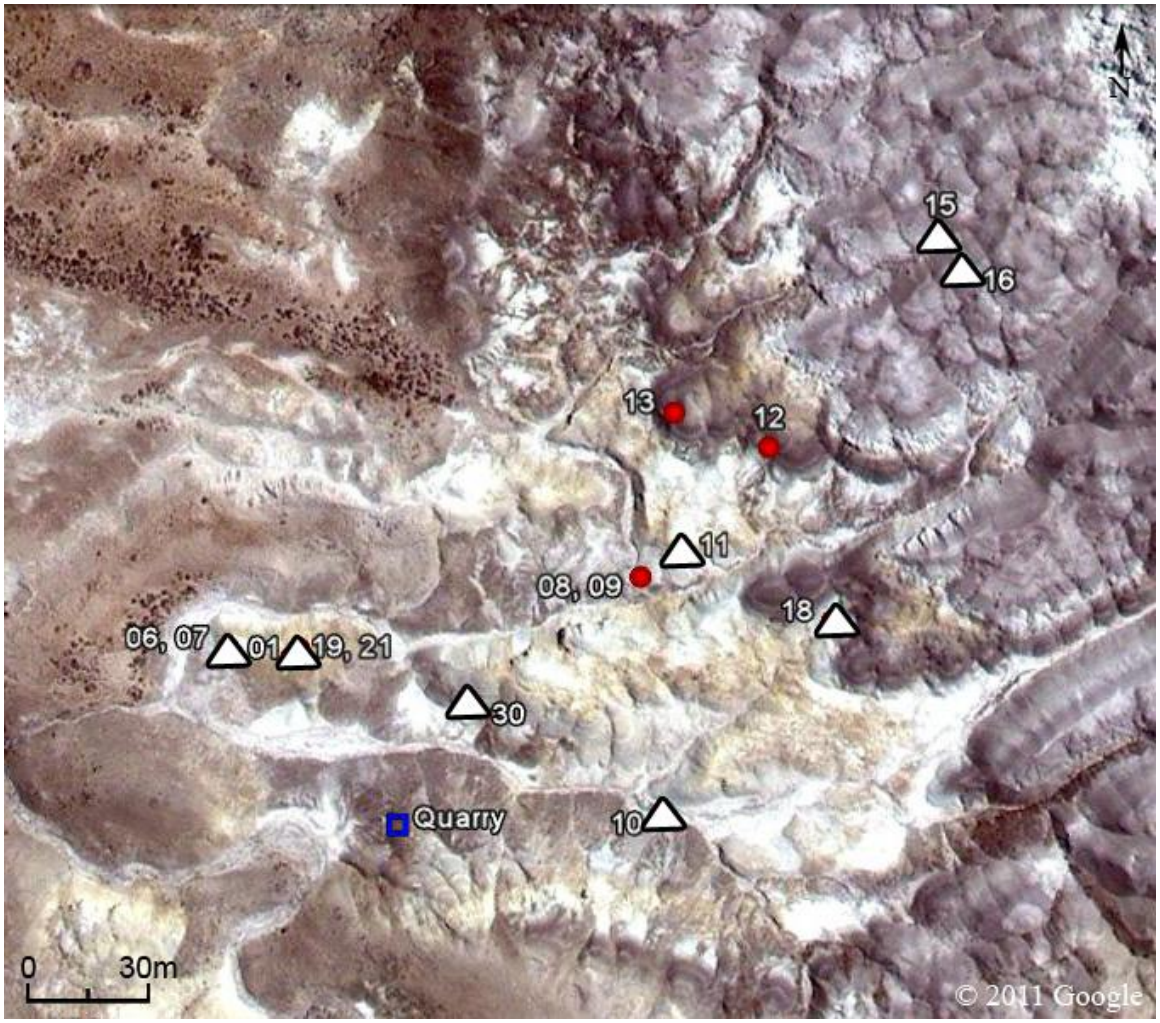

Figure 3.3. A map showing the northern site. The red circles indicate where fossil wood samples of angiosperms were collected,while the white triangles indicate where fossil wood samples of gymnosperms were collected. The blue square shows the relationship of the fossil wood collected to a titanosaur quarry.

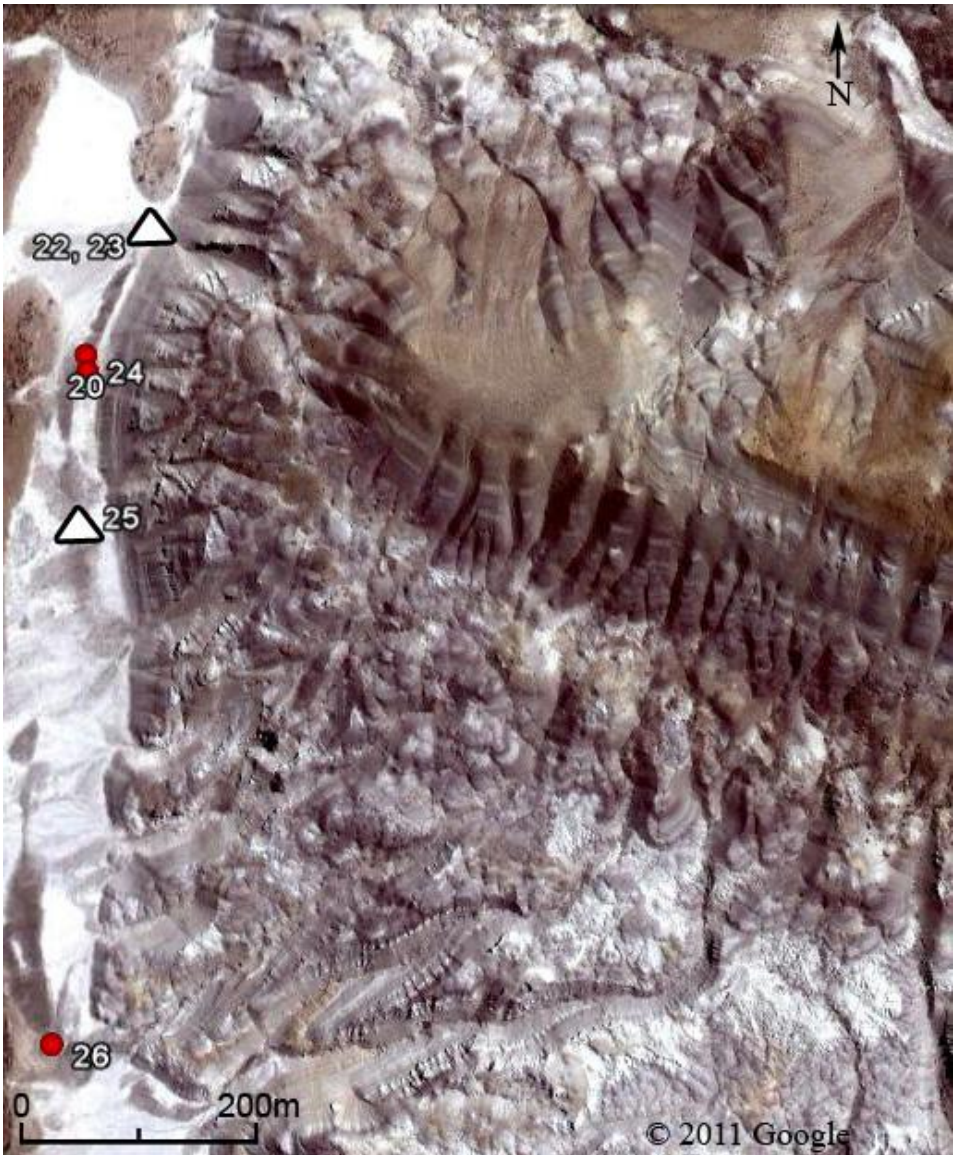

Figure 3.4. A map showing the soutwestern sites. The red circles indicate where fossil wood samples of angiosperms were collected, while the white triangles indicate where fossil wood samples of gymnosperms were collected.

Table 3.1. Anatomical Features of angiosperm wood from the Cerro Fortaleza Formation.

Feature	MPM-13 *Hedycaryoxylon sp. A*	MPM-20 *Hedycaryoxylon sp. A*
Growth rings	distinct (specimen), absent (thin section)	distinct
Vessels		
porosity	diffuse	diffuse
arrangement	diffuse to locally radial	diffuse
groupings	solitary, paired, rarely grouped (3 vessel groupings)	solitary, very rarely paired
tangential diameter (µm)	mean 78.16; st dev 11.74; median 40.50; range 21-71	mean 69.84; st dev 12.37; median 33; range 18-72
number per mm^{-2}	mean 25.30; st dev 4.45; median 25; range 19-32	mean 30.60; st dev 7.03; median 30; range 26-47
cross-sectional shape	oval, round	oval, round
perforation plates	scalariform	scalariform
scalariform bar number	(+)15 to 32	(+)20 to 31
intervessel pitting	scalariform to opposite	scalariform to opposite
vessel-ray pitting	scalariform	scalariform
helical thickenings	absent	absent
tyloses	common	rare
Fibers		
pitting	distinct bordered pits (RLS and TLS)	distinct bordered pits (RLS)
septate	present	present
Axial parenchyma	present	absent
distribution	diffuse	diffuse
crystals	absent	absent
Rays		
width (cells)	mean 4.36; st dev. 1.52; median 4; range 2-8	mean 4.28; st dev. 0.97; median 4; range 3-6
height (µm)	mean 1142.76; st dev. 482.51; median 1065; range 467-2173	mean 1077.2; st dev. 395.59; median 1007; range 463-1728
number per mm	mean 14.80; st dev. 1.23; median 15; range 12-16	mean 14.30; st dev. 1.16; median 14; range 13-16
cellular composition	procumbent, square, upright, sheath cells	procumbent, square, upright, sheath cells

Table 3.1. Continued.

Feature	MPM-12 *Hedycaryoxylon sp. A*	MPM-24 *Hedycaryoxylon sp. A*
Growth rings	distinct	distinct
Vessels		
porosity	diffuse	semi-ring (?) to diffuse
arrangement	diffuse to locally radial	diffuse to locally radial
groupings	solitary, paired, rarely grouped (3-5 vessel groupings)	solitary, paired, occassionally grouped (2-7 vessel groupings)
tangential diameter (µm)	mean 54; st dev 14.73; median 51; range 25-90	mean 90.94; st dev 14.12; median 44; range 21-78
number per mm^{-2}	mean 31.60; st dev. 7.23; median 33.5; range 21-38	mean 51.70; st dev 11.05; median 54.5; range 33-65
cross-sectional shape	(oval)	oval, round
perforation plates	scalariform	scalariform
scalariform bar number	12 to +20	(+)9 to 13
intervessel pitting	scaliariform to opposite	scalariform to opposite
vessel-ray pitting	simple oval to scalariform	scalariform
helical thickenings	absent	absent
tyloses	rare	common
Fibers		
pitting	simple, minutely bordered pits (few) (TLS)	simple, minutely bordered pits (TLS)
septate	present	present
Axial parenchyma	extremely rare	present
distribution	diffuse	diffuse
crystals	absent	
Rays		
width (cells)	mean 5.20; st dev. 1.85; median 5; range 1-9	mean 7.08; st dev. 3.17; median 6; range 4-17
height (µm)	mean 976.72; st dev. 229.64; median 978; range 514-1431	mean 927.76; st dev. 394.09; median 869; range 409-1594
number per mm	mean 14.20; st dev. 0.42; median 14; range 14-15	mean 8.10; st dev. 1.29; median 8; range 6-10
cellular composition	procumbent, square, upright, sheath cells	procumbent, square, sheath cells

Table 3.1. Continued

Feature	MPM-26 *Nothofagoxylon corrugatus*
Growth rings	weakly distinct
Vessels	
porosity	semi-ring to diffuse
arrangement	radial to diffuse
groupings	solitary
tangential diameter (µm)	mean 64.16; st dev 19.07; median 61; range 35-101
number per mm^{-2}	mean 30.20; st dev 5.09; median 29; range 23-39
cross-sectional shape	oval
perforation plates	simple and scalariform
scalariform bar number	20-40
intervessel pitting	scalariform to opposite
vessel-ray pitting	round, scalariform
helical thickenings	absent
tyloses	common
Fibers	
pitting	distinct bordered pits (RLS)
septate	present
Axial parenchyma	absent
distribution	absent
crystals	absent
Rays	
width (cells)	mean 2.2; st dev. 0.58; median 2; range 1-3
height (µm)	mean 714.84; st dev. 170.74; median 739; range 337-1074
number per mm	mean 12.20; st dev. 1.23; median 12; range 11-14
cellular composition	procumbent, square, upright

Figure 3.5. Field photographs of the angiosperm fossil wood from the Cerro Fortaleza Formation. a. MPM-13 *Hedycaryoxylon sp. A* (holotype). b. MPM-12 *Hedycaryoxylon sp. A.* c. MPM-20 *Hedycaryoxylon sp. A.* d. MPM-24 *Hedycaryoxylon sp. A.* e. MPM-26 *Nothofagoxylon corrugatus*.

Table 3.2. Comparison of *Hedycaryoxylon* species modified from Poole and Gottwald (2001)

Growth rings	***H. sp. A* nov. sp.**	***H. tambourissoides***
Age and locality	Late Cretaceous, Argentina	Late Cretaceous, Antarctica
Growth rings	weakly distinct-distinct	weak-indistinct
Vessels		
porosity	diffuse	diffuse
groupings	solitary,rarely radial groups or clusters (3-5 vessel groupings)	solitary, radial groups and clusters of up to 4
tangential diameter (µm)	mean 73.24; range 21-90	mean 89; range 50-150
number per mm^{-2}	mean 34.8; range 19-65	range 10-32
perforation plates	scalariform	scalariform
scalariform bar number	9 to 32	6 to 12
intervessel pitting	scalariform to opposite	opposite, elongate, weakly scalariform
vessel-ray pitting	scalariform	oval to weakly scalariform
tyloses	present	present
Fibers		
pitting	simple to distinct bordered pits	?
septate	present	present
Axial parenchyma	present	present
distribution	scanty paratracheal	paratracheal
crystals	absent	absent
Rays		
width (cells)	mean 5.23; range 1-17 (mainly 3, 4 and 5)	range 1-18 (mainly 4, 7 and 18)
height (mm)	mean 1.03; range 0.46-2.17	range 0.35-5
cellular composition	heterocellular, procumbent, square, upright, sheath cells	heterocellular with square and procumbent body cells, square-upright marginal cells, sheath cells

Table 3.2. Continued.

Growth rings	***H. hortonioides***	***H. subaffine***
Age and locality	Late Cretaceous, South Africa	Late Cretaceous, Germany
Growth rings	Absent	absent/indistinct
Vessels		
porosity	diffuse	diffuse
groupings	solitary, radial or slightly diagonal groups of 2-3	solitary, radial groups of up to 4, tangential pairs
tangential diameter (µm)	mean 55; range 30-70	mean 55; range 45-90
number per mm^{-2}	24-76	~30
perforation plates	Scalariform	scalariform
scalariform bar number	14 to 34	10 to 24
intervessel pitting	scalariform	opposite, elongate, scalariform
vessel-ray pitting	large, oval, scalariform	large, oval, scalariform
tyloses	present	absent
Fibers		
pitting	?	?
septate	occasional	present
Axial parenchyma	present	present
distribution	apotracheal, diffuse, very few single cells	prismatic, scarce, diffuse, occasionally vasicentric
crystals	present near vessels	absent
Rays		
width (cells)	range 1-11 (mainly 4)	range 2-12 (mainly 5-10)
height (mm)	range 0.80-2.00	range 0.60-4.00
cellular composition	heterocellular with 1-3 rows of procumbent marginal cells, sheath cells	heterocellular with 1-4 rows of upright marginal cells, sheath cells

Table 3.2. Continued.

Growth rings	***H. vasicentrosum***
Age and locality	Early Tertiary, Germany
Growth rings	absent/indistinct
Vessels	
porosity	diffuse
groupings	solitary, short radial groups
tangential diameter (µm)	mean 85; range 60-125
number per mm^{-2}	?
perforation plates	scalariform
scalariform bar number	18 to 45
intervessel pitting	scalariform, opposite at ends of vessel elements
vessel-ray pitting	scalariform
tyloses	present
Fibers	
pitting	?
septate	present
Axial parenchyma	present
distribution	paratracheal; vasicentric scanty
crystals	present
Rays	
width (cells)	range 1-9 (mainly 4-8)
height (mm)	range ~1.30-3.50
cellular composition	heterocellular with single row of upright marginal cells, occasional rhombic crystals present

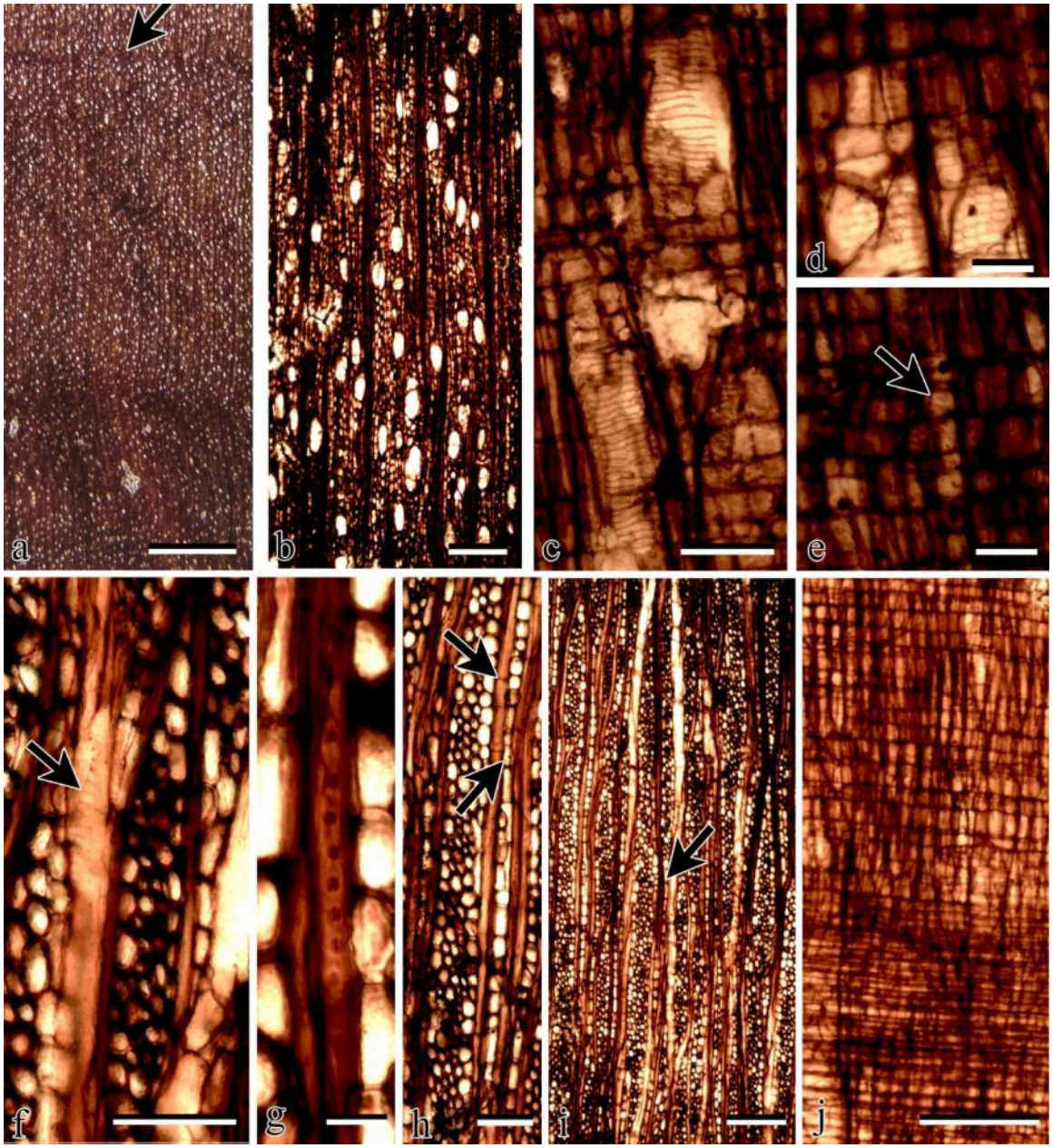

Figure 3.6. *Hedycaryoxylon* sp. A. a. TS with growth rings (arrow). MPM-12; scale bar = 2.5 mm. b. TS showing diffuse porous wood; scale bar = 250 µm. c. RLS showing scalariform perforation plates; scale bar = 100 µm. d, e. RLS showing oval to scalariform vessel-ray pits; scale bars = 50 µm. f. TLS showing scalariform intervessel pitting (arrow); scale bar = 100 µm. g. TLS showing ground fiber with minute bordered pitting; scale bar = 50 µm. h. TLS showing septate fibers (upper arrow) and sheath cell (lower arrow); scale bar = 100 µm. i. TLS showing multiseriate rays and sheath cells (arrow) scale bar = 250 µm. j. RLS showing procumbent, square and upright cells; scale bar = 250 µm. b-j, MPM-13 (holotype).

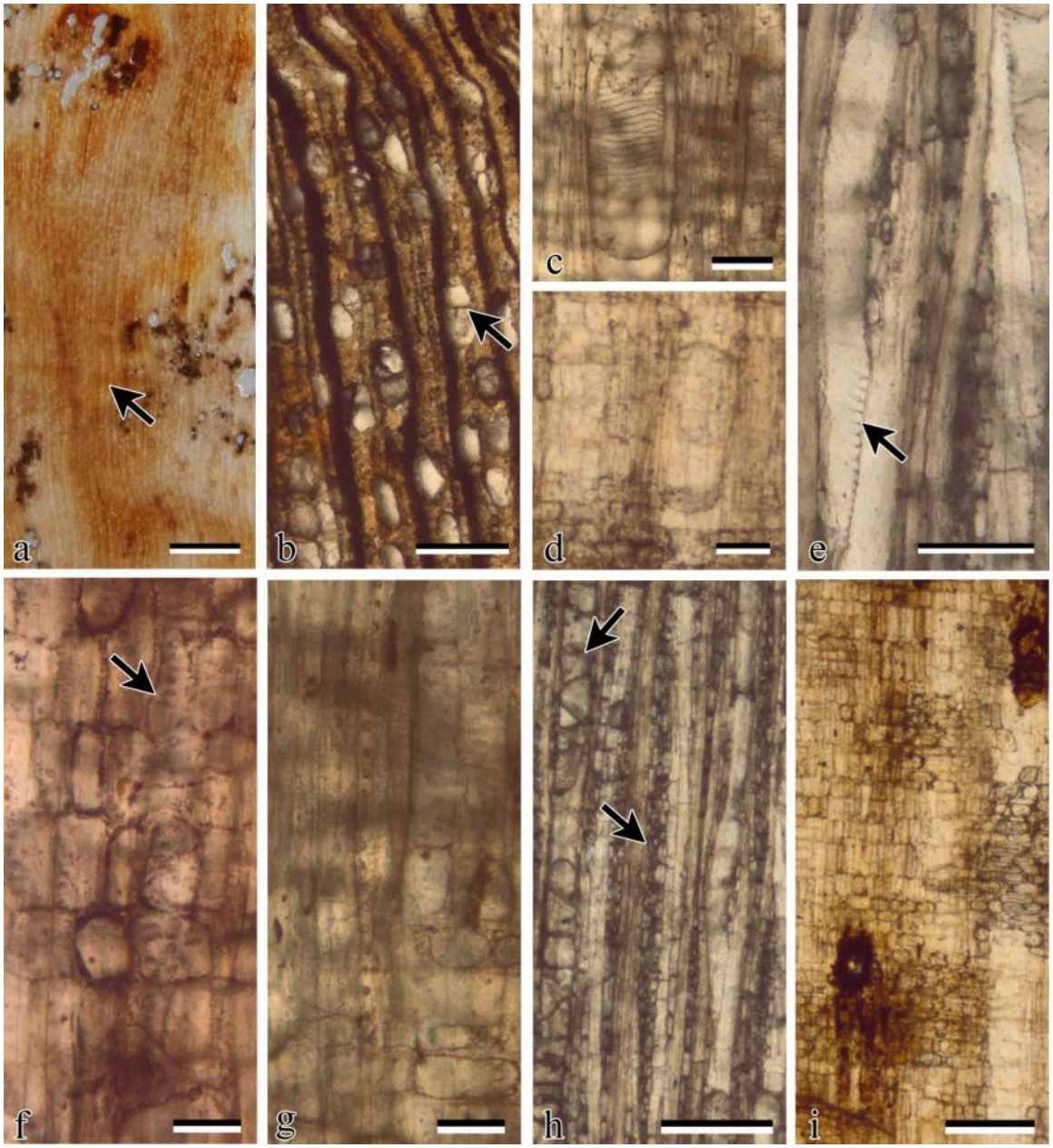

Figure 3.7. *Nothofagoxylon corrugatus*. MPM-26. a. TS showing one faint growth ring (arrow); scale bar = 2.5 mm. b. TS showing diffuse porous wood, solitary vessels, tyloses (arrow) and undulating region; scale bar = 250 µm. c. RLS showing scalariform perforation plate; scale bar = 100 µm. d. RLS showing simple perforation plate; scale bar = 100 µm. e. TLS showing scalariform intervessel pitting; scale bar = 100 µm. f. RLS showing simple vessel-ray pitting (arrow); scale bar = 100 µm. g. RLS showing ground fiber with minute bordered pitting; scale bar = 100 µm. h. TLS showing rays (lower arrow) and tyloses (upper arrow); scale bar = 250 µm. i. RLS showing cellular composition of ray; scale bar = 250 µm.

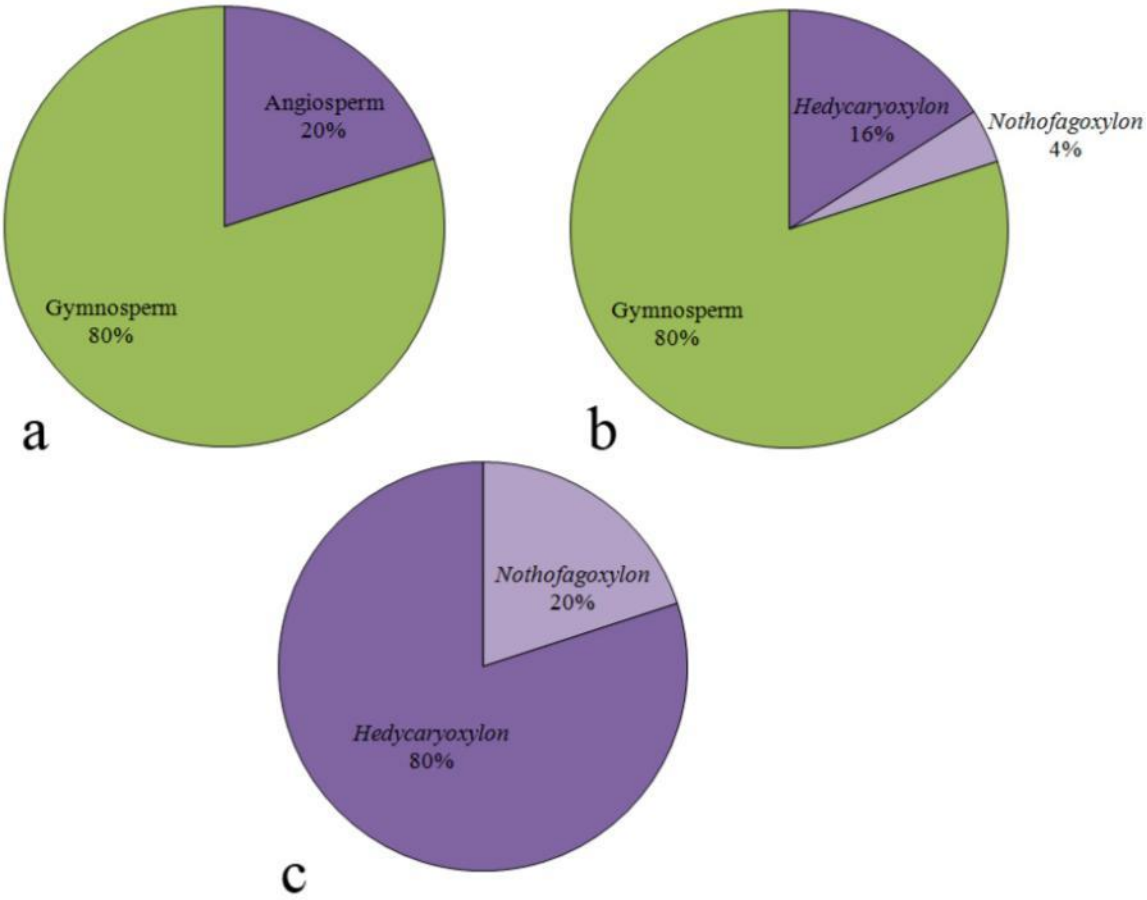

Figure 3.8. The percentages of angiosperm wood from the Cerro Fortaleza Formation. a. Percentage of angiosperm wood to gymnosperm wood. b. Percentage of each angiosperm morphogenera to the overall percentage of wood collected from the Cerro Fortaleza Formation. c. Percentage of each angiosperm morphogenera.

CHAPTER 4: NEONATAL TEETH IN DIRECT ASSOCIATION WITH A MATURE *TALENKAUEN SANTACRUCENSIS*

INTRODUCTION

The abundance and diversity of South American ornithopod dinosaurs has increased over the past two decades through discoveries such as *Talenkauen* (Novas et al., 2004), *Macrogryphosaurus* (Calvo et al., 2008), *Notohypsilophodon* (Martínez, 1998), *Gasparinisaura* (Coria and Salgado, 1996a; Salgado et al., 1997) and *Anabisetia* (Coria and Calvo, 2002). Despite these recent discoveries, the Gondwanan ornithopod record is incomplete compared to that of the Northern Hemisphere. Moreover, only *Gasparinisaura cincosaltensis* is known from multiple individuals representing different ontogenetic stages, from older juveniles to mature adults (Coria and Salgado, 1996a; Salgado et al., 1997).

The Cerro Fortaleza Formation is located in Santa Cruz Province, southern Argentina. The formation is exposed along the Río La Leona between Lagos Argentino and Viedma and along the southern shore of Lago Viedma (Barrancas Blancas) (Arbe, 2002; Arbe and Hechem, 1984; Novas et al., 2002). The Cerro Fortaleza Formation interdigitates with and overlies the Anita Formation (Campanian) and is overlain by the Irene Formation (Maastrichtian). The Anita Formation has been biostratigraphically dated using ammonite biozones and the Irene Formation with palynological biozones (Arbe and Hechem, 1984; Kraemer and Riccardi, 1997; Macellari et al., 1989; Povilauskas et al., 2008). Thus, the Cerro Fortaleza Formation must be Campanian-Maastrichtian? in age. This formation ranges in thickness from 350 m on Cerro Fortaleza

to 390 m at Barrancas Blancas (Arbe, 2002; Marenssi et al., 2003). It is characterized by lithified fluvial sands, overbank mud deposits, and paleosols deposited in fluvial, fluvial-palustrine and coastal plain environments on the northeastern margin of the Austral Basin (Arbe, 2002; Arbe and Hechem, 1984; Kraemer and Riccardi, 1997; Macellari et al., 1989; Marenssi et al., 2003; Novas et al., 2002). The Cerro Fortaleza Formation has also been referred to as the Pari Aike Formation, Chorrillo Formation and the Mata Amarilla Formation (Feruglio, 1938a, b, 1944; Goin et al., 2002; Kraemer and Riccardi, 1997; Leanza, 1972; Novas et al., 2002; Nullo et al., 1981a; O'Gorman and Varela, 2010; Varela, 2010a).

A distinct dinosaurian fauna consisting of ornithopod, sauropod, and theropod taxa has been described from the Cerro Fortaleza Formation which include: *Talenkauen santacrucensis* (Novas et al., 2004), *Puertasaurus reuili* (Novas et al., 2005b), *Orkoraptor burkei* (Novas et al., 2008), *Austrocheirus isasii* (Ezcurra et al., 2010) and a new genus and species of titanosaur is currently under study. Microvertebrate remains containing, elasmobranch teeth (*Archaeolamna kopingensis*), semionotiform/lepisoteid scales, dipnoan teeth, testudine fragments and theropod teeth have also been identified (Schroeter et al., in prep). Poorly preserved leaf impressions from indeterminate conifers and cycads have also been discovered but not yet described (Novas et al., 2002; Novas et al., 2008). Furthermore, fossilized angiosperm and gymnosperm wood is found throughout the formation (Egerton et al., 2010).

Talenkauen santacrucensis (MPM-10001) was discovered on the southern coast of Lago Viedma (Lat. 49° 51’ 16.2” S, Long. 72° 06’ 26.3” W) on Cerro Los Hornos in 2000. This specimen was encased in a well-cemented, medium-grained sandstone

interpreted as having been deposited in a fluvial channel. *T. santacrucensis* (Novas, 2004), a medium-sized ornithopod, was the first formally described dinosaur from the Cerro Fortaleza Formation (Figure 4.1a, b). This taxon is described from a partially articulated skeleton that includes: premaxilla, maxilla, predentary, dentary, teeth, 9 cervical, 16 dorsal, and 4 sacral vertebrae, ribs, mineralized intercostals plates, pectoral and pelvic girdles, and fore- and hindlimbs (Novas et al., 2004). *Talenkauen* has many iguanodontian synapomorphies, such as: rhomboid-shaped maxillary teeth with a prominent primary ridge on the labial surface of the crown; V-shaped predentary with processes for dentary articulation; presacral count of 9 cervical and 16 dorsal vertebrae; sigmoidal-shaped ilium that is shorter than the femur; and a mediolaterally, dorsoventrally deep pubis with prepubic process (Norman, 2004; Novas et al., 2004). This taxon also has plate-like, ossified structures between the anterior dorsal ribs. Novas et al. (2004) suggested that these structures are uncinate processes that may have aided in respiration, such as in extant Aves. Comparable plate-like structures are present in other ornithopods (e.g. *Thescelosaurus*, *Hypsilophodon*); however, there is little consensus as to the function of these structures (Butler and Galton, 2008; Codd and Manning, 2007; Codd et al., 2008). Novas et al. (2004) regarded *Talenkauen* as a euiguanodontian closely related to *Gasparinisaura* and *Anabisetia*.

Institutional Abbreviation. MPM, Museo Padre Molina, Río Gallegos, Santa Cruz.

MATERIAL

Two minute teeth and bone fragments were recovered during preparation of the body block of MPM-10001. They were found close to the rib cage. The two teeth were imaged using a scanning electron microscope (Phillips XL30) at the Museo Argentino de Ciencias Naturales. Because the teeth were found associated with the body block of *T. santacrucensis*, the Museo Padre Molina choose to assign them the same museum number as the holotype of this species.

DESCRIPTION

The small isolated teeth from the MPM-10001 body block are symmetrical and labial lingually compressed (Figure 4.1). The minute tooth crowns are approximately1 mm apicobasal height and 1.7 mm mesodistal width. A centrally located primary ridge occurs on the lingual surface with five secondary ridges accompanying the primary ridge. The secondary ridges run parallel to sub-parallel, relative to the primary ridge, and each leads to a marginal denticle (Figure 4.2b, c). The labial surface of the crown is enameled and has a steeply inclined wear facet (Figure 4.2a). Microstriae occur on the surface of the crown (Figure 4.2d, e). There is a cingulum at the base of the crown. The roots are not preserved.

DISCUSSION

The centrally located primary ridge, bilateral symmetry and five marginal denticles on the lingual surface indicate that these are dentary teeth from a basal ornithopod. Labial lingual compression of the crown and secondary ridges ending in marginal denticles are common in euornithopods (Norman et al., 2004). The dentary teeth of the mature *Talenkauen* individual (MPM-10001) are triangular with a central primary coronal ridge on the lingual surface. Five to six secondary apical ridges occur on either side of the primary ridge and run parallel to sub-parallel to the latter, similar to the condition in the juvenile MPM-10001 teeth (Figure 4.3). Basally, the lateral margins form broad ridges that merge with the primary ridge to form a moderate cingulum. Similarly in both the mature and juvenile MPM-10001 specimens, the lingual surface of the dentary teeth also possesses ridges; however, in the mature MPM-10001 individual, the dentary teeth have between 9-12 ridges. The dentary teeth of the mature MPM-10001 individual become mesodistally compressed and labial lingually expanded basally. Wear facets are steeply inclined on the labial surface in both the mature and juvenile MPM-10001specimens.

Other South American ornithopods (*Gasparinisaura cincosaltensis* and *Anabiestia saldiviai)* share the same dental morphology as observed in other euornithopods (Norman et al., 2004). *Gasparinisaura* dentary teeth have smooth labial surfaces; the features of the lingual surface are unknown. The number of marginal denticles in *Gasparinisaura* are the same as those in small MPM-10001 specimen (Coria and Salgado, 1996a). However, marginal denticle number can vary within individuals and cannot be reliably used as a diagnostic character (Norman et al., 2004). *Anabiestia*

has lingual ridges on the dentary teeth but does not appear to have a primary ridge (Coria and Calvo, 2002).

A recent taphonomic study on human teeth has shown that transportation in medium and coarse-grained sediments leads to extensive pitting and polishing of the enamel, respectively (King et al., 1999). Despite being encased in a medium-grained sandstone, the juvenile MPM-10001 teeth do not display any pitting or polishing other than a small chip on one of the teeth (Figure 4.2e). This suggests that these teeth were not transported any great distance.

Well-defined, steeply inclined wear facets and microstriae occur on the labial surfaces of the teeth (Figure 4.1a). Wear facets have been documented from embryonic ornithopods (*Maiasaura peeblesorum* and *Hypracrosaurus stebingeri*) and initially led some authors to misidentify embryos as hatchlings (Horner, 1999; Horner and Currie, 1994; Horner and Makela, 1979). Thus, wear facets alone do not necessarily indicate that the small MPM-10001 teeth were from a hatchling. However, the combination of wear facets and microstriae do indicate whether an individual is a hatchling or not. Typical microwear occurs as scratching or pitting of various sizes, shapes and orientations on the enamel surface of a tooth from mastication or food processing (Godon, 1988; Teaford, 1988; Walker et al., 1978). The microstriae on the enamel of the juvenile MPM-10001 teeth are overall uniform in apicobasal height. Therefore, the striations on MPM-10001 are due to the processing of food, indicating the individual was not embryonic.

Embryonic and hatchling ornithopod dinosaurs are extremely rare and have only been named and described from North America (*Dryosaurus* sp., *Hypacrosaurus stebingeri*, *Maiasaura peeblesorum, Orodromeus makelai, Tenontosaurus tilletti*) and

Europe (*Telmatosaurus transsylvanicus*) (Carpenter, 1994; Forster, 1990; Grigorescu et al., 2010; Horner, 1999; Horner and Currie, 1994; Horner and Weishampel, 1988). Of those listed above, only *Tenontosaurus tilletti* juveniles have been found associated with adult skeletons (Forster, 1990).

CONCLUSIONS

The size, wear patterns and tooth morphology of the minute teeth found in the body block of a mature individual of *Talenkauen santacrucensis* (MPM-10001) indicates that this material is most likely attributable to a juvenile *Talenkauen*, possibly a recent hatchling. This is the first record of a neonatal ornithopod dinosaur from South America and is only the second known in direct association with a mature skeleton. The direct association with a mature specimen does not preclude parental care during and after hatching in ornithischian dinosaurs although more evidence would be required to examine this hypothesis.

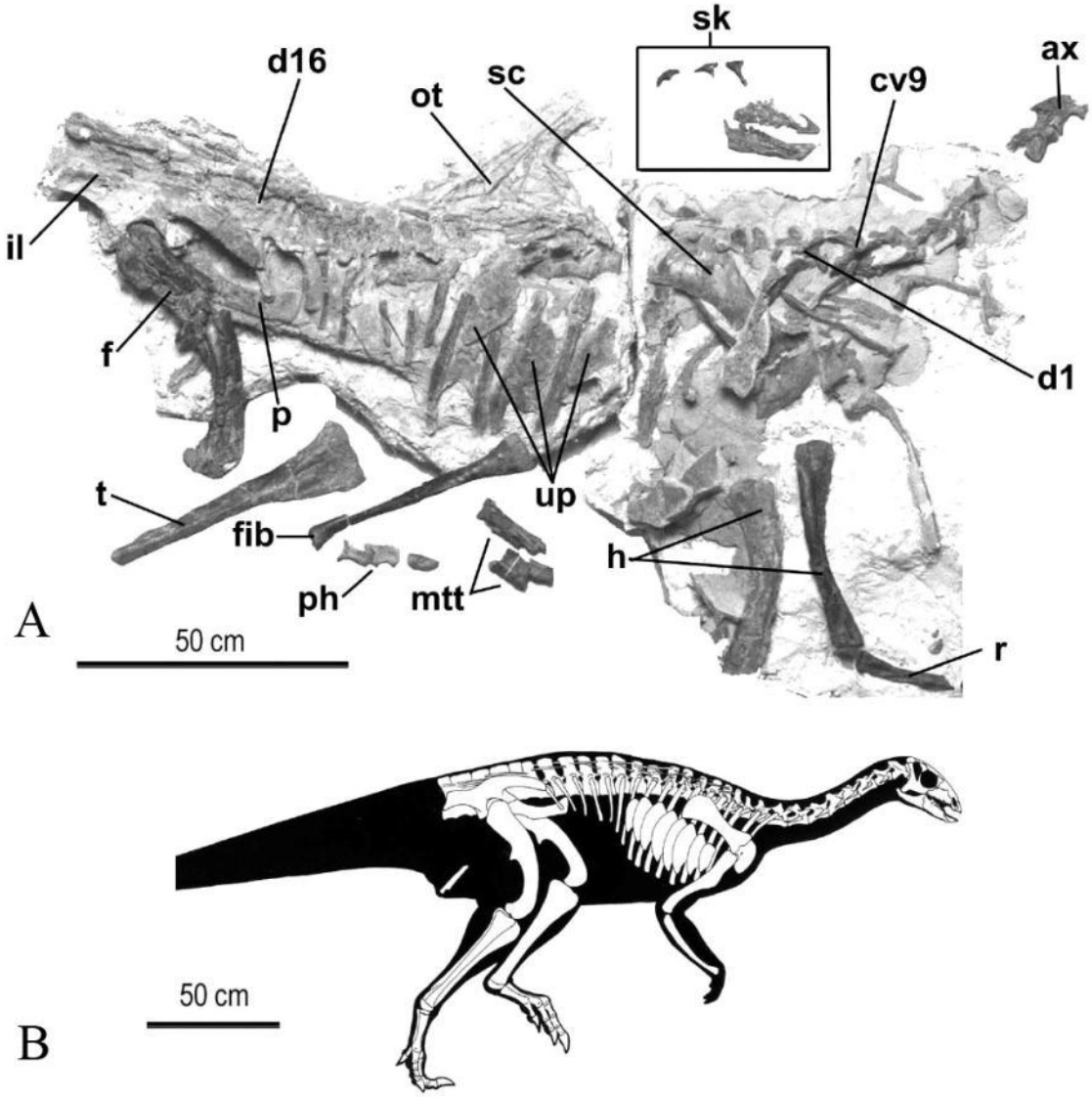

Figure 4.1. MPM-10001. a. Partially articulated body block of *Talenkauen santacrucensis*. b. Reconstruction of *T. santacrucensis* (Novas et al., 2004).

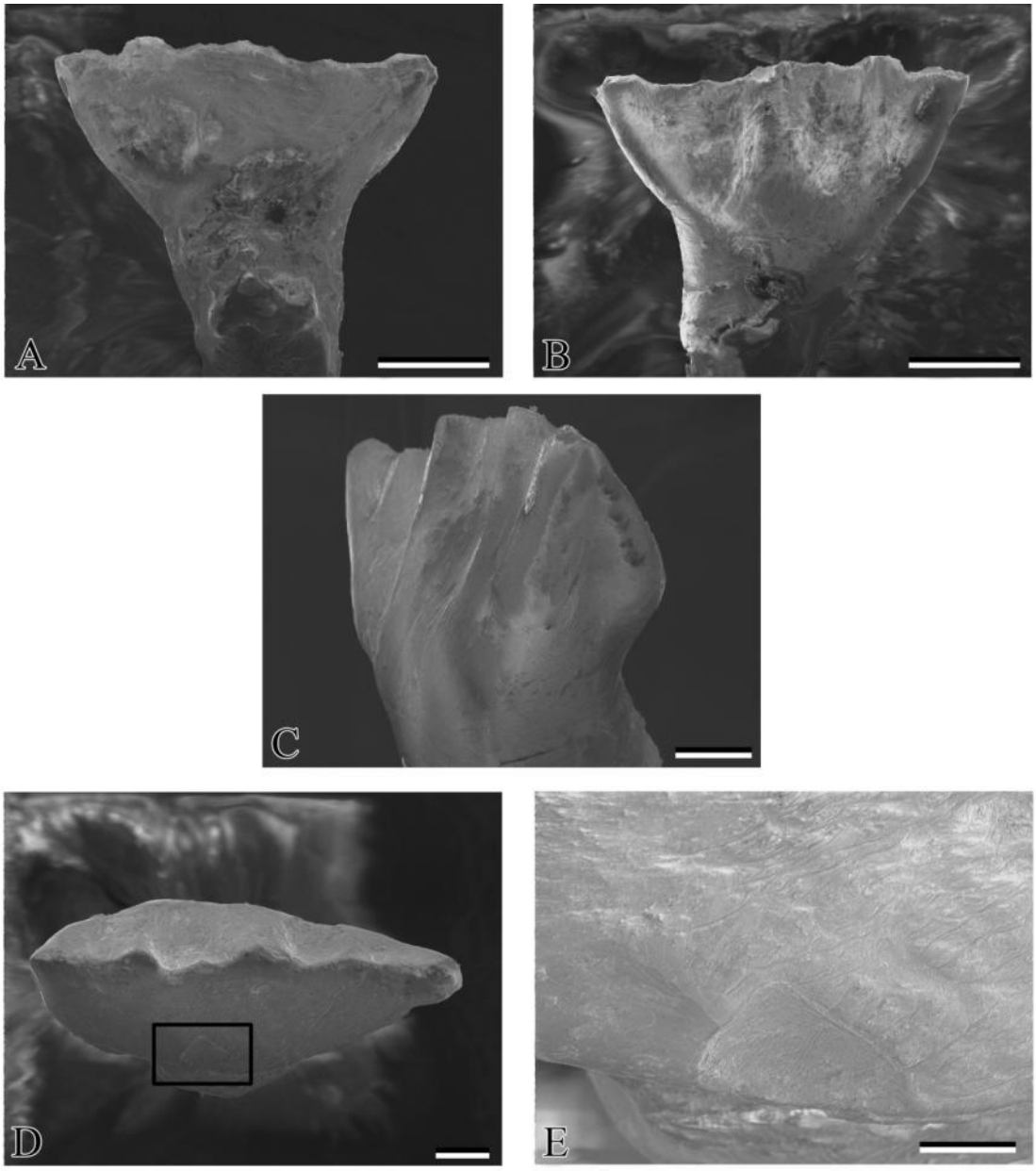

Figure 4.2. MPM-10001 neonatal teeth. a. Labial view of tooth 1; scale bar = 500 µm. b. Lingual view of tooth 1; scale bar = 500 µm. c. Medial view of lingual surface of tooth 2; scale bar = 200 µm. d. Occlusional view of tooth 2; scale bar = 200 µm. e. Microwear on labial surface of crown of tooth 2; scale bar = 100 µm.

Figure 4.3. MPM-10001 left dentary in lateral view (above) and medial view (below). Scale bar equals 5 cm.

CHAPTER 5: ASSOCIATED SHARK VERTEBRAE FROM THE CRETACEOUS- PALEOGENE BOUNDARY OF NEW JERSEY

INTRODUCTION

The endoskeleton of sharks (Chondrichthyes) consists primarily of hyaline and calcified cartilage. Rather than being replaced by endochondral bone, like most other vertebrates, sharks retain a cartilaginous skeleton. The cartilage is strengthened by the deposition of polygons of hydroxyapatite onto the cartilage. Vertebral centra are the most calcified part of the skeleton (Applegate, 1967; Compagno, 1999). In modern sharks (Neoslachians), the centra is uncalcified since this is where the notochord travels (Compagno, 1999). Therefore, the predominantly cartilaginous skeleton of sharks has a lower preservational potential than bone. Fossil shark vertebrae typically occur as isolated centra, and more rarely, associated to semi-articulated specimens (e.g. Blanco-Piñón et al., 2005; Gottfried et al., 1996; Gottfried and Fordyce, 2001; Shimada, 2008; Shimada and Cicimurri, 2006).

An Elasmobranch skeleton is described here (NJSM 21876) is comprised of 51 associated vertebrae from the basal Hornerstown Formation in Gloucester County, New Jersey. The specimen is associated with a *Cucullaea-Turritella* assemblage along with two articulated caudal vertebrae, a coracoid and a humerus from a crocodylian. The shark vertebrae morphology is consistent with a lamnoid-type centra.

GEOLOGICAL BACKGROUND

The Inversand Pit is a surface quarry used to mine glauconite and is located in Gloucester County, New Jersey. Glauconite, often referred to as marl and greensand, is utilized for the manufacture of "Greensand Plus" and "Manganese Greensand" which are commercial products used for water treatment. The quarry exposes a stratigraphic section that ranges from the Late Cretaceous through to the Pleistocene. The Hornerstown Formation (Late Cretaceous?-Paleocene) is currently being mined for glauconite (Gallagher, 1993, 2002; Lacovara and Gallagher, 2006).

The quarry pit encompasses approximately 2-3 acres and has a vertical relief of approximately 15 m (Gallagher, 1993, 2002). Five formations are exposed in the mine: Navesink (Maastrichtian), Hornerstown (Paleogene), Vincentown (Paleogene), Kirkwood (Miocene), and Pensauken (Pleistocene) formations (Gallagher, 1993, 2002; Lacovara and Gallagher, 2006). In this study, only the Navesink and the Hornerstown formations will be discussed.

The Navesink Formation exposure is approximately 2 m thick at the Inversand quarry and consists of brown to olive green, unconsolidated, bioturbated glauconitic sand which ranges in size from clay to small, sand-sized particles (Gallagher, 1993; Minard et al., 1969; Owens et al., 1970). Glauconite ($(K, Na)(Fe^{+3}, Al, Mg)_2(Si, Al)_4O_{10}(OH)_2$) is a phyllosilicate mineral that consists of small aggregations of indistinct grains that form in highly productive, low energy, marine sedimentary environments (Obasi et al., 2011). The base of the formation is primarily a light- to dark-brown glauconite, often referred to

as "chocolate marl," which is a function of little influx of terrigenous sediments. The base is also characterized by abundant marine fossils such as *Exogyra* spp. (Gallagher, 1993, 2002). As the section continues upwards, the brown hue of the glauconite becomes less distinct as the green hue becomes more distinct. This color change is due to a decrease in clay content and an increase in terrigenous sediments. Above the basal sequence, a fossiliferous layer containing marine invertebrates and both aquatic and terrestrial vertebrate fossils can be found (Gallagher, 1993, 2002). Vertebrate fossils recovered from this stratum to date include: Chondrichthyes, Osteichthyes, Mosasauridae, Crocodyliformes, Hadrosauridae, and Dryptosauridae (Gallagher, 2002). The terrestrial vertebrate remains can be attributed to animals that died on or near the coast and whose bodies subsequently washed into the Atlantic Ocean (Gallagher, 1993). This environment would provide conditions favorable to preservation and fossilization because low dissolved oxygen levels would still persist periodically (Gallagher, 1993). The Navesink Formation is interpreted as a near-shore shelf environment (Gallagher, 1993; Wolfe, 1977). The age of the formation is considered to be ~70-66 Ma based on $^{87}Sr/^{86}Sr$ radioactive isotopes (Sugarman et al., 1995).

The Hornerstown Formation (Upper Cretaceous?-Paleocene) exposure is approximately 5.5 m thick at the Inversand quarry and consists of olive green, unconsolidated, clay to sand-sized glauconitic sediments (Gallagher, 1993; Minard et al., 1969). The formation contains several fossiliferous layers. The Main Fossiliferous Layer (MFL) is the lower-most level. It occurs approximately 20 cm above the Navesink/Hornerstown boundary and is approximately 25-30 cm thick (Gallagher, 1993; Obasi et al., 2011). The fossils found within this layer include both invertebrate and

vertebrate remains. The invertebrate fauna includes a rich assemblage of sponges (*Peronidella* spp.), corals (Scleractinia), oyster shells (*Pycnodonte* spp.), steinkerns of bivalves (*Cucullaea* spp.), gastropods (*Turritella* spp.) and brachiopods (*Oleneothyris* spp.). The vertebrate assemblage from the MFL includes at least: six species of Chondrichthyes, two species of Osteichthyes, eight species of Chelonia, six species of Mosasauridae, one species of Plesiosauria, six species of Crocodylia and eight species of Aves (Gallagher, 1993, 2002). The Hornerstown Formation is interpreted to represent a highly productive, low energy, mid- to outer shelf marine environment (Gallagher, 1993; Obasi et al., 2011). The age and relationship of the Hornerstown Formation and the Navesink Formation has been widely discussed (see Obasi et al., 2011). Recent research suggests that the Navesink/Hornerstown boundary (including the MFL) contains faunal remains (a thanatocoenosis) that accumulated immediately after the bolide impact at the Cretaceous/Paleogene boundary (Obasi et al., 2011).

In 2008, 51 articulated/associated elasmobranch vertebrae (NJSM 21876) were discovered in the Main Fossiliferous Layer (MFL) of the Hornerstown Formation at the Inversand Quarry in Sewell, New Jersey. All the vertebrae were located in glauconitic sands within an area of 40 cm by 55 cm.

METHODS

The vertebrae were collected by plaster jacketed while still *in situ* (Figure 5.1). During transport, several of the vertebrae shifted. The relative position of each vertebra

and any associated fossils were mapped before they were removed from the jacket (Figure 5.2). The specimen was then curated in the collections of the New Jersey State Museum (NJSM 21876).

Measurements of the shark vertebrae were taken using digital calipers. When applicable, the vertebrae were measured from the edges of the cranial and caudal surfaces of all centra. Each measurement was repeated three times in order to account for variations on the surface of every vertebra. These measurements were averaged for the final value. Dorsoventral and transverse diameters were taken from both the cranial and caudal surfaces. The craniocaudal length of the centra was measured dorsoventrally and laterally across the center of the centra (Figure 5.3).

The final values for each measurement were used in the following statistical tests. A two-tailed, paired *t*-test was used to determine if there were any significant differences in the dorsoventral or transverse diameter between the cranial and caudal surfaces of each centrum. The correlation coefficient was calculated to determine if there was a relationship between the dorsoventral and the transverse diameter; the dorsoventral length and the lateral length; the dorsoventral diameter and the dorsoventral length; and the transverse diameter and the lateral length.

Additionally, the sizes of the centra were analyzed in order to determine whether or not the vertebrae could have come from a single animal or from an accumulation of individuals. Gottfried et al. (1996) examined 15 lamniform shark (*Carcharodon carcharias*) vertebral columns in order to ascertain the size relationship of centra in precaudal vertebrae. They found that the ratio of the "widest" (largest transverse

diameter) precaudal centrum to the smallest and last precaudal centrum is between 60%-69% (mean = 63.9%, standard deviation = 2.5). Following this ratio, the estimated size of the last precaudal centrum for the fossil vertebrae described here was calculated by multiplying 63.9% from the largest transverse diameter (27.45 mm). The vertebrae that were below the 63.9% value were removed and the correlation coefficients were recalculated for the dorsoventral diameter and the dorsoventral length and the transverse diameter and the lateral length.

An analysis of covariance test (ANOVA) was used to examine the relationships of the location of different groups of vertebrae within the jacket. Three apparent groups of vertebrae were then compared. All statistical analyses were conducted using the statistical software package SAS®.

A standard X-ray (0.78 kV for 0.01 seconds) was taken of five of the most complete vertebrae using a portable X-ray (MinXray Model HF100) in order to ascertain the number of incremental growth lines. The X-rays were then scanned into Adobe Photoshop™ and the image inverted in order to make the growth lines clearer.

DESCRIPTION

The vertebrae, NJSM 21786, are disk-shaped with concentric rings (annuli) on the cranial and caudal surfaces. These surfaces are smooth and are raised into a slight ridge around the periphery of the vertebrae. These are the only smooth edges that can be measured for the dorsoventral diameter andtransverse diameter. There appears to be

some dorsoventral compression of the centra that does not appear to be taphonomic. The lateral periphery of the centra is slightly lower than the cranial and caudal surfaces. Craniocaudally oriented lamellae occur on the lateral-most surfaces of the vertebrae. The mean dorsoventral diameter of the centra is 22.37 mm with a range of 8.63-28.04 mm. The average craniocaudal thickness is 11.42 mm with the range being 5.94-16.21 mm. Paired basidorsal and basiventral foramina occur on the dorsal and ventral surfaces, respectively. The mean foramina size of these is 3.66 mm with a range of 0.84 -5.51 mm. An "X"-shape going through the centra and can be clearly seen in the x-ray image (Figure 5.4). Branching radii can also be seen radiating from the center of the centra laterally. Concentric growth rings can also be seen in an X-ray image. Heavily ossified, irregular regions occur in four vertebrae. The lateral laminae in these vertebrae are either locally obscured or, in the case of one vertebra, destroyed.

RESULTS

The dorsoventral diameters measured from both the cranial and caudal edges are not statistically significant (p-value = 0.24). The same is also true for the cranial and caudal surfaces for the transverse diameters (p-value = 0.31). Thus, the cranial and caudal surfaces of the centra are approximately the same size. The correlation of the dorsoventral diameter and the trnsverse diameter is significant ($r^2 = 0.94$, p-value < 0.001). Additionally, the correlation between the dorsoventral length and the lateral length ($r^2 = 0.83$, p-value < 0.001); the dorsoventral diameter and the dorsoventral length

($r^2 = 0.73$, p-value < 0.001); and the transverse diameter and the lateral length ($r^2 = 0.87$, p-value < 0.001) are also all significant (Figure 5.5).

The estimated "width" of the last precaudal centrum is calculated to be 17.54 mm. Five vertebrae are below this value and have been removed from the dataset. After removing these data points, the new r^2 value for the dorsoventral diameter and the dorsoventral length ($r^2 = 0.92$, p-value < 0.001) and the lateral diameter and the lateral length ($r^2 = 0.94$, p-value < 0.001) is higher (Figure 5.6). The vertebrae in the jacket did not form any significant groupings except for those in the southeastern region (p-value < 0.001) (Figure 5.7). Additionally, the X-ray did reveal the presence of growth lines; however, the number of growth lines is difficult to establish (Figure 5.4).

DISCUSSION

The degree of morphological variation of vertebrae in extant and extinct sharks is poorly known (Applegate, 1967; Cailliet et al., 2006; Gottfried et al., 1996; Shimada, 2008). Therefore, without teeth or cranial elements, the exact taxonomic placement of NJSM 21786 cannot be confidently determined. However, lamnoid-type vertebrae are characteristic of extant lamniform sharks and can be used to identify centra of extinct forms. Extant clades containing lamnoid vertebrae include Orectolobidae, Odontaspidae, Alopiidae, Rhincodontidae, Cetorhinidae and Lamnidae (Applegate, 1967). Shark remains from the basal Hornerstown Formation are known primarily from teeth (*Cretalamna appendiculata*, *Squatina* sp., *Squalicorax pristodontus* and *Odontaspis*

cuspidata) and isolated vertebrae (Gallagher, 1993, 2002). Of the shark taxa known, *Cretalamna appendiculata*, *Squalicorax pristodontus* and *Odontaspis cuspidata* are lamniform sharks. Thus, these vertebrae probably belong to one of these species.

Based on the linear regression values of the diameters and the lengths of the centra, the shark vertebrae in NJSM 21786 appear to represent a single animal. There is a significant correlation between the diameters and the lengths of the vertebrae. However, when evaluating the dataset as a whole, the linear regression line of the diameters and the lengths has an r^2 range of between 0.73 and 0.87. A few outliers reduce this value. By using the mean width ratio of the widest precaudal centrum to that of the last precaudal centrum from extant *Carcharodon carcharias* (63.9%), the five vertebrae with the lowest lateral diameter values are assumed to be caudal vertebrae and were therefore removed from the analysis. The revised r^2 values for the centra diameters and widths range from 0.92 to 0.94 (Figure 5.6).

The vertebrae in the jacket did not form any significant groupings except for those vertebrae in the southeastern region (p-value < 0.001). The vertebrae from this region may have been articulated in life (Figure 5.7).

CONCLUSIONS

The elasmobranch vertebrae described here from the basal Hornerstown Formation appear to be from a single animal. The exceptional preservation of these

vertebrae along with that of other partially articulated vertebrate specimens, including turtles, crocodyliformss and osteichthyans suggests little to no reworking.

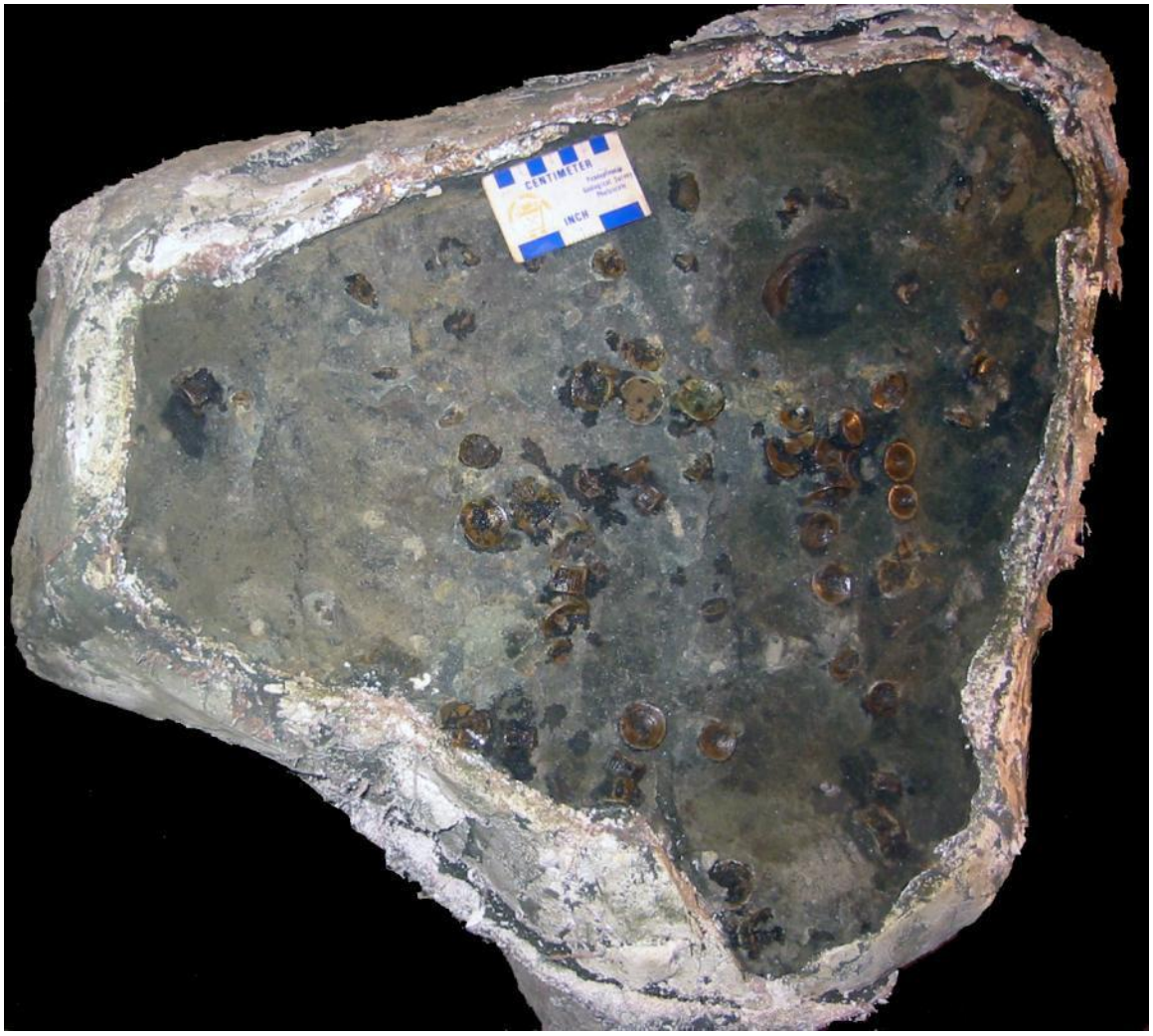

Figure 5.1. Shark vertebrae (NJSM 21876) from the Hornerstown Formation.

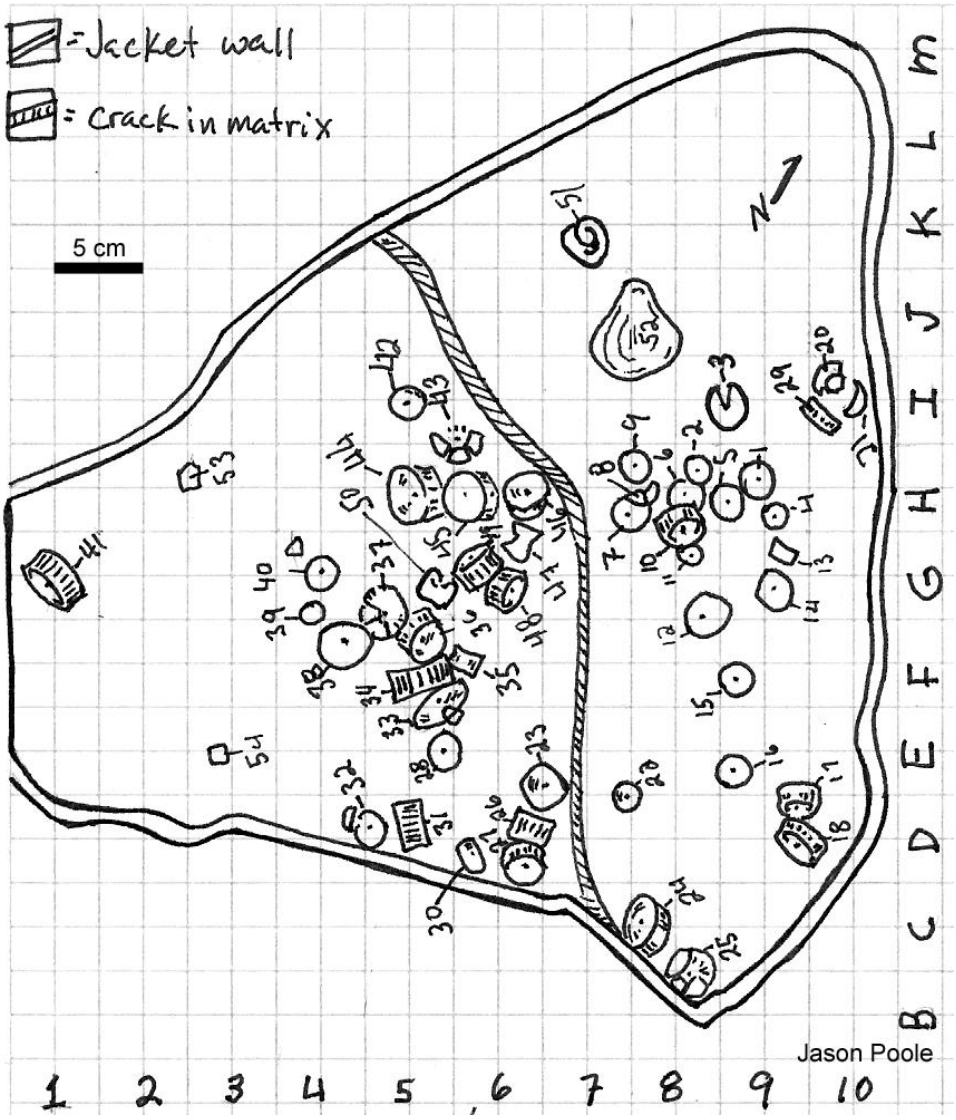

Figure 5.2. Map of field jacket containing NJSM 21876 and the location of individual vertebrae. Note that some sediment shifting occurred during transport.

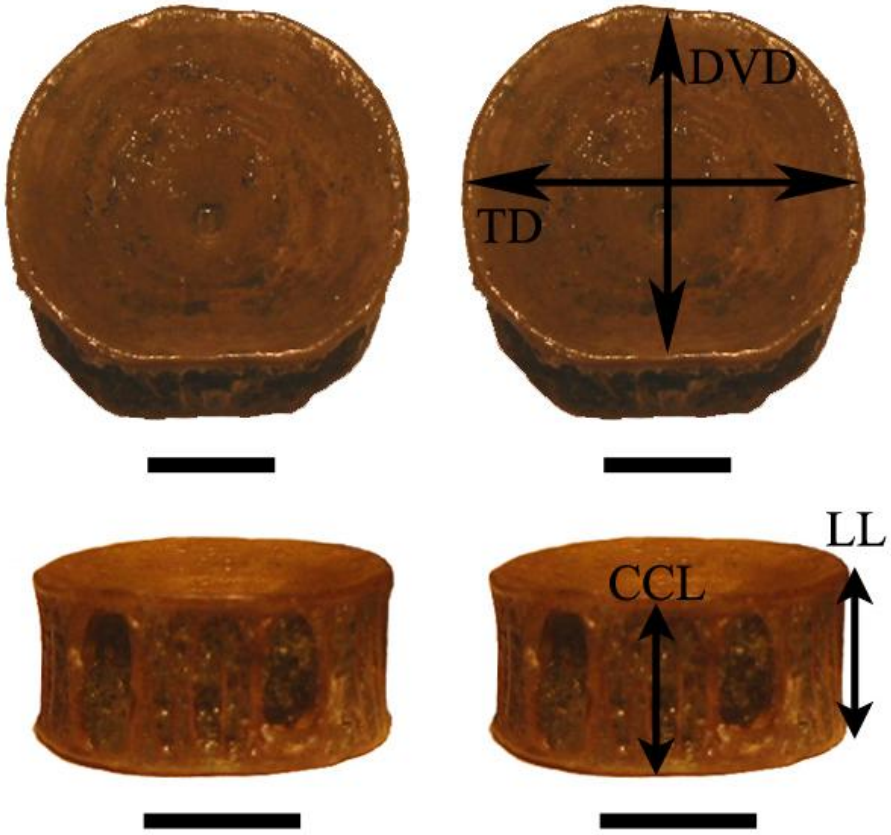

Figure 5.3. A typical centrum of NJSM 21876 indicating where measurements were taken. DVD, dorsoventral diameter; TD, lateral diameter; CCL, craniocaudal length; and LL lateral length. Scale bar = 10 mm.

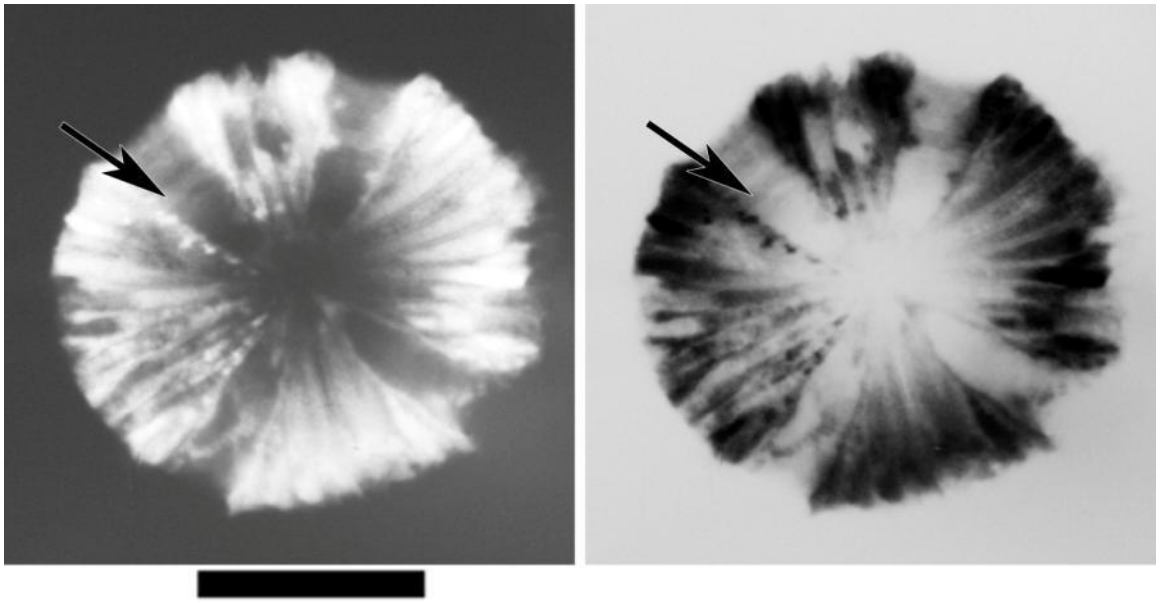

Figure 5.4. X-ray (left) and the inverse image (right) of a centrum of NJSM 21876. Arrows are pointing to growth lines. Scale bar = 10 mm.

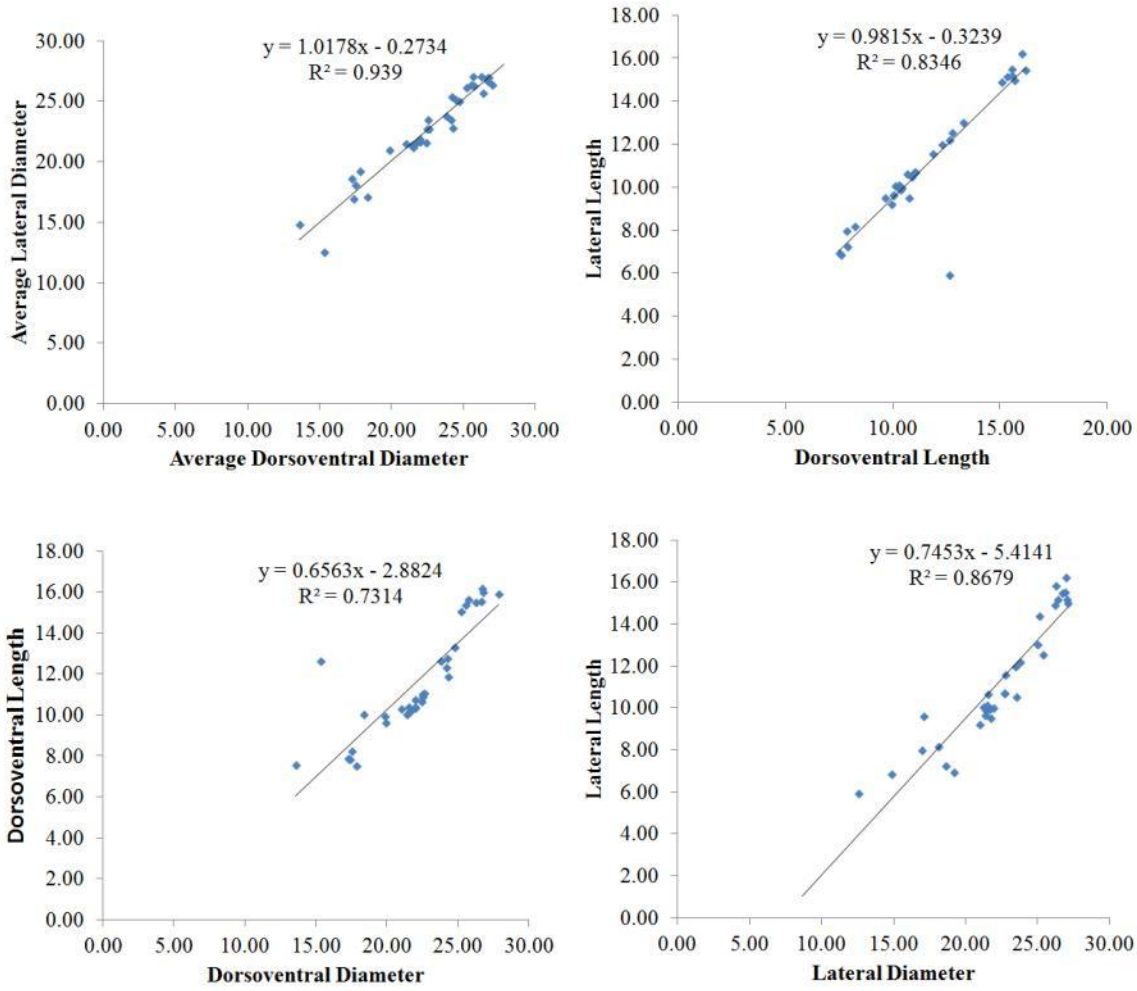

Figure 5.5. Linear regression lines of vertebral measurements from NJSM 21876.

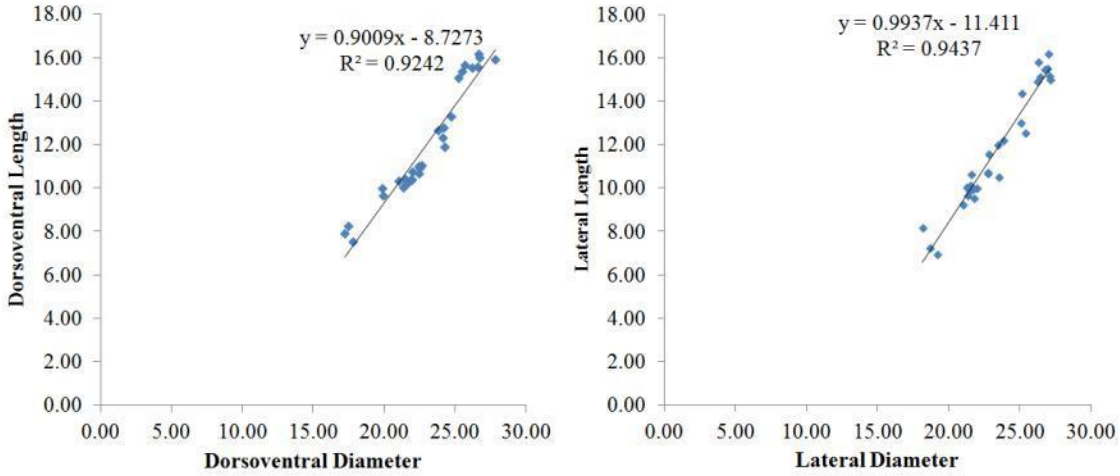

Figure 5.6. Linear regression lines from NJSM 21786 of vertebral measurements greater than 17.54 mm.

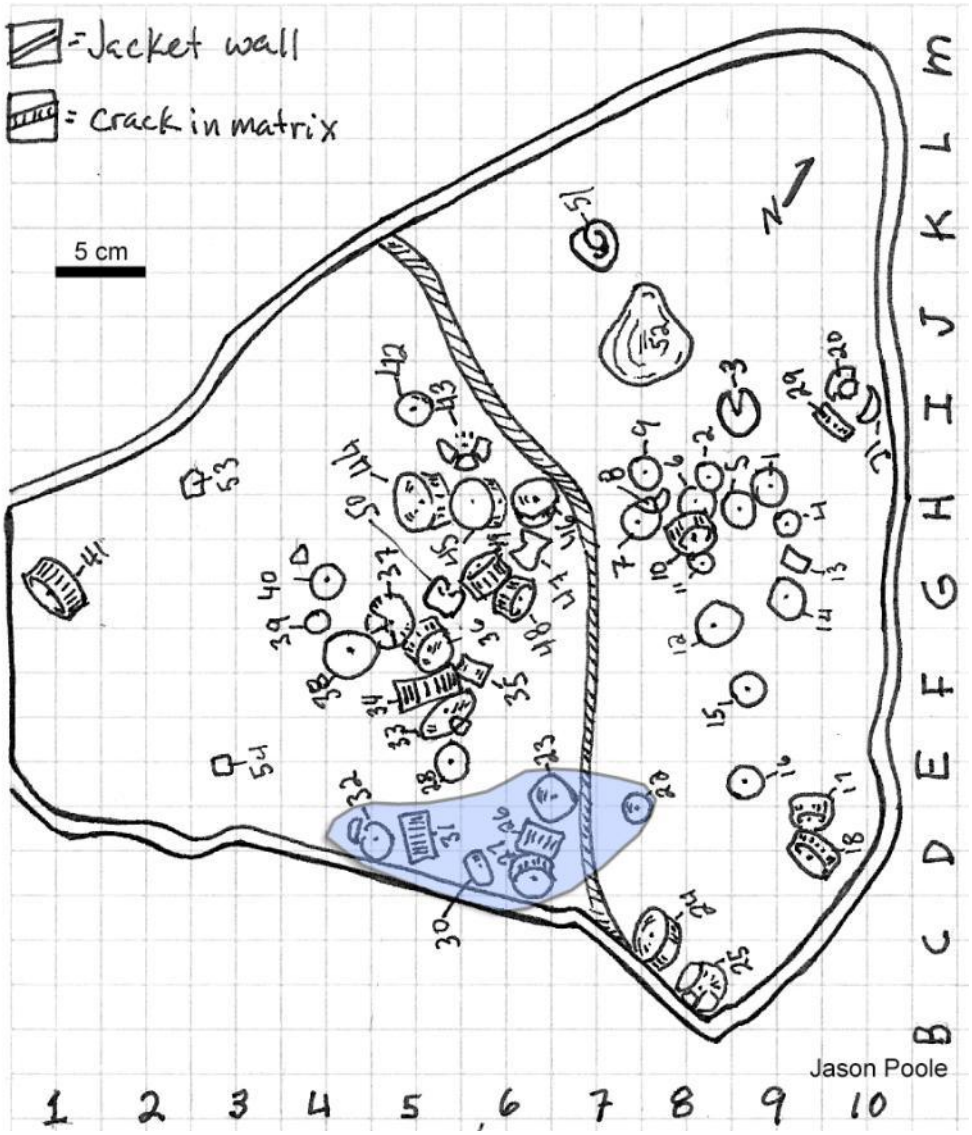

Figure 5.7. Map of jacket containing NJSM 21786. Shaded area represents the only significant grouping (p-value <0.001).

REFERENCES

Agnolin, F., 2010, A new species of the genus *Atlantoceratodus* (Dipnoiformes: Ceratodontoidei) from the Uppermost Cretaceous of Patagonia and a brief overview of fossil dipnoans from the Cretaceous and Paleogene of South America: Brazilian Geographical Journal: Geosciences and Humanities research medium, v. 1, p. 162-210.

Ali, J.R., and Aitchison, J.C., 2008, Gondwana to Asia: Plate tectonics, paleogeography and the biological connectivity of the Indian sub-continent from the Middle Jurassic through latest Eocene (166-35 Ma): Earth-Science Reviews, v. 88, p. 145-166.

Ameghino, F., 1893, Sobre la presencia de vertebrados de aspecto mesozoico en la formación Santacruceña de la Patagonia austral: Revista del Jardín Zoológico de Buenos Aires, v. 1, p. 76-84.

—, 1898, Sinopsis geológico-paleontológica, Segundo conso de la República Argentina: Buenos Aires, p. 112-255.

—, 1899a, Nota preliminar sobre el *Loncasaurus argentinus*, un representante de la Familia de los Megalosauridae en la República Argentina: Anais de Societa de Ciencias de Argentina, v. 47, p. 61-62.

—, 1899b, Supelmento: La Plata.

—, 1900, Mamíferos del Cretácico inferior de la Patagonia (Formación de las areniscas abigarradas): Comunicación del Museo Nacionales, Buenos Aires, v. 3, p. 1-568.

—, 1906, Les formations sédimentaires du Crétacé supérieur et du Tertiaire de Patagonie: Anales del Museo Nacional, Buenos Aires, ser. 3, v. 15, p. 1-568.

Andrews, H.N., Jr., 1936, A New Sequoioxylon from Florissant, Colorado: Annals of the Missouri Botanical Garden, v. 23, p. 439-446.

Apesteguia, S., Agnolin, F.L., and Claeson, K., 2007, Review of Cretaceous dipnoans from Argentina (Sarcopterygii: Dipnoi) with descriptions of new species: Revista del Museo Argentino de Ciencias Naturales, v. 9, p. 27-40.

Applegate, S.P., 1967, A survey of shark hard parts, *in* Gilbert, P.W., Mathewson, R.F., and Rall, D.R., eds., Sharks, Skates, and Rays: Baltimore, The Johns Hopkins Press, p. 37-67.

Arbe, H.A., 1986, El Cretácico de la Cuenca Austral: sus ciclos de sedimentación: Buenos Aires, University of Buenos Aires.

—, 1987, El Cretácico de la Cuenca Austral: Boletín de Informaciones Petroleras, v. 9, p. 91-110.

—, 2002, Análisis estratigráfico del cretácico de la cuenca austral, *in* Haller, M.J., ed., Geología y Recursos Naturales de Santa Cruz. Relatorio del XV Congreso Geológica Argentino, Volume I: El Calafate, Buenos Aires, p. 103-128.

Arbe, H.A., and Hechem, J.J., 1984, Estratigrafía y facies de depositos continentales, litorales y marinos del Cretacico Superior, Lago Argentino, Provincia de Santa Cruz: Noveno Congreso Geologico Argentino, S.C. de Bariloche, Actas, v. 7, p. 124-158.

Archangelsky, S., Barreda, V., Passalia, M.G., Gandolfo, M., Prámparo, M., Romero, E., Cúneo, R., Zamuner, A., Iglesias, A., Llorens, M., Puebla, G.G., Quattrocchio, M., and Volkheimer, W., 2009, Early angiosperm diversification: evidence from southern South America: Cretaceous Research, v. 30, p. 1073-1082.

Arrondo, O.G., 1983, Informe estudio paleontológico: Yac. Petrol. Fiscales. Inf. Inéd., Buenos Aires.

Barbeau, J., David L., Olivero, E.B., Swanson-Hysell, N.L., Zahid, K.M., Murray, K.E., and Gehrels, G.E., 2009, Detrital-zircon geochronology of the eastern Magallanes foreland basin: Implications for Eocene kinematics of the northern Scotia Arc and Drake Passage: Earth and Planetary Science Letters, v. 284, p. 489-503.

Barefoot, A.C., and Hankins, F.W., 1982, Identification of Modern and Tertiary Woods: Oxford, Oxford University Press, 189 p.

Barreda, V., and Archangelsky, S., 2006, The southernmost record of tropical pollen grains in the mid-Cretaceous of Patagonia, Argentina: Cretaceous Research, v. 27, p. 778-787.

Berry, E., 1928, Tertiary fossil plants from the Argentine Republic: Proceedings of the United States National Museum, Washington, v. 73, p. 1-27.

Berry, E.W., 1937, Upper Cretaceous Plants from Patagonia: Science, v. 86, p. 221-222.

Bhardwaj, D.C., 1952, On some interesting Jurassic woods from Rajmahal Hills, Bihar: Proceedings of the 39th Indian Science Congress, Calcutta, India, v. 3, p. 31-32.

—, 1953, Jurassic woods from the Rajmahal Hills, Bihar: The Palaeobotanist, v. 2, p. 59-70.

Bianchi, J.L., 1967, Informe preliminar acerca de los perfiles estratigáficos realizados en el sector occidental de la Cuenca Austral, durante las campañas 1964-5 y 1965-66: Yac. Petrol. Fiscales. Inf. Inéd., Buenos Aires.

Biddle, K.T., Uliana, M.A., Mitchum, R.M., Fitzgerald, M.G., and Wright, R.C., 1986, The stratigraphic and structural evolution of the central and eastern Magallanes Basin, southern South America: Special Publications of the International Association of Sedimentologists, v. 8, p. 41-61.

Blakey, R.C., 2008, Gondwana paleogeography from assembly to breakup: A 500 m.y. odyssey: Geological Society of America Special Papers, v. 441, p. 1-28.

Blanco-Piñón, A., Shimada, K., and González-Barba, G., 2005, Lamnoid vertebrae from the Agua Nueva Formation (Upper Cretaceous: lower–middle Turonian), NE Mexico: Revista Mexicana de Ciencias Geológicas, v. 22, p. 19-23.

Blokhina, N., Afonin, M., and Kodrul, T., 2010, Fossil wood of <i>Sequoioxylon burejense</i> sp. nov. (Taxodiaceae) from the Upper Cretaceous of the Zeya-Bureya Basin (Russian Far East): Paleontological Journal, v. 44, p. 1231-1239.

Brea, M., Matheos, S.D., Raigemborn, M.S., Iglesias, A.R.I., Zucol, A.F., and Prámparo, M., 2011, Paleoecology and paleoenvironments of Podocarp trees in the Ameghino Petrified forest (Golfo San Jorge Basin, Patagonia, Argentina): Constraints for Early Paleogene paleoclimat: Geologica Acta, v. 19, p. 13-28.

Burmeister, H., 1892, Nuevos datos sobre el Territorio Patagónico de Santa Cruz.: Revista Museo La Plata, v. 4, p. 227-256.

—, 1901, Memoria sobre el territorio de Santa Cruz: Buenos Aires, Imprenta De "La Nación", 104 p.

Butler, R.J., and Galton, P.M., 2008, The 'dermal armour' of the ornithopod dinosaur *Hypsilophodon* from the Wealden (Early Cretaceous: Barremian) of the Isle of Wight: a reappraisal: Cretaceous Research, v. 29, p. 636-642.

Cailliet, G., Smith, W., Mollet, H., and Goldman, K., 2006, Age and growth studies of chondrichthyan fishes: the need for consistency in terminology, verification, validation, and growth function fitting: Environmental Biology of Fishes, v. 77, p. 211-228.

Calvo, J.O., Porfiri, J.D., and Novas, F.E., 2008, Discovery of a new ornithopod dinosaur from the Portezuelo Formation (Upper Cretaceous), Neuquén, Patagonia, Argentina: Arquivos do Museu Nacional, Rio de Janeiro, v. 65, p. 471-483.

Cambiaso, A.V., Novas, F.E., Lirio, J., and Nunez, H., 2002, Un nuevo dinosario ornithopodo del Cretacio Superior de la Isla James Ross, Peninsula Antarctica: VIII Congresso Argentino de Paleontologia y Bioestratigrafia, Resumenes, p. 61.

Cantrill, D.J., and Nagalingum, N.S., 2005, Ferns from the Cretaceous of Alexander Island, Antarctica: Implications for Cretaceous phytogeography of the Southern Hemisphere: Review of Palaeobotany and Palynology, v. 137, p. 83-103.

Cantrill, D.J., and Poole, I., 2002, Cretaceous patterns of floristic change in the Antarctic Peninsula, *in* Crame, J.A., and Owen, A.W., eds., Palaeobiogeography and biodiversity change: The Ordovician and Mesozoic-Cenozoic radiations, Volume 194: London, Geological Society of London, p. 141-152.

—, 2005, Taxonomic turnover and abundance in Cretaceous to Tertiary wood floras of Antarctica: implications for changes in forest ecology: Palaeogeography, Palaeoclimatology, Palaeoecology, v. 215, p. 205-219.

Carlquist, S., 2010, Comparative Wood Anatomy: Systematic, Ecological and Evolutionary Aspects of Dicotyledon Wood: New York, Springer-Verlag, 447 p.

Case, J.A., Martin, J.E., Chaney, D.S., Reguero, M., Marenssi, S.A., Santillana, S.M., and Wooodburne, M.O., 2000, The first duck-billed dinosaur (Family Hadrosauridae) from Antarctica: Journal of Vertebrate Paleontology, v. 20, p. 612-614.

Case, J.A., Martin, J.E., and Reguero, M., 2007, A dromaeosaur from the Maastrichtian of James Ross Island and the Late Cretaceous Antarctic dinosaur fauna, *in* Cooper, A., Raymond, C., and Team, I.E., eds., Antarctica: a Keystone in a Changing World -- Online Proceedings for the Tenth International Symposium on Antarctic Earth Sciences, Volume 2007-1047, SRP 083: U.S. Geological Survey Open-File Report: Washington, D.C., U.S. Geological Survey, p. 1-4.

Cione, A.L., Gouiric, S., Goin, F., and Poiré, D., 2007, *Atlantoceratodus*, a new genus of lungfish from the Upper Cretaceous of South America and Africa: Revista del Museo de La Plata, Paleontología, v. 10, p. 1-112.

Codd, J., and Manning, P., 2007, Uncinate processes: a unique synapomorphy for manirptoran and avian theropods?: Journal of Vertebrate Paleontology, v. 27, p. 60A.

Codd, J.R., Manning, P.L., Norell, M.A., and Perry, S.F., 2008, Avian-like breathing mechanics in maniraptoran dinosaurs: Proceedings of the Royal Society of London B, v. 275, p. 157-161.

Compagno, L.J.V., 1999, Endoskeleton, *in* Hamlett, W.C., ed., Sharks, skates and rays. The biology of elasmobranch fishes: Washington D. C., Johns Hopkins Press, p. 69-92.

Conwentz, H., 1885, Árboles fósiles del Río Negro: Boletín de la Academia de Ciencias (Córdoba), v. 7, p. 435-456.

Coria, R.A., and Calvo, J.O., 2002, A new iguanodontian ornithopod from Neuquen Basin, Patagonia, Argentina: Journal of Vertebrate Paleontology, v. 22, p. 503-509.

Coria, R.A., and Salgado, L., 1996a, A basal Iguanodontian (Ornithischia: Ornithopoda) from the Late Cretaceous of South America: Journal of Vertebrate Paleontology, v. 16, p. 445-457.

—, 1996b, '*Loncosaurus argentinus*' Ameghino, 1899 (Ornithischia, Ornithopoda): a revised description with comments on its phylogenetic relationships: Ameghiniana, v. 33, p. 373-376.

Crame, J.A., Francis, J.E., Cantrill, D.J., and Pirrie, D., 2004, Maastrichtian stratigraphy of Antarctica: Cretaceous Research, v. 25, p. 411-423.

Crame, J.A., Pirrie, D., Riding, J.B., and Thompson, W.A., 1991, Campanian-Maastrichtian (Cretaceous) stratigraphy of the James Ross Island area, Antarctica: Journal of the Geological Society, v. 148, p. 1125-1140.

Crane, P.R., 1987, Vegetational consequences of the angiosperm diversification, *in* Friis, E.M., Chaloner, W.G., and Crane, P.R., eds., The origins of angiosperms and their biological consequences: Cambridge, Cambridge University Press, p. 107-144.

Creber, G.T., and Francis, J.E., 1999, Fossil tree-ring analysis: palaeodendrology, *in* Jones, T.P., and Rowe, N.P., eds., Fossil Plants and Spores: Modern Techniques: London, Geological Society, p. 245-250.

Crié, L., 1889, Beiträge zur Kenntniss der fossilen Flora einiger Inseln des südpacifischen und indischen Oceans: Palaeontologische Abhandlungen, v. 5, p. 77-87.

Crisafulli, A., 2004, Nuevos registros de la xilotafoflora de la Formación Yaguarí, Pérmico Superior de Uruguay: Revista Museo Argentino Ciencias Naturales, nueva serie, v. 5, p. 169-180.

Crisafulli, A., and Herbst, R., 2008, Maderas gimnospérmicas de la Formación Solca (Pérmico Inferior), provincia de La Rioja, Argentina: Ameghiniana, v. 45, p. 737-751.

—, 2009, Gymnospermous woods (Coniferales, Taxales, and Ginkgoales) from the Upper Permian Tacuary Formation, Eastern Paraguay: Palaeobiodiversity and Palaeoenvironments, v. 89, p. 95-109.

Darwin, C., 1833-1834, Banda Oriental notebook, Darwin Online, http://darwin-online.org.uk/.

—, 1846, Geological observations of South America. The Geology of the Voyage of the Beagle, under the command of Capt. Fitzroy, R.N. during the years 1832 to 1836: London, Smith Elder and Co., 279 p.

Davies, T.J., Barraclough, T.G., Chase, M.W., Soltis, P.S., Soltis, D.E., and Savolainen, V., 2004, Darwin's abominable mystery: Insights from a supertree of the angiosperms: Proceedings of the National Academy of Sciences of the United States of America, v. 101, p. 1904-1909.

Del Fueyo, G.M., 1998, Coniferous woods from the Upper Cretaceous of Patagonia, Argentina: Revista Española de Paleontología, v. 13, p. 43-50.

Dolezych, M., Jochmann, M., and Gröschke, A., 2010, The fossil wood and resin of *Taxodioxylon vanderburghi*i nov spec. in Paleogene sediments of Svalbard: Palaeontographica. Abt. B, v. 284, p. 159-181.

Dolezych, M., and Van Der Burgh, J., 2004, Xylotomische Untersuchungen an inkohlten Hölzern aus dem Braunkohlentagebau Berzdorf (Oberlausitz, Deutschland): Feddes Repterorium, v. 115, p. 397-437.

Dutra, T.L., and Batten, D.J., 2000, Upper Cretaceous floras of King George Island, West Antarctica, and their palaeoenvironmental and phytogeographic implications: Cretaceous Research, v. 21, p. 181-209.

Eagles, G., and König, M., 2008, A model of plate kinematics in Gondwana breakup: Geophysical Journal International, v. 173, p. 703-717.

Eckhold, 1923, Die Hoftüpfel bei rezenten und fossilen Coniferen: Jahrbuch Königliche Preussischen Geologischen Landesanstalt, v. 42, p. 472-505.

Egerton, V.M., Williams, C.J., and Lacovara, K., 2010, Climatic and floral latitudinal gradients between Late Cretaceous South Smerica and Antarctica: Paleobiogeographical implications for southernmost Gondwana: Journal of Vertebrate Paleontology, p. 84A.

Ezcurra, M.D., Agnolin, F.L., and Novas, F.E., 2010, An abelisauroid dinosaur with a non-atrophied manus from the Late Cretaceous Pari Aike Formation of southern Patagonia: Zootaxa, v. 2450, p. 1-25.

Falcon-Lang, H.J., 2003, Growth interruptions in silicified conifer woods from the Upper Cretaceous Two Medicine Formation, Montana, USA: implications for palaeoclimate and dinosaur palaeoecology: Palaeogeography, Palaeoclimatology, Palaeoecology, v. 199, p. 299-314.

—, 2005, Intra-tree variability in wood anatomy and its implications for fossil wood systematics and palaeoclimatic studies: Palaeontology, v. 48, p. 171-183.

Falcon-Lang, H.J., and Cantrill, D.J., 2000, Cretaceous (Late Albian) coniferales of Alexander Island, Antarctica. 1: Wood taxonomy: a quantitative approach: Review of Palaeobotany and Palynology, v. 111, p. 1-17.

—, 2001, Leaf phenology of some mid-Cretaceous polar forests, Alexander Island, Antarctica: Geological Magazine, v. 138, p. 39-52.

Feruglio, E., 1935, Relaciones estratigráficas y faunísticas entre los estratos cretáceos y terciarios en la región del Lago Argentino y en la del Golgo de San Jorge (Patagonia): Boletin de Informaciones Petroleras, Yacimientos e Industrias: Revista Mensual Publicada Bajo el Patrocinio de la Direccion General de Yacimientos Petroliferos Fiscales, v. 128, p. 69-93.

—, 1938a, El Cretáceo Superior del lago San Martin: Physis, v. 12, p. 293-338.

—, 1938b, La nomenclatura estratigráfica de la Patagonia y Tierra del Fuego: Una reunión de Geólogos de YPF y el problema de la Terminología Estratigráfica. Boletín de Informaciones Petroleras, p. 82-95.

—, 1938c, Relaciones Estratigráficas entre el Patagoniano y el Santacruciano en la Patagonia Austral: Revista del Museo de La Plata. Sección Geología, v. 4, p. 128-159.

—, 1944, Estudios geolóficos y glaciológicosen la región del lago Argentino (Patagonia): Boletin de la Academia Nacional de Ciencias, v. 37, p. 3-255.

FitzRoy, R., 1839, Narrative of the surveying voyages of His Majesty's Ships Adventure and Beagle between the years 1826 and 1836, describing their examination of the southern shores of South America, and the Beagle's circumnavigation of the globe. Proceedings of the second expedition, 1831-36, under the command of Captain Robert Fitz-Roy, R.N.: London, Henry Colburn.

Florin, 1940, The Tertiary fossil conifers of south Chile and phytogeographical significance, with a review of fossil conifers of southern lands: Kungl. Sven. Vetenskapsakad. Handl., v. 19, p. 1-107.

Forster, C.A., 1990, Evidence for juvenile groups in the ornithopod dinosaur *Tenotosaurus tilletti* Ostrom: Journal of Paleontology, v. 64, p. 164-165.

Fossa-Mancini, E., 1938, Criterios adoptados en la nueve terminologia estratigrafica para algunas regiones Argentinas: Una reunión de Geólogos de YPF y el problema de la Terminología Estratigráfica. Boletín de Informaciones Petroleras, p. 61-65.

Francis, J., Ashwoth, A., Cantrill, D.J., Crame, J.A., Howe, J., Stephens, R., -M., T.A., and Thorn, V., 2008, 100 Million years of Antarctic climate evolution: Evidence from fossil plants, *in* Cooper, A.K., Barrett, P.J., Stagg, H., Storey, B., Stump, E., Wise, W., and team, t.I.e., eds., 10th International Symposium on Antarctic Earth Sciences: Washington, DC, The National Academies Press, p. 19-27.

Francis, J.E., and Poole, I., 2002, Cretaceous and early Tertiary climates of Antarctica: evidence from fossil wood: Palaeogeography, Palaeoclimatology, Palaeoecology, v. 182, p. 47-64.

Frenguelli, J., 1936, El Banco Verde de Paso Niemann del Río Chico en el Chubut y sus diatomeas: Revista del Museo de La Plata. Sección Geología, v. 1, p. 3-65.

—, 1953, La Flora fósil de la región del Alto Río Chalía en Santa Cruz (Patagonia) Notas del Museo de la Plata, v. 16, p. 239-257.

Furque, G., 1973, Descripición geológica de la Hoja 58 b, lago Argentino. : Servicio Nacional de Minería y Geología, Boletín, v. 140, p. 1-49.

Furque, G., and Camacho, H.H., 1972, El Cretácico Superior y terciario de la región austral del Lago Argentino (Provincia de Santa Cruz): Actas 4º Jornadas Geológicas Argentinas, v. 3, p. 61-75.

Gallagher, W.B., 1993, Ther Cretaceous/Tertiary mass extinction event in the northern Atlantic coastal plain: The Mosasaur, v. 5, p. 75-154.

—, 2002, Faunal changes across the Cretaceous-Tertiary (K-T) boundary in the Atlantic coastal plain of New Jersey: Reconstructing the marine community after the K-T mass-extinction event, *in* Koeberl, C., and MacLeod, K.G., eds., Catastrophic Events and mass Extinctions: Impacts and Beyond Boulder, Geological Society of America, p. 291-301.

Gasparini, Z., Olivero, E., Scasso, R., and Rinaldi, C., 1987, Un ankylosaurio (Reptilia, Ornithischia) Campaniano en el continente Antartico: Anais do X Congresso Brasileiro de Paleontologia, v. 1, p. 131-141.

Gerards, T., Damblon, F., Wauthoz, B., and Gerrienne, P., 2007, Comparison of cross-field pitting in fresh, dried and charcoalified softwoods: IAWA Journal, v. 28, p. 49-60.

Gnaedinger, S., 2007a, Planoxylon Stopes, Protelicoxylon Philippe y Herbstiloxylon nov. gen. (Coniferales) de la Formación La Matilde (Jurásico Medio), provincia de Santa Cruz, Argentina: Ameghiniana, v. 44, p. 321-335.

—, 2007b, Podocarpaceae woods (Coniferales) from middle Jurassic La Matilde formation, Santa Cruz province, Argentina: Review of Palaeobotany and Palynology, v. 147, p. 77-93.

Godon, K.D., 1988, A review of methodolgy and qunantification in dental microwear analysis: Scanning Microscopy, v. 2, p. 1139-1147.

Goin, F.J., Poiré, D.G., de la Fuente, M.S., Cione, A.L., Novas, F.E., Bellosi, E.S., Ambrosio, A., Ferrer, O., Canessa, N.D., Carloni, A., Ferigolo, J., Ribeiro, A.M., Sales Viana, M.S., Reguero, M.A., Vucetich, M.G., Marenssi, S., de Lima Filho, M.F., and Agostinho, S., 2002, Paleontología y geología de los sedimentos del Cretácico Superior aflorantes al sur del Río Shehuen (Mata Amarilla, Provincia de Santa Cruz, Argentina): Actas del XV Congreso Geológico Argentino.

Göppert, H.R., 1850, Monographie der fossilen Coniferen.: Verhandelingen van de Hollandsche Maatschappij der Wetenschappen te Harlem, v. 12.

Gothan, W., 1905, Zur Anatomie lebender und fossiler Gymnospermen-Hölzer: Abh. Preuss. Geol. Landslt., v. 44, p. 1-108.

—, 1915, Die Hoftüpfel bei rezenten und fossilen Coniferen, *in* Jaworski, E., ed., Beitra¨ge zur Kenntnis des Jura in Süd-Amerika: Teil II. Neues Jahrb, Volume 40, F. Mineral. Geol. und Pal. Beil. Bd., p. 364– 456.

Gottfried, M.D., Compagno, L.J.V., and Bowman, S.C., 1996, Size and Skeletal Anatomy of the Giant "Megatooth" Shark Carcharodon megalodon, *in* Klimley, A.P., and David, G.A., eds., Great White Sharks: San Diego, Academic Press, p. 55-66.

Gottfried, M.D., and Fordyce, R.E., 2001, An associated specimen of *Carcharodon angustidens* (Chondrichthyes, Lamnidae) from the Late Oligocene of New Zealand, with comments on *Carcharodon* interrelationships: Journal of Vertebrate Paleontology, v. 21, p. 730-739.

Gottwald, H., 1992, Hölzer aus marinen Sanden des Oberen Eozän von Helmstedt (Niedersachsen): Palaeontographica Abteilung B, v. 225, p. 27-103.

Harland, M., Francis, J.E., Brentnall, S.J., and Beerling, D.J., 2007, Cretaceous (Albian-Aptian) conifer wood from Northern Hemisphere high latitudes: Forest composition and palaeoclimate: Review of Palaeobotany and Palynology, v. 143, p. 167-196.

Hartig, T., 1848, Beiträge zur Geschichte der Pflanzen und zur Kenntnis der norddeutschen Braunkohlen-Flora: Bot. Zeitung (Berlin), v. 6, p. 122-128, 137-141, 166-172 adn 185-190.

Hass, H., and Rowe, T., 1999, Thin sections and wafering, *in* Jones, T.P., and Rowe, N.P., eds., Fossil Plants and Spores: Modern Techniques: London, The Geological Society.

Hay, W.W., DeConto, R.M., Wold, C.N., Wilson, K.M., Voigt, S., Schulz, M., Wold, A.R., Dullo, W.-C., Ronov, A.B., Balukhovsky, A.N., and Söding, E., 1999, Alternative global Cretaceous paleogeography, *in* Barrera, E., and Johnson, C.C., eds., Evolution of the Cretaceous Ocean-Climate System, Volume Geological Society of America Special Paper: Boulder, Geological Society of America, p. 1-47.

Herbst, R., Brea, M., Crisafulli, A., Gnaedinger, S., Lutz, A., and Martínez, L., 2007, La Paleoxilología en la Argentina. Historia y desarrollo: Ameghiniana, v. 11, p. 57-71.

Hoadley, B.R., 1990, Identifying Wood: Accurate Results with Simple Tools: Newtown, The Taunton Press.

Hooker, J.J., Milner, A.C., and Sequeira, S.E.K., 1991, Short note: an ornithopod dinosaur from the Late Cretaceous of west Antarctica: Antarctic Science, v. 3, p. 331-332.

Horner, J.R., 1999, Egg clutches and embryos of two hadrosaurian dinosaurs: Journal of Vertebrate Paleontology, v. 19, p. 607-611.

Horner, J.R., and Currie, P.J., 1994, Embyonic and neonatal morphology and ontogeny of a new species of *Hypacrosaurus* (Ornithischia, Lambeosauridae) from Montana and Alberta, *in* Carpenter, K., Hirsch, K.F., and Horner, J.R., eds., Dinosaur Eggs and Babies: Cambridge, Cambridge University Press, p. 312-336.

Horner, J.R., and Makela, R., 1979, Nest of juveniles provides evidence of family structure among dinosaurs: Nature, v. 282, p. 296-298.

Huene, F.v., 1929, Los Saurisquios y Ornitiscquios del Cretáceo Argentino: Anales del Museo de La Plata, v. 3, p. 1-196.

IAWA, C., 1989, IAWA list of microscopic features for hardwood identification: International Association of Wood Anatomists Bulletin, New Series, v. 10, p. 219-332.

—, 2004, List of microscopic features for softwood identification: International Association of Wood Anatomists Journal, v. 25, p. 1-70.

Iglesias, A.R.I., Artabe, A.E., and Morel, E.M., 2011, The evolution of Patagonian climate and vegetation from the Mesozoic to the present: Biological Journal of the Linnean Society, v. 103, p. 409-422.

Iglesias, A.R.I., Zamuner, A.B., Poire, D.G., and Larriestra, F., 2007, Diversity, taphonomy and Palaeoecology of an angiosperm flora from the Cretaceous (Cenomanian-Coniacian) in southern Patagonia, Argentina, Volume 50, p. 445-466.

InsideWood, 2004-onwards, Published on the internet.

Jaworski, E., 1915, Beiträge zur Kenntnis der Jura in Sudamerika: Neues Jahrbuch Min. Geol. Paläonto, v. 40, p. 364-456.

—, 1926a, Beitriige zur Paliontologie und Stratigraphie des Lias, Doggers, Tithons und der Unterkreide in den Kordilleren im Süden der Provinz Mendoza (Argentinien). Teil I. Lias und Dogger: Geologische Rundschau, v. 17a, p. 373-427.

—, 1926b, La fauna del Lías y Dogger de la Cordillera Argentina en la parte meridional de la provincia de Mendoza: Academia Nacional de Ciencias (Coroba), v. 4, p. 135-317.

Keidel, J., 1917, Über das patagonische Tafelland, das patagonische Geröll und ihre Beziehungenzu den geologischen Erscheinungen im argentinischen Andengebiet und Litoral: Zeitschrift Deutsche Wissenschaftliche Verein, v. 3, p. 219-245, 311-333.

King, T., Andrews, P., and Boz, B., 1999, Effect of taphonomic processes on dental microwear: American Journal of Physical Anthropology, v. 108, p. 359-373.

Kraemer, P.E., and Riccardi, A.C., 1997, Estratigrafía de la región comprendida entre los lagos Argentino y Viedma (49° 40'-50° 10' lat. S), Provincia de Santa Cruz: Revista de la Asociacíon Geológica Argentina, v. 52, p. 333-360.

Kraus, G., 1870, Bois fossiles de Coniféres, *in* Schimper, W.P., ed., Traité de Paléontologie végétale, Volume 2, Baillère, Strasbourg, p. 363-385.

Kräusel, R., 1920, Nachträge zur Tertiärflora Schlesiens, I: Jahrb. Preuβ. Geol. Landesanst, v. 39, p. 329-460.

—, 1924, Beitrage zur Kenntnis der fossilen Flora Sudamerikas. I. Fossile Hölzer aus Patagonien und benachbarten Gebieten: Arkiv för Botanik, v. 19, p. 1-36.

—, 1949, Die fossilen Koniferen Hölzer (Unter Ausschluss von Araucarioxylon Kraus) II: Kritische Untersuchungen zur Dianostik lebender und fossiler Koniferen-Hölzer: Palaeontographica. Abt. B, v. 89, p. 83-203.

Kunzmann, L., 2007, Araucariaceae (Pinopsida): Aspects in palaeobiogeography and palaeobiodiversity in the Mesozoic: Zoologischer Anzeiger - A Journal of Comparative Zoology, v. 246, p. 257-277.

Lacovara, K.J., and Gallagher, W.B., 2006, From the K/T to the beach: the coastal deposits of southern New Jersey: Geological Society of America Field Trip Guide of Annual Meeting, 2006, Philadelphia, v. 18, p. 1-32.

Lacovara, K.J., Harris, J.D., Lamanna, M.C., Novas, F.E., Martínez, R.D., Luna, M., Ibiricu, L.M., Ambrosio, A., and Casal, G.A., 2004, An enormous sauropod from the Maastrichtian Pari Aike Formation of southernmost Patagonia: Journal of Vertebrate Paleontology, v. 22, p. 81A.

Lagabrielle, Y., Goddéris, Y., Donnadieu, Y., Malavieille, J., and Suarez, M., 2009, The tectonic history of Drake Passage and its possible impacts on global climate: Earth and Planetary Science Letters, v. 279, p. 197-211.

Leanza, A.F., 1972, Andes Patagónicos australes: Geolocía Reginal Argentina, Academia Nacional de Ciencias, Córdoba p. 689-706.

LePage, B., Yang, H., and Matsumoto, M., 2005, The Evolution and Biogeographic History of *Metasequoia*, *in* LePage, B.A., Williams, C.J., Yang, H., ed., The geobiology and ecology of Metasequoia: New York, Springer-Verlag, p. 3-114.

LePage, B.A., 2007, The Taxonomy and Biogeographic History of Glyptostrobus Endlicher (Cupressaceae): Bulletin of the Peabody Museum of Natural History, v. 48, p. 359-426.

Li, Z.X., and Powell, C.M., 2001, An outline of the palaeogeographic evolution of the Australasian region since the beginning of the Neoproterozoic: Earth-Science Reviews, v. 53, p. 237-277.

Lutz, H.J., 1930, A New Species of Cupressionoxylon (Goeppert) Gothan From the Jurassic of South Dakota: Botanical Gazette, v. 90, p. 92-107.

Lydekker, R., 1893, The dinosaurs of Patagonia: Anales del Museo de La Plata, v. 2, p. 1-14.

Macellari, C.E., Barrio, C.A., and Manassero, M.J., 1989, Upper Cretaceous to Paleocene depositional sequences adn standstone petrography of southwestern Patagonia (Argentina and Chile): Journal of South American Earth Sciences, v. 2, p. 223-239.

Mädel, E., 1960, Monimiaceen-Hölzer aus den oberkretazischen Umzamba-Schichten von Ost-Pondoland (S-Afrika): Senckenbergiana Lethaea, v. 41, p. 331-391.

Marenssi, S.A., Casadio, S., and Santillana, S.N., 2003, Estratigrafía y sedimentología de las unidades del Cretácico superior-Paleógeno aflorantes en la margen sureste del lago Viedma, provincial de Santa Cruz, Argentina: Rev. Asoc. Geol. Argent., v. 58, p. 403-416.

Martínez, L., and Lutz, A.I., 2007, Especies nuevas de Baieroxylon Greguss y Circoporoxylon Kräusel en las Formaciones Rayoso y Huincul (Cretácico), provincia del Neuquén, Argentina.: Ameghiniana, v. 44, p. 537-546.

Martínez, R.D., 1998, *Notohypsilophodon comodorensis* gen. et sp. nov. Un Hypsilophodontidae (Ornitischia: Ornithopoda) del Cretacico Superior de Chubut, Patagonia central, Argentina: Acta Geologica Leopoldensia, v. 21, p. 119-135.

Metcalfe, C.R., 1987, Anatomy of the dicotyledons. Second edition, Volume 3. Magnoliales, Illiciales and Laurales: Oxford, Clarendon Press.

Metcalfe, C.R., and Chalk, L., 1950, Anatomy of the dicotyledons: Volumes 1 and 2: Oxford, Clarendon Press, 1500 p.

—, 1983, Anatomy of the dicotyledons. Second edition, Volume 2. Wood structure and conclusion of general introduction: Oxford, Claredon Press.

Minard, J.P., Owens, J.P., Sohl, N.F., Gill, H.E., and Mello, J.F., 1969, Cretaceous–Tertiary boundary in New Jersey, Delaware, and eastern Maryland: U.S. Geological Survey, Bulletin, v. 1274H, p. 1-33.

Molnar, R.E., Angriman, L.A., and Gasparini, Z., 1996, An Antarctic Cretaceous theropod: Memoirs of the Queensland Museum, v. 39, p. 669-674.

Morgans, H.S., Hesselbo, S.P., and Spicer, R.A., 1999, The Seasonal Climate of the Early-Middle Jurassic, Cleveland Basin, England: PALAIOS, v. 14, p. 261-272.

Nishida, M., Ohsawa, T., Nishida, H., and Rancusi, M.H., 1992, Permineralized coniferous woods from the XI Region of Chile, central Patagonia: Research Institute of Evolutionary Biology, v. 7, p. 47-59.

Nishida, M., Ohsawa, T., and Ranxusi, M.H., 1990, Miscellaneous notes on the petrified coniferous woods from central Chilean Patagonia, XI Region, Chile., *in* Nishida, M., ed., Report of the Paleobotanical Survey to Patagonia, Chile, Chiba University, p. 21-29.

Norman, D.B., 2004, Basal Iguanodontia, *in* Weishampel, D.B., Dodson, P., and Osmólska, H., eds., The Dinosauria, Second Edition: Berkeley, University of California Press, p. 413-437.

Norman, D.B., Sues, H.-D., Witmer, L.M., and Coria, R.A., 2004, Basal Ornithopoda, *in* Weishampel, D.B., Dodson, P., and Osmólska, H., eds., The Dinosauria, Second Edition: Berkeley, University of California Press, p. 393-412.

Novas, F.E., Bellosi, E.S., and Ambrosio, A., 2002, Los "Estratos con Dinosaurios" del Lago Viedma y Rio La Leona (Cretacico, Santa Cruz): sedimentología y contenido fosilífero: Actas del XV Congreso Geologico Argentino (CD-ROM), v. 315, p. 1-7.

Novas, F.E., Cambiaso, A.V., and Ambrosio, A., 2004, A new basal iguanodontian (Dinosauria, Ornithischia) from the Upper Cretaceous of Patagonia: Ameghiniana, v. 41, p. 75-82.

Novas, F.E., de Valais, S., and Vickers-Rich, P., 2005a, A large Cretaceous theropod from Patagonia, Argentina, and the evolution of carcharodontosaurids: Naturwissenschaften, v. 92, p. 226–230.

Novas, F.E., Ezcurra, M.D., and Lecuona, A., 2008, *Orkoraptor burkei* nov. gen. et sp., a large theropod from the Maastrichtian Pari Aike Formation, Southern Patagonia: Cretaceous Research, v. 29, p. 468-480.

Novas, F.E., Salgado, L., Calvo, J.O., and Agnolin, F., 2005b, Giant titanosaur (Dinosauria, Sauropoda) from the Late Cretaceous of Patagonia: Revista del Museo Argentino de Ciencias Naturales, n.s., v. 7, p. 37-41.

Nullo, F.E., Panza, J.L., and Blasco de Nullo, G., 1999, Jurásico y Cretácico del la Cuenca Austral, *in* Caminos, R., ed., Geología Argentina Volume 29: Buenos Aires, SEGEMAR, p. 528-535.

Nullo, F.E., Proserpio, C.A., and Blasco de Nullo, G., 1981a, El Cretacico de la Cuenca Austral entre el Lago San Martín y río Turbio, *in* Volkheimer, W., ed., Cuencas sedimentarias del jurásico y cretácico de América del Sur, Volume 1: Buenos Aires.

—, 1981b, Estratigrafía del Cretácico superior en el Cerro Indice y alrrededores, Provinica de Santa Cruz, Actas 8° Congreso Geológico Argentino, Volume 3: Buenos Aires, p. 373-387.

O'Gorman, J.P., and Varela, A.N., 2010, The oldest lower Upper Cretaceous plesiosaurs (Reptilia, Sauropterygia) from southern Patagonia, Argentina: Ameghiniana, v. 47, p. 447-459.

Obasi, C.C., Terry, D.O., Jr., Myer, G.H., and Grandstaff, D.E., 2011, Glauconite Composition and Morphology, Shocked Quartz, and the Origin of the Cretaceous(?) Main Fossiliferous Layer (MFL) in Southern New Jersey, U.S.A: Journal of Sedimentary Research, v. 81, p. 479-494.

Oviedo, E.S., 1982, Geología de la Valle del rio Leona. Provincia de Santa Cruz [Unpublished thesis]: Buenos Aires, Universidad de Buenos Aries.

Owens, J.P., Minard, J.P., Sohl, N.F., and Mello, J.F., 1970, Stratigraphy of the post-Magothy Upper Cretaceous formations in southern New Jersey and northern Delmarva Peninsula, Delaware and Maryland U.S. Geological Survey, Professional Paper v. 674, p. 1-60.

Panti, C., Pujana, R.R., Zamaloa, M.C., and Romero, E.J., 2011, Araucariaceae macrofossil record from South America and Antarctica: Alcheringa: An Australasian Journal of Palaeontology, p. 1-22.

Pasad, M.N.V., 1981, New species of fossil wood Planoxylon from Late Paleozoic of Irian Jaya, Indonesia: Bulletin of the Geological Research and Development Centre v. 5, p. 37-40.

Passalia, M.G., 2007, A mid-Cretaceous flora from the Kachaike Formation, Patagonia, Argentina: Cretaceous Research, v. 28, p. 830-840.

Philippe, M., 1993, Nomenclature générique des trachéidoxyles fossiles mésozoïques à champs araucarioïdes: Taxon, v. 42, p. 74-80.

—, 2011, How many species of Araucarioxylon?: Comptes Rendus Palevol, v. 10, p. 201-208.

Philippe, M., Bamford, M., McLoughlin, S., Alves, L.S.R., Falcon-Lang, H.J., Gnaedinger, S., Ottone, E.G., Pole, M., Rajanikanth, A., Shoemaker, R.E., Torres, T., and Zamuner, A., 2004, Biogeographic analysis of Jurassic-Early Cretaceous wood assemblages from Gondwana: Review of Palaeobotany and Palynology, v. 129, p. 141-173.

Philippe, M., and Bamford, M.K., 2008, A key to morphogenera used for Mesozoic conifer-like woods: Review of Palaeobotany and Palynology, v. 148, p. 184-207.

Philippe, M., and Hayes, P., 2010, Reappraisal of two of Witham's species of fossil wood with taxonomical and nomenclatural notes on Planoxylon Stopes, Protocedroxylon Gothan and Xenoxylon Gothan: Review of Palaeobotany and Palynology, v. 162, p. 54-62.

Philippe, M., Quiroz, D., and Torres, T., 2000, Early Cretaceous fossil wood from Aysen area (Patagonia, Chile) and their bearings on the role of the Araucariaceae in the Andean forest at this time: IX Congreso Geolo´gico Chileno, Puerto Varas, Chile v. 2, p. 235-239.

Piatnitzky, A., 1936, Estudio geológico de la región del Río Chubut y del Río Genoa: Boletín de Informaciones Petroleras, v. 13, p. 83-118.

Piatnizky, A., 1936, Observations geológicas en el oeste de Santa Cruz: Boletín de Informaciones Petroleras, v. 165, p. 45-85.

Podgorny, I., 2005, Bones and devices in the constitution of paleontology in Argentina at the end of the nineteenth century: Science in Context, v. 18, p. 249-283.

Poole, I., 2002, Systematics of Cretaceous and Tertiary *Nothofagoxylon*: Implications for Southern Hemisphere biogeography and evolution of the Nothofagaceae: Australian Systematic Botany, v. 15, p. 247-276.

Poole, I., and Cantrill, D., 2001a, Fossil Woods From Williams Point Beds, Livingston Island, Antarctica: A Late Cretaceous Southern High Latitude Flora: Palaeontology, v. 44, p. 1081-1112.

Poole, I., Cantrill, D., and Utescher, T., 2005, A multi-proxy approach to determine Antarctic terrestrial palaeoclimate during the Late Cretaceous and Early Tertiary: Palaeogeography, Palaeoclimatology, Palaeoecology, v. 222, p. 95-121.

Poole, I., and Cantrill, D.J., 2001b, Forests of the Polar Night: Geoscientist, v. 11, p. 4-6.

Poole, I., Cantrill, D.J., Hayes, P., and Francis, J., 2000a, The fossil record of Cunoniaceae: new evidence from Late Cretaceous wood of Antarctica?: Review of Palaeobotany and Palynology, v. 111, p. 127-144.

Poole, I., and Francis, J.E., 1999, The first record of fossil atherospermataceous wood from the upper Cretaceous of Antarctica: Review of Palaeobotany and Palynology, v. 107, p. 97-107.

—, 2000, The First Record of Fossil Wood of Winteraceae from the Upper Cretaceous of Antarctica: Ann Bot, v. 85, p. 307-315.

Poole, I., and Gottwald, H., 2001, Monimiaceae *sensu lato*, an element of Gondwanan polar forests: Evidence from the late Cretaceous-early tertiary wood flora of Antarctica: Australian Systematic Botany, v. 14, p. 207-230.

Poole, I., Gottwald, H., and Francis, J.E., 2000b, Illicioxylon, an Element of Gondwanan Polar Forests? Late Cretaceous and Early Tertiary Woods of Antarctica: Ann Bot, v. 86, p. 421-432.

Poole, I., Hunt, R.J., and Cantrill, D.J., 2001, A Fossil Wood Flora from King George Island: Ecological Implications for an Antarctic Eocene Vegetation: Ann Bot, v. 88, p. 33-54.

Poole, I., Mennega, A.M.W., and Cantrill, D.J., 2003, Valdivian ecosystems in the Late Cretaceous and Early Tertiary of Antarctica: further evidence from myrtaceous and eucryphiaceous fossil wood: Review of Palaeobotany and Palynology, v. 124, p. 9-27.

Poole, I., Richter, H., and Francis, J., 2000c, Evidence for Gondwanan origins for Sassafras (Lauraceae)? Late Cretaceous fossil wood of Antarctica: IAWA, v. 21, p. 463-475.

Povilauskas, L., Barreda, V., and Marenssi, S., 2008, Polen y esporas de la Formación La Irene (Maastrichtiano), sudoeste de la provincia de Santa Cruz, Argentina: primeros resultados: Geobios, v. 41, p. 819-831.

Povilauskas, L., Palamarczuk, S., Barreda, V., Bellosi, E.S., Novas, F., Ambrosio, A., and Ottone, G., 2003, Edad y paleoambiente de depósitos del Cretácico tardío del so de la provincia de Santa Cruz: Evidencias palinológicas XIII Simposio Argentino de Paleobotánica y Palinología.

Powell, J.E., 2003, Revision of South American Titanosaurid sinosaurs: palaeobiological, palaeobiogeographical and phylogenetic aspects: Records of the Queen Victoria Museum, v. 111, p. 1-173.

Prabhakar, M., 1987, Palynology of the Upper Gondwana deposits of Rampur area, Pranhita Godavari Basin, Andhra Pradesh, India: Journal of the Palaeontological Society of India, v. 32, p. 114-121.

Pujana, R.R., Umazano, A.M., and Bellosi, E.S., 2007, Maderas fósiles afines a Araucariaceae de la Formación Bajo Barreal, Cretácico Tardío de Patagonia central (Argentina): Revista Museo Argentino Ciencias Naturales, nueva serie, v. 9, p. 161-167.

Quattrocchio, M.E., Martinez, M.A., Pavisich, A.C., and Volkheimer, W., 2006, Early Cretaceous palynostratigraphy, palynofacies and palaeoenvironments of well sections in northeastern Tierra del Fuego, Argentina: Cretaceous Research, v. 27, p. 584-602.

Quattrocchio, M.E., Volkheimer, W., Borrromei, A.N.A.M., and MartÍNez, M.A., 2011, Changes of the palynobiotas in the Mesozoic and Cenozoic of Patagonia: a review: Biological Journal of the Linnean Society, v. 103, p. 380-396.

Raigemborn, M.S., Brea, M., Zucol, A.F., and Matheos, S.D., 2007, Early Paleogene climate at mid latitude in South America: Mineralogical and paleobotanical proxies from continental sequences in Golfo San Jorge basin (Patagonia, Argentina): Geologica Acta, v. 7, p. 125-145.

Rajanikanth, A., and Sukh-Dev, A., 1989, The Kota Formation: Fossil flora and Stratigraphy: Geophytology, v. 19, p. 52-64.

Riccardi, A.C., 2008, El Museo de La Plata en el avance del conocimiento geológico a fines del Siglo XIX: Serie correlación geológica, p. 109-126.

Riccardi, A.C., and Rolleri, E.O., 1980, Cordillera Patagónica Austral, En II Simposio Geología Regional Argentina, Volume 2, Academia Nacional de Ciencias, Córdoba, p. 1173-1306.

Roll, A., 1936, Informe sobre la estructura de Pari Aike (región de Mata Amarilla): Yac. Petrol. Fiscales. Inf. Inéd., Buenos Aires

Ru-feng, W., Yu-fei, W., and Yong-zhe, C., 1996, Cupressinoxylon jiayinense, a new species of the Late Cretaceous from Heilongjiang Province, China: IAWA Journal, v. 17, p. 319-326.

Salard, M., 1968, Contribution a la connaisance de la flore fossile de la Nouvelle Caledonie: Palaeontographica Abteilung B, v. 124, p. 1-44.

Salgado, L., 2007, Patagonia and the study of its Mesozoic reptiles, *in* Gasparini, Z., Salgado, L., and Coria, R.A., eds., Patagonian Mesozoic Reptiles: Bloomington, Indiana University Press, p. 1-28.

Salgado, L., Coria, R.A., and Heredia, S.E., 1997, New materials of *Gasparinisaura cincosaltensis* (Ornithischia, Ornithopoda) from the Upper Cretaceous of Argentina: Journal of Paleontology, v. 71, p. 933-940.

Scher, H.D., and Martin, E.E., 2006, Timing and Climatic Consequences of the Opening of Drake Passage: Science, v. 312, p. 428 - 430.

Schroeter, E.R., Egerton, V.M., Ibiricu, L.M., and Lacovara, K.J., in prep, The first occurrence of *Archaeolamna kopingensis* (Lamniformes: Archaeolamnidae) in South America (Santa Cruz Province, Argentina).

Shimada, K., 2008, Ontogenetic Parameters and Life History Strategies of the Late Cretaceous Lamniform Shark, Cretoxyrhina mantelli, Based on Vertebral Growth Increments: Journal of Vertebrate Paleontology, v. 28, p. 21-33.

Shimada, K., and Cicimurri, D.J., 2006, The oldest record of the Late Cretaceous anacoracid shark, *Squalicorax pristodontus* (Agassiz), from the Western Interior, with comments on *Squalicorax* phylogeny, *in* Lucas, S.G., and Sullivan, R.M., eds., Late Cretaceous Vertebrates from the Western Interior, Volume 35: New Mexico Museum of Natural History and Science Bulletin: Albuquerque, New Mexico Museum of Natural History and Science, p. 177-184.

Spalletti, L.A., and Franzese, J.R., 2007, Mesozoic Paleogeography and Paleoenvironmental Evolution of Patagonia (Southern South America), *in* Gasparini, Z., Salgado, L., and Coria, R.A., eds., Patagonian Mesozoic Reptiles: Bloomington Indiana University Press, p. 29-49.

Stewart, W.N., and Rothwell, G.W., 1993, Paleobotany and the Evolution of Plants: Cambridge, Cambridge University Press.

Stopes, M.C., 1916, An Early Type of the Abietineae (?) from the Cretaceous of New Zealand: Annals of Botany, v. os-30, p. 111-125.

Sugarman, P.J., Miller, K.G., Bukry, D., and Feigenson, M.D., 1995, Uppermost Campanian–Maastrichtian strontium isotopic, biostratigraphic, and sequence stratigraphic framework of the New Jersey Coastal Plain: Geological Society of America,Bulletin, v. 107, p. 19-37.

Süss, H., 1960, Ein Monimiaceen-Hölzer aus der oberen Kreide Deutschlands *Hedycaryoxylon subaffine* (Vater) nov. comb.: Senckenbergiana Lethaea, v. 41, p. 317-330.

Tarmian, A., Azadfallah, M., Gholamiyan, H., and Shahverdi, M., 2011, Inter-Tracheid and cross-field pitting in compression wood and opposite wood of Norway Spruce (*Picea abies* L.): Notulae Scientia Biologicae, v. 3, p. 145-151.

Taylor, T.N., Taylor, E.L., and Krings, M., 2009, Paleobotany: The Biology and Evolution of Fossil Plants: New York, Elsevier Inc., 1230 p.

Teaford, M.F., 1988, A review of dental microwear and diet in modern mammals: Scanning Microscopy, v. 2, p. 1149-1166.

Terada, K., Asakawa, T.O., and Nishida, H., 2006a, Fossil woods from the Loreto Formation of Las Minas, Magallanes (XII) Region, Chile, *in* Nishida, H., ed., Post-Cretaceous Floristic Changes in Southern Patagonia, Chile, Chuo University.

Terada, K., Asakawa, T.O., and Nishida, M., 2006b, Fossil woods from Arroyo Cardenio, Chile Chico Province, Aisen (XI) Region, Chile, *in* Nishida, M., ed., Post-Cretaceous floristic changes in Southern Patagonia, Chile, Chuo University.

Torres, T., and Philippe, M., 2002, Nuevas especies de Agathoxylon y Baieroxylon del Lías de La Ligua (Chile) con una evaluación del registro paleoxilológico en el Jurásico de Sudamérica: Revista Geológica de Chile, v. 29, p. 151-163.

Torrey, R.E., 1923, The comparative anatomy and phylogeny of the Coniferales, Part. 3: Mesozoic and Tertiary coniferous woods: Mem. Boston Soc. Nat. Hist, v. 6, p. 39-106.

Vagyani, B.A., and Mahabale, T.S., 1974, A new species of fossil Gymnospermous wood Planoxylon Stopes from Adhari (m.s.): The Palaeobotanist, v. 21.

Varela, A.N., 2009, Accommodation/sediment supply fluvial deposition controlled by base level changes and relative sea level fluctuations in the Mata Amarilla Formation (Early Upper Cretaceous), Southern Patagonia, Argentina. , 9th International Conference on Fluvial Sedimentology. *Actas Geológica Lilloana*., Volume 21, p. 66.

—, 2010a: La Plata, University of La Plata.

—, 2010b, Paleosol development in response to extrinsic and intrinsic factors: The Mata Amarilla Formation (lower Upper Cretaceous), an example of southern Patagonia, *in* Schwarz, E., Georgieff, S., Piovano, E., and Ariztegui, D., eds., 18th International Sedimentological Congress: Mendoza, Argentina, p. 892.

Varela, A.N., Richiano, S., and Poiré, D.G., 2010, Distinguishing tsunamis shell bed deposit using sedimentologic and taphonomic features: an example from (Lower Upper Cretaceous) Southern Patagonia, Argentina, *in* Schwarz, E., Georgieff, S., Piovano, E., and Ariztegui, D., eds., 18th International Sedimentological Congress, p. 893.

Vaudois, N., and Privé, C., 1971, Révision des bois fossiles de Cupressaceae: Palaeontographica. Abt. B, v. 134, p. 61-86.

Veevers, J.J., 2004, Gondwanaland from 650-500 Ma assembly through 320 Ma merger in Pangea to 185-100 Ma breakup: supercontinental tectonics via stratigraphy and radiometric dating: Earth-Science Reviews, v. 68, p. 1-132.

Visscher, G.E., and Jagels, R., 2003, Separation of *Metasequoia* and *Glyptostrobus* (Cupressaceae) based on wood anatomy: IAWA Journal, v. 24, p. 439-450.

Vozenin-Serra, C., and Salard-Cheboldaeff, M., 1992, Les bois minéralisés permo-triasiques de Nouvelle-Calédonie. Implications phylogénetique et paléogéographique: Palaeontographica Abteilung B, v. 225, p. 1-25.

Walker, A., Hoeck, H.N., and Perez, L., 1978, Microwear of Mammalian Teeth as an Indicator of Diet: Science, v. 201, p. 908-910.

Wheeler, E.A., and Baas, P., 1998, Wood identification: A review: IAWA Journal, v. 19, p. 241-264.

Wheeler, E.A., and Lehman, T.M., 2005, Upper Cretaceous-Paleocene conifer woods from Big Bend National Park, Texas: Palaeogeography, Palaeoclimatology, Palaeoecology, v. 226, p. 233-258.

—, 2009, New Late Cretaceous and Paleocene dicot woods of Big Bend National Park, Texas and review of Cretacous wood characteristics: IAWA, v. 30, p. 293-318.

Williams, C.J., Trostle, K.D., and Sunderlin, D., 2010, Fossil wood in coal-forming environments of the late Paleocene-early Eocene Chickaloon Formation: Palaeogeography, Palaeoclimatology, Palaeoecology, v. 295, p. 363-375.

Willis, K.J., and McElwain, J.C., 2002, The Evolution of Plants: Oxford, Oxford University Press, 378 p.

Wolfe, P.E., 1977, The Geology and Landscapes of New Jersey: New York, Crane, Russak and Company.

Wood, R.C., and Patterson, B., 1973, A fossil trionychid turtle from South America: Breviora, v. 405, p. 1-10.

APPENDIX A: FOSSIL GYMNOSPERM WOOD SAMPLE DESCRIPTIONS AND PLATES

Agathoxylon

MPM-8

Growth ring boundaries are distinct and abrupt with a narrow latewood zone (Figure 1a). False rings are present. The average radial diameter of the earlywood tracheids is 30 µm (range 15-41 µm) and the average tangential diameter is 22 µm (15-31 µm). Axial parenchyma are absent. The radial walls of the tracheids only contain uniseriate bordered pitting with an average bordered pit diameter of 10 µm (range 7-16 µm). These pits touch neighboring pits with some deformation occurring. This is consistent with araucarian radial pitting (Figure 1b, c). No resin canals were observed. Rays are comprised of ray parenchyma. Cross-field pits appear to be araucarioid and consist of 2-6 small pits (Figure 1d). Tangential rays are exclusively uniseriate with a mean ray height of 3.96 cells (standard deviation 1.48) with a range being 2-9 cells (Figure 1e, f).

MPM-21

Growth rings can be distinguished, but are not well preserved (Figure 2a, b). The tracheids have undergone significant deformation; however the diameters of some unaltered tracheids could still be recorded (radial diameter = 30 µm; tangential diameter = 22 µm) (Figure 2b). Axial parenchyma are absent. Bordered pitting on the tracheid radial wall is exclusively uniseriate with the majority of the pits touching (Figure 2c, d).

The average bordered pit diameter is 15 µm with a range of 11-18 µm. No resin canals were observed. Ray parenchyma are horizontal with smooth end walls. Cross-field pits consist of 2-6, unordered, crowded pits with narrow, angled, elliptical apertures consistent with araucarioid cross-field pits (Figure 2d). Tangential rays are predominantly uniseriate (96%) with some rays containing biseriate sections (Figure 2e, f). The average tangential ray length is 6.05 cells with the range being 1-15 cells (standard deviation 3.29).

MPM-23

Growth rings are distinct with a narrow latewood zone (3-6 cells wide). The transition may either be gradual or abrupt (Figure 3a, b). False rings are present (Figure 3b). Axial parenchyma are absent. No resin canals were observed. The average tracheid diameters are, radially, 44 µm (range, 24-76 µm) and tangentially, 36 µm (range, 22-67 µm). Bordered pitting on the radial wall of the tracheids is either uniseriate or biseriate with the former dominant (97%). Biseriate pitting occurs as both alternate (two occurrences) and opposite (one occurrence) (Figure 3c). The majority of bordered pits on the tracheids touch adjacent pits with some deformation occurring. The average diameter of the bordered pits is 17 µm with a range of 8-24 µm. In radial longitudinal section, ray parenchyma are commonly filled with resin (Figure 3d, e, f). The end walls of the ray parenchyma are smooth with no additionally thickenings. Ray tracheids are absent. Cross-field pits consist of 2-6, ordered to unordered, crowded pits with narrow, angled, elliptical apertures consistent with araucarioid cross-field pits (Figure 3d). The tangential

ray cells are all uniseriate. The mean ray height is 8.31 cells (standard deviation 6.27) with a range of 1-28 cells per ray (Figure 3e, f).

MPM-32

Growth rings are distinct with a narrow latewood zone (1-6 cells high). Several growth rings are separated by cell failure at the latewood/earlywood boundary ("frost ring") (Figure 4a, b). Axial parenchyma are absent. The average radial diameter of the earlywood tracheids is 35 µm (range 20-47 µm) and the average tangential diameter is 30 µm (18-49 µm). Bordered pitting on the radial walls of the tracheids is predominantly uniseriate (79%) and locally biseriate (21%) (Figure 4c, d). Alternate biseriate pitting is exclusive throughout the specimen. The bordered pits are araucarian and have an average diameter of 16 µm and a range of 11-22 µm. Ray tracheids are absent while ray parenchyma are abundant. Ray parenchyma are horizontal and have smooth end walls. Cross-field pits consist of 2-6, unordered, crowded pits per cross-field with narrow, angled, elliptical apertures consistent with araucarioid cross-field pits (Figure 4d). Spiral checking can be seen in several tracheids throughout the sample (Figure 4d). Tangential rays are predominantly uniseriate (69%) with some rays containing biseriate sections. The average tangential ray length is 6.48 cells with the range being 1-19 (standard deviation 3.95) (Figure 4e, f). Bordered pits occur on the tangential wall of the tracheid (Figure 4f).

Planoxylon

MPM-9

Growth ring boundaries are distinct with a narrow latewood zone and some earlywood crushing (Figure 5a, b). False rings are present throughout the specimen (Figure 5a, b). Axial parenchyma are present but rare. The mean earlywood tracheid diameter, radially, is 47 µm (range 29-79 µm) and, tangentially, is 39 µm (range 23-63 µm). Bordered pitting on the radial wall of the tracheid is a mix of both araucarian (dominant) and abietinean and consists of uniseriate (98%) and rare biseriate (exclusively alternate) pits (Figure 5c, d). The biseriate pits are restricted to the end walls of the tracheids (Figure 5d). Bordered pits are circular; although, more often, they are semi-circular due to slight compression from neighboring pits (Figure 5c, d). The average diameter of the bordered pits is 14 µm with the range being 8-20 µm. Spiral checking is present in some tracheids. Cross-field pits are araucarioid, cupressoid and piceoid and contain 1-6 pits per cross-field, with the majority containing 2-4 pits and rarely 5-6 pits. These pits are commonly obliquely angled with the pit aperture elliptical to slit-like (araucarioid and cupressoid); although some apertures are rounded (piceoid) (Figure 5e, f). Ray tracheids are absent. Abietineentüpfelungen (‘abietinean pitting’) can be identified on the transverse walls of some of the ray cells in both RLS and TLS (Figure 5g, h). In TLS, rays are predominantly uniseriate (97%) with some local biseriation (Figure 5i). The mean ray height is 8.7 cells with a range being 2-21 cells. Tangential tracheid walls contain some bordered pits (Figure 5i).

Cupressinoxylon

MPM-26b

Growth rings are distinct and have a narrow latewood zone of only two to six cells thick (Figure 8a, b). A few false rings are present. Axial parenchyma are diffuse (Figure 8b). The mean earlywood tracheid radial and tangential diameters are 25 µm (range 14-39 µm) and 24 µm (range 11-41 µm), respectively. The radial walls of the tracheids contain only uniseriate bordered pits (mean diameter 12 µm); however, most of the length of the tracheid is smooth (Figure 8c). The bordered pits are either isolated or form short chains of 2-8 pits; however, they rarely touch (Figure 8c, d). The apertures of the bordered pits are either elliptical or slit-like. Ray parenchyma have smooth walls and ray tracheids are absent (Figure 8c). Rays are commonly resin-filled. Cross-field pits consist of 1-2 bordered pits per cross-field with an aperture narrower than the border and angled ~45° (Figure 8d, e). These features are consistent with cupressoid pits. Spiral checking on the tracheid wall occurs in small sections throughout the specimen. Tangential rays are uniseriate with no biseriation present in the thin section (Figure 8f, g). The average ray height is 4.5 cells with a range from 1-11 cells (standard deviation 2.21). A few bordered pits occur on the tangential wall of the tracheids (Figure 8).

Taxodioxylon sp. 1

MPM-10

Growth rings are distinct and abrupt with a narrow latewood zone (5-8 cells) (Figure 7a, b). False rings are present (Figure 7b). The tracheids are square to hexagonal in shape and have a mean radial diameter of 30 µm (range 15-42) and mean tangential diameter of 26 µm (range 15-42) (Figure 7b, c). Axial parenchyma are diffuse and occurs in both the latewood and the earlywood (Figure 7b, c). Beading occurs on the end walls of the axial parenchyma. The radial walls of the tracheids bear bordered pits that average 14 µm in diameter and have a range of 8-19 µm. The bordered pits are predominantly abietinean; however sections of araucarian pitting occur (Figure 7d). Cross-field pits consist of 2 or 4 taxodioid-cupressoid pits with both narrow and wide apertures (Figure 7e, f). Ray parenchyma have sub-horizontal, smooth walls and are commonly filled with dark, resinous material (Figure 7d, e, f). Ray tracheids are absent. Tangential rays are uniseriate with an average 5.76 cells high (standard deviation 3.33) with a range of 2 to 18 cells (Figure 7g).

MPM-15

Growth rings are distinct with an abrupt, narrow latewood zone (Figure 8a, b). False rings are present (Figure 8b). In transverse section, the tracheids are square to hexagonal in shape with the mean radial and tangential earlywood tracheid diameters being 31 µm (range 16-55 µm) and 27 µm (range 13-43 µm), respectively. The radial wall of the

tracheids predominately contain uniseriate bordered pitting (99%) (Figure 9c, d), and rarely biseriate alternate pitting (Figure 9e). Bordered pitting on the radial wall of the tracheids consists of a mixture of abietinean and araucarian pitting, depending on the depth of field, with the former being dominant (Figure 9c, d, e). These bordered pits range in size from 9-19 µm with the average being 14 µm. Axial parenchyma are rare and occur in both the earlywood and the latewood (Figure 8b). Moderate beading occurs on some of the transverse end walls of some of the axial parenchyma (Figure 8f). Ray parenchyma are horizontal with smooth end walls. Ray tracheids are absent. Cross-field pitting consists of 2 to 4 small, unorganized taxodioid/cupressoid pits (Figure 8d). In tangential longitudinal section, the ray height ranges from 2 to 11 cells with the average being 4.49 cells (Figure 9g).

MPM-16

Growth rings are distinct with both thick (less than 5 cells thick) and thin latewood (1-3 cells) zone and false rings are present (Figure 9a, b, c). Possible wound wood is present (Figure 9c). Axial parenchyma are rare and contain pitting on some of the end walls. The tracheids are square to hexagonal in shape. The average tracheid diameters are, radially, 29 µm (range 16-44 µm) and, tangentially, 36 µm (range 22-67 µm). The radial walls of the trachieds contain exclusively uniseriate abietinean bordered pitting (Figure 9d). The average bordered pit diameter is 12 µm (range 6-15 µm). Ray parenchyma walls are smooth. Ray tracheids are absent. Cross-field pitting consists of 2-4 small taxodioid/cupressoid pits per cross-field (Figure 9e, f). The average ray height in

tangential section is 4.74 cells (standard deviation 2.04) with a range being 2-14 cells per ray. Rays are exclusively uniseriate (Figure 9g).

MPM-18

This specimen is from a branch (Figure 10a). Growth rings are distinct with a narrow latewood zone and a wide earlywood zone. False rings are present (Figure 10b). Axial parenchyma are diffuse. The tracheids are square to hexagonal in shape. The average radial tracheid diameter is 27 µm (range 13-39) and tangential diameter is 25 µm (range 13-43 µm). The tracheid radial walls contain bordered abietinean pitting with the average pit diameter being 11 µm (range 7-14 µm) (Figure 10c, d). Ray parenchyma walls are smooth and straight; ray tracheids are not present. Cross-field pitting consists of 2-4 taxodioid pits per cross-field, with the majority containing 2 pits per cross-field (Figure 10d). In tangential longitudinal section, ray height ranges from 1 to 8 cells high with the average being 3.64 cells high (standard deviation 1.31) (Figure 10e). Beading is present on the transverse end walls of axial parenchyma (Figure 10f).

***Taxodioxylon* sp. 2**

MPM-11b

Growth rings are abrupt with a narrow latewood zone (2-6 cells thick) and a wide earlywood zone (Figure 11a, b). The earlywood has been crushed in many of the growth rings (Figure 11b). False rings are present. Axial parenchyma are diffuse and occur in

both the earlywood and the latewood. Beading is present on the transverse end walls of some of the axial parenchyma (Figure 11e). The tracheids are rectangular to hexagonal in shape. The mean radial earlywood tracheid diameter is 27 µm (range 16-40 µm) and the mean tangential tracheid diameter is 26 µm (range 10-37 µm). The radial walls of the tracheids bear abundant araucarian bordered pits and possible xenoxylon bordered pit (Figure 10c, d). Bordered pits are predominately uniseriate (99%) with one set of opposite biseriate pits. The average diameter of the bordered pits is 16 µm (range 12-27 µm). Ray parenchyma horizontal and end walls are smooth and straight; ray tracheids are absent (Figure 11c, f). Rays are often filled with a dark resinous material. Cross-field pitting consists of 1-2 obliquely angled taxodioid/cupressoid pits in both the earlywood and the latewood (Figure 11f). In tangential longitudinal section, ray height ranges from 2-21 cells high with the average being 7.26 cells high (standard deviation 4.22). Rays are predominately uniseriate (98%) with some local biseriation (Figure 11g, h).

Podocarpoxylon

MPM-6

This material is poorly preserved. Growth rings are distinct and abrupt (Figure 12a, b). The average earlywood tracheid diameters are 41 µm (range 14-53 µm) radially and 35 µm (range 23-47) tangentially. Bordered pitting on the radial walls of the tracheids is predominantly uniseriate with some local biseriation (one set of opposite biseriation) (Figure 12d, e). The bordered pits are widely spaced apart and have an average diameter of 13 µm with a range of 9-16 µm. Cross-field pits have an elliptical aperture consistent

with podocarpoid cross-field pits (Figure 12e, f). The tangential mean ray height is 4.39 (standard deviation 2.01) with a range of 2 to 12 cells (Figure 12g).

MPM-11a

Growth rings are abrupt with a narrow latewood zone (Figure 13a, b). The earlywood is crushed in many of the growth rings (Figure 13b). Axial parenchyma are diffuse but rare. The average radial diameter of the earlywood tracheids is 34 µm (range 22-45 µm) and the tangential diameter is 29 µm (14-41 µm). The radial wall of the tracheids bear abietinean bordered pits that have an average diameter of 13 µm (range 9-16 µm) (Figure 13c). Ray parenchyma have sub-horizontal, smooth walls and are commonly filled with resinous material (Figure 13c, d). Ray tracheids are absent. Cross-field pits are podocarpoid-cupressoid with mostly 2 pits per cross-field (Figure 13d). Cross-field pits are a mix between having a narrow or wide aperture. Tangential rays are predominately uniseriate (97%) with some local biseriation. Tangential ray height averages 9.09 cells (standard deviation 5.92) with a range of 2 to 25 cells (Figure 13e, f).

MPM-25

Growth rings are distinct; the transition of earlywood to latewood is typically abrupt (only 3-9 latewood cells thick). A few growth rings do show a gradual transition. False rings are present and are 2-3 cells thick (Figure 14a, b). Axial parenchyma are present, but are not abundant (Figure 14b). The average earlywood tracheid diameters are 38 µm

(range 24-62 µm) and 28 µm (range 14-49 µm) radially and tangentially, respectively. Bordered pitting on the radial walls of the tracheids are predominantly uniseriate (99%) with only a few occurrences of adjacent and opposite biseriate. The bordered pits are round and form short chains of closely associated (less than one cell space apart) with some pits touching (Figure 14c, d). The mean bordered pit diameter is 14 µm with the range being 10-18 µm. Ray tracheids are absent. Ray parenchyma are horizontal and have smooth, unpitted walls. Cross-field pitting generally occurs as 1-2 pits per cross-field that contain sub-parallel, narrow apertures consistent with podocarpoid pits (Figure 14d). In tangential section, rays are predominately uniseriate (97%) (Figure 14g). The average tangential ray length is 10.13 cells with a range being 1-37 cells.

MPM-30

Growth rings are distinct; the transition of earlywood to latewood is typically abrupt (only 3-4 latewood cells thick). A few growth rings do show a gradual transition (Figure 15a). Five false rings are present in the thin section (Figure 15b). Axial parenchyma are present, but are not abundant (Figure 14b). The average diameter of the tracheids radially is 22 µm (range 14-30 µm) and tangentially 23 µm (13-37 µm). Bordered pitting on the radial walls of the tracheids are predominantly uniseriate (99%) with only one occurrence of adjacent biseriate. The bordered pits are round with the apertures either round to slit-like and form short chains of touching or closely associated (less than one cell space apart) pits (abietinean pitting) (Figure 15c, d). The average bordered pit width is 11 µm with a range of 7-14 µm. In radial section, spiral checking (spiral grooves) on the

tracheid walls occurs periodically throughout the thin section at approximately a 45 degree angle (Figure 15c, d). Ray tracheids are absent. Ray parenchyma are horizontal and have smooth, unpitted walls. Cross-field pitting generally occurs as a single, sub-parallel, narrow aperture (podocarpoid) (Figure 15d). Tangential rays are predominately uniseriate (99%) with only one incidence of biseriation (Figure 15d, e). The average tangential ray length is 4.43 cells with a range being 2-11 cells (standard deviation 2.08).

MPM-31

Growth rings are distinctly marked by thickened latewood tracheids with rings being 3-9 cells wide (Figure 16a, b). False rings are present and are 2-3 cells thick. The average radial tracheid diameter is 44 µm (range 22-61 µm) and tangential diameter is 32 µm (range 22-61 µm). The radial walls of the tracheids contain bordered uniseriate pitting (97%). Biseriate alternate pitting was only observed in two tracheids, while biseriate opposite pitting only occurs in one tracheid. The average bordered pit size is 15 µm with a range of 10-21 µm. The bordered pits are relatively close to each other; however, because there is little to no deformation, they are considered abietinean pitting (Figure 16c). Axial parenchyma are rare. Ray parenchyma are commonly filled with a dark material and ray tracheids are absent (Figure 16d, e). Cross-field pitting varies with 2-4 pits per field, with two vertical-sub vertical slit-like pits (podocarpoid) predominating (Figure 16d, e). The tangential ray height averages 6.24 cells (standard deviation 4.11) with a range of 2-20 cells per ray (Figure 16 e, f).

Gymnosperm indet.

MPM-1

Growth rings are present, but not very well-defined (Figure 17a, b). Axial parenchyma is very abundant and commonly filled with dark material (Figure 17b, c, f, g). The end walls of the axial parenchyma are smooth. The average tracheid diameters are, radially, 39 µm (range 20-58 µm) and, tangentially, 32 µm (range 19-43 µm). Bordered pitting on the radial walls of the tracheids is not well-preserved, thus it is impossible to ascertain the size or arrangement of the bordered pits (Figure 17c). Cross-field pits are preserved in some cross-fields. They occur as 1-2, round to slightly elliptical pits per cross-field (1 being most common) (Figure 17d, e). Tangential rays are short with an average length being 3.76 cells (range 1-8 cells) (Figure 17g). Putative family assignments may be Podocarpacacea, Cupressaceae or Cephalotaxaceae based on the presence of diffuse axial parenchyma (Richter et al. 2004). The type of cross-field pitting in the specimen suggests that the wood may belong to *Taxodioxylon*.

MPM-7

Growth rings are distinct and contain a thick latewood zone and some earlywood crushing (Figure 18a, b). False rings are present. The average earlywood tracheid radial and tangential diameters are 36 µm (range 15-49 µm) and 29 µm (range 15-49 µm), respectively. Axial parenchyma is abundant and diffuse in both the earlywood and the latewood (Figure 18b). The end walls of the parenchyma are smooth. Parenchyma are

often filled with dark resinous material (Figure 18c, f). The radial walls of the tracheids contain bordered pitting, although poor preservation prevents identification of abietinean or araucarian pitting. Some possible taxodioid cross-field pits are preserved (Figure 18d). Tangential rays are exclusively uniseriate with an average ray height of 3.95 cells and range of 1-9 cells (Figure 18e). There appears to be organic crystal deposits in the axial parenchyma in most of the specimens (Figure 18f). Due to poor preservation, MPM-07 can only be confidently identified as Gymnosperm. Putative family assignments may be Podocarpacacea, Cupressaceae or Cephalotaxaceae based on the presence of diffuse axial parenchyma (Richter et al. 2004). The type of cross-field pitting in the specimen suggests that the wood may belong to *Taxodioxylon*.

MPM-19

Growth rings are distinct with a thick latewood zone (Figure 19a, b). False rings are present and are only a few cells thick (Figure 19a). Axial parenchyma is diffuse in both the earlywood and the latewood (Figure 19b). The end walls of the parenchyma are smooth. The tracheid radial walls contain bordered pitting, although poor preservation prevents identification of abietinean or araucarian pitting (Figure 19c, d). Cross-field pits cannot be confidently identified to any particular type (Figure 19d). Tangential rays are exclusively uniseriate with an average ray height of 3.76 cells (standard deviation 1.76) and range of 1-11 (Figure 19e, f). Due to poor preservation, MPM-19 can only be confidently identified as Gymnosperm indet. Putative family assignments may be

Podocarpacacea, Cupressaceae or Cephalotaxaceae based on the presence of diffuse axial parenchyma (Richter et al. 2004)

MPM-22

Growth rings are distinct with particular zones of thick latewood banding (Figure 20a, b). Smaller latewood rings occur between the thick latewood banding (Figure 20a). Axial parenchyma is abundant and diffuse in both latewood and earlywood (Figure 20b). They are commonly filled with material including possible organic crystals (Figure 20c). The axial parenchyma have smooth end walls (Figure 20c). Due to poor preservation, only a few bordered pits on the radial wall of the tracheids can be identified. Only a few cross-field pits are preserved and they look to be taxodioid (Figure 20 e, f). Tangential rays appear to be uniseriate with the mean ray height of 3.85 cells (based on 20 rays; standard deviation 1.84) (Figure 20g). Due to poor preservation, Specimen 22 can only be confidently identified as Gymnosperm indet. Putative family assignments may be Podocarpacacea, Cupressaceae or Cephalotaxaceae based on the presence of diffuse axial parenchyma (Richter et al. 2004).

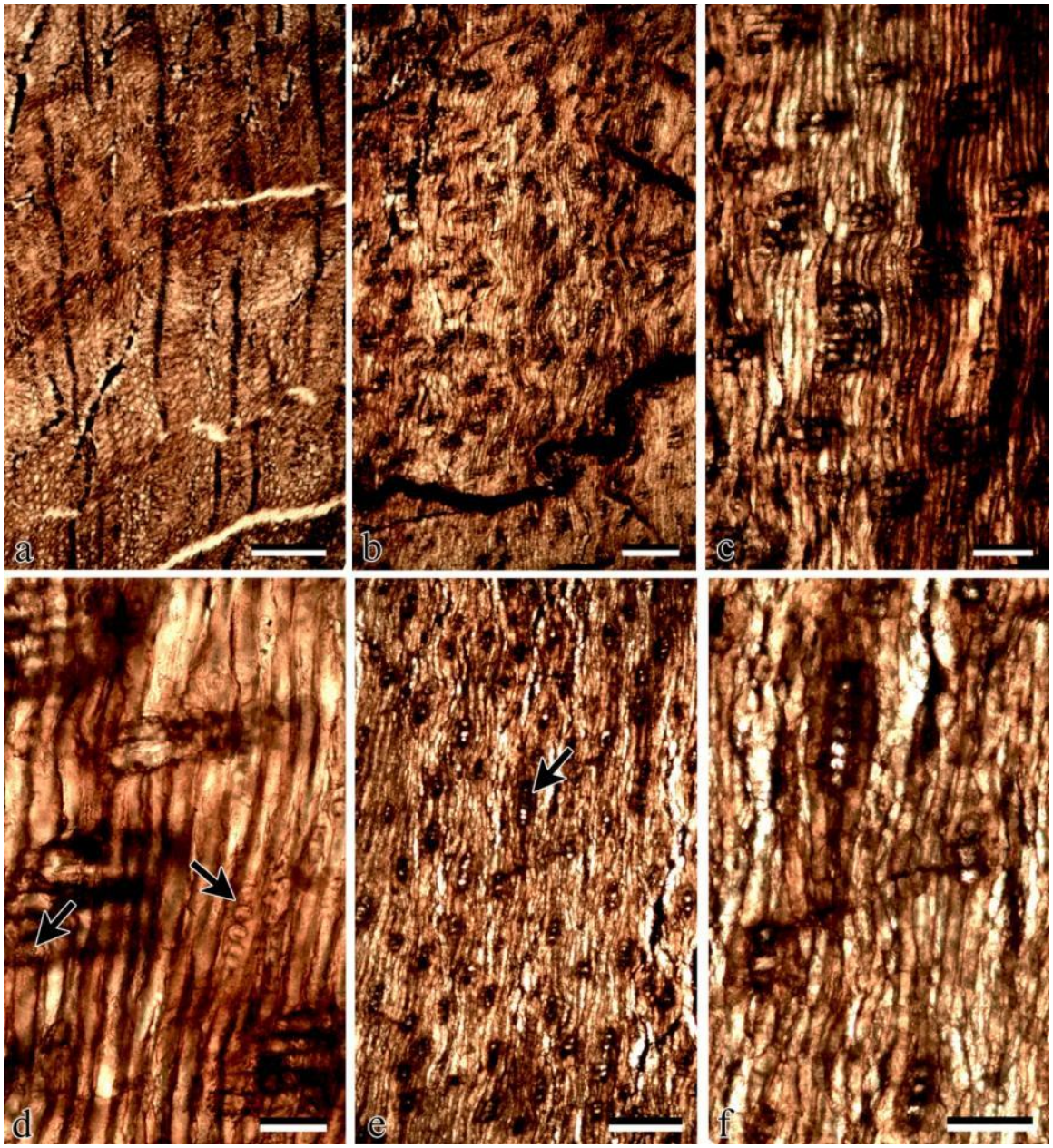

Figure A.1. Agathoxylon sp. MPM-8. a. TS showing growth rings, scale bar = 250 µm. b. RLS showing araucarian bordered pitting on the tracheids, scale bar = 250 µm. c. RLS showing araucarioid tracheid uniseriate bordered pits, scale bar = 100 µm. d. RLS showing araucarioid cross-field pits (left arrow) and araucarian bordered pitting (right arrow), scale bar = 50 µm. e, f. TLS showing short, uniseriate rays (arrow), scale bars = 100 µm (e) and 50 µm (f).

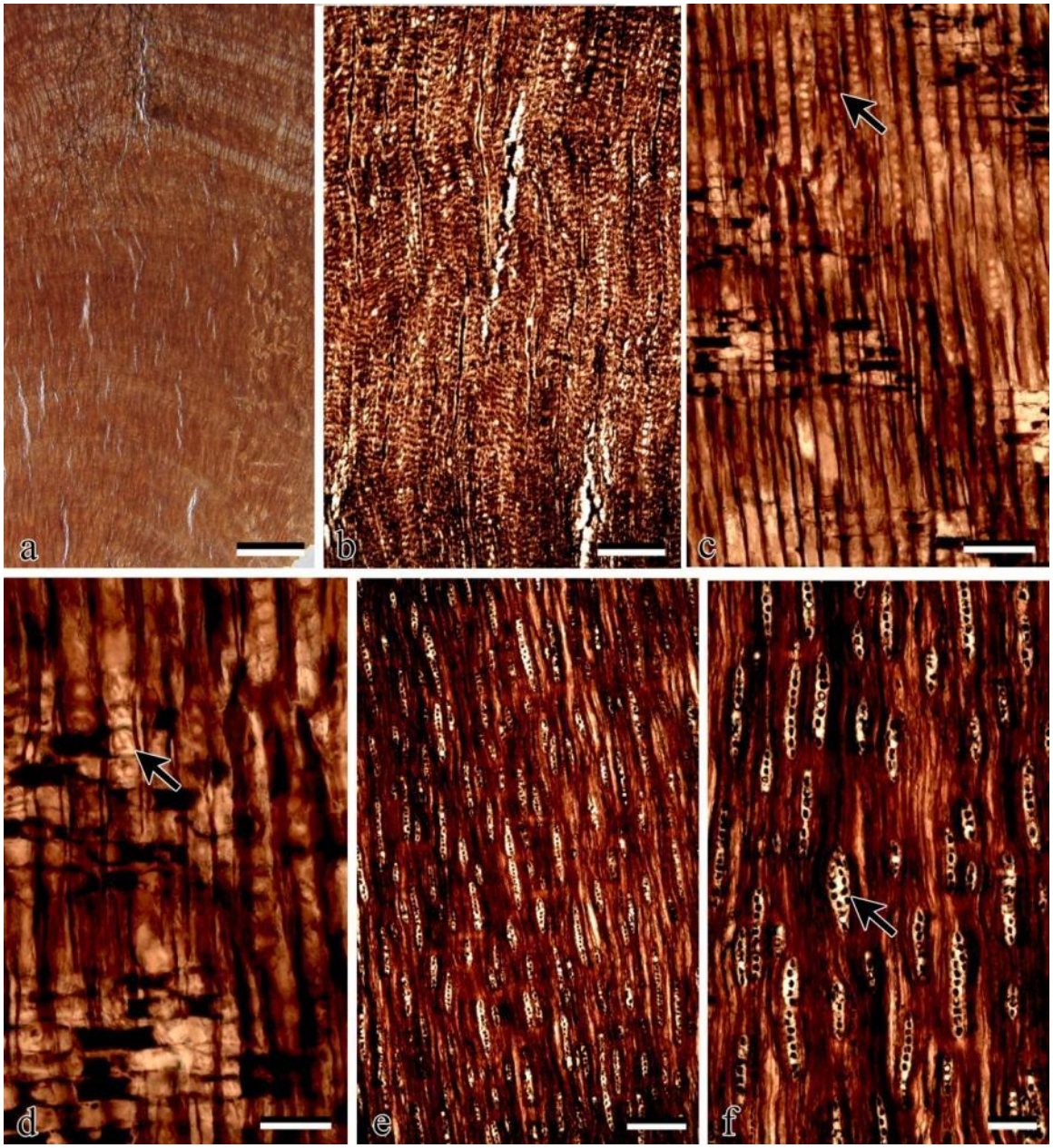

Figure A.2. *Agathoxylon* sp. MPM-21. a. TS showing growth rings, scales bar = 2.5 mm. b. TS showing growth rings and tracheids, scale bar = 250 µm (b). c. RLS showing uniseriate bordered pits on the radial walls of the tracheids (arrow), scale bar = 100 µm. d. RLS showing araucarioid cross-field pits (arrow), scale bar = 50 µm. e. TLS showing uniseriate and biseriate rays, scale bar = 250 µm. f. TLS showing uniseriate and biseriate rays (arrow), scale bar = 100 µm.

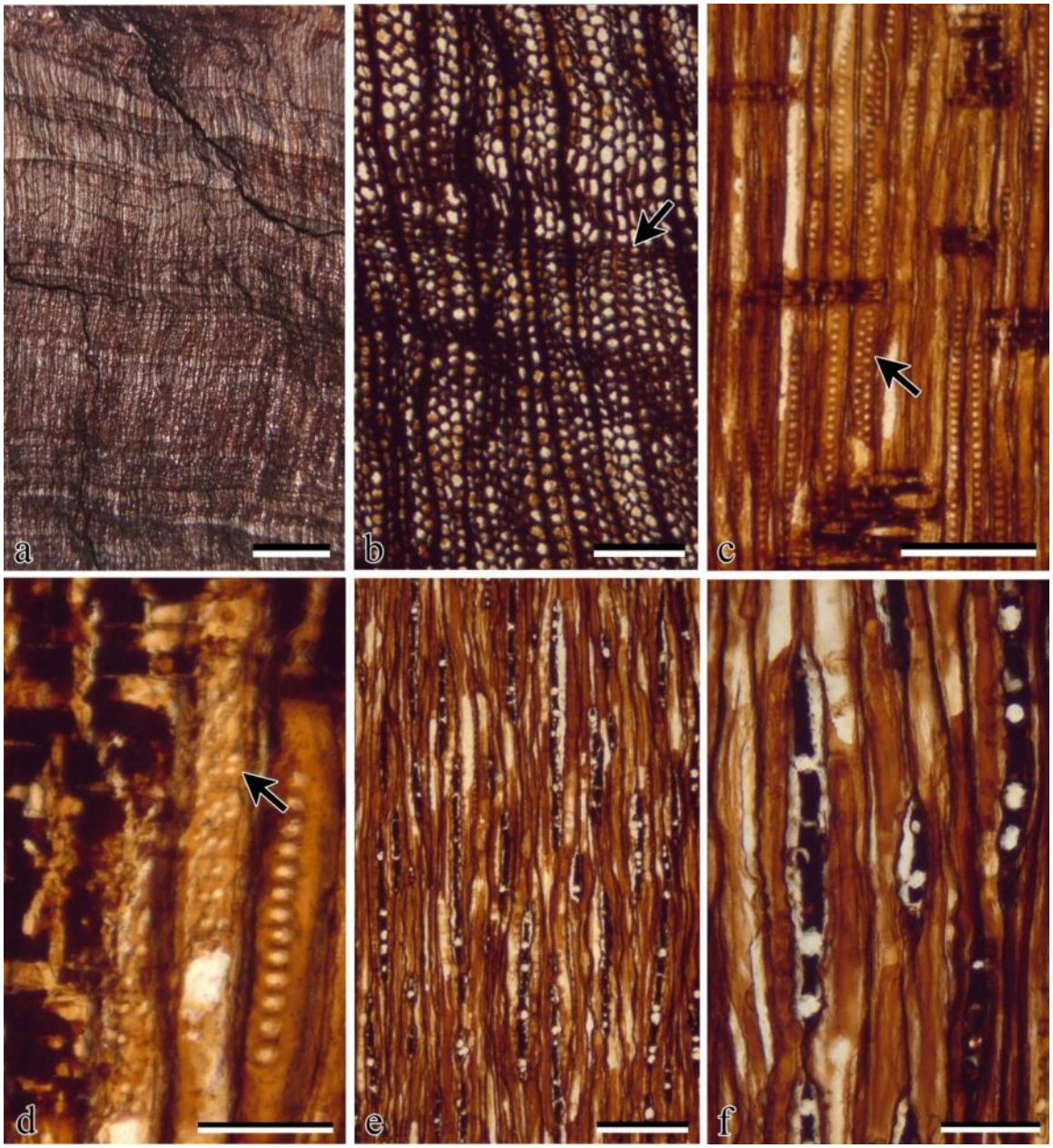

Figure A.3. *Agathoxylon* sp. MPM-23. a. TS showing growth rings, scale bar = 2.5 mm. b. TS showing false rings (arrow), scale bar = 250 µm. c. RLS showing araucarian uniseriate and alternate biseriate pitting (arrow), scale bar = 250 µm. d. RLS showing araucarioid cross-field pits (arrow), scale bar = 100 µm. e, f. TLS showing tangential rays, scale bars = 250 µm (e) and 100 µm (f).

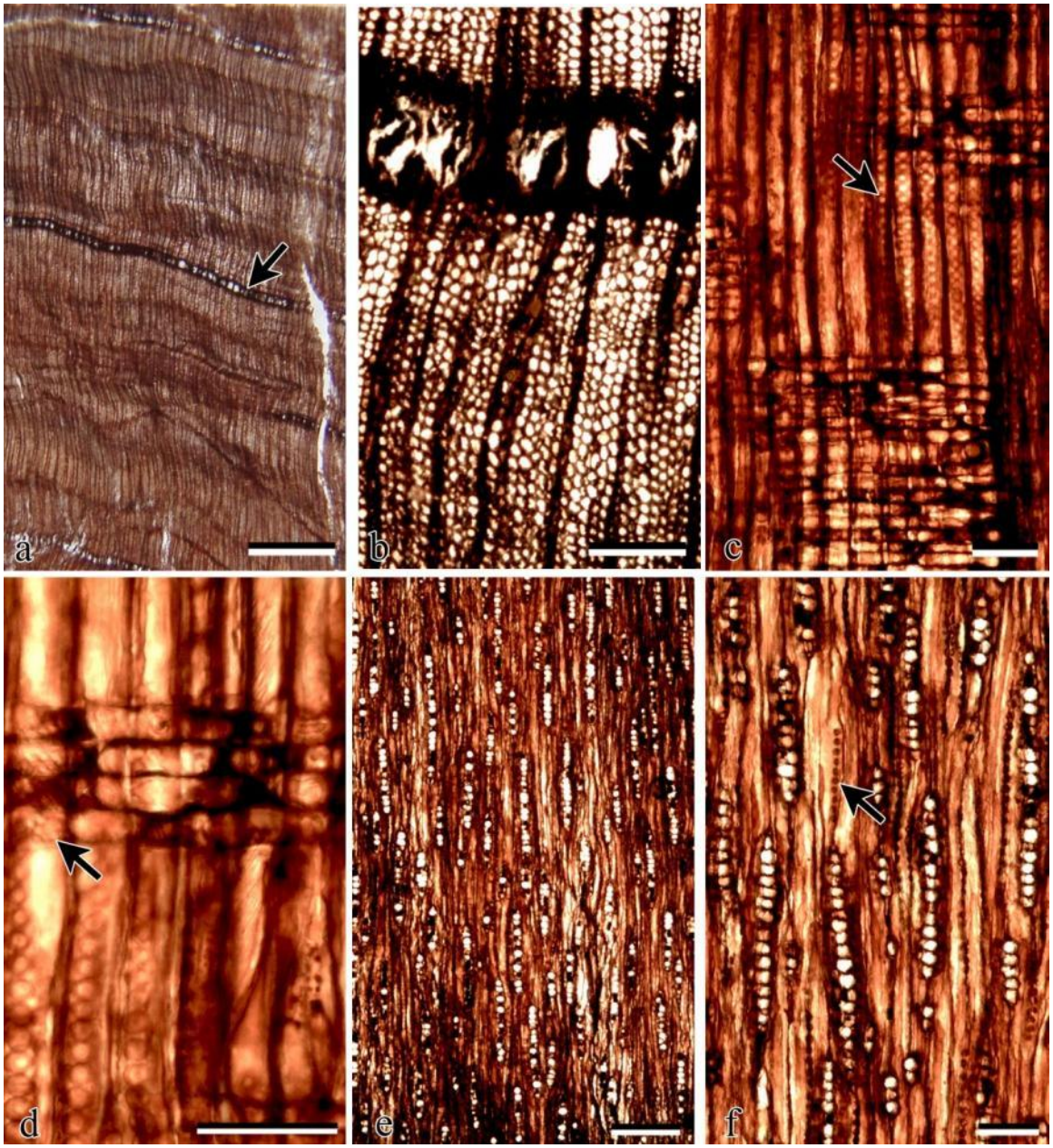

Figure A.4. *Agathoxylon* sp. MPM-32. a. TS showing growth rings and frost rings (arrow), scale bar = 2.5 mm. b. TS showing growth rings and frost ring, scale bar = 250 µm. c. RLS with uniseriate (arrow) and biseriate alternate pitting on the tracheid walls, scale bar = 100 µm. d. RLS with the arrow pointing to araucarioid cross-field pitting, scale bar = 100 µm. e. TLS showing predominantly uniseriate rays, scale bar = 250 µm. f. TLS showing uniseriate rays and pitting on tangential wall of some tracheids, scale bar = 100 µm.

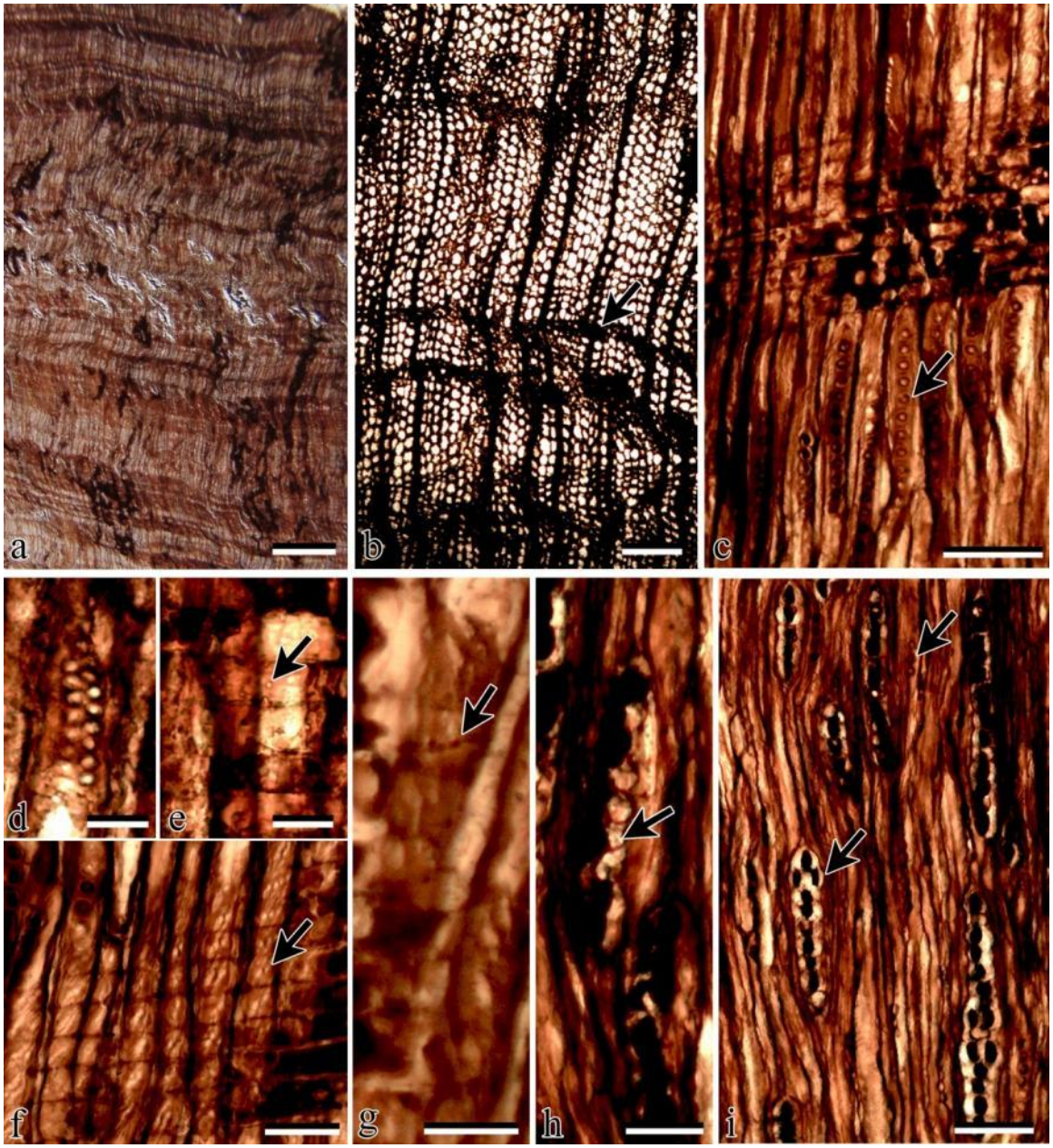

Figure A.5. *Planoxylon* sp. MPM-9. a. TS showing growth rings, scale bar = 2.5 mm. b. TS showing growth rings and false rings (arrow), scale bar = 250 µm. c. RLS showing rays and uniseriate bordered pitting (arrow), scale bar = 100 µm. d. RLS showing rare, alternate biseriate tracheid pitting, scale bar = 50 µm. e. RLS showing rounded (piceoid) cross-field pitting (arrow), scale bar = 25 µm. f. RLS showing obliquely angled, slit-like (cupressoid) cross-field pitting (arrow), scale bar = 50 µm. g, h. RLS and TLS showing abietineentüpfelungen (arrows) in the ray cells, scale bars = 25 µm (g) and 50 µm (h). i. TLS showing bordered pits (upper arrow) and uniseriate and biseriate (lower arrow) rays, scale bar = 100 µm.

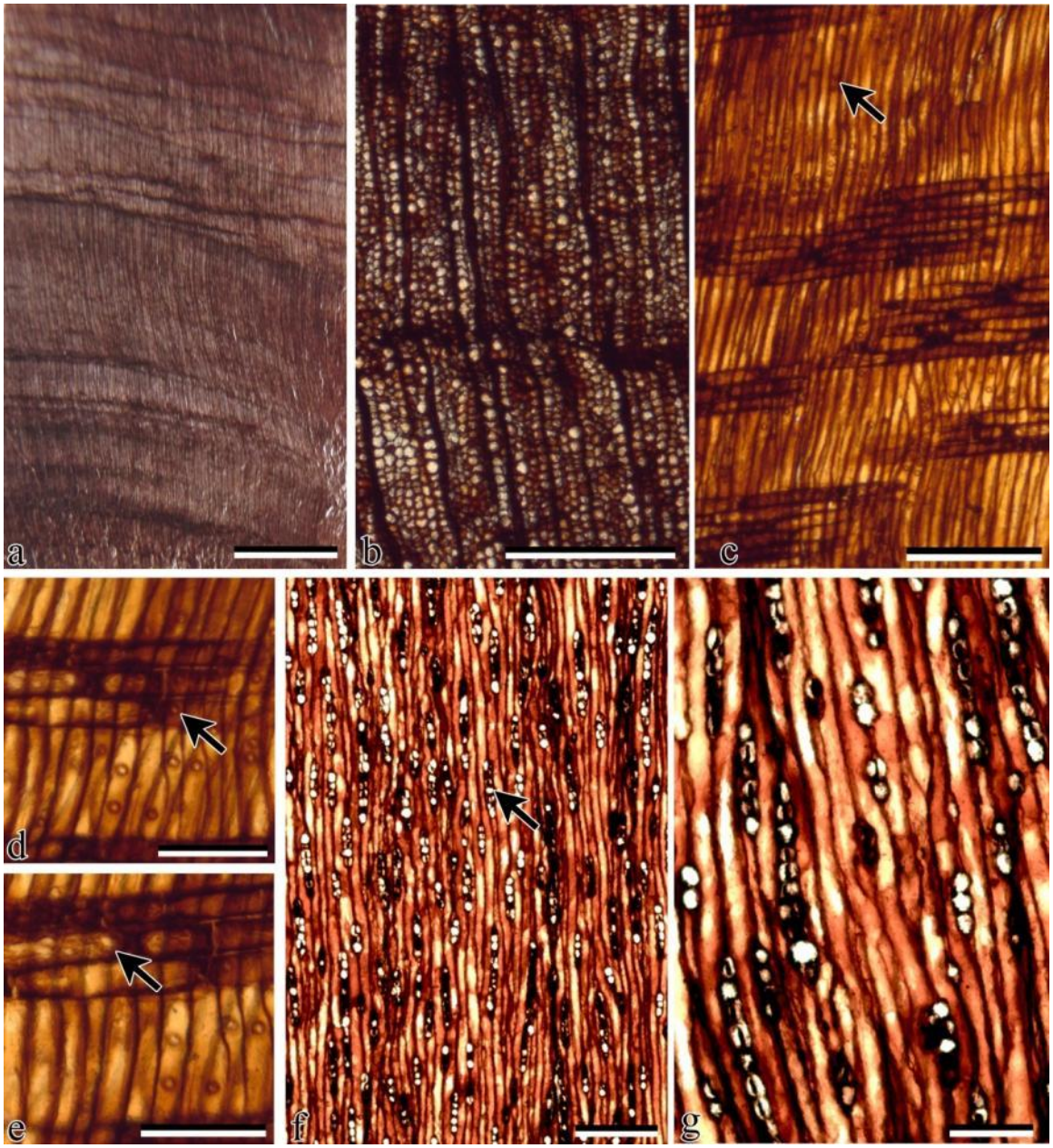

Figure A.6. *Cupressinoxylon* sp. MPM-26b. a. TS showing growth rings, scale bar = 2.5 mm. b. TS showing growth rings, scale bar = 500 µm. c. RLS showing abietinean pitting and rays, scale bar = 250 µm. d, e. RLS showing cupressoid cross-field pits (arrow), scale bar = 100 µm. f. TLS showing uniseriate rays (arrow), scale bar = 250 µm. g. TLS showing uniseriate rays, scale bar = 100 µm.

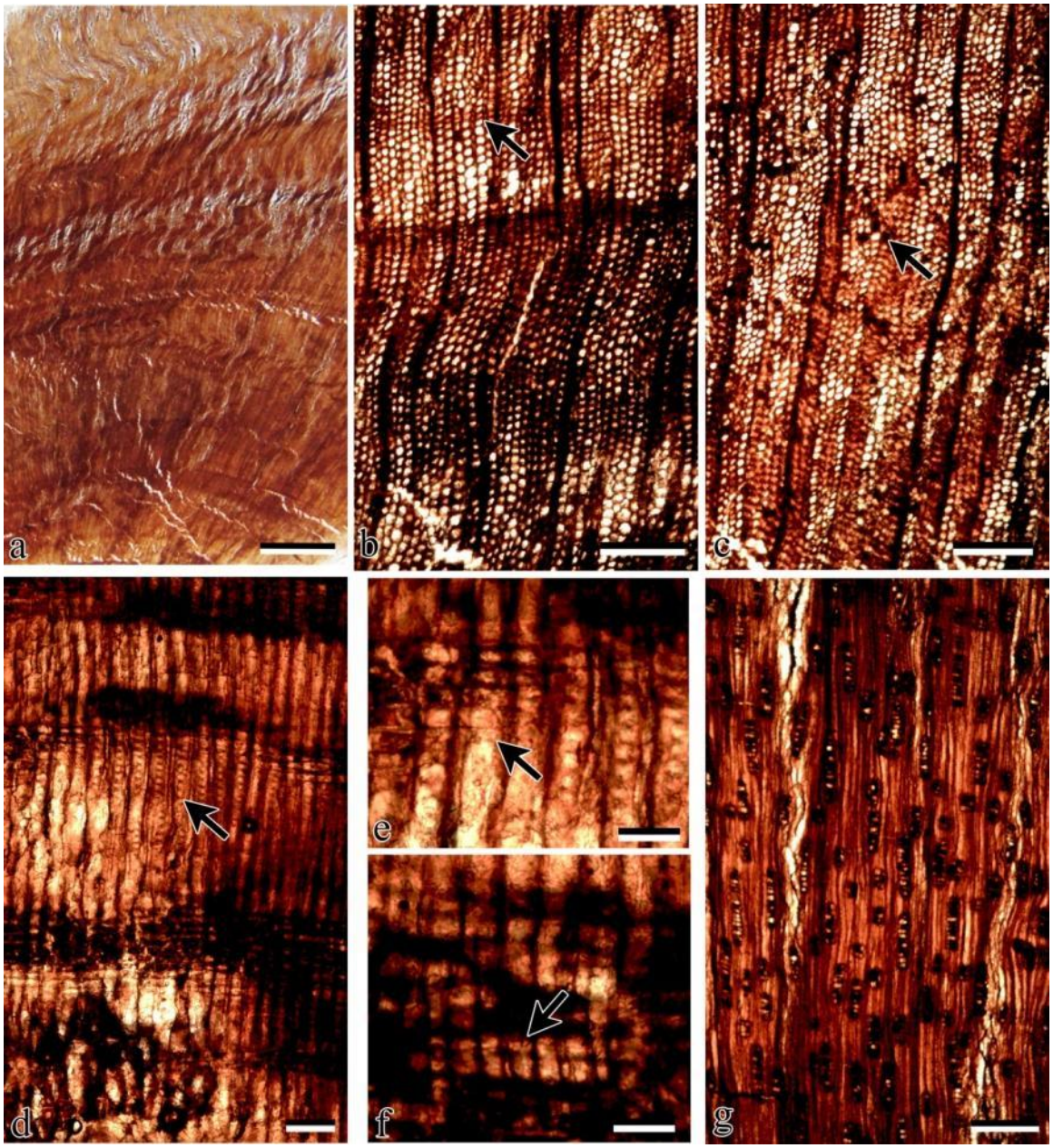

Figure A.7. Taxodioxylon sp. 1. MPM-10. a. TS showing growth rings, scale bar = 2.5 mm. b. TS showing growth rings and possible false ring, scale bar = 250 µm. c. TS showing diffuse axial parenchyma (arrow) in earlywood, scale bar = 250 µm. d. RLS showing bordered pitting of the tracheid wall (arrow) and rays, scale bar = 100 µm. e, f. RLS showing taxodioid-cupressoid cross-field pitting (arrow), scale bars = 50 µm. g. TLS showing uniseriate rays, scale bar = 250 µm.

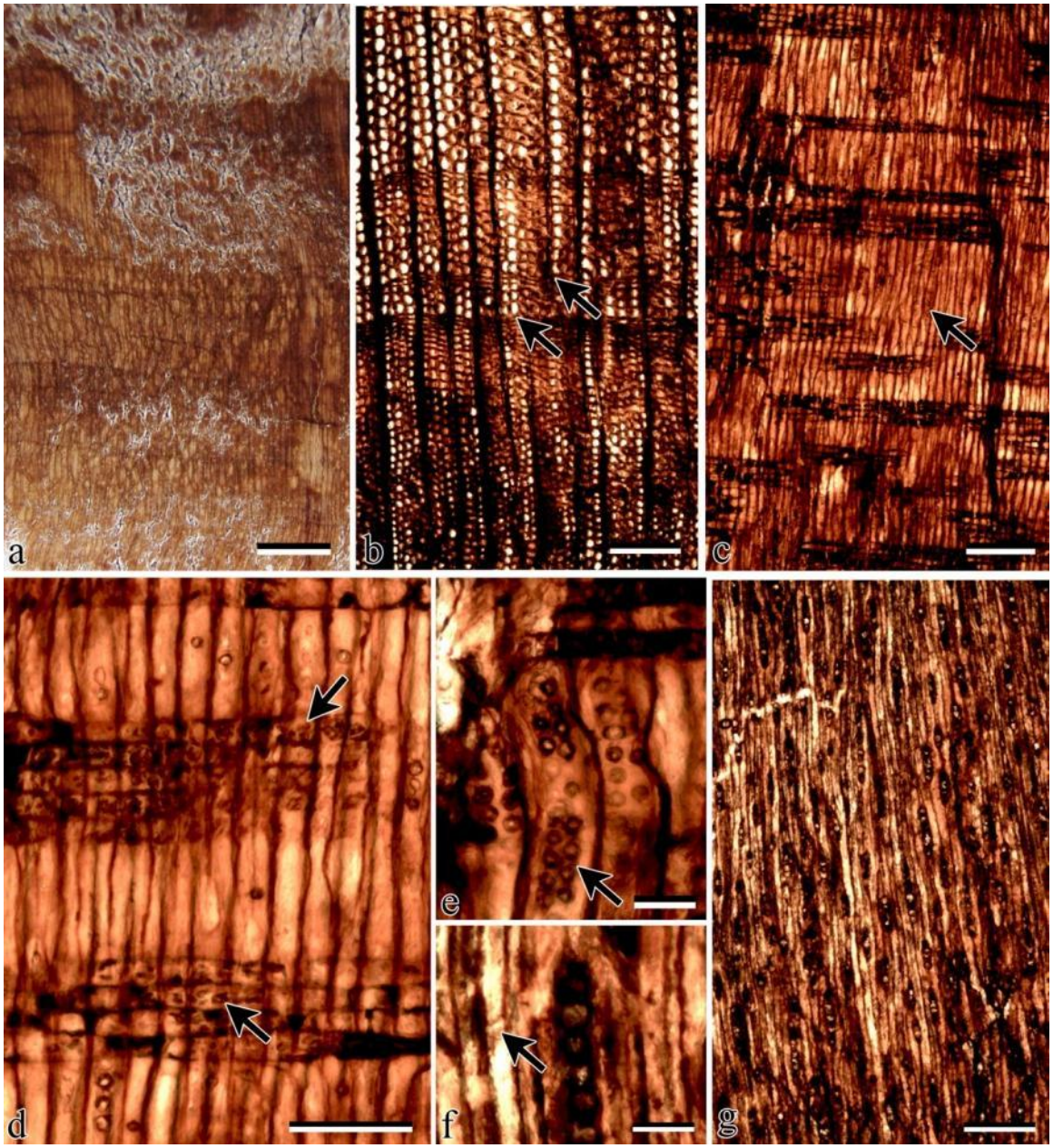

Figure A.8. *Taxodioxylon* sp. 1. MPM-15. a. TS showing growth rings, scale bar = 2.5 mm. b. TS showing growth rings (lower arrow) and false ring (upper arrow), scale bar = 250 µm. c. RLS showing abietinean pitting (arrow) and rays, scale bar = 250 µm. d. RLS showing small, obliquely angled taxodioid cross-field pits (arrow), scale bar = 100 µm. e. RLS showing alternate and opposite biseriate bordered pitting, scale bar = 50 µm. f. TLS showing pitting on an axial parenchyma (arrow), scale bar = 50 µm. g. TLS showing uniseriate tangential rays, scale bar = 250 µm.

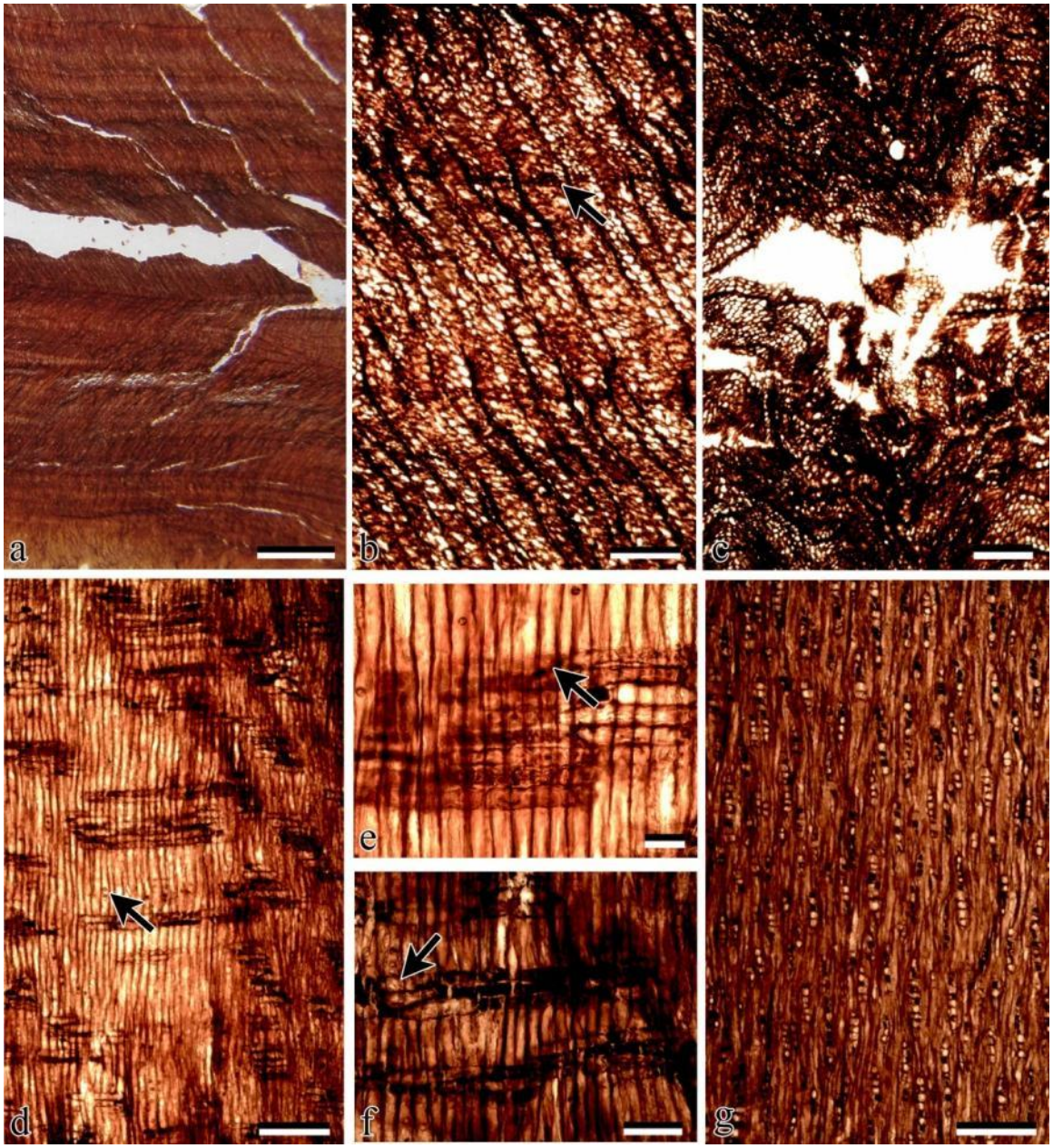

Figure A.9. *Taxodioxylon* sp. 1. MPM-16. a. TS showing growth rings, scale bar = 2.5 mm. b. TS showing growth rings (arrow), scale bar = 250 µm. c. TS showing wound wood (?), scale bar = 250 µm. d. RLS showing abietinean bordered pitting (arrow) on the tracheid walls, scale bar = 250 µm. e, f. RLS showing cross-field pitting (arrow), scale bars = 50 µm (e) and 100 µm (f). g. TLS showing uniseriate tangential rays, scale bar = 250 µm.

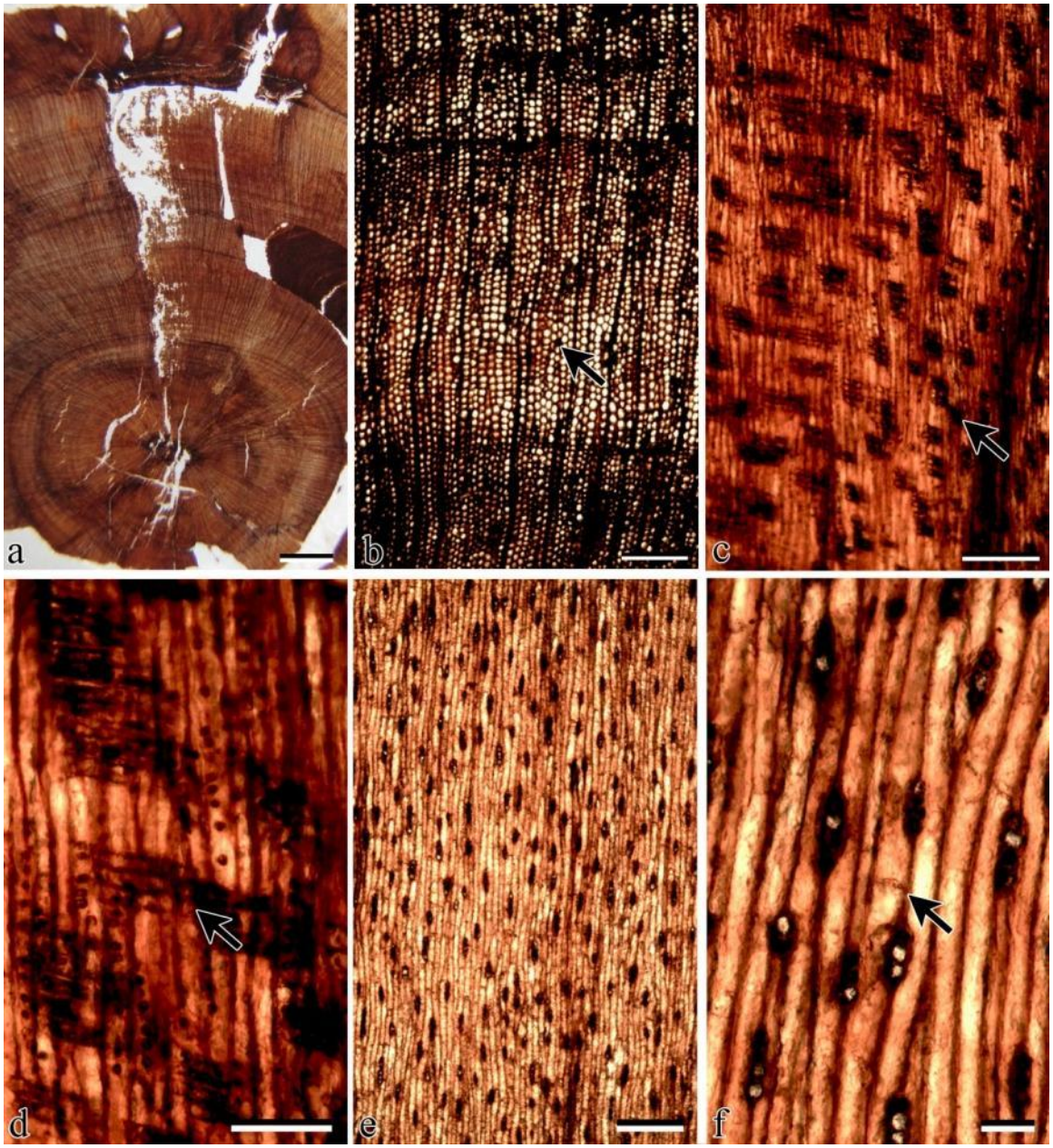

Figure A.10. *Taxodioxylon* sp. 1. MPM-18. a. TS showing pith and growth rings, scale bar = 2.5 mm. b. TS showing growth rings, false ring, and diffuse axial parenchyma (arrow), scale bar = 250 µm. c. RLS showing rays (arrow), scale bar = 250 µm. d. RLS showing cross-fields with taxodioid cross-field pits (arrow), scale bar = 100 µm. e. TLS showing short rays, scale bar = 250 µm. f. TLS showing beading on the end walls of the axial parenchyma (arrow), scale bar = 50 µm.

Figure A.11. *Taxodioxylon* sp. 2. MPM-11b. a. TS showing growth rings, scale bar = 2.5 mm. b. TS showing growth rings (arrow), scale bar = 250 µm. c. RLS showing abietinean pitting (arrow) and rays, scale bar = 250 µm. d. RLS showing possible xenoxylon bordered pitting on the tracheid walls (arrow), scale bar = 50 µm. e. TLS showing beading on the end walls of the axial parenchyma (arrow), scale bar = 25 µm. f. RLS showing small, obliquely angled taxodioid cross-field pits (arrows), scale bar = 50 µm. g. TLS showing tangential uniseriate rays, scale bar = 250 µm. h. TLS showing uniseriate and biseriate (arrow) tangential rays, scale bar = 100 µm.

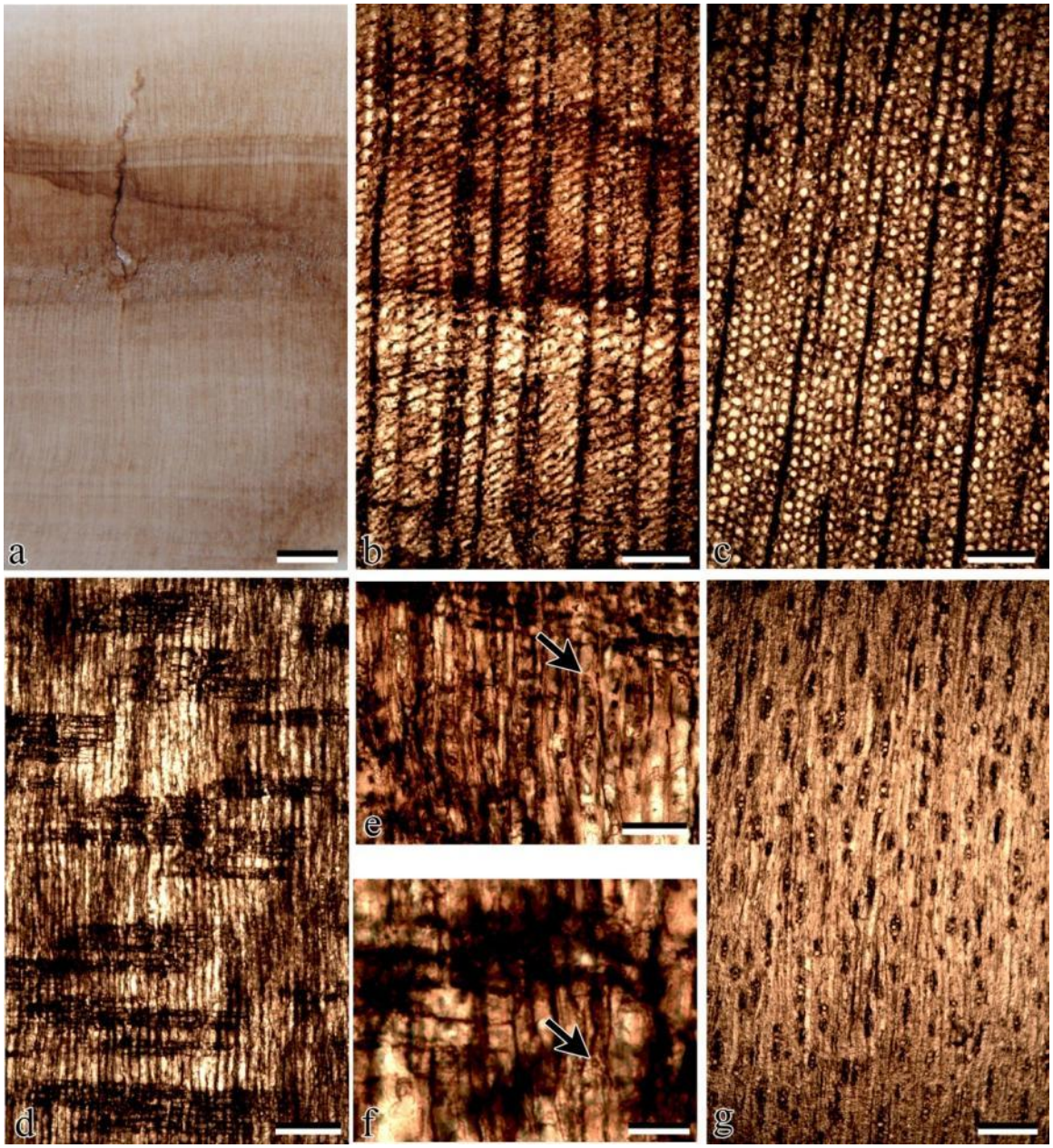

Figure A.12. *Podocarpoxylon* sp. MPM-6. a. TS showing growth rings, scale bar = 2.5 mm. b. TS showing growth ring, scale bar = 250 µm. c. TS showing axial parenchyma, scale bar = 250 µm. d. RLS showing rays and tracheid bordered pitting, scale bar = 250 µm. e. RLS showing uniseriate abietinean pitting on the tracheid walls (arrow), scale bar = 100 µm. f. RLS showing podocarpoid cross-field pits (arrow), scale bar = 50 µm. g. TLS showing uniseriate rays, scale bar = 250 µm.

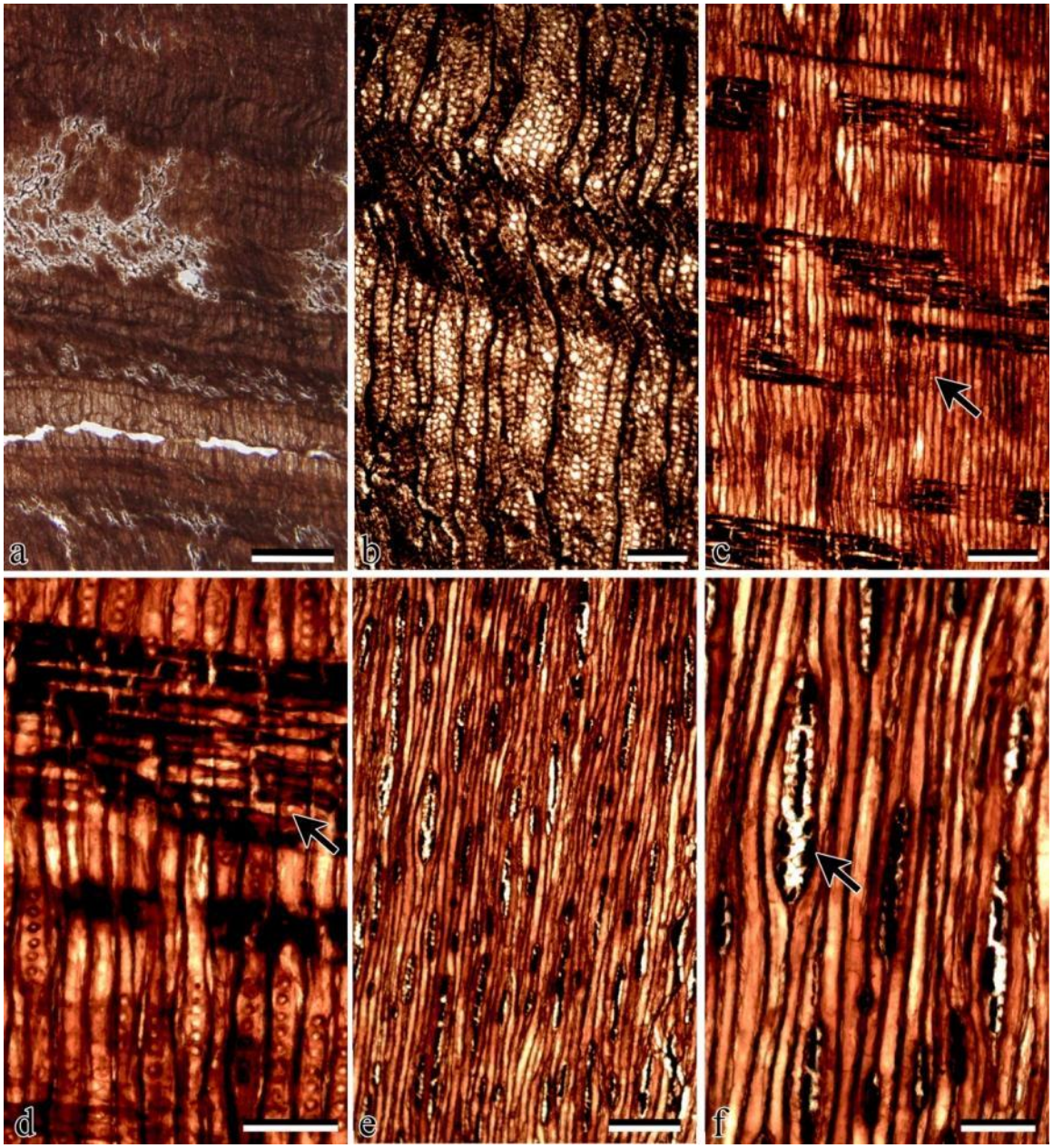

Figure A.13. *Podocarpoxylon* sp. MPM-11a. a. TS showing growth rings, scale bar = 2.5mm. b. TS showing growth rings and axial parenchyma, scale bar = 250 µm. c. RLS showing abietinean bordered pitting (arrow) and rays, scale bar = 250 µm. d. RLS showing podocarpoid-cupressoid cross-field pits (arrow), scale bar = 100 µm. e. TLS showing uniseriate rays, scale bar = 250 µm. f. TLS showing a biseriate ray (arrow), scale bar = 100 µm.

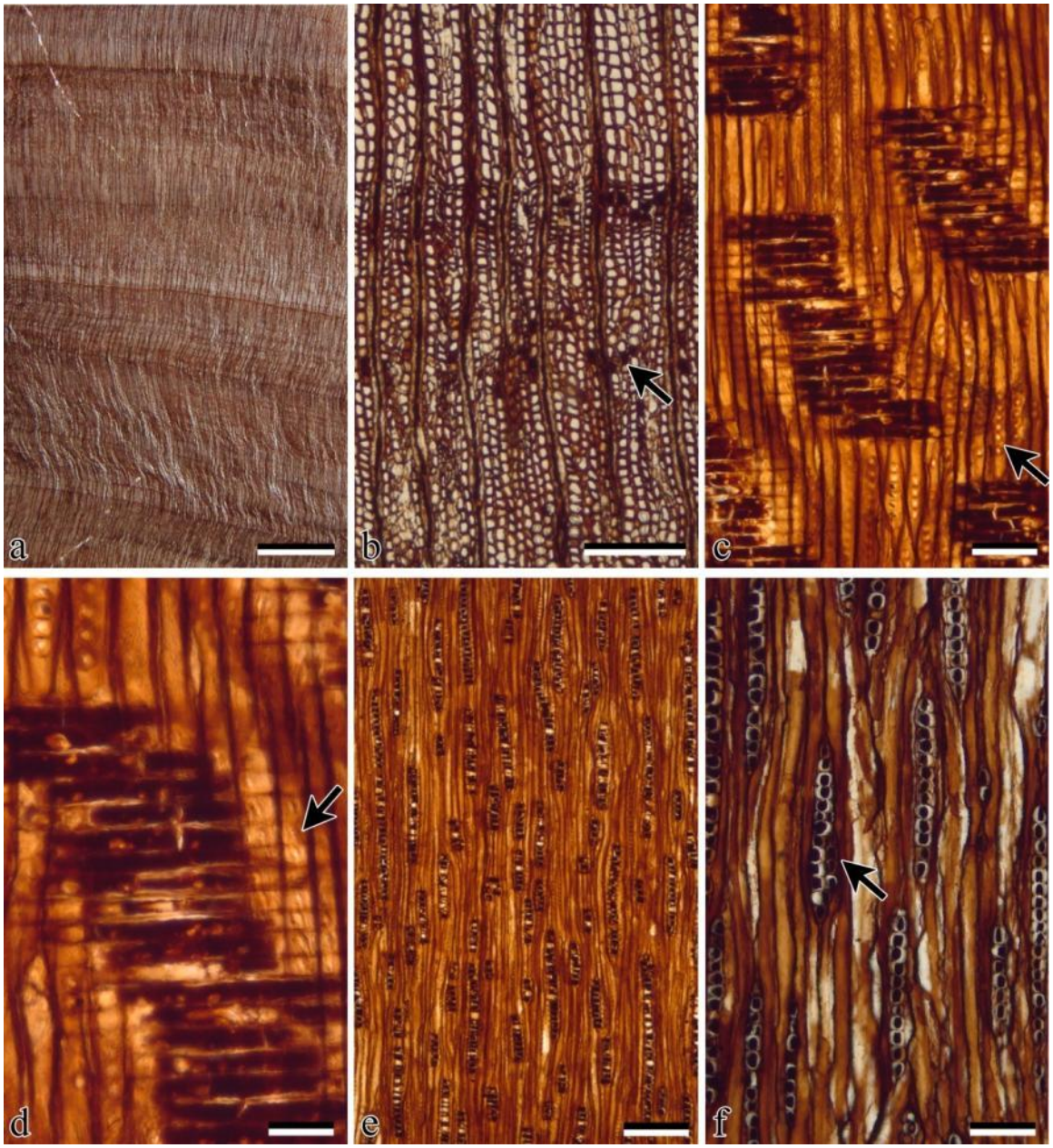

Figure A.14. *Podocarpoxylon* sp. MPM-25. a. TS showing growth rings, scale bar = 2.5 mm. b. TS showing a growth ring and axial parenchyma (arrow), scale bar = 250 µm. c. RLS showing abietinean pitting (arrow) on the radial wall of the tracheids, scale bar = 200 µm. d. RLS showing narrow slit-like podocarpoid cross-field pitting (arrow), scale bar = 100 µm. e. TLS showing uniseriate rays, scale bar = 250 µm. f. TLS showing uniseriate rays, scale bar = 100 µm.

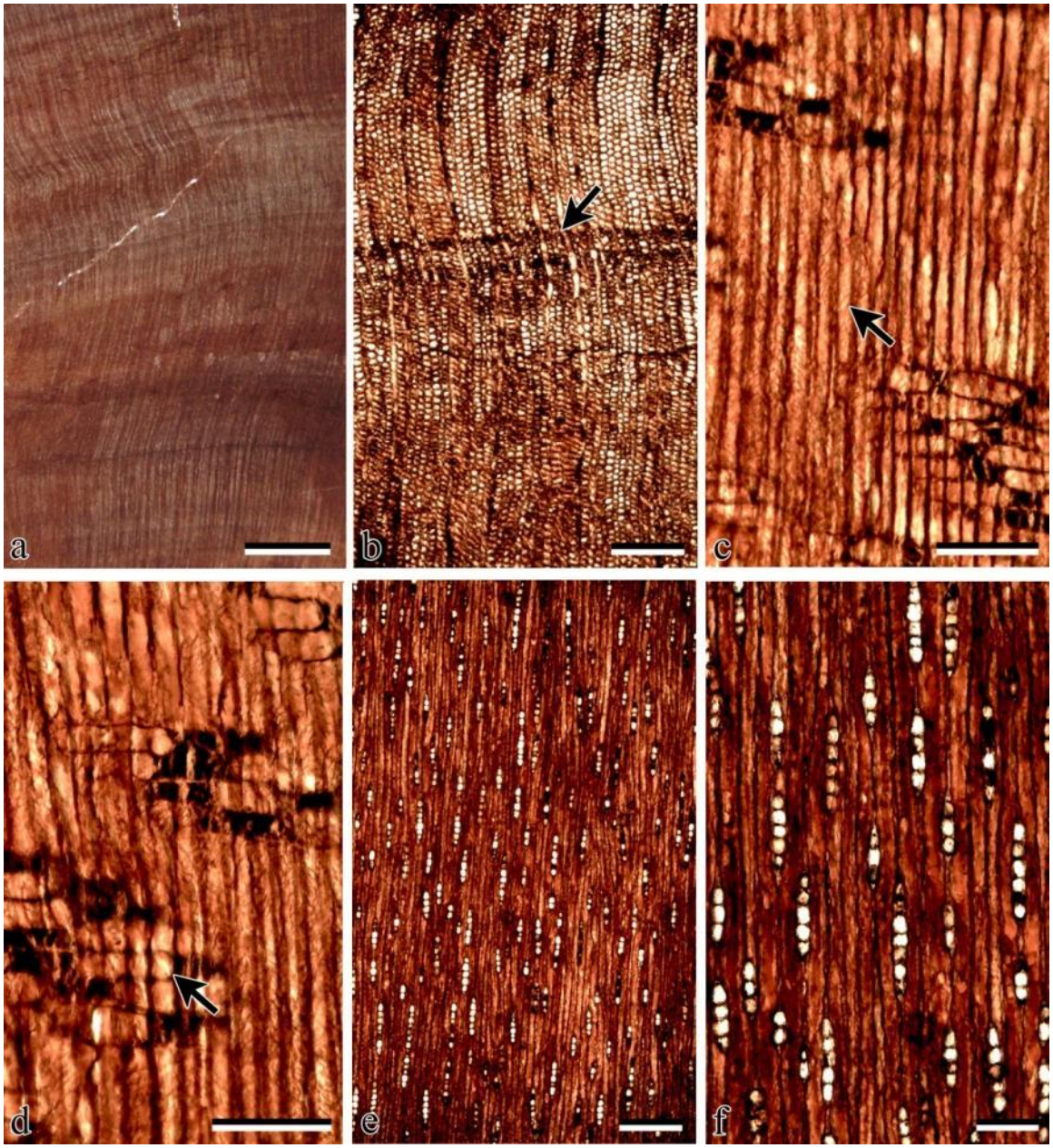

Figure A.15. *Podocarpoxylon* sp. MPM-30. a. TS showing growth rings, scale bar = 2.5 mm. b. TS showing a false ring just after a true growth ring (arrow), scale bar = 250 µm. c. RLS showing spiral checking (arrow) in the tracheid walls, scale bar = 100 µm. d. RLS showing abietinean pitting and silt-like podocarpoid cross-field pitting (arrow), scale bar = 100 µm. e, f. TLS showing tangential rays, scale bar = 250 µm (e) and 100 µm (f).

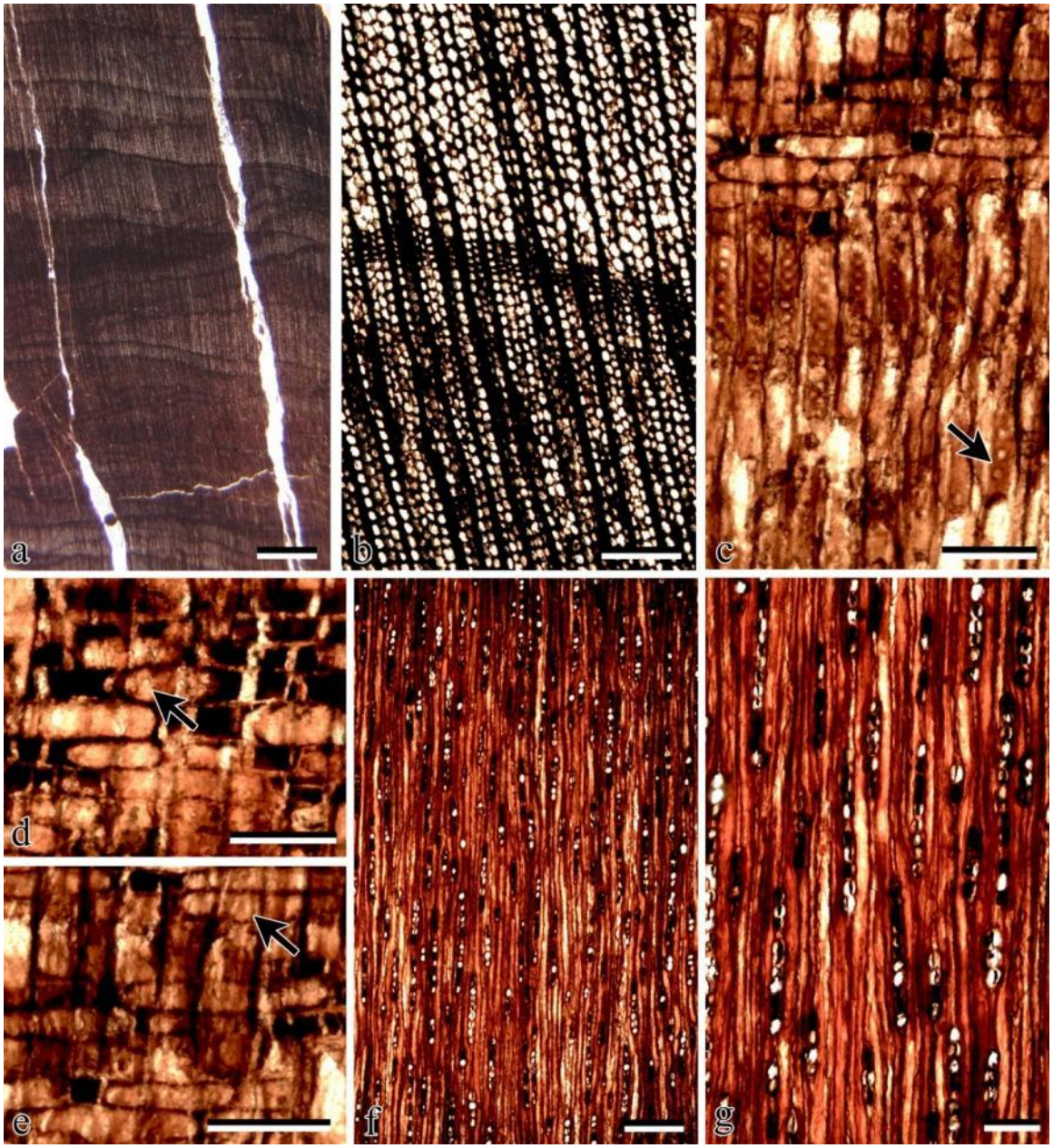

Figure A.16. *Podocarpoxylon* sp. MPM-31. a. TS showing growth ring, scale bar = 2.5 mm. b. TS showing growth ring (arrow), scale bar = 250 µm. c. RLS showing abietinean uniseriate pitting on the tracheids (arrow), scale bar = 100 µm. d, e. RLS showing podocarpoid cross-field pitting (arrows), scale bars = 100 µm. f, g. TLS showing uniseriate rays, scale bars = 250 µm (f) and 100 µm (g).

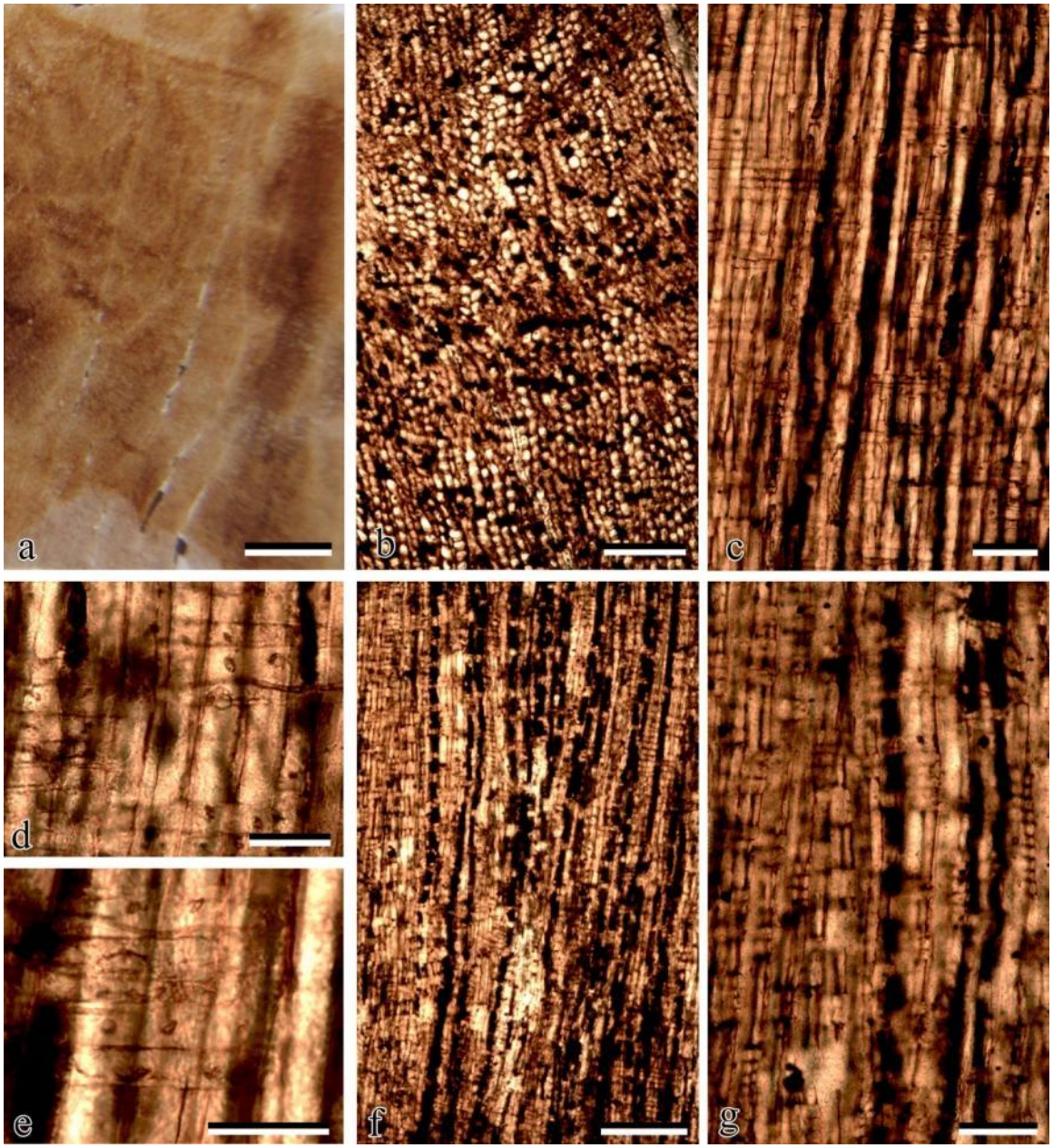

Figure A.17. Gymnosperm indet. MPM-1. a. TS showing growth rings, scale bar = 2.5mm. b. TS showing diffuse axial parenchyma, scale bar = 250 µm. c. RLS showing rays, scale bar = 100 µm. d, e. RLS showing taxodioid cross-field pits, scale bars = 50 µm. f., g. TLS showing short, uniseriate rays, scale bars = 100 µm (f) and 50 µm (g).

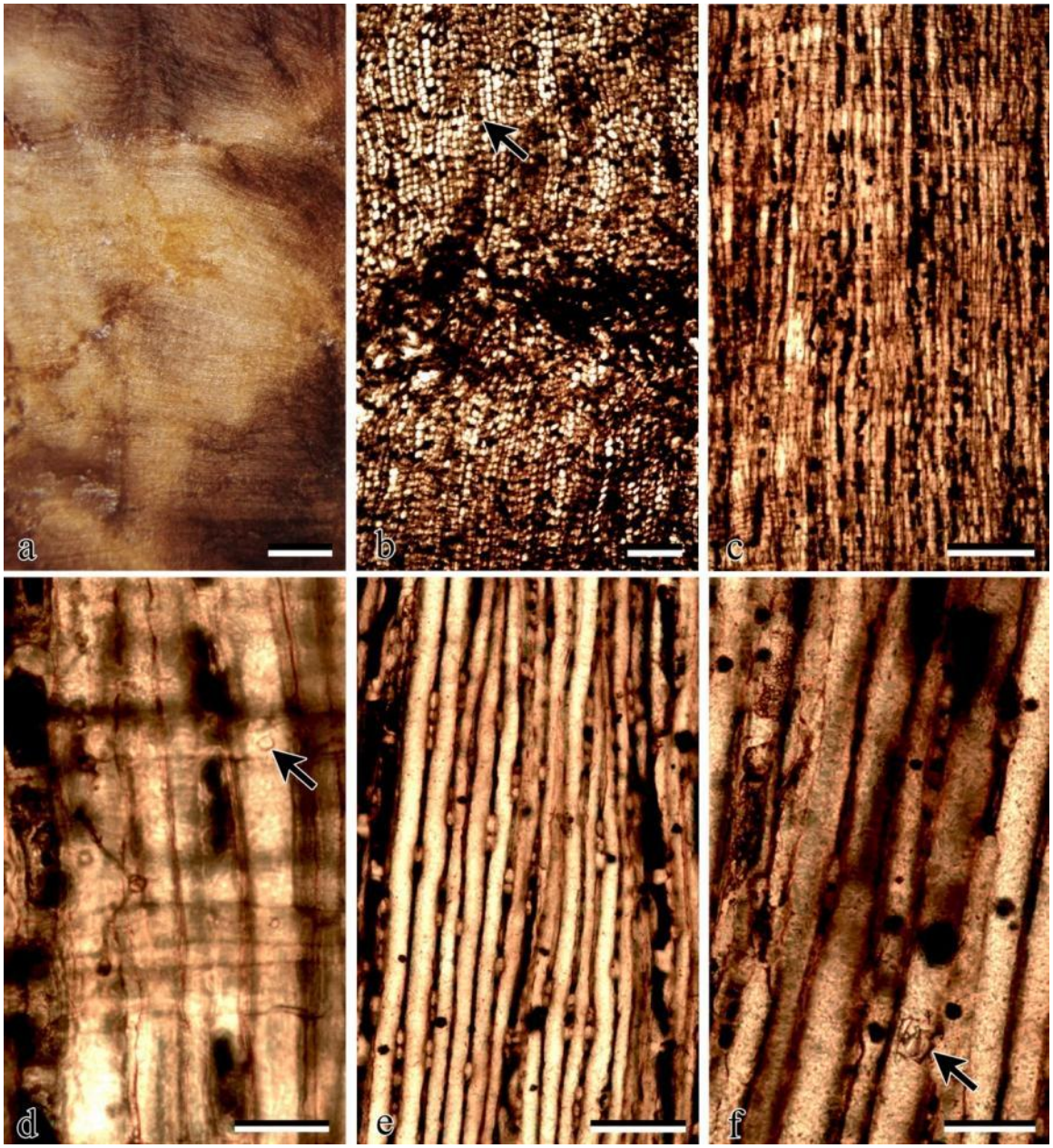

Figure A.18. Gymnosperm indet. MPM-7. a. TS showing growth rings, scale bar = 2.5 mm. b. TS showing growth ring and diffuse axial parenchyma, scale bar = 250 µm. c. RLS showing rays, scale bar = 250 µm. d. RLS showing rays and taxodioid cross-field pits (arrow), scale bar = 50 µm. e. TLS showing short tangential rays, scale bar = 100 µm. f. TLS showing possible organic crystal deposit, scale bar = 25 µm.

Figure A.19. Gymnosperm indet. MPM-19. a. TS showing growth rings, scale bar = 2.5 mm. b. TS showing growth rings and diffuse axial parenchyma (arrow), scale bar = 250 µm. c. RLS showing rays and possible cross-field pits, scale bar = 250 µm. d. RLS showing rays and possible cross-field pits (arrow), scale bar = 50 µm. e. TLS showing tangential rays, scale bar = 250 µm. f. TLS showing axial parenchyma and rays, scale bar = 100 µm.

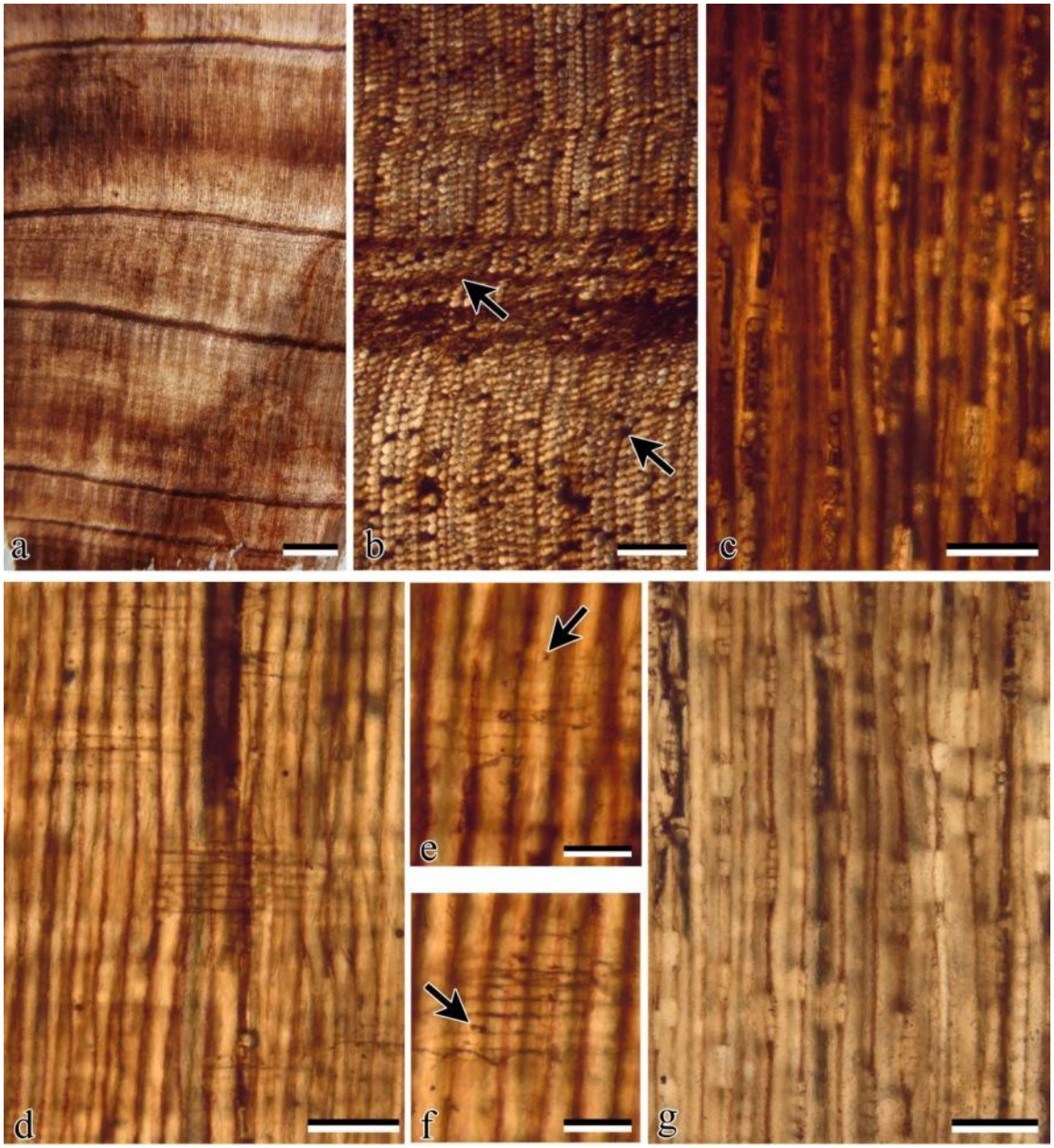

Figure A.20. Gymnosperm indet. MPM-22. a. TS showing growth rings, scale bar = 2.5mm. b. TS showing growth rings including false rings (upper arrow) and diffuse axial parenchyma (lower arrow), scale bar = 250 µm. c. TLS showing axial parenchyma with smooth end walls, scale bar = 100 µm. d. RLS showing rays, scale bar = 100 µm. e, f. RLS showing possible taxodioid cross-field pits, scale bars = 50 µm. g. TLS showing short, uniseriate rays, scale bar = 100 µm.

APPENDIX B: FOSSIL ANGIOSPERM WOOD SAMPLE DESCRIPTIONS AND PLATES

Hedycaryoxylon sp. A sp. nov.

MPM-13 (holotype)

MPM-13 have been broken from permineralized logs that are at least a half meter in diameter. Growth rings are weakly distinct and can be distinguished based upon fiber diameter (Figure B.1a, b). The growth rings in MPM-13 can only be distinguished in the hand sample. The vessels are diffuse porous and are randomly arranged to loosely radially arranged (Figure B.1a, b). They have a circular to oval outline and occur predominantly as solitary vessels, but occasionally occur as paired and rarely in radial multiples or in clusters (3vessels per grouping). Vessel walls are thin compared to fibers and parenchyma. The mean tangential diameter of the vessel lumina is 78.16 µm with a range of 21-71 µm. The average number of vessels per square millimeter is 25.30 vessels with a range of 19-32 vessels. Perforation plates are scalariform with between 15-32 bars per plate (Figure B.1c). Vessel-ray pitting consists of simple, horizontal (scalariform) pits (Figure B.1d, e). Intervessel pitting is scalariform (Figure B.1f). Helical thickenings in vessel elements are absent. Tyloses are common. Ground tissue fibers contain distinct bordered pits that can be seen in both radial and tangential longitudinal section (Figure B.1g). Both septate and nonseptate fibers occur in the specimen (Figure B.1f). Fiber walls are thin to thick. Axial parenchyma is diffuse and is occasionally paratracheal, occurring either above and/or below a vessel. Rays are predominantly multiseriate with a

mean width of 4.36 cells (range, 2-8 cells) with the majority of the rays being 3 or 4 cells wide (Figure B.1h). Uniseriate rays are extremely rare. The mean ray height is 1.14 mm with a range of 0.47-2.17 mm. The mean number of rays per millimeter is 14.80 rays with a range of 12-16 rays. Ray cells are procumbent (centrally located in the ray), square and upright (toward the margins of the ray). Larger sheath cells predominantly occur at the ends of the rays and often extend the rays an additional 0.25-0.5 mm (Figure B.1h,i).

MPM-12

Growth rings are distinct with thick-walled latewood fibers and tracheids (Figure B.2a,b). Thinner-walled early wood appears to have been crushed resulting in distortion of the earlywood (Figure B.2b). The wood is diffuse porous (Figure B.2a). Vessels are predominantly solitary, occasionally paired, and rarely grouped (3-5 vessel) (Figure B.2b). The mean tangential diameter of vessels is 54 µm with a range of 25-90 µm (standard deviation 14.73; median 51). The average number of vessels per mm^2 is 31 with a range of 21 to 38. Tyloses rarely occur in vessels. Perforation plates are scalariform and consist of 12 to +20 fine bars per plate (average 18 in complete plates) (Figure B.2c). Intervessel pits are predominately scalariform but a few opposite pits are present (Figure B.2e). Intervessel pit diameter is between 25µm and 35µm. Vessel-ray pitting consists of simple pits that are oval (horizontal) to scalariform pits (Figure B.2d). Helical thickenings are absent. Ground tissue fibers rarely contain simple, distinct, minute pits that can be seen in tangential longitudinal section (Figure B.2f). Septate fibers are present

and have thin to thick walls (Figure B.2g). Axial parenchyma are rare. In tangential section, rays are greater than 1 mm long (mean 0.98 mm, range 0.51-1.43 mm) and are multiseriate with 4-9 cells at the widest point of the rays (Figure B.2h). There are 8.10 (range 6-10) rays per mm when measured perpendicular to the ray axis. Rays consist of centrally located procumbent cells and marginal square and upright cells (Figure B.2i).

MPM-20

Growth ring boundaries are distinct with thickened tracheids and less vessels in the latewood (Figure B.3a, b). Vessels are the approximately the same size in both the earlywood and latewood (diffuse porous); however, the frequency of vessels is higher in the earlywood (Figure B.3b). Vessels are round to oval (where not deformed) and are predominately solitary and rarely occur in pairs (Figure B.3b). The mean tangential diameter of the vessels is 69.84 (standard deviation 12.37, median 33) with a range of 18-72. The number of vessels per square millimeter averages 30.60 (standard deviation 7.03, median 30) with a range of 26-47. Tyloses are rare. Perforation plates are scalariform with between 20 and 31 bars per plate(Figure B.3c). Intervessel pitting is scalariform to opposite (Figure B.3d). Vessel-ray pits are simple, horizontal (scalariform) with reduced borders (Figure B.3e). Helical thickenings are absent. Fiber walls are thin to thick and contain abundant bordered pitting that can been seen predominately in radial longitudinal section and only rarely in tangential longitudinal section (Figure B.3c). Septate fibers are present (Figure B.3f). Axial parenchyma are absent. The average ray width is 4.28 cells (standard deviation 0.97, median 4) with a

range of 3-6 cells (Figure B.3f, g). Ray length averages 1077.2 µm (standard deviation 395.59 µm, median 1007 µm) with a range of 463-1728 µm (Figure B.3g). The number of rays per millimeter averages 14.3 (standard deviation 1.16, median 14) with a range of 13-16. Ray parenchyma consists of centrally located procumbent cells and marginally located square/ upright cells (Figure B.3h).

MPM-24

Growth ring boundaries are distinct; primarily due to crushing of vessels and fibers (Figure B.4 a, b). MPM-24 appears to be diffuse porous (Figure B.4b, c). Vessels are predominately solitary; however, they do occur in small clusters of 2-7 (2-3 being most common) (Figure B.4c). Vessel walls are thin and tyloses in the vessel are common (Figure B.4 b). The mean tangential diameter of the vessels is 90.94 µm (standard deviation 14.12 µm, median 44 µm) with a range of 21-78 µm. The number of vessels per square millimeter averages to be 51.70 vessels (standard deviation 11.05, median 54.5) with a range of 33-65 vessels. Perforation plates are scalariform with approximately 9 to 15 pits per plate (Figure B.4 d). Intervessel pits are scalariform to opposite (Figure B.4 f). Vessel ray pits are simple horizontal pits (scalariform) with a weakly defined border (Figure B.4 e). Helical thickenings are absent. Both septate and non-septate fibers are present (Figure B.4 h). Fibers are thin to thick-walled and contain minute, distinctly bordered pits (Figure B.4 g). They occasionally dissect multiseriate rays (Figure B.4 i). Axial parenchyma are rare. Rays are multiseriate with an average width of 7.08 cells (standard deviation 3.17, median 6) and a range of 4-17 cells (Figure B.4 i). The mean

ray length is 927.76 µm (standard deviation 394.09 µm, median 869 µm) with a range of 409-1594 µm. The number of rays per millimeter averages 8.1 (standard deviation 1.29, median 8) with a range of 6-10 rays. The rays are heterocellular and are composed of procumbent and square cells (Figure B.4 j).

Nothofagoxylon triseriatum

MPM-26

This sample was collected from a spoil pile at the base of an outcrop of interbedded channel sands and muds (Figure B.5). There are no other geological formations, other than the Cerro Fortaleza Formation, on the hill above where the specimen was found. It notably has ancient insect borings on it and through it (Figure B.5e). There are only a few distinct growth rings present (Figure B.5a, b). In most cases, the growth ring boundaries are relatively indistinct with minimal structural changes (i.e. vessel density and fiber thickness) except for an undulating band (Figure B.5 b). The wood is semi-ring diffuse porous to diffuse porous. The vessels are almost exclusively solitary (Figure 3.7b). The number of vessels per square millimeter averages 30.20 (standard deviation 5.09, median 29) with a range of 23-39. The vessels are oval-shaped with the long axis being radially aligned (Figure B.5b). The mean tangential diameter of the vessel is 64.16 µm (standard deviation 19.07 µm, median 61 µm) with a range of range 56-92 µm. Both simple and scalariform perforation plates are present, the latter being dominant (Figure B.5c, d). Scalariform perforation plates consist of 20-40 bars. Vessel-ray pits have simple borders with mostly rounded pits and fewer scalariform pits (Figure B.5f).

Intervessel pits are predominantly scalariform; however, opposite pits do occur (Figure B.5e). Tyloses are very common (Figure B.5b, h). Fibers are thin-walled and contain distinct bordered pits that can be seen in radial longitudinal section (Figure B.5g). Septate fibers are present. Axial parenchyma appear to be absent. Rays are primarily biseriate (average number of cells, 2.2); uniseriate and triserate rays are less common (Figure B.5h). The average height of the rays is 714.84 µm (standard deviation, 1.23 µm, median 739 µm) with a range of 337-1074 µm. The average number of rays per square millimeter is 12.20 (standard deviation, 1.23; median 12) with the range begin 11-14 rays. The cellular composition of the rays is procumbent, square and upright cells (Figure B.5i).

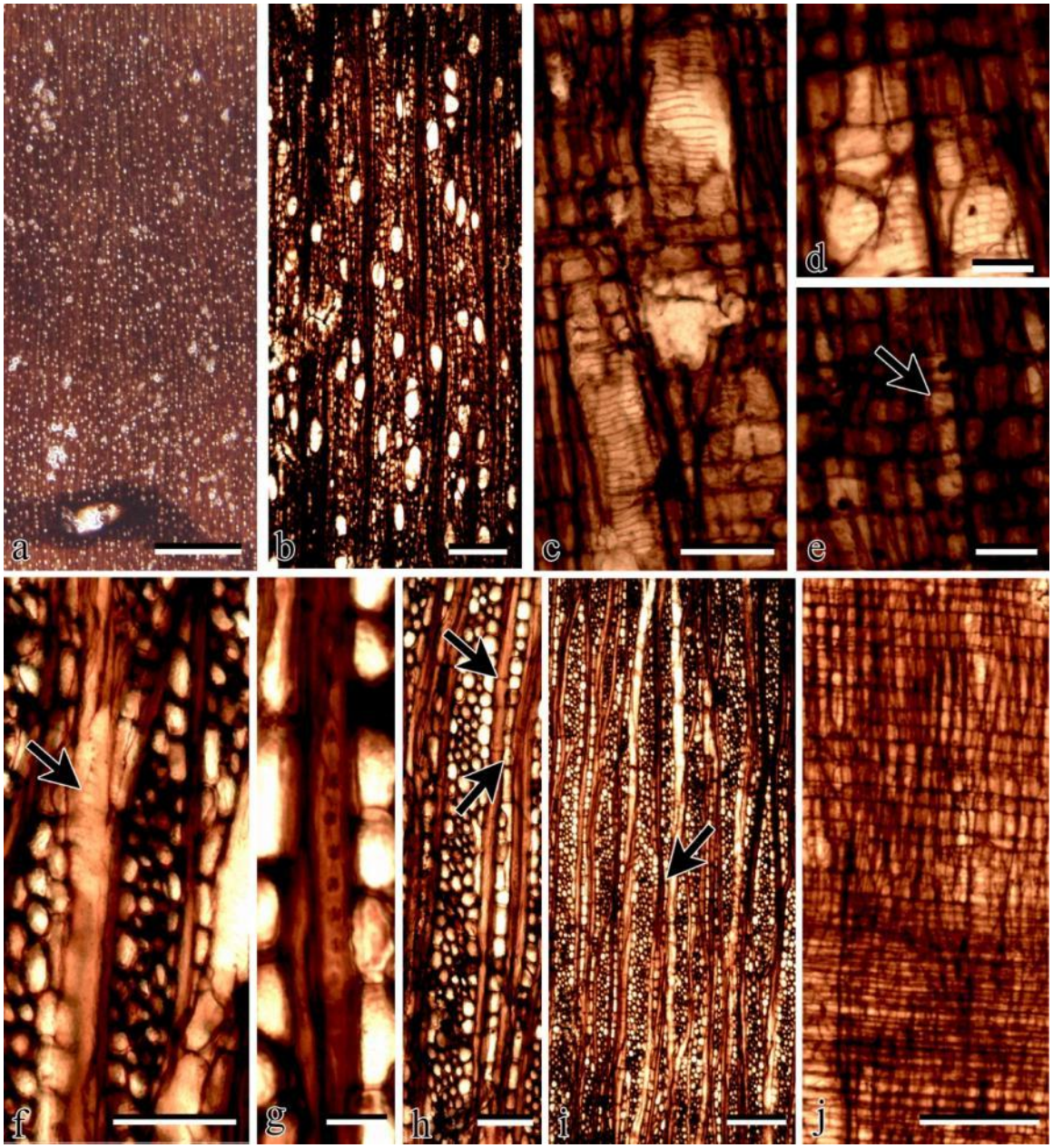

Figure B.1. *Hedycaryoxylon* sp. A. MPM-13. a. TS showing diffuse porous wood; scale bar = 2.5 mm. b. TS showing diffuse porous wood; scale bar = 250 µm. c. RLS showing scalariform perforation plates; scale bar = 100 µm. d, e. RLS showing oval to scalariform vessel-ray pits; scale bars = 50 µm. f. TLS showing scalariform intervessel pitting (arrow); scale bar = 100 µm. g. TLS showing ground fiber with minute bordered pitting; scale bar = 50 µm. h. TLS showing septate fibers (upper arrow) and sheath cell (lower arrow); scale bar = 100 µm. i. TLS showing multiseriate rays and sheath cells (arrow) scale bar = 250 µm. j. RLS showing procumbent, square and upright cells; scale bar = 250 µm.

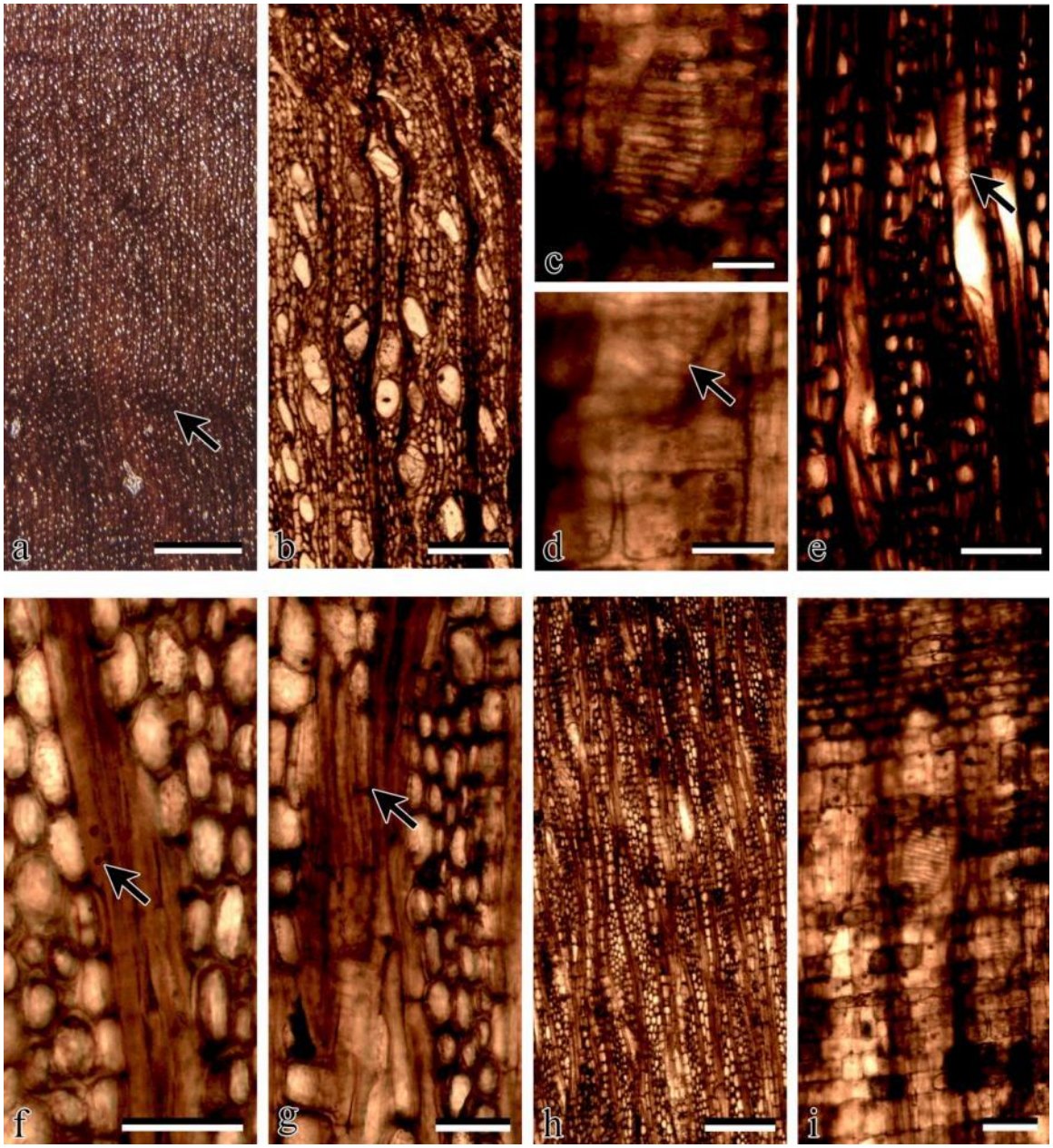

Figure B.2. *Hedycaryoxylon* sp. A. MPM-12. a. TS showing growth rings (arrow) and diffuse porous wood; scale bar = 2.5 mm. b. TS showing diffuse porous wood and crushed vessels; scale bar = 250 µm. c. RLS showing scalariform perforation plate; scale bar = 100 µm. d. RLS showing oval to scalariform vessel-ray pits (arrow); scale bar = 50 µm. e. TLS showing scalariform intervessel pitting (arrow); scale bar = 50 µm. f. TLS showing ground fiber with minute bordered pitting (arrow); scale bar = 50 µm. g. TLS showing septate fibers (arrow); scale bar = 50 µm. h. TLS showing multiseriate rays; scale bar = 250 µm. i. RLS showing rays with procumbent, square and upright cells; scale bar = 100 µm.

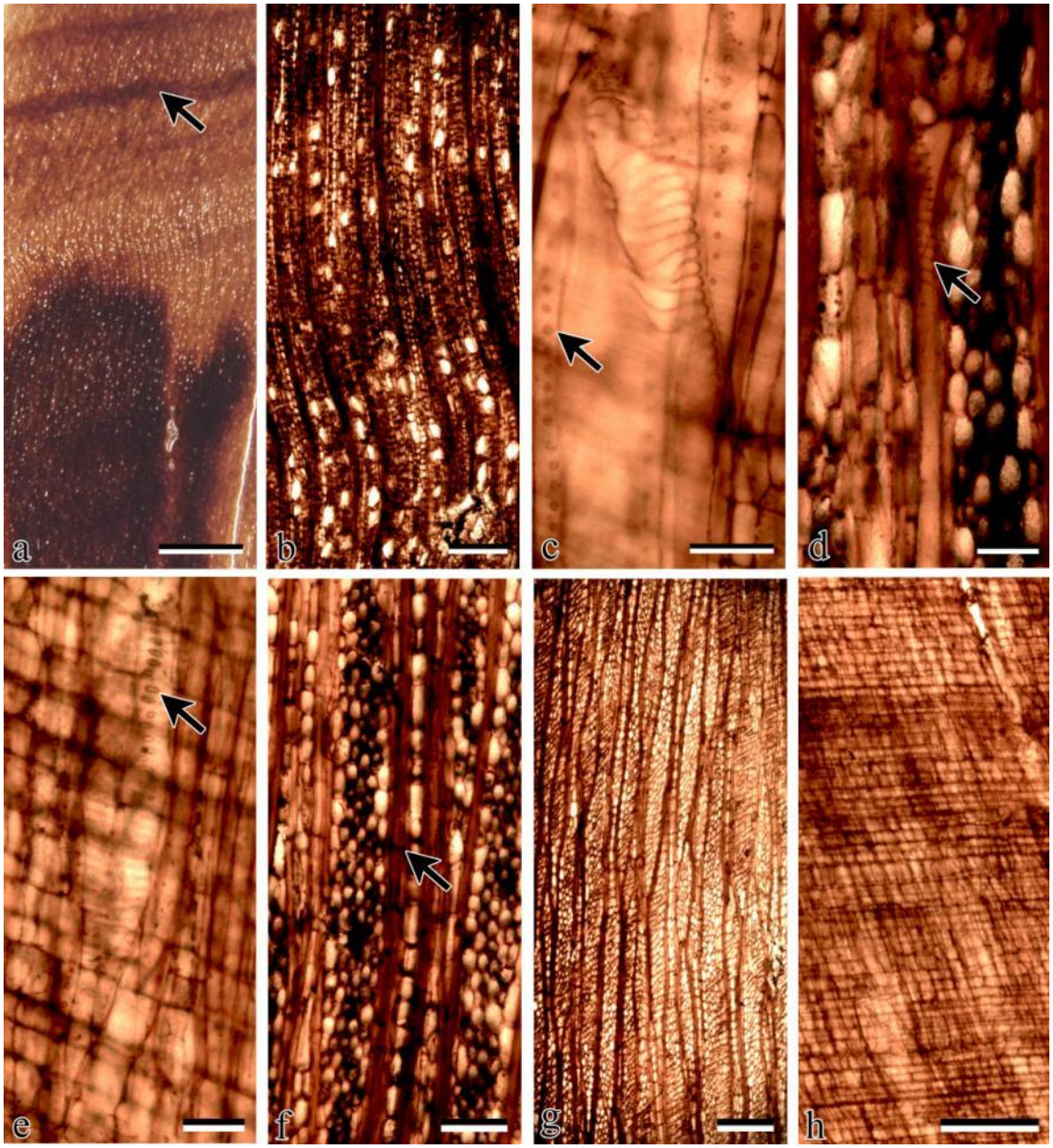

Figure B.3. *Hedycaryoxylon* sp. A. MPM-20. a. TS with growth rings (arrow); scale bar = 2.5 mm. b. TS showing diffuse porous wood, thickened fibers at growth rings, solitary and rarely paired vessels; scale bar = 250 µm. c. RLS showing scalariform perforation plate and fibers with bordered pitting (arrow), scale bar = 50 µm. d. TLS showing scalariform intervessel pitting (arrow); scale bar = 50 µm. e. RLS showing simple vessel-ray pitting; scale bar = 50 µm. f. TLS showing septate fibers (arrow); scale bar = 100 µm. g. TLS showing multiseriate rays; scale bar = 250 µm. h. RLS showing cellular composition of rays; scale bar = 250 µm.

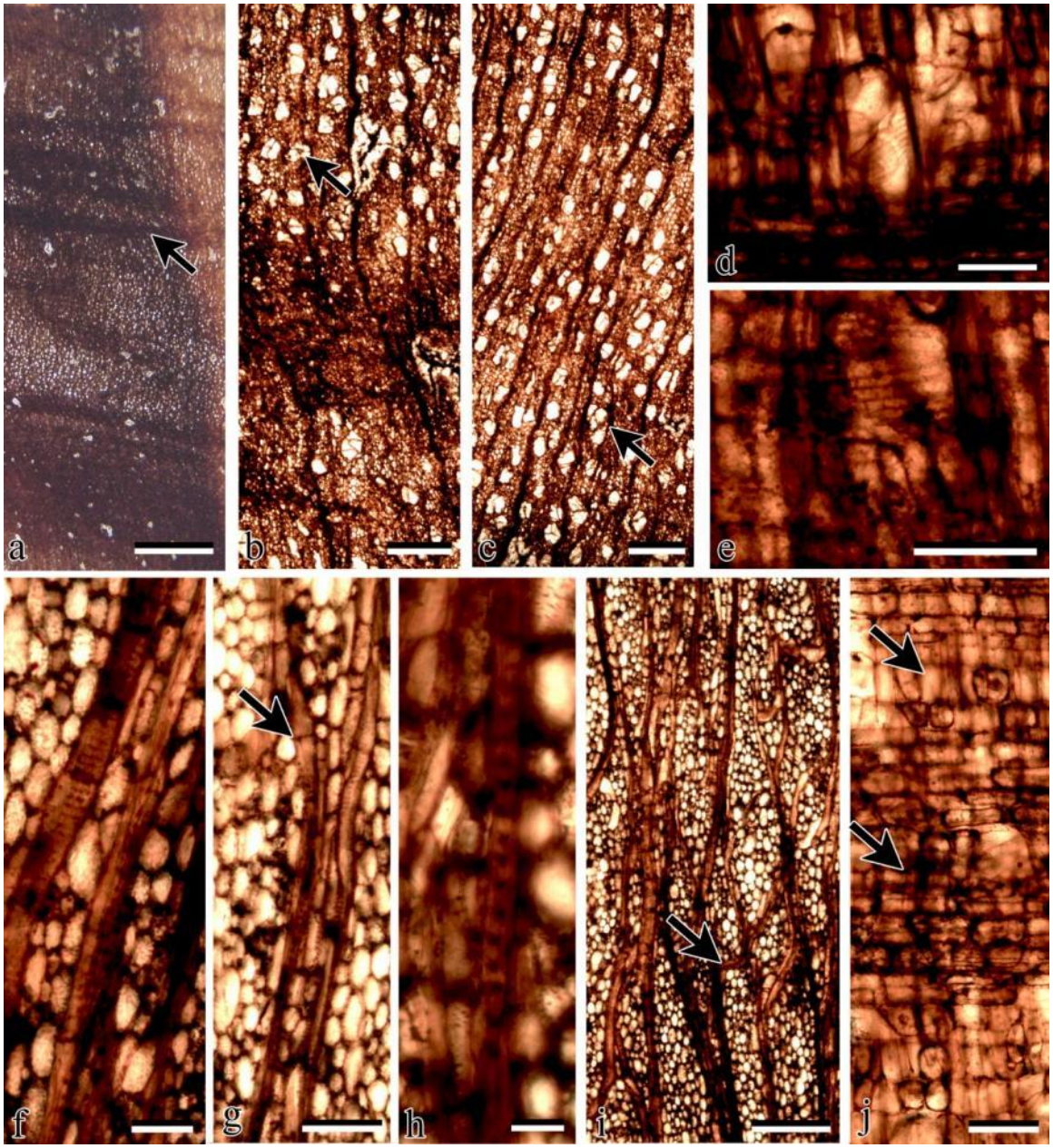

Figure B. 4. *Hedycaryoxylon* sp. A. MPM-24. a. TS with growth rings; scale bar = 2.5 mm. b. TS showing a growth ring, diffuse porous wood and tyloses (arrow); scale bar = 250 µm. TS showing diffuse porous wood and vessel cluster (arrow), scale bar = 250 µm. d. RLS showing scalariform perforation plates, scale bar = 50 µm. e. RLS showing simple vessel-ray pitting, scale bar = 100 µm. f. TLS showing scalariform intervessel pitting, scale bar = 50 µm. g. TLS showing fiber with bordered pitting, scale bar = 25 µm. h. TLS showing septate fibers (arrow), scale bar = 100 µm. i. TLS showing multiserate rays and fiber dissecting ray (arrow), scale bar = 250 µm. j. RLS showing procumbent (lower arrow) and upright (upper arrow) ray cells, scale bar = 100 µm.

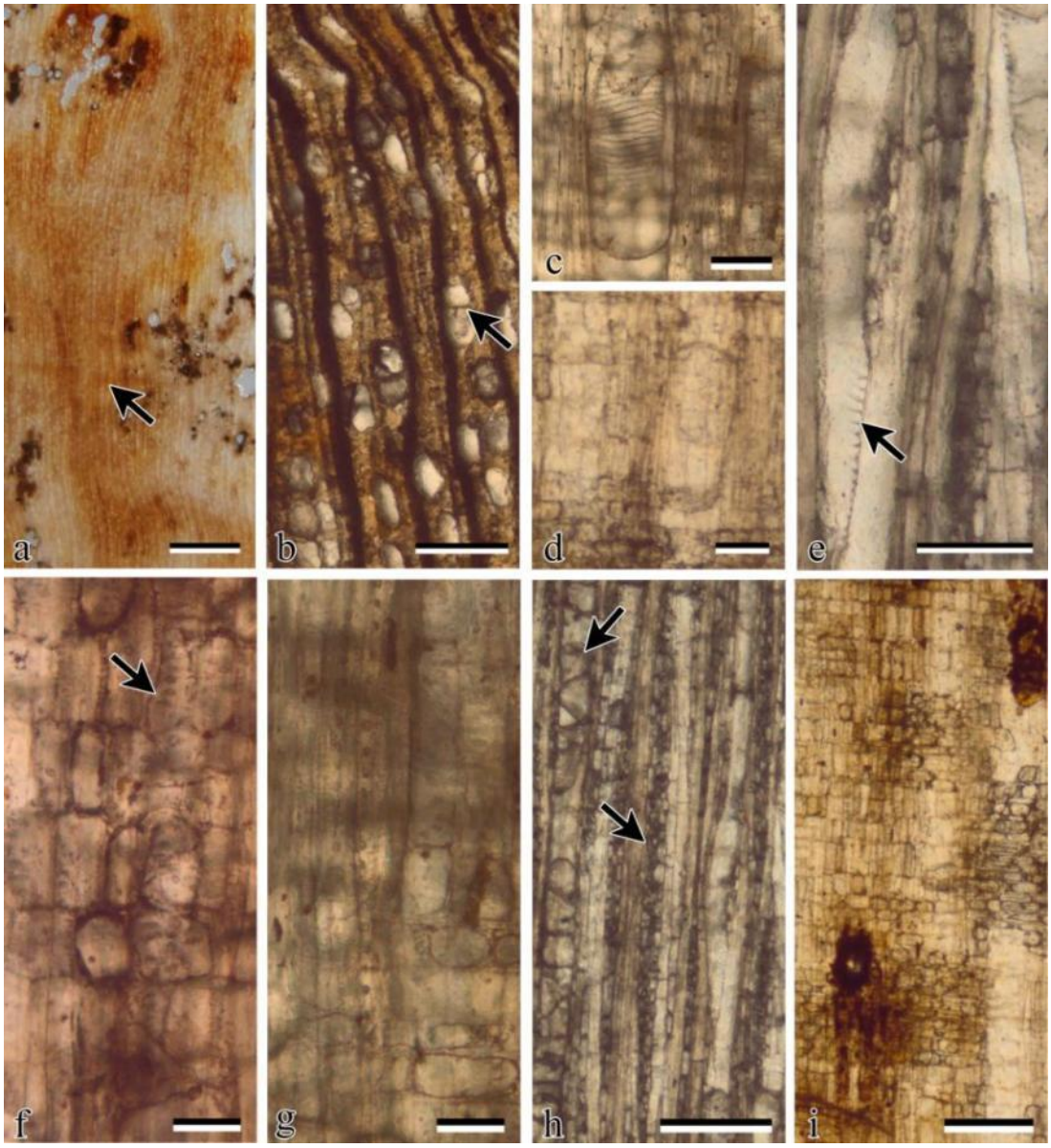

Figure B.5. *Nothofagoxylon corrugatus*. MPM-26. a. TS showing one faint growth ring (arrow); scale bar = 2.5 mm. b. TS showing diffuse porous wood, solitary vessels, tyloses (arrow) and undulating region; scale bar = 250 µm. c. RLS showing scalariform perforation plate; scale bar = 100 µm. d. RLS showing simple perforation plate; scale bar = 100 µm. e. TLS showing scalariform intervessel pitting; scale bar = 100 µm. f. RLS showing simple vessel-ray pitting (arrow); scale bar = 100 µm. g. RLS showing ground fiber with minute bordered pitting; scale bar = 100 µm. h. TLS showing rays (lower arrow) and tyloses (upper arrow); scale bar = 250 µm. i. RLS showing cellular composition of ray; scale bar = 250 µm.

APPENDIX C: ELASMOBRANCH VERTEBRAL MEASUREMENTS.

Vertebrae ID	Diameter						
	Dorsoventral 1	Dorsoventral 2	TVS 1	TVS 2	Dorsoventral Average	TVS Average	Average Diameter
1	23.83	24.50	22.51	24.42	24.17	23.46	23.81
2	21.74	22.17	22.11	21.75	21.96	21.93	21.95
3	22.49		22.84	22.57	22.49	22.71	22.60
4	21.51	21.25	21.81	20.88	21.38	21.34	21.36
5	22.44	22.85	22.78	22.64	22.65	22.71	22.68
6	21.73	21.30	21.54	21.31	21.52	21.43	21.47
7	23.83	24.65	25.98	24.76	24.24	25.37	24.80
8	17.23	17.79	18.04	18.20	17.51	18.12	17.82
9	22.04	21.40		21.60	21.72	21.60	21.66
10	25.69	27.65	26.22	27.20	26.67	26.71	26.69
11	21.79	22.17	21.66	21.68	21.98	21.67	21.83
12	23.78	25.73	23.69	26.38	24.75	25.04	24.90
13		18.36	16.49	17.71	18.36	17.10	17.73
15	21.88	23.17	23.72	23.31	22.53	23.51	23.02
16	22.00		21.97	21.51	22.00	21.74	21.87
17	23.59						
20		24.29	21.77	23.83	24.29	22.80	23.54
21	17.79			8.63		8.63	8.63
22	20.79	21.26	21.69	21.28	21.02	21.48	21.25
23	25.77		26.27		25.77	26.27	26.02
26	23.47	27.02	25.51	26.87	25.24	26.19	25.72
27	28.04	27.64			27.84		27.84
28	15.51	19.01	19.15	18.12	17.26	18.64	17.95
30	24.94	26.48	27.24	26.95	25.71	27.09	26.40
31	26.27	22.59			24.43		24.43
32	25.81			15.79		15.79	
33	26.52	27.03	26.93	27.03	26.78	26.98	26.88
34	26.59	20.91			23.75		23.75
35	17.37		17.32	16.64	17.37	16.98	17.18
36	23.75	27.33	26.42		25.54	26.42	25.98
37							
38	27.28	25.53	25.70		26.41	25.70	26.05

Vertebrae ID	Diameter						
	Dorsoventral 1	Dorsoventral 2	TVS 1	TVS 2	Dorsoventral Average	TVS Average	Average Diameter
39		17.83	19.35	19.06	17.83	19.21	18.52
41	27.02	27.05	26.36		27.04	26.36	26.70
42	18.27	12.45	12.68	12.44	15.36	12.56	13.96
44							
45	26.37				26.37		26.37
46	26.64	26.60	26.63	27.17	26.62	26.90	26.76
49	26.12	26.34	27.45	26.62	26.23	27.04	26.63
55	22.76	26.16	24.75	25.53	24.46	25.14	24.80
56	19.19	20.54	21.44	20.58	19.87	21.01	20.44
57	22.49	25.17	22.88	24.73	23.83	23.81	23.82
58							
60	12.59	14.60	15.45	14.27	13.60	14.86	14.23
61	18.79	21.11			19.95		19.95
48a	21.98	22.92	20.30	22.81	22.45	21.56	22.00
48b	21.76	21.32		21.24	21.54	21.24	21.39
45							

Vertebrea ID	Length	
	Dorsoventral	Lateral
1	12.31	11.98
2	10.35	10.02
3	11.01	10.70
4	10.04	9.66
5	11.05	10.71
6	10.38	9.88
7	12.77	12.55
8	8.23	8.19
9	10.27	9.96
10	16.18	15.47
11	10.41	9.96
12	13.30	13.03
13	10.03	9.63
15	10.90	10.52
16	10.74	9.53
17		
20	11.87	11.58
21	8.46	
22	10.30	10.12
23		15.83
26	15.08	14.91
27	15.92	
28	7.88	7.24
30	15.66	14.99
31		
32	15.76	
33	16.00	16.21
34		
35	7.84	7.98
36	15.35	15.16
37	15.15	
38		
39	7.51	6.93
41		
42	12.63	5.94
44	7.62	
45		

Vertebrea ID	Length	
	Dorsoventral	Lateral
46	15.57	15.51
49	15.53	15.18
55		14.38
56	9.96	9.23
57	12.64	12.21
58		10.41
60	7.57	6.87
61	9.63	9.50
48a	10.67	10.64
48b	10.13	10.06
45		

VITAE

Victoria M. Egerton

Education

2011	Ph.D. Drexel University, Department of Biology "The Geology, and Paleoecology of the Cerro Fortaleza Formation, Patagonia (Argentina)"
2005	B.Sc. Florida State University, Department of Biology
2003	B.Sc. Mississippi State University, Department of Geoscience

Academic Positions

2011-Current	Post-doctoral research associate, Faculty of Life Sciences, University of Manchester
2011-2006	Graduate Student, Department of Biology, Drexel University
2011-2006	Teaching Assistant, Department of Biology, Drexel University
2005-2009	Fossil Preparation Laboratory Manager, Academy of Natural Sciences, Philadelphia
2004-2005	Project Manager, Diatomware Database, Florida State University
2004	Intern, Department of Paleobiology, Smithsonian National Museum of Natural History
2004-2003	Museum Assistant, Mississippi State University
2003-2002	Student Teaching Assistant, Department of Geology, Mississippi State University

Publications

Wise, S.W., Olney, M., Covington, J.M., **Egerton, V.M.,** Jiang, S., Kulhanek, D.K., Rambeen, S., Schrader, H., Sims, P.A., Wood, A.S., Davis, A., Davenport, D.R., Doepler, N., Falcon, W., Lopez, C., Pressley, T., Swedberg, O.L., and Harwood, D.M., 2007, Cenozoic Antarctic DiatomWare/BugCam: An Aid for Research and Teaching, in Cooper, A.K., and al, C.R.R.e., eds., Online Proceeding of the 10th ISAES, Volume 17, USGS Open-File Report 2007-1047 Short Research Paper, p. 1-4.

Egerton, V.M., and Mylroie, J.E., 2004, Preliminary investigations of 15 fossil reefs on San Salvador Island, Bahamas, In: Davis, R.L., Gamble, D.W. (Eds.), Proceedings of the 12th Symposium on the Geology of the Bahamas and Other Carbonate Regions. Gerace Research Center, San Salvador, Bahamas, p. 13–23.